

Rheology of Coating Systems

By

Pieter Lafras Moolman

Thesis submitted in partial fulfilment of requirements for the degree of Master of Science in
Engineering (Chemical Engineering) in the Department of Chemical Engineering at the University
of Stellenbosch



Supervisor: Prof. J.H. Knoetze

Stellenbosch
April 2003

Declaration

I, the undersigned, hereby declare that the work contained in this thesis is my own original work and that I have not previously in its entirety or in part, submitted it at any university for a degree.

Pieter Lafras Moolman

18 February 2003

Abstract

Desired behaviour of paint during processing, storage, application and after application is of great importance in the coatings industry. Rheology (the study of flow and deformation behaviour) is used as a method to investigate the behaviour of the flow and deformation properties of the paint during these stages. Some of the more important phenomena that can occur during these stages, which were examined rheologically, are:

- i. The rheological behaviour of certain complex raw materials during processing – vesiculated beads suspensions
- ii. The paint behaviour during storage – in-can stability, e.g. phase separation and sedimentation of particles;
- iii. The paint during application – ease of application, spatter, etc.;
- iv. The paint behaviour after application – sag, layer thickness, levelling (ability to hide brush marks), etc.

A *rheometer* was used to obtain rheological curves from a paint sample (± 1 ml). Correct interpretation of these curves, which display rheological properties of the sample such as the viscosity, shear stress, structural strength and many more, produced information about the properties mentioned in i, ii, iii and iv above. It was found that the rheological data correlated well with empirical tests carried out in the laboratory for spatter, sag, levelling behaviour and in-can stability of the paint.

A wide variety of paints were studied ranging from tough/durable outdoor paints to smooth/velvety indoor paints. The rheological behaviour explained the specific end-use properties of the paints. Paints from two different companies were compared on a rheological basis. In some cases large differences in rheological behaviour were observed. Rheology modifiers were tested on a new paint. It was found that specific rheology modifiers could be incorporated into the formulation to give the specific rheological behaviour required. Rheological modelling was performed and it was found that the flow behaviour of paint could be modelled accurately with existing viscosity models (Ostwald/de Waal, Bingham, Casson, Herschel-Bulkley, Cross and Philips-Deutsch). Other rheological properties of paint were also modelled successfully with a simple linear regression model.

Rheology was also used as a method to examine the flow and deformation properties of vesiculated beads, a component of paint with very complex rheology. The most important factors that influence the rheological behaviour of the vesiculated beads were determined. It was found that the type of manufacturing process for the beads affected the rheological behaviour. The effect of the raw materials used to manufacture the vesiculated beads were rheologically determined.

Opsomming

Dit is baie belangrik dat verf die gewenste gedrag moet toon tydens berging, vervaardiging, tydens aanwending en direk na aanwending. Reologie (die studie van vloeï- en vervorming) word gebruik as a metode om die vloeï- en vervormingseienskappe van verf gedurende bogenoemde stadia te ondersoek. Sommige van die belangriker verskynsels wat gedurende hierdie stadia kan plaasvind, is d.m.v reologiese toetse ondersoek. Die verskynsels is as volg:

- i. Die reologiese gedrag van komplekse grondstowwe soos gevesikuleerde partikel suspensies.
- ii. Verfgedrag tydens berging – stabiliteit van verf in die blik, bv. faseskeiding en sedimentasie van partikels
- iii. Verfgedrag tydens aanwending – gemak van aanwending, spatsels
- iv. Verfgedrag direk na aanwending – afsakking, dikte van verflaag, vloeï-eienskappe

‘n Reometer is gebruik om die reologiese kurwes te bepaal deur gebruik te maak van ± 1 ml monster. Korrekte interpretasie van hierdie kurwes, wat onder meer eienskappe soos viskositeit, spanning en struktuursterkte insluit, lei tot inligting wat die verskynsels in i, ii, iii en iv kan verklaar. Daar is gevind dat inligting wat verkry is i.v.m die verskynsel van spatsels, afsakking, vloeï en die stabiliteit van verf in die blik, goed korreleer met empiriese toetse wat in die laboratorium uitgevoer is.

‘n Groot verskeidenheid van verwe, wat wissel van duursame/sterk buitemuurse verf, tot fluweelsagte binnenshuise verf, is ondersoek. Die reologiese toetse het daarin geslaag om die eienskappe van die eindproduk suksesvol te verduidelik. Verf van twee verskillende maatskappye is ook met mekaar vergelyk op ‘n reologiese grondslag. Daar is by sommige van die verwe aansienlike verskille in die reologiese gedrag gevind. ‘n Nuwe verf is gebruik om die uitwerking van reologie modifiseerders te ondersoek. Daar is gevind dat daar spesifieke reologie modifiseerders bestaan wat unieke reologiese gedrag verseker. Reologiese modellering is gedoen op verf en daar is gevind dat die vloeïgedrag van die verf akkuraat gemodelleer kan word deur van die bestaande viskositeitsmodelle gebruik te maak (Ostwald/de Waal, Bingham, Casson, Herschel-Bulkley, Cross en Philips-Deutsch). Ander reologiese eienskappe is gemodelleer deur gebruik te maak van eenvoudige regressie modelle.

Daar is ook van reologiese tegnieke gebruik gemaak om die vloeï en vervormingseienskappe van gesuspendeerde gevesikuleerde partikels, wat as 'n grondstof vir verf gebruik word, te ondersoek. Die belangrikste faktore wat die reologiese gedrag beïnvloed het, was onder meer die verskillende prosesse waarmee die gevesikuleerde partikels vervaardig is. Die effek van sekere van die grondstowwe wat gebruik word om die gevesikuleerde partikels te vervaardig, is ook reologies ondersoek.

This work is dedicated to my mother and father

Acknowledgements

I would like to thank Plascon Research Centre for their financial support throughout my studies and for providing the Paar Physica MCR 300 rheometer used for experimental work.

A special word of thanks to my supervisor, Prof. Hansie Knoetze, for his support and guidance over the past two years.

I would like to express my gratitude towards my family who supported me throughout this project.

To Cara Fouche, who always succeeded in putting a smile on my face when times were difficult.

Table of Contents

Chapter 1	Introduction	1
1.1	Rheology	1
1.2	Rheology in the coating industry	1
1.3	Importance of this study	2
1.4	Aims of this study	2
Chapter 2	Literature Review	4
2.1	Rheology	4
2.2	Rheometry	5
2.2.1	Instruments	5
2.2.2	Test types	6
2.3	Data interpretation	9
2.3.1	Flow curves	9
2.3.2	Amplitude sweeps	11
2.3.3	Frequency sweeps	12
2.3.4	Three-interval-thixotropy-test (3-ITT)	14
2.3.5	Time test	16
2.4	Vesiculated bead and polymeric thickener rheology	17
2.5	Dispersion rheology and stability of a dispersion	21
2.6	Paint rheology	25
2.6.1	Flow and viscosity curves	26
2.6.2	Amplitude sweeps	27
2.6.3	Frequency sweeps	27
2.6.4	Three-interval-thixotropy-test (3-ITT)	28
2.7	Rheology modifiers	30
2.8	Modelling	33

Chapter 3	Experimental	35
3.1	Test instrumentation	35
3.1.1	Rheometer	35
3.1.2	Measuring systems	36
3.2	Test types	42
3.2.1	Rotational tests	42
3.2.2	Oscillatory tests	43
Chapter 4	Rheological Properties of Vesiculated Beads	45
4.1	Background	45
4.2	Chemical and physical composition of vesiculated beads dispersion	46
4.3	Manufacturing processes of vesiculated beads	48
4.3.1	The emulsification process in an emulsion reactor	48
4.3.2	The Cowles process	50
4.3.3	The homogenisation process	51
4.3.4	Discussion of results	51
4.3.5	Conclusions	59
4.3.6	Implications of differences in manufacturing processes	59
4.3.7	Concluding remarks	60
4.4	Effect of raw materials on rheology of vesiculated beads	61
4.4.1	Effect of hydroxy-ethyl-cellulose (HEC)	61
4.4.2	Effect of polyvinyl-alcohol (PVOH)	71
4.4.3	Effect of diethylene-triamine (DETA)	81
4.4.4	Effect of LMA	88
4.5	Effect of physical properties – particle size	92
4.5.1	Viscosity curves	93
4.5.2	Amplitude sweeps	95
4.5.3	Frequency sweeps	96
4.5.4	Conclusions	98
4.5.5	Practical implications	98
4.6	Effect of manufacturing parameters	99

4.6.1 Effect of number of passes	99
4.6.2 Effect of geometry of plungers	102
4.7 Curing of beads	105
4.8 Conclusions	108
Chapter 5	Rheological Properties of Pigment & Extender-Free Paint (PE-Free Paint)
	110
5.1 Concept of new paint	110
5.2 Chemical properties of new paint	110
5.3 Rheology of new paint	111
5.3.1 Viscosity curves	112
5.3.2 Amplitude sweeps	114
5.3.3 Frequency sweeps	118
5.3.4 Three-interval-thixotropy-test (3-ITT)	125
5.4 Conclusions	130
Chapter 6	Rheological Properties of Paint
	132
6.1 Rheological characterisation of commercial paints of company ABC	133
6.1.1 Group I	134
6.1.2 Group II	143
6.2 Rheological comparison of paints from company ABC and XYZ	152
6.2.1 Water-based paints	153
6.2.2 Solvent-based paints	160
6.3 Comparison of a high-quality (expensive) and a low-quality (inexpensive) paint in terms of rheological behaviour	167
6.3.1 Viscosity curves	167
6.3.2 Amplitude sweeps	168
6.3.3 Frequency sweeps	170
6.3.4 Three-interval-thixotropy-test (3-ITT)	171
6.3.5 Conclusions	173
6.4 The consistency of the paint manufacturing process	174

6.4.1	Viscosity curves	174
6.4.2	Amplitude sweeps	177
6.4.3	Frequency sweeps	180
6.4.4	Time sweeps	182
6.4.5	Three-interval-thixotropy-test (3-ITT)	183
6.4.6	Conclusions	184
6.5	Conclusions	186
Chapter 7	Rheology Modifiers	187
7.1	Background	187
7.2	Chemistry of rheology modifiers	187
7.2.1	ASE chemistry	188
7.2.2	HEUR chemistry	188
7.2.3	HASE chemistry	190
7.3	Formulating with rheology modifiers	190
7.3.1	Formulating with alkali swellable emulsions (ASE)	192
7.3.2	Formulating with HEUR rheology modifiers	193
7.3.3	Formulating with HASE rheology modifiers	194
7.3.4	The compatibility between dispersants and associative thickeners	194
7.4	Discussion of results	195
7.4.1	Acrysol ASE60	195
7.4.2	Acrysol RM8W and Acrysol RM2020	201
7.4.3	Acrysol RM5	209
7.5	Conclusions	216
Chapter 8	Modelling	218
8.1	Approximation functions for flow and viscosity curves of paint	218
8.1.1	Possible flow behaviour of paints	219
8.1.2	Model functions for flow behaviour for paint with a yield point	220
8.1.3	Model functions for flow behaviour of shear-thinning paints	228
8.1.4	Model functions for flow behaviour of paints without yield points	230
8.2	Approximation functions for flow and viscosity curves of dispersions	233

8.2.1	The Ostwald / de Waal model for vesiculated beads dispersion	233
8.2.2	The Casson model for vesiculated beads dispersion	234
8.2.3	The Herschel-Bulkley model for vesiculated beads	235
8.3	Paint modelling – Simple linear regression	236
8.3.1	Background	236
8.3.2	Regression model	238
8.3.3	Modelling the yield point of paint X	239
8.3.4	Modelling the behaviour of paint X in the LVER	240
8.4	Conclusions	242
8.4.1	Modelling of paints	246
8.4.2	Modelling of vesiculated beads dispersion	243
8.4.3	Simple linear regression model for modelling of certain rheological behaviour of a paint	244
Chapter 9	Conclusions and Recommendations	245
9.1	Conclusions	245
9.2	Recommendations	246
Chapter 10	Future Work	247
References		248
Appendix A	Rheology	252
Appendix B	Typical Rheological Behaviour of Coatings	264
Appendix C	Glossary of Rheological and Coating Terms	276
Appendix D	Raw Data	283
Appendix E	Raw Data (on CD)	

List of Figures:

Chapter 2:

Figure 2-1: Flow and viscosity behaviour for 1) Newtonian, 2) Shear-thinning and 3) Shear-thickening substances	10
Figure 2-2: Typical viscosity behaviour for a paint	11
Figure 2-3: Determination of yield point from amplitude sweep	12
Figure 2-4: Typical rheological behaviour of systems under frequency oscillation	13
Figure 2-5: Typical G' and G'' curves in a 3-ITT	15
Figure 2-6: Time-dependent behaviour of substances without a chemical reaction	16
Figure 2-7: A typical viscosity profile for a coating	26
Figure 2-8: Test method for determining structural recovery after high shear	28

Chapter 3:

Figure 3-1: Photo of Physica MCR 300 (Modular Compact Rheometer) with power supply unit	36
Figure 3-2: Photo of measuring system	37
Figure 3-3: The cone-and-plate measuring system	38
Figure 3-4: Plate-and-plate measuring system	40

Chapter 4:

Figure 4-1: A SEM photograph of the vesiculated beads ($\times 500$ times)	45
Figure 4-2: PBT impeller blade for emulsification process	49
Figure 4-3: Disc turbine impeller blade for Cowles process	50
Figure 4-4: Viscosity curves for vesiculated beads produced by each of the three different processes	52
Figure 4-5: Amplitude sweeps for the three different vesiculated beads samples	54
Figure 4-6: Relationship between G' and shear rate for vesiculated beads	55
Figure 4-7: Amplitude sweep with stress on x-axis for vesiculated beads	56
Figure 4-8: Frequency sweeps with complex viscosity on y-axis	58
Figure 4-9: Effect of HEC content on viscosity curves for vesiculated beads	62
Figure 4-10: Effect of HEC content on the amplitude sweeps for vesiculated beads	63
Figure 4-11: Relationship between amount of HEC and G' values in the LVER	64
Figure 4-12: Effect of HEC content on amplitude sweeps for vesiculated beads (stress on x-axis)	65
Figure 4-13: Relationship between yield point and the amount of HEC	65
Figure 4-14: Effect of HEC content on frequency sweeps for vesiculated beads	66
Figure 4-15: Effect of HEC content on frequency sweeps ($\tan \delta$ vs. frequency)	67
Figure 4-16: Effect of HEC content on structural recovery	69
Figure 4-17: Effect of PVOH content on viscosity curves for vesiculated beads	73
Figure 4-18: Effect of PVOH content on amplitude sweeps	74
Figure 4-19: Relationship between G' and amount of PVOH	75
Figure 4-20: Effect of PVOH content on amplitude sweeps (stress values on x-axis)	76
Figure 4-21: Relationship between yield stress and amount of PVOH	77
Figure 4-22: Effect of PVOH content on the frequency sweeps	78
Figure 4-23: Effect of PVOH content on the structural recovery curves	79

Figure 4-24: Effect of DETA content on the viscosity curves	82
Figure 4-25: Effect of DETA content on amplitude sweeps	84
Figure 4-26: Liquid-/solid-like behaviour in LVER	85
Figure 4-27: Effect of DETA content on the frequency sweeps	86
Figure 4-28: Effect of DETA content on structural recovery curves	87
Figure 4-29: Effect of LMA on viscosity curves	89
Figure 4-30: Effect of LMA on the amplitude sweeps	90
Figure 4-31: Effect of LMA on the frequency sweeps	91
Figure 4-32: Effect of particle size on viscosity curves	93
Figure 4-33: Relationship between low-shear viscosity ($\dot{\gamma} = 1 \text{ s}^{-1}$) and stirrer speed	94
Figure 4-34: Correlation between particle size (PS), particle size distribution (PSD) and stirrer speed	94
Figure 4-35: Effect of particle size on the amplitude sweep	95
Figure 4-36: Relationship between G' , G'' in the LVER and the stirrer speed	96
Figure 4-37: Effect of particle size on frequency sweeps	97
Figure 4-38: Effect of number of passes on the amplitude sweep	100
Figure 4-39: Effect of number of passes on the frequency sweep	101
Figure 4-40: Effect of plunger geometry on amplitude sweeps	103
Figure 4-41: Effect of plunger geometry on the frequency sweeps	104
Figure 4-42: Rheological parameters during curing reaction at 70°C	105
Figure 4-43: SEM photos taken at different stages during the curing of the vesiculated beads	106
Figure 4-44: Initial changes in character of the vesiculated beads during the curing reaction at 70°C	107

Chapter 5:

Figure 5-1: Comparison between viscosity curves of PE-free paints (blue) and standard paints (red)	112
Figure 5-2: Amplitude sweeps for PE-free paints with Ucar as coalescent	115
Figure 5-3: Amplitude sweeps for PE-free paints with Coasol as coalescent	115
Figure 5-4: Relationship between G' and beads/emulsion ratio	116
Figure 5-5: Apparent yield points obtained from amplitude sweeps	117
Figure 5-6: Frequency sweep for PE-free paints with Ucar as coalescent	118
Figure 5-7: Frequency sweep for PE-free paints with Coasol as coalescent	119
Figure 5-8: Trendlines for G' and G'' in high-frequency range for JE4/Coasol	120
Figure 5-9: Trendlines for G' and G'' at high-frequency range for JE5/Ucar	120
Figure 5-10: Degree of spatter	121
Figure 5-11: Comparison between spatter of standard paints (paint C) and PE-free paint (paint PE)	122
Figure 5-12: Comparative results for degree of spatter (laboratory vs. frequency sweep)	124
Figure 5-13: Loss factor in low-frequency range	125
Figure 5-14: Comparison between laboratory results and the power-law parameter, n , obtained from the 3-ITT for the levelling behaviour of the PE-free paints and the standard paints	127
Figure 5-15: Correlation between layer thickness and structural recovery (G')	129

Chapter 6:

Figure 6-1: Viscosity curves for group I paints	134
Figure 6-2: Amplitude sweeps for group I paints	136

Figure 6-3: Frequency sweeps for group I paints	139
Figure 6-4: 3-ITT curves for group I paints	140
Figure 6-5: Viscosity curves for group II paints	143
Figure 6-6: Amplitude sweeps for group II paints	145
Figure 6-7: Frequency sweeps for group II paints	147
Figure 6-8: Spatter behaviour for ceiling paint and high-quality matt paint	149
Figure 6-9: 3-ITT curves for group II paints	150
Figure 6-10: Viscosity curves for water-based paints of company ABC and XYZ	153
Figure 6-11: Amplitude sweeps for water-based paints of companies ABC and XYZ	155
Figure 6-12: Amplitude sweeps for water-based paints of companies ABC and XYZ (shear stress on x-axis)	156
Figure 6-13: Frequency sweeps for water-based paints of companies ABC and XYZ	157
Figure 6-14: 3-ITT curves for water-based paints of companies ABC and XYZ	159
Figure 6-15: Viscosity curves for solvent-based paints of companies ABC and XYZ	161
Figure 6-16: Amplitude sweeps for solvent-based paints of companies ABC and XYZ	162
Figure 6-17: Amplitude sweep expressed in terms of shear stress	163
Figure 6-18: Frequency sweeps for solvent-based paints of companies ABC and XYZ	164
Figure 6-19: 3-ITT curves for solvent-based paints of companies ABC and XYZ	165
Figure 6-20: Viscosity curves for high- and low-quality paints	167
Figure 6-21: Amplitude sweeps for high- and low-quality paints	169
Figure 6-22: Frequency sweeps for low- and high-quality paints	170
Figure 6-23: 3-ITT for the high- and low-quality paints	172
Figure 6-24: Viscosity curves for three different paints	175
Figure 6-25: Amplitude sweeps for three EPL-30 paint samples	178
Figure 6-26: Amplitude sweeps expressed with $\tan \delta$ on the y-axis	179
Figure 6-27: Frequency sweeps for EPL-30 paints	180
Figure 6-28: Time sweeps for EPL-30 paints	182
Figure 6-29: Three-interval-thixotropy-test curves for EPL-30 paints	183

Chapter 7:

Figure 7-1: Chemical structure of typical HEUR thickener	189
Figure 7-2: Effect of pH on viscosity for rheology modifiers that are pH sensitive	191
Figure 7-3: Effect of pH on viscosity (0.54% Acrysol ASE 60)	192
Figure 7-4: Effect of pH on viscosity (0.89% Acrysol ASE 60)	192
Figure 7-5: Effect of pH on viscosity (1.24% Acrysol ASE 60)	193
Figure 7-6: Viscosity curves with Acrysol ASE 60	195
Figure 7-7: Amplitude sweeps for Acrysol ASE 60	196
Figure 7-8: Frequency sweeps for Acrysol ASE 60	198
Figure 7-9: Storage stability of paint with Acrysol ASE 60 (4 weeks)	199
Figure 7-10: Structural recovery with Acrysol ASE 60	200
Figure 7-11: Effect of Acrysol RM2020/RM8W on viscosity curves	202
Figure 7-12: Effect of Acrysol RM2020/RM8W on amplitude sweeps	204
Figure 7-13: Effect of Acrysol RM2020/RM8W on frequency sweeps	205
Figure 7-14: Storage stability of paint with Acrysol RM2020/RM8W (4 weeks)	206
Figure 7-15: Effect of Acrysol RM2020/RM8W on the structural recovery	207
Figure 7-16: Effect of Acrysol RM5 on viscosity curves	209
Figure 7-17: Effect of Acrysol RM5 on amplitude sweeps	211
Figure 7-18: Effect of Acrysol RM5 on frequency sweeps	212
Figure 7-19: Storage stability of paint with Acrysol RM5 (4 weeks)	213
Figure 7-20: Effect of Acrysol RM5 on the structural recovery	214

Chapter 8:

Figure 8-1: Different types of flow behaviour for paints	219
Figure 8-2: Bingham model-fit for paint with a yield point	221
Figure 8-3: Casson model-fit for paint with a yield point	222
Figure 8-4: Herschel-Bulkley model-fit for paint with a yield point	224
Figure 8-5: Amplitude sweep for paint with yield point	226
Figure 8-6: Ostwald / de Waal model-fit for paint with shear-thinning behaviour	229
Figure 8-7: Cross model-fit for model without yield point	231
Figure 8-8: Philips-Deutsch model-fit for paint without a yield point	233
Figure 8-9: Ostwald / de Waal model-fit	233
Figure 8-10: Casson model-fit	234
Figure 8-11: Herschel-Bulkley model-fit	235
Figure 8-12: Error % for modelling of viscosity data by means of different modelling techniques	238
Figure 8-13: Modelled yield point data for paint X	239
Figure 8-14: Modelled cross-over point (in terms of stress) for paint X	241
Figure 8-15: Modelled cross-over point (in terms of frequency) for paint X	241

Chapter 9:

Figure 9-1: Rheology in the paint manufacturing process	245
---	-----

List of Tables**Chapter 2:**

Table 2-1: Parameters for characterising a system of dispersed particles	22
Table 2-2: Typical shear rates in the coatings industry	25

Chapter 3:

Table 3-1: Technical specifications of MCR 300	35
--	----

Chapter 4:

Table 4-1: Chemical and physical composition of the vesiculated beads dispersion	46
Table 4-2: Physical properties of vesiculated beads samples	52
Table 4-3: Properties of vesiculated beads samples with different levels of HEC	61
Table 4-4: Amount of PVOH in each sample	72
Table 4-5: Amount of DETA in each sample	82
Table 4-6: Effect of DETA on low and high-shear viscosity	83
Table 4-7: Degree of structural recovery after 80 seconds	87
Table 4-8: Particle size with corresponding Cowles impeller speed	92

Chapter 5:

Table 5-1: Chemical composition of PE-free paint given as % of total mass	111
Table 5-2: Power-law parameters, K and n for PE-free and standard paints with R ² -values	113
Table 5-3: Beads/emulsion ratio	116
Table 5-4: Laboratory values for spatter	123
Table 5-5: Laboratory values for levelling and the power-law parameter, n	126

Chapter 6:

Table 6-1: Description of paints	133
Table 6-2: Power-law parameter, n, for viscosity curves of group I paints	135
Table 6-3: tan δ values in the LVER for group I paints	137
Table 6-4: Structural strength (G') and quality for group I paints	137
Table 6-5: Yield points for group I paints obtained from amplitude sweeps	138
Table 6-6: Percentage structural recovery for paints of group I	141
Table 6-7: Structural strengths (G') of group II paints	146
Table 6-8: Yield points of group II paints	146
Table 6-9: Description of paints manufactured by two different companies	152
Table 6-10: High- and low-shear viscosities of water-borne paints	154
Table 6-11: Comparison between water-based paints from companies ABC and XYZ	160
Table 6-12: Comparison between solvent-based paints from companies ABC and XYZ	166
Table 6-13: Cost of high- and low-quality paints	167
Table 6-14: Structural recovery for high- and low-quality paints	172
Table 6-15: Comparison between high- and low-quality paints	173
Table 6-16: Viscosity values at various shear rates	175
Table 6-17: Power-law parameters for power-law model	176

Table 6-18: Power-law parameters, n and K	176
Table 6-19: Yield points	179
Table 6-20: Difference in slopes of G' and G'' curves in the high-frequency range of the frequency sweep	181
Table 6-21: Time for 75% structural recovery	184

Chapter 7:

Table 7-1: Chemical composition of latex paint	190
Table 7-2: Effect of rheology modifiers on PE-free paint	216

Chapter 8:

Table 8-1: Model predictions for yield points	225
Table 8-2: Model groups for flow behaviour of paint	227
Table 8-3: Factor levels for paint X	236
Table 8-4: Regression coefficients for simple linear regression model for predicting yield points	240
Table 8-5: Regression coefficients for simple linear regression model for prediction of the cross-over point for paint X	242
Table 8-6: Correlation coefficients for simple linear regression model for behaviour of a paint in the LVER	244

Nomenclature

Latin characters (lower-case letters)

a_i	Regression coefficient	[-]
c	Herschel-Bulkley viscosity	[Pas]
d_{max}	Maximum particle diameter	[m]
f	Frequency	[Hz]
h	Cone tip truncation	[m]
k	Constant	
l	Length	[m]
s	Deflection	[m]
r	Radius	[m]
t	Time	[s]
$\tan \delta$	Loss factor	[-]
v	Velocity	[m/s]
x,y	Coordinates, e.g. in the Cartesian coordinate system	

Latin characters (capital letters)

D	Impeller diameter	[m]
F	Force	[N]
G	Shear modulus	[Pa]
G^*	Complex modulus	[Pa]
G'	Storage modulus	[Pa]
G''	Loss modulus	[Pa]
G_{Cr}	Cross-over point between G' and G''	[Hz]
H	Distance between tow parallel plates	[m]
K	Consistency index	[Pas ⁿ]
K_I	Constant for impeller blades	
LVER	Linear viscoelastic range	[Pa]
M_R	Molecular weight	[kg/mol]
N	Impeller speed	[rpm]

N_Q	Pumping number	[revolution ⁻¹]
N_{Re}	Impeller Reynolds number	[-]
P	Pressure	[Pa]
PS	Particle size	[m]
PSD	Particle size distribution	[m]
Q	Volumetric flow rate	[m ³ /s]
Q_{eff}	Effective volumetric pumping rate	[m ³ /s]
R^2	R-square value	[-]
Re	Reynolds number	[-]
R_{MS}	Measuring system radius	[m]
R_p	Radius of particle	[m]
Sg	Specific gravity	[kg/m ³]
T	Tank diameter	[m]
X	Variable	

Greek symbols

η	Shear viscosity	[Pas]
η'	Real part of complex viscosity	[Pas]
η''	Imaginary part of complex viscosity	[Pas]
η^*	Complex viscosity	[Pas]
η_B	Bingham flow coefficient	[Pas]
η_C	Casson flow coefficient	[Pas]
η_0	Zero-shear viscosity	[Pas]
η_∞	Infinite-shear viscosity	[Pas]
γ	Strain	[%]
γ_A	Strain amplitude for oscillatory tests	[%]
$\dot{\gamma}$	Shear rate	[s ⁻¹]
$\dot{\gamma}_w$	Shear rate at wall	[s ⁻¹]
$\dot{\gamma}_{app}$	Apparent shear rate	[s ⁻¹]
$\dot{\gamma}_{av}$	Average shear rate	[s ⁻¹]

$\dot{\gamma}_{emulsion}$	Shear rate in emulsion reactor	[s ⁻¹]
$\dot{\gamma}_{Cowles}$	Shear rate in Cowles process	[s ⁻¹]
$\dot{\gamma}_{homogeniser}$	Shear rate in homogeniser	[s ⁻¹]
τ	Shear stress	[Pa]
τ_A	Shear stress amplitude for oscillatory tests	[Pa]
τ_B	Bingham yield stress	[Pa]
τ_C	Casson yield stress	[Pa]
τ_{HB}	Herschel-Bulkley yield stress	[Pa]
τ_w	Shear stress at wall	[Pa]
τ_L	Limit of LVER	[Pa]
τ_y	Yield stress	[Pa]
α	Cone angle	[°]
δ	Phase shift angle, loss angle	[°]
ω	Angular frequency	[rad/s]
π	Pi	[-]
ϕ_c	Critical volume fraction	[-]
ϕ_s	Solids volume fraction	[-]
σ	Correlation coefficient	[-]

Superscript

*	Complex
®	Registered
m	Power-law parameter related to compressibility
n	Power-law exponent
p	Herschel-Bulkley index
TM	Trade mark

Subscript

A	Amplitude
app	Apparent
av	Average
Cr	Cross-over
gradient	Gradient
i	$i=1,2,3\dots$
layer	Layer
max	Maximum
mean	Mean value
MS	Measuring system
particle	Particle
w	Wall
y	Yield

CHAPTER 1 Introduction

1.1 Rheology

In 1678 Robert Hooke developed his ‘True theory of elasticity’ which forms the basic theory behind classical elasticity. At the other end of the spectrum, in 1687, Isaac Newton published his theory on an ideal viscous liquid [Barnes et al., 1989]. The term ‘rheology’ was invented by Professor Bingham and this definition was accepted when the American Society of Rheology was founded in 1929.

Rheology: The study of the deformation and flow of matter [Barnes et al., 1989].

This definition of rheology allows for the study of behaviour of all matter, including the classical extremes of a Hookean solid and a Newtonian liquid.

It was only in the nineteenth century that scientists began to have doubts about matter that did not behave ideally viscous or ideally elastic, after experiments were carried out with a liquid-like material that could not be described by Newton’s law and a solid-like material that could not be described by Hooke’s law. These intermediate substances, which are viscoelastic, are called complex fluids or, in more modern-day terms, Maxwell fluids. Paint is a Maxwell fluid.

While it is true that the classical definition of a ‘liquid’ as opposed to ‘solid’ provides a basis for deciding whether a substance is a solid or a liquid, the classical definition is inadequate not only for many everyday purposes, but for engineering ones as well.

1.2 Rheology in the Coatings Industry

Coatings are subject to very different forms of stresses. Applying paint on a surface (brushing and rolling) usually results in high shear rates of $\pm 10^6 \text{ s}^{-1}$ depending on the thickness of the layer and

the speed of application. In contrast, during adhesion to the surface (levelling and sagging), only small forces act on the paint, so that the resulting shear rates are smaller than 10^{-3} s^{-1} .

Besides the influence of the shear rate on the rheology behaviour, there are also shear-rate-dependent phenomena that have to be considered which are time dependent, such as thixotropic behaviour. In addition, elastic behaviour may occur which can influence the flow properties.

It is therefore obvious that paint will respond very diversely to these different forms of stresses. Rheology is used to investigate the behaviour of paint during all the above-mentioned processes in the coating industry.

1.3 Importance of Study

The total global consumption of paint in 2000 was estimated at 23 million tonnes [Busato, 2001], of which $\pm 40\%$ was for decorative coatings [Gous, 2002]. Increasing requirements in paint quality necessitate accurate control of the application properties. For paints, the flow behaviour is a decisive quality characteristic. Accurate flow and deformation behaviour is investigated by means of rheology.

This study provides valuable information concerning the flow and deformation behaviour of some of South Africa's more familiar paints.

1.4 Aims of this Study

The present study was undertaken to promote a better understanding of the underlying factors in coating rheology. This is still a relatively new field of research. It was only in the late 1990s that rheological instruments got sophisticated enough to carry out measurements that simulated actual phenomena in the coating industry.

More specifically, the objectives of this study were:

- To use rheology as a method to investigate the factors influencing the stability and flow/deformation behaviour of a raw material (vesiculated beads) used in the coating industry;
- To use rheology as a method to investigate the performance of a coating containing this specific raw material as one of the main components of the formulation;
- To use rheology as a method to investigate flow and deformation properties of paint that influence its performance. These properties are:
 - In-can stability during storage (phase separation, sedimentation)
 - Workability (mixing, pumping, pouring)
 - Application behaviour (ease of application, spatter)
 - Behaviour after application (levelling, layer thickness, sag);
- To use rheology as a method to investigate how paint performance can be enhanced by using rheology modifiers.

CHAPTER 2 Literature Review

2.1 Rheology

Rheology was first acknowledged as a science in its own right around the beginning of the 20th century. However, scientists have long been interested in the behaviour of liquids and solids. A list of interesting historical developments is given by Mezger [2002]. Some of the more important developments are as follows:

- 15th century: Leonardo da Vinci examines the bending behaviour of solids.
- 1663: Blaise Pascal philosophises on ideal liquids without any flow resistance.
- 1676: Robert Hooke derives the ‘Elasticity Law’.
- 1687: Isaac Newton derives the ‘Viscous Law’.
- 1705: Jacob and Johan Bernoulli formulated the Bernoulli equation.
- 1820: Henri Navier develops a theory about the flow behaviour of ideal viscous fluids, which later leads to the Navier/Stokes relation.
- 1839: G. Hagen designs the first capillary viscometer.
- 1885: Osborne Reynolds observes shear thickening behaviour in highly concentrated suspensions.
- 1890: Kelvin and Voigt publish studies on viscoelastic solids.
- End of 19th century: Stormer designs the first torque-controlled rotational viscometer.
- 1929: Founding of the world’s first ‘Society of Rheology’ by Bingham.
- 1951: Weissenberg presents the ‘Rheogoniometer R1’, the first rheometer.
- 1970: Flow-curve analysis begins to replace single-point measurements in industry.
- 1980: Digital control of instruments, analysis and storage of data using computers and software.
- 1983: The company Bohlin presents the first rheometer with an air bearing.
- 1985: The company Physica presents its first viscometer.
- 1992: The company Rheologica presents its first rheometer.
- 1995: Physica presents a rheometer with technology for very rapid tests.
- 2001: Physica presents the Direct Strain Oscillation mode for tests at very small deflection angles.

It is therefore evident that rheology is a fast-growing field of study with important advances in rheometry taking place at the beginning of the 21st century. The term *rheometry* is used when referring to the measuring technology used to determine rheological data. According to Mezger [2002] this includes the measuring systems, instruments and test and analysis methods used to obtain rheological information about a substance.

2.2 Rheometry

2.2.1 Instruments

It was shown in the previous section (section 2.1 – Rheology) that it was only in the 1980s that a variety of companies started to develop rheometers, thereby illustrating the importance of rheology and the instruments used for rheological testing. These days the use of a rheometer that can perform tests in both the controlled stress and controlled strain modes is almost essential in obtaining the desired results.

2.2.1.1 Rheometer

The word *rheometer* refers to an instrument that can measure rheological properties, in contrast to a *viscometer* which can only be used for viscosity measurements. It is essential to be able to obtain more than merely the viscosity of a substance in order to be able to obtain rheological data that can provide important information about the character of the sample as well. Some of the more important behaviour that can be obtained from rheometry is as follows (specifically for paint industry) [Mezger, 2002]:

- Sedimentation of particles in a suspension;
- Levelling due to surface tensions;
- Sagging under gravitational forces;
- Tube or pipe-line flow;
- Mixing, stirring;
- Painting, brushing, spraying;
- Wet grind of pigments;
- Rolling and high-speed coating.

These processes occur at the very small shear rates of 10^{-6} s^{-1} to the very high shear rates of 10^6 s^{-1} . Therefore highly dynamic and sensitive rheometers are required to simulate these shear rates accurately and it was only in the 1980s that these types of rheometers became commercially available.

Various rheometrical techniques exist that can simulate these shear rates accurately. Barnes et al. [1989] describes how these shear rates are obtained with the use of a rheometer with different measuring devices (cone-and-plate, plate-and-plate). Mezger [2002] also distinguishes between different measuring systems for the rheometer including the cone-and-plate and the plate-and-plate measuring systems and gives guidelines on how to choose the measuring system for a specific test and sample. These guidelines are very useful, especially for operators who are not *that* familiar with the test instrumentation. However, the experienced rheologist knows that each sample is unique and therefore also requires unique judgement in terms of rheometrical choices to be made. Advantages, disadvantages and limitations of each system are also discussed. It is useful to keep these limitations in mind while rheological tests are performed, so that reliable rheological data is obtained. It is possible for almost anyone to perform a rheological test on a rheometer, but whether the data are actually representative of the behaviour of the substance is another question.

A rheometer is a highly sensitive instrument that must be handled with great care in order not to damage the air bearing which drives the measuring system. Operating instructions for the specific rheometer used for this study, the Physica MCR 300, are given by Langenbucher [2001] in the operating manual. The operating manual also gives standard test procedures.

2.2.2 Test Types

Tests procedures for the following standard test types are given by Langenbucher [2001] in the operating manual for the Physica MCR 300 rheometer:

- Standard oscillatory tests:

Oscillatory tests are used to examine all kinds of viscoelastic behaviour. These types of tests are almost always used to investigate the character of the sample. Therefore information about the character of the sample can be obtained by performing the following test types in the oscillatory mode without destroying the structure of the sample:

- Amplitude sweep: This test method is mostly used to determine the LVER (linear viscoelastic range) of the material;
 - Frequency sweep: This tests method is time related and therefore gives valuable information about the behaviour of the material during long and short time-scale behaviour;
 - Time test: This test method is used to investigate the behaviour of the material over a certain duration of time to determine the structural changes that are taking place;
 - Structural decomposition/recovery test: This test method is used to investigate the structural decomposition/recovery that is taking place within the sample, usually after a high-shear load. This test method is especially of great importance in the paint industry, because it enables one to investigate the structural recovery of a coating directly after application;
 - Temperature test: The response of a sample to controlled temperature variations gives valuable data about the character of the sample.
- Standard rotational tests:
Rotational tests are mostly used to obtain the flow and viscosity curves.

- Flow/viscosity curve: This test method relates the flow ($\tau = f(\dot{\gamma})$) and viscosity behaviour ($\eta = f(\dot{\gamma})$) to a range of shear rates and can therefore be used to obtain the behaviour of a sample at the shear rates mentioned for most of the processes in section 2.2.1.1

The following rotational tests are used to obtain the same rheological information as mentioned for the oscillatory tests above; however, the behaviour of the sample is obtained under shear and not at very small deformations.

- Time test;
- Relaxation test;
- Structure decomposition/recovery;
- Temperature test.

These test types (oscillatory and rotational) can also be combined/changed to obtain even more precise rheological information about the sample.

It can therefore be seen that sufficient test types exist to obtain representative information about the flow and deformation properties of the sample; however, results obtained from these test types are inconclusive if the following parameter settings are not performed correctly:

- Time duration for test;
- Time duration for each point;
- Data point distribution;
- Shear rate/shear stress profile;
- Temperature profile;
- Gap control during measurement;
- Strain and frequency control in oscillatory tests;
- Direct strain control;
- Control of dynamics during measurement.

As mentioned earlier, there are guidelines for these parameter settings; however, experience has shown that a proper knowledge of the physical and chemical character of the sample is also required to ensure accurate parameter settings that will reflect the true rheological behaviour of the sample.

Rheometry can also be used to investigate the rheological behaviour of a sample during specific scenarios. Some of these scenarios are as follows:

- Challenges in characterisation of concentrated suspensions [Chander, 1997];
- Small amplitude oscillatory shearing as a method not to significantly deform the fluid's microstructure [Larson, 2000];
- Rheological test methods for the sagging behaviour of coatings [Mezger et al., 1998];
- Rheological test methods for simulation of the coating application process [Mezger, 1999];
- New techniques for paint and coating applications [Mezger, 1999].

2.3 Data Interpretation

It is important to have good knowledge of the chemical and physical composition of the sample and the capabilities and restrictions of the rheometer before interpretation of the data is attempted or even before the tests are performed. The interpretation of the data will be misleading if the test is not performed within the limitations of the rheometer or if the character of the sample is not well understood. For example, if a measurement of the steady-state viscosity at very low shear rates is required and the time duration for data-point collection is not long enough, then the transient viscosity will be measured instead of the steady-state viscosity.

The data interpretation of the most frequently used test types follows, given that the tests are performed with the appropriate parameter settings.

2.3.1 Flow Curves

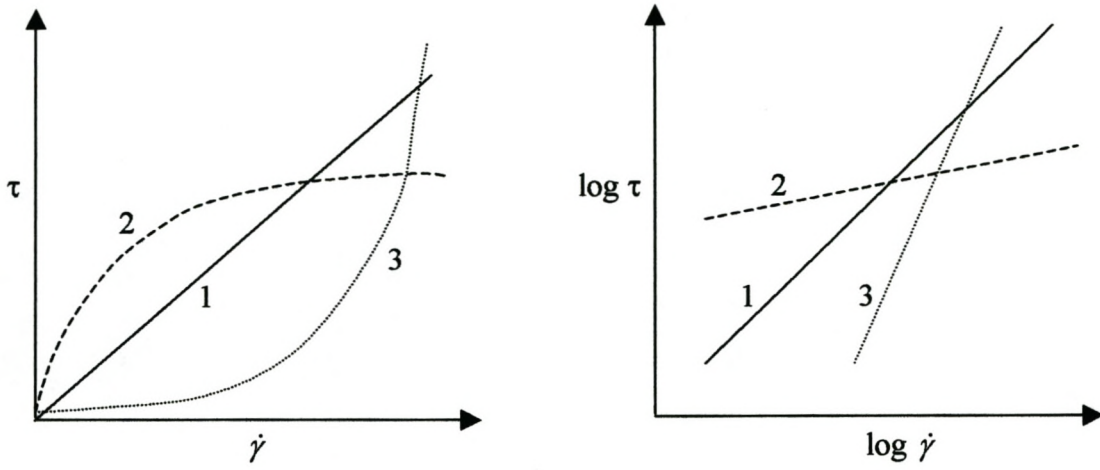
According to Barnes et al. [1989], viscosity is traditionally regarded as the most important rheological property as it immediately gives an indication of the substance's resistance to flow. Mezger [1999] has, however, indicated that the viscosity curve alone is not sufficient in paint rheology for quality assurance.

Mezger [2002] distinguishes between three different types of flow and viscosity curves:

1. Newtonian
2. Pseudoplastic
3. Dilatant.

These different types of behaviour are illustrated in the following figure.

Comparison of flow curves:



Comparison of viscosity curves:

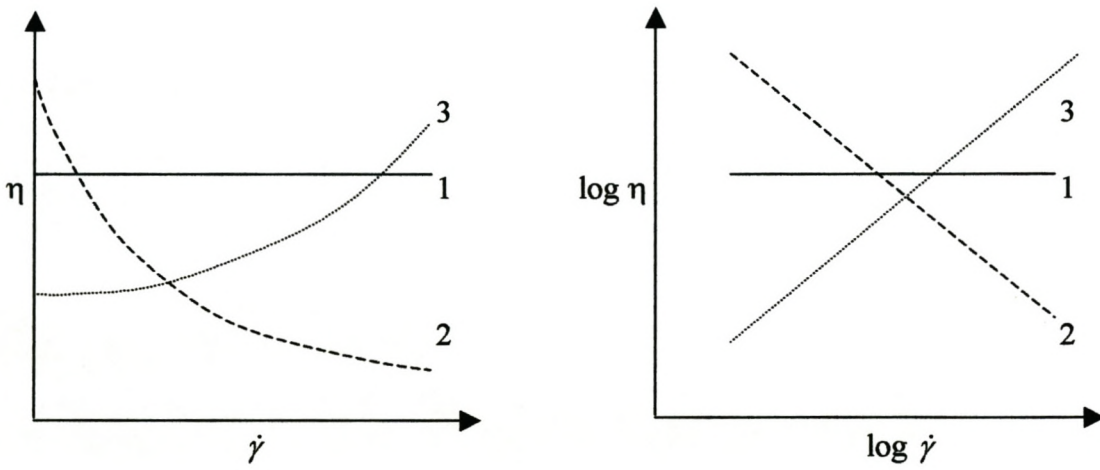


Figure 2-1: Flow and viscosity behaviour for 1) Newtonian, 2) Shear-thinning and 3) Shear-thickening substances

Coatings usually display shear-thinning behaviour to allow for the following appropriate behaviour illustrated in Figure 2-2 [Prideaux, 1993].

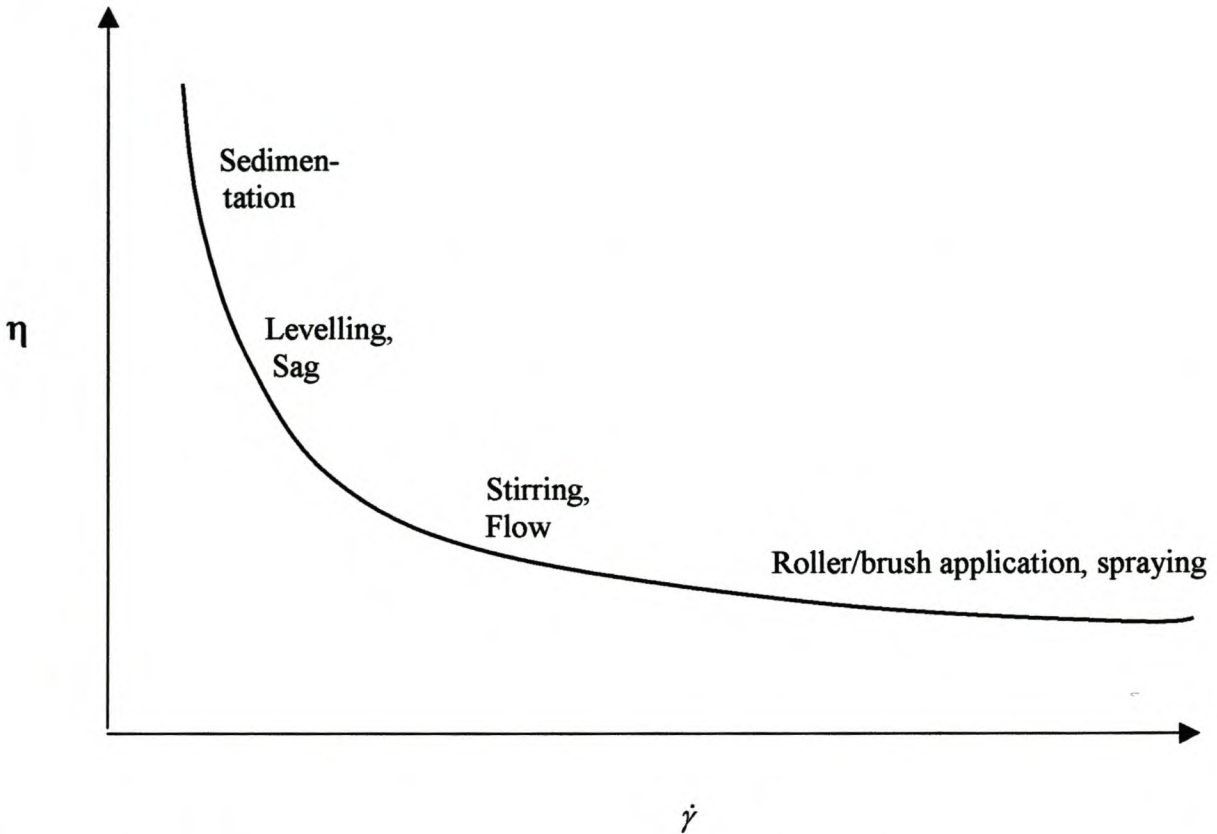


Figure 2-2: Typical viscosity behaviour of a paint [Prideaux, 1993]

2.3.2 Amplitude Sweeps

Mezger [2002] explains the need of the amplitude sweep (see Figure 2-3):

1. Investigation of the character of the sample: With small amplitudes, in the linear viscoelastic range (LVER), both the storage modulus (G') and the loss modulus (G'') run at a constant plateau. A solid-like character predominates when $G' > G''$ and a liquid-like character when $G'' > G'$.
2. Determination of the limit of the linear viscoelastic range (LVER): This is a very important test as it reveals the range within which further tests must be performed when information about the elastic and viscous character of the sample is required.

3. Determination of the yield point of a sample. There are two interpretations of the yield point:

- i. τ_{Y1} : Deviation of the G' curve from the constant plateau values in the LVER;
- ii. τ_{Y2} : Cross-over point with the analogy that the sample flow when $G'' > G'$.

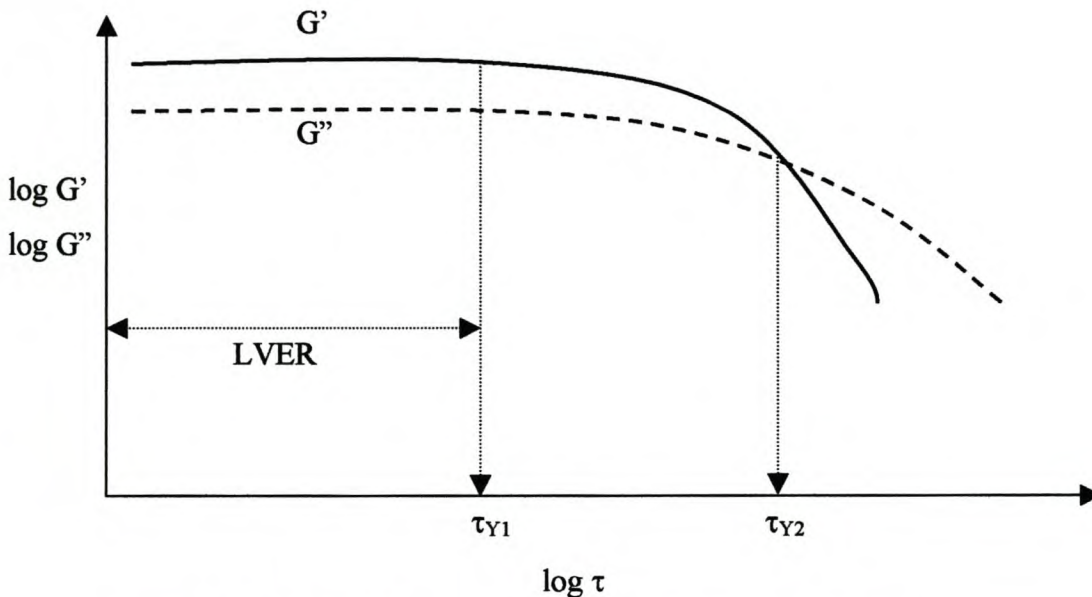


Figure 2-3: Determination of yield point from amplitude sweep

2.3.3 Frequency Sweeps

Barnes et al. [1989] states that quantifying a substance as pure elastic, pure viscous or viscoelastic is not sufficient. If a wide range of stress is applied over a wide range of time, or frequency, it is possible to observe liquid-like behaviour in solids and solid-like behaviour in liquids and therefore attempting to label a material as solid or liquid can be difficult.

Mezger [1999] states that this type of test provides significant information for the investigation of internal structures, e.g. when comparing structural strengths of dispersions. The following behaviour of certain systems under frequency oscillation are given (see Figure 2-4):

1. Behaviour of unlinked polymers:

No primary chemical valency bonds or secondary physical bonds occur between the molecules. Already with small shearing forces or movements, these molecules are capable of slowly sliding off from each other and partly disentangling.

2. Behaviour of cross-linked polymers:

Chemical primary principal valency bonds fix these networks. As a consequence, the sliding of the main molecular chains from others has become impossible without a destruction of the network.

3. Behaviour of dispersions and gels:

In most dispersions and gels, the solid-like character G' predominates over the liquid-like character G'' .

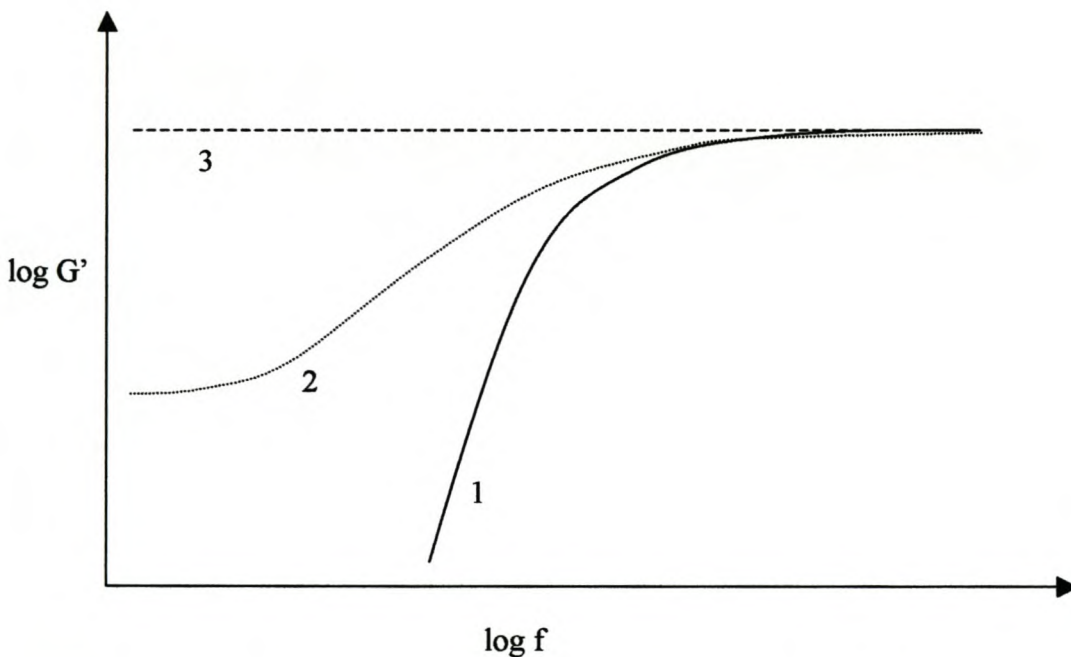


Figure 2-4: Typical rheological behaviour of systems under frequency oscillation [Mezger, 2002]

All three types of behaviour are observed in the coating industry at some stage of the manufacturing process.

Mezger [2002] further explains how the frequency sweep can be used instead of the conventional method (flow curves) to determine the behaviour of the sample below its yield point. The frequency sweep provides several measuring values for G' which can also be used to characterise the consistency of the sample at rest. Mostly G' values at the smallest frequencies of the measuring diagram are used to characterise the structural strength at rest, and rarely the G'' values. Both G' and G'' can be used to characterise the sample and not only one point as in the flow curve.

Not only is the shape of the curves given in Figure 2-4 indicative of the character of the sample but of the relationship between G' and G'' as well. Liquid-like behaviour of a substance in the low- and high-frequency range has very definitive implications on the short (high frequencies) and long (low frequencies) time-scale behaviour. So does the predominance of the solid-like behaviour in the low- and high-frequency range as well. Paints are subjected to both the low- and high-frequency range during storage and application behaviour, respectively, and therefore correct interpretation of the frequency sweep data is of great importance in the paint industry.

2.3.4 Three-Interval-Thixotropy-Test (3-ITT)

The interpretation of the data obtained from this test is of great importance in the coatings industry. This is a relative new type of test method which has been made possible by advances in the technology of the test instrumentation.

Mezger [2002] explains why this test method for determination of the thixotropy behaviour is the preferred method – thixotropic behaviour refers to the decrease in the structural strength during the load phase *and* the regeneration during the rest phase. This test method simulates the decrease in structural strength *as well as* the regeneration, while other methods only simulate the decrease in structural strength. A sample is therefore thixotropic only when the process is completely reversible.

Various methods for analysing the structural recovery of a sample after a high-shear load exist. These methods are given by Mezger [2002] and include the following ways of interpreting the data (see Figure 2-5):

- Thixotropy value as the difference in the G' values – this value is calculated in the following way:

$$\Delta G' = G'_{\max} - G'_{\min}$$

- Total thixotropy time – this is the time the sample takes to recover from G'_{\min} to G'_{\max}
- Thixotropy time required to reach a certain percentage of regeneration – this is the time period the sample takes to recover a certain percentage of its original structural strength ($G'(100\%)$), e.g. 75% structural recovery
- Thixotropy time required to reach the cross-over point, $G' = G''$ – if $G' > G''$ in the first interval and $G'' > G'$ in the second, then this is the time period required to reach the cross-over point ($G' = G''$).
- Percentage of regeneration during a previously defined time period – this is when G' values are compared to the original structural strength over a period of time during the recovery phase.

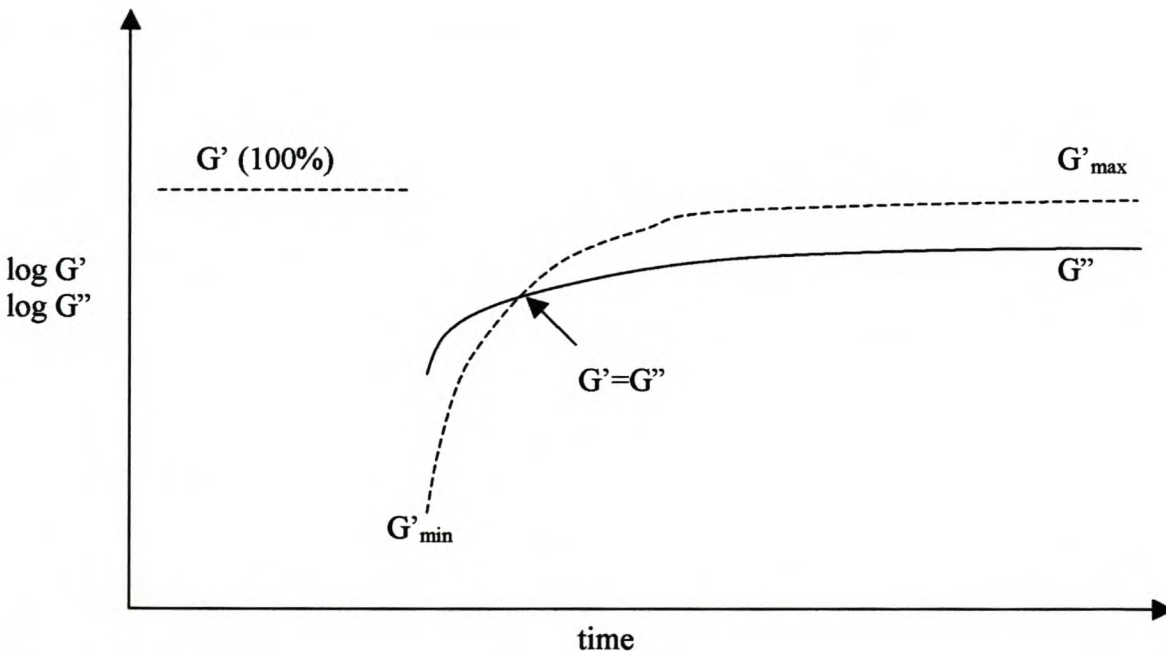


Figure 2-5: Typical G' and G'' curves in a 3-ITT

2.3.5 Time Test

This test aims to determine the influence of the shear load on the physical properties, e.g. showing the change in structural strength (G') over time. Mostly G' is plotted against time.

From the time test it is possible to determine the following type of time-dependent behaviour [Mezger, 2002]:

1. Time-dependent behaviour of substances *without* chemical reaction

These tests are used to investigate the stability of samples with no chemical reaction and therefore only temporary physical changes are recorded. Typical curves for G' values are given below in Figure 2-6.

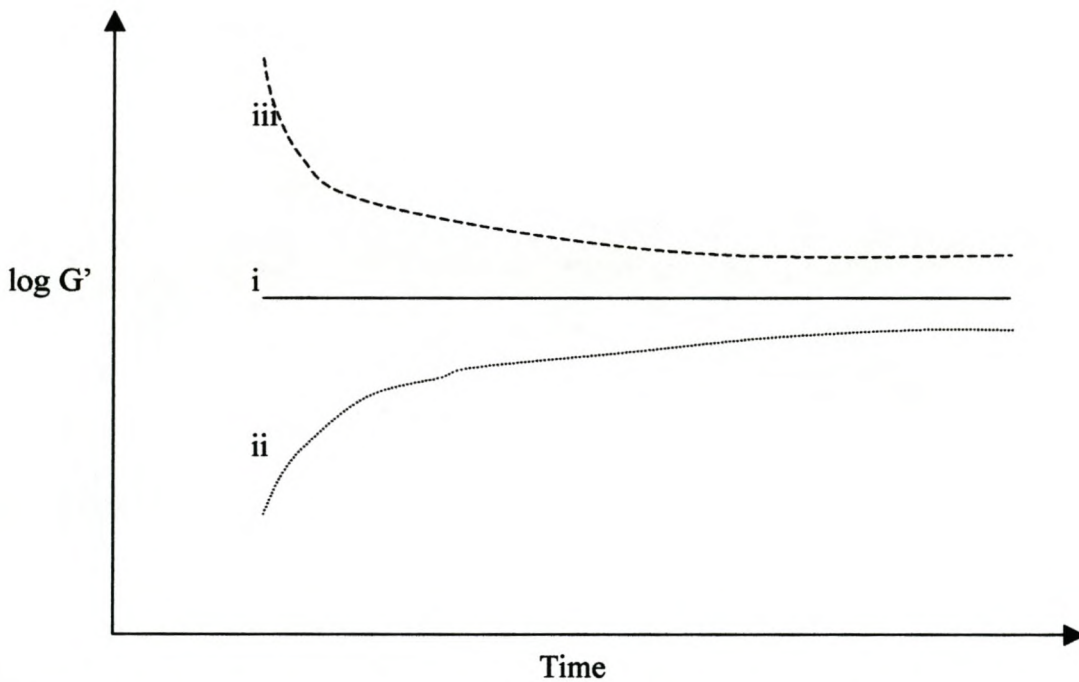


Figure 2-6: Time-dependent behaviour for substances without a chemical reaction

The following types of behaviour are observed in Figure 2-6:

- i. Time-independent, stable structure;
- ii. Building up of structure, e.g. due to mechanical entanglements;
- iii. Structural decomposition due to disentanglements.

2. Time-dependent behaviour of substances *with* chemical reaction

These tests are used to investigate the consistency of samples for which chemical reactions are taking place during the measurement. The time curves are evaluated immediately after the chemical reaction has begun and after long times when the chemical reaction is completed. The reaction process is recorded by way of changes of the rheological parameters G' and G'' with time. Typical curves for G' are also illustrated in Figure 2-6:

- i. Stable structure;
- ii. Building up of structure, e.g. during curing reactions;
- iii. Structural decomposition, e.g. destruction of macromolecules.

It is of great importance to plot both the G' and G'' curves for substances undergoing a chemical reaction. The significance lies in the cross-over point - the cross-over point ($G' = G''$) marks the transition between solid-like and liquid-like behaviour. Solidification can be due to glass formation or by network formation (gelation).

2.4 Vesiculated Bead and Polymeric Thickener Rheology

In order to be able to explain the rheological behaviour of any material, it is necessary to understand the chemical and physical composition of the material. Perrins et al. [1994] describes the vesiculated polymer beads as multi-vesiculated beads that consist of a solid polymer matrix, formed usually from a cross-linked polymer, in which are incorporated numerous vesicles of an aqueous phase. It can therefore be seen that quite complicated rheological behaviour is expected from the vesiculated beads dispersion.

Concentrated suspensions of solid particles, as the vesiculated beads (24% - 28% solids), are highly sensitive to shear forces acting on them. According to Gunning [1975], the shear rate during manufacture plays an important role. He also states that there is a critical shear rate, above which the incidence of distorted clusters of granules occur, which is unacceptable in the manufacture of matt paints. The critical shear rate is commonly much lower than the shear rate, which can be used to prepare the uninitiated dispersion of globules, and hence at initiation and activation it is usual practice to reduce the speed of agitation.

Not only is the rheology of the vesiculated beads very dependent on the physical properties of the vesiculated bead particles, but also on the chemical composition of the dispersion. For example, DETA (di-ethyl tri-amine), the amine compound used for neutralisation of the acid groups in the polyester, is amongst others, one of the most influential chemical compounds on the rheology of the dispersion. According to a Tioxide® report [1981]; it has also been found that when the amount of the amine component of the promoter system is increased, the viscosity of the emulsion may be adversely affected. For example, DETA may cause excessive thickening and/or instability of the emulsion when present in excessive amounts.

Other rheological research on the vesiculated beads is not well documented in the literature. However, Terblanche [2002] examined the viscosity development of the vesiculated beads during production as well as the rheological behaviour of the vesiculated beads after production. He found the beads to display the following rheological behaviour:

- The non-Newtonian behaviour could be modelled by the power-law model;
- Viscoelastic behaviour;
- Shear-thinning behaviour;
- Thixotropic behaviour.

Polymeric Thickener Rheology

Extensive literature exists on the polymeric thickeners used in the vesiculated beads dispersion, hydroxy ethyl cellulose (HEC) and poly vinyl alcohol (PVOH). However, the literature often examined either HEC or PVOH in the presence of a latex network different from vesiculated bead particles. However, understanding the functionality of HEC and PVOH makes it possible to use

these literature references as basic guidelines for understanding the possible rheological behaviour of the beads in the presence of HEC and PVOH.

According to Karickhoff [1984], polymeric thickeners such as PVOH and HEC show special utility when used to thicken coating compositions, especially coating compositions containing vesiculated polymeric beads as part of the pigmentation. The use of PVOH and HEC overcomes the limitations of prior thickeners that do not provide a completely acceptable combination of low- and high-shear viscosities. PVOH and HEC act as thickening agents in water to form the aqueous phase and impart excellent high shear-rate viscosities and still allow excellent flow and levelling as the coating dries.

Other literature that could possibly be used to explain some of the rheological behaviour observed in the vesiculated beads dispersion is given by Kiratzis et al. [1998] for the examination of particulate systems in the presence of HEC. He found the following, amongst other rheological observations:

- A linear increase in G' was observed with increase in HEC concentration.
- It was also observed that a threshold concentration of HEC is required, above which a significant change in rheological properties is recorded.
- Above a certain solids volume fraction (ϕ_s), the yield stress follows a power law of the form:

$$\tau_y = \phi_s^n$$

The dependency becomes of a higher order as the HEC content decreases.

- At solids fractions higher than 20%, G' becomes greater than G'' , indicating the formation of a three-dimensional network. Thus, at higher solid contents, significant particle interaction starts taking place, dictating the rheological properties of the dispersion. Similar behaviour is followed by the elastic modulus and the elastic modulus follows a power law of the form:

$$G' = \phi_s^n$$

- According to Liang et al. [1993] the differences in the structure between different HEC/particulate systems are shown in both the yield stress τ and the elastic modulus G' . The difference in structure is, however, clearer in the behaviour of G' than that for τ . This should be expected as G' is a more sensitive parameter to the changes in the flocculated structure than τ . While both G' and τ are related to the strength of the bonds, G' is predominantly determined by the number of particle bonds. On the other hand, τ is dictated both by the strength and the number of bonds and is consequently less sensitive to the flocculated structure.
- The dependence of G' on the molecular weight of the HEC was also examined. Increasing values for G' in the LVER were observed for increases in the molecular weight of the HEC and vice versa.
- At high solids content and high HEC concentrations, the response of the system becomes predominantly elastic at low frequencies. HEC causes the formation of 'topological restraints' comprised of chains of particles.
- It was found that at low strains G' and G'' are independent of the amplitude of oscillation up to a critical strain γ_c . At amplitudes above the critical strain, both G' and G'' are amplitude dependent, with G' decreasing monotonically and, at high HEC concentrations, G'' going through a maximum.
- For steady-state shear, non-Newtonian behaviour is noted and a Sisko type model for shear-thinning behaviour can adequately describe the data. The frequency-dependent viscosity can be defined as:

$$|\eta^*| = \frac{\sqrt{G' + G''}}{\omega}$$

Another study performed by Liang et al. [1993] also examined concentrated sterically stabilised latex dispersions in the presence of HEC. He found the following rheological behaviour, amongst others:

- The effect of HEC on the viscoelastic properties of a polystyrene latex dispersion was investigated using steady-state and oscillatory techniques. The storage modulus G' was measured as a function of the volume fraction of the latex, volume fraction of the polymer and particle size. The results showed an increase in the G' with increase in volume fraction of the polymer as expected. However, G' increased with increase in particle size, which was opposite to what was found previously. It was also found that the molecular weight of the HEC did not significantly affect the dependence of G' on the volume fraction of the latex.

These observations by Kiratzis et al. [1998] and Liang et al. [1993] will be used as guidelines when investigating the effect of HEC on the rheology of the vesiculated beads, keeping in mind that the latexes were different from the vesiculated beads dispersion.

In the same manner Nommensen et al. [1999] examined the properties of polymerically stabilised suspensions by a polymer layer on the surface of the suspended particles. Therefore, his work closely resembles the polymerically stabilised vesiculated beads by means of PVOH. With the aid of a model, the so called 'lubrication model', he related the elastic properties of the suspension to the polymer fraction. This 'lubrication model' will be used as a model that can provide a possible rheological explanation regarding the effect of different levels of PVOH on the rheology of the vesiculated beads.

2.5 Dispersion Rheology and Stability of a Dispersion

Many of the substances used in the coatings industry can be classified as dispersions. Therefore, some sort of relation can be drawn between the rheology of paint and the rheology of dispersions. Another advantage is that there is a great deal of literature available regarding dispersion rheology;

however, due to this fact one must also be very specific in obtaining literature that is applicable to the present study. Literature that was thought to be applicable to this study is discussed below.

- The rheology of sterically stabilised dispersions and lattices were examined by Mewis et al. [2000]. Data sets are used to predict properties such as viscosity, yield stress, shear-thickening and viscoelastic behaviour. The procedures presented by Mewis et al. [2000] can be used qualitatively to predict the viscosity of the vesiculated beads dispersion.

Characterisation of concentrated suspensions was found to be very difficult due to the vast range of the possible parameters governing the suspension. The challenges on characterisation of concentrated suspensions were examined by Chander [1997]. The success in obtaining the desired stability and rheology of suspensions depends on the ability to predict correctly the system response from characteristics of the particles and the suspending medium. Behaviour of concentrated suspensions was predicted by Chander [1997] by relating rheological properties measured in diluted suspensions. He examined the following parameters for characterising a system of dispersed particles:

Table 2-1: Parameters for characterising a system of dispersed particles

Disperse phase properties:	Size distribution Particle shape Density Surface energy Homogeneity
Continuous phase:	Aqueous Non-aqueous Dissolved substances
Interfacial properties:	Electric double-layer Zeta potential Adsorption density Packing of molecules in the adsorbed layer Thickness of adsorbed layer
Colloid properties:	Percent solids Stability

Methods of characterising stability of concentrated dispersions have not been standardised and there is a large variation in techniques and methodology. In general, rheological properties of concentrated suspensions vary considerably due to:

- Hard sphere interaction;
- Double-layer repulsion;
- Sterical stabilisation;
- Weakly or strongly flocculated suspensions;
- History of dispersion;
- Wide distribution of particle sizes;
- Slip near the walls during measurements.

The rheological behaviour of concentrated suspensions is already relatively complex as it is and according to Gupta [2000] becomes even more complex if the liquid phase is non-Newtonian, which it is for the vesiculated beads dispersion. It can therefore be seen that rheological characterisation of the vesiculated beads dispersion is considered to be a daunting task, not yet undertaken by anyone. Therefore, existing literature that dealt with material closely resembling the vesiculated beads dispersion is of great importance.

It was found that Liang et al. [1992] had performed extensive studies on very similar concentrated suspensions. Liang et al. [1992] performed rheological studies on concentrated polystyrene latexes, sterically stabilised by poly(ethylene oxide) chains. The complex modulus G^* , the storage modulus G' and the loss modulus G'' were obtained as a function of frequency at various latex volume fractions. Results indicated that the dispersion changed from being more viscous ($G'' > G'$) to more elastic ($G' > G''$) over a narrow range of volume fractions of the particles. Increasing the solid particle volume fraction increased the elastic modulus by several orders of magnitude as did the dynamic viscosity. Under these conditions, the latex dispersion behaves as an elastic gel which can be fitted by a power-law equation $G' = k\phi^m$ where m is related to the compressibility of particles.

Furthermore, Liang et al [1992] also found that the smaller particles had considerably higher G' values than the larger ones. It was also found that increasing the polymer volume fraction results in a plateau value for G' , whereas the Bingham yield stress values increased continuously. This was

found to be related to the increase of the polymer volume fraction, while the storage modulus is a measure of the number of bonds formed in the flocculated structure.

Stability of a Dispersion

The sedimentation stability is a very significant aspect for the evaluation of dispersions. Long-term storability as well as closed-circuit stability in pipelines is required over days, weeks or even months. Mezger [1999] suggested three different test methods for investigating the stability of a dispersion. These tests are as follows:

1. **Yield Point:** The more strongly a network of a substance is developed, the lower is the sedimentation tendency of particles. The more strongly the solid particles are embedded into the superstructure, the higher is their yield point.
2. **Storage modulus G' :** The storage modulus stands for the stability of the dispersion and thus characterises the internal structural forces. A higher structural strength at rest, which is measured under minimum load in the LVER, provides improved particle compound and counteracts a phase separation. The increased stiffness of the superstructure avoids sedimentation processes and is indicated through higher G' values. To judge the sedimentation behaviour, the values occurring at low loads should be applied, i.e. for the amplitude sweep at minimum deformation and for the frequency sweep at low frequencies.

Mezger [2002] also states that G' and G'' curves run parallel to each other in the frequency sweep, showing little slope for stable dispersions and that a relatively constant structural strength can be found through the full frequency range.

3. **Zero-shear viscosity:** The zero-shear viscosity can be determined provided that the disperse character is not predominant. The zero-shear viscosity can be determined by flow curves but more precisely by looking at the lowest frequencies of the frequency sweep. The higher the zero-shear viscosity, the higher is the resistance against sedimentation.

2.6 Paint Rheology

Apart from literature given for the interpretation of rheological curves in general (see section 2.3 – Data Interpretation), there is also detailed literature on interpretation of rheological properties specifically for coatings.

Typical shear rates in the coatings industry, according to Mezger [1999], are given in Table 2-2 below.

Table 2-2: Typical shear rates in the coatings industry

Process	Shear Rate [s^{-1}]
Sedimentation of particles:	10^{-6} to 10^{-2}
Surface levelling:	10^{-2} to 10^{-1}
Sagging:	10^{-2} to 10^{-1}
Immersing:	10^0 to 10^2
Pipe flow, pumping:	10^0 to 10^3
Mixing, stirring:	10^1 to 10^3
Filling into containers:	10^2 to 10^4
Painting, brushing, spreading:	10^2 to 10^4
Rolling, printing:	10^2 to 10^6
Spraying, knife-coating:	10^2 to 10^6

Table 2-2 shows that typical shear rates in the coatings industry range from $10^{-6} s^{-1}$ to $10^6 s^{-1}$. The following are some of the more important shear-related processes [Mezger, 1999]:

1. At very low shear rates:
 - Dispersion stability (separation and sedimentation behaviour) and long-term storage stability;
 - Time-dependent behaviour directly after application, e.g. levelling, sagging and layer thickness.

2. At medium shear rates:

- Workability, which is an indication of the flow behaviour during mixing, stirring, pouring, etc.

3. At high shear rates:

- Application behaviour.

2.6.1 Flow and Viscosity Curves

Coatings have complex structures and therefore complex flow behaviour; they cannot be described by only one viscosity value, because most coatings show pseudoplastic behaviour (see Figure 2-7).

Furthermore, Mezger [1999] stated that investigation of *only* the viscosity curves is not sufficient to obtain information on properties such as sagging and levelling behaviour.

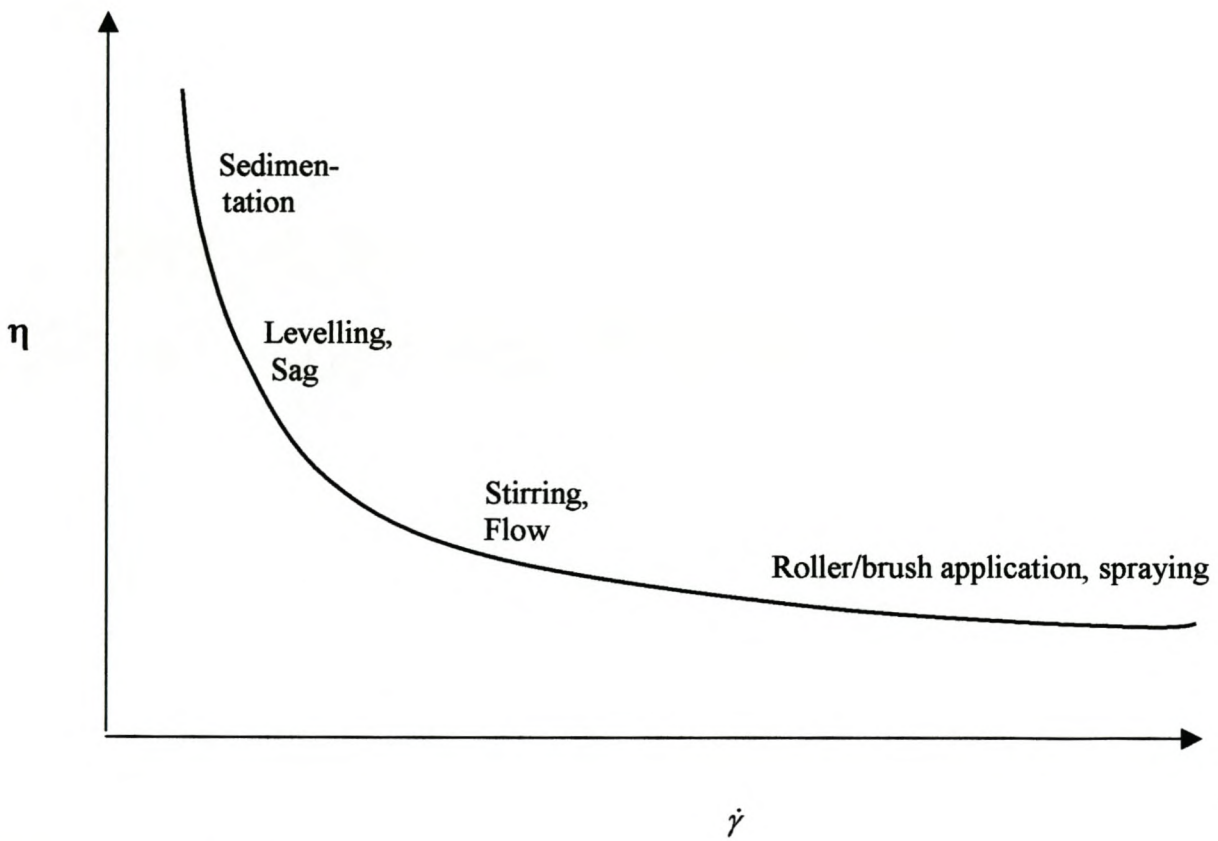


Figure2-7: A typical viscosity profile for a coating [Prideaux, 1993]

2.6.2 Amplitude Sweeps

The importance of the amplitude sweeps in the coatings industry was examined by Eidam [1997] and Mezger [1999].

- Eidam [1997] described how the amplitude sweeps can be used as a better test method than a flow curve to determine the yield points of paints. They are defined as being the limits of the LVER. For this G' and G'' were measured. The yield point was determined as the measuring point at which the first point of one of the curves deviated from the constant plateau value. A sample with $G'' > G'$ in the LVER displays no yield point relevant for coatings.
- Mezger [1999] examined the character and stability under low-shear conditions by means of the LVER of the amplitude sweep. The structural strength of the paint is examined in terms of the storage modulus G' .

2.6.3 Frequency Sweeps

Mezger [1999] used the frequency sweep to indicate whether paints are likely to sediment. The behaviour of the G' and G'' curves in the low-frequency range (long time-scale behaviour) gives information on possible sedimentation behaviour. According to Mezger [1999], a paint will sedimentate when $G'' > G'$ in the low-frequency range of the frequency sweep. The shape of the G' and G'' curves gives information about the stability of the paint – G' and G'' curves that run parallel to each other with only a slight slope are usually stable over the whole frequency range.

Wollny [2002] stated that the behaviour of the G' and G'' curves in the high-frequency range (short time-scale behaviour) can be used to determine the spatter behaviour of a paint – a paint is likely to spatter when $G'' > G'$ in the high-frequency range of the frequency sweep.

2.6.4 Three-Interval-Thixotropy-Test (3-ITT)

According to Mezger [1999], thixotropic behaviour in rheological terms mean both characterising the decrease of the structural strength under a shear load *and* the increase of the structural strength of the unloaded sample afterwards. Historically, different test methods were used to measure thixotropy, e.g. measuring the thixotropic value (TV) or the hysteresis area (HA), but these methods only characterise the structural decomposition under a shear load, but not the more important structural recovery after the shear load.

Mezger [1999] examined a test method that realistically simulated the application process by three test intervals. The intervals are as follows:

1. Low-shearing: Determination of the structure at rest as the initial state before application;
2. High-shearing: Destruction of paint structure (simulates application of paint);
3. Low-shearing: Determination of the structural regeneration over time after application.

Input data for the test method are given in Figure 2-8 below.

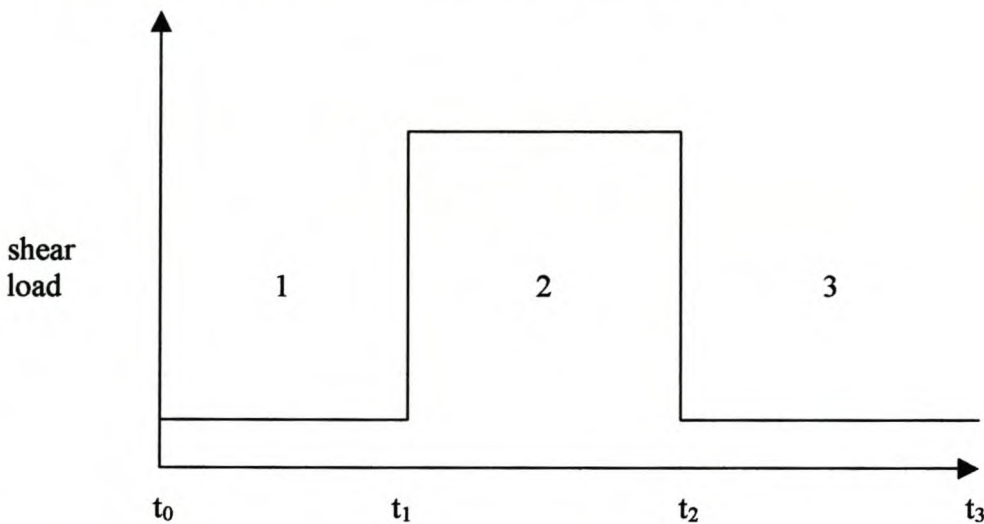


Figure 2-8: Test method for determining structural recovery after high shear

Mezger [1999] remarked that using the following modes (rotational or oscillatory) resulted in simulating the application process most accurately:

1. Low shearing – oscillatory mode (interval 1 and 3 in Figure 2-8);
2. High shearing – rotational mode (interval 2 in Figure 2-8).

The advantage of performing the 3-ITT in the combined mode (oscillation and rotational) is that the oscillatory test gives two parameters, G' and G'' . Therefore more information about the character of a sample can be obtained by using two parameters in the oscillatory mode rather than only one parameter (viscosity) in the rotational mode.

The combined test method also has further advantages. Since even very small rotational speeds lead to higher deformations compared to the limited deformation with a LVER oscillatory test, the combination of oscillation and rotation in one experiment has the advantage that during the rest interval quasi-zero shear conditions can be simulated better by using oscillatory tests in the LVER than by using rotational tests. On the other hand, high-shear conditions can be simulated in a better way with rotational tests rather than with oscillatory tests.

The practical implications of the test are as follows [Mezger, 1999]:

- If a crossover-point exists ($G''=G'$) in the third interval, it is important to know the time until the cross-over point. If $G' > G''$ in the first interval and $G'' > G'$ in the third interval, then the cross-over point indicates the transition point between the liquid- and solid-like character. Examining the liquid- and solid-like character of the paint after the high shear is important in explaining the levelling and sagging behaviour of the paint.
- As long as $G'' > G'$, the coating shows a liquid-like character and:
 - can flow under its own gravity to fill hollow spaces;
 - can flow after application and therefore prevents brush marks;
 - allows for degassing of the film;
 - orientation of solid particles;
 - can lead to undesired sagging behaviour.
- When $G' > G''$, the sample has solid-like character and:
 - sagging of paint is limited;
 - ensures desired layer thickness;
 - prevents demixing of components of the paint.

- Structural recovery that takes place too fast leads to poor levelling, whereas a too slow recovery causes sagging of the paint and thus, as a consequence, an insufficient layer thickness [Mezger, 1999].

(See Appendix C – Glossary of rheological terms for definitions of sagging, levelling, etc.).

Cohu et al. [1994] examined the levelling of thixotropic coatings by means of the 3-ITT. Rheological measurements showed that the rheology of non-evaporative coatings can be described fully by using the five parameters that were used in the computation of the levelling viscosity. These five parameters are the following:

1. Infinite shear-rate viscosity, η_{∞}
2. Yield stress, τ_y
3. Power-law index, n
4. Rate of recovery, ξ
5. Rate of recovery power-law index, β .

It was shown that the steady-state viscosity of the fluid is irrelevant in the description of the levelling behaviour.

2.7 Rheology Modifiers

In order to obtain the proper viscosity to maintain the suspension of pigments in the paint and to provide improved application characteristics, water-based paints normally require the addition of thickener to adjust their viscosity characteristics [Karickhoff, 1984].

In the paper of Kastner [2001] a short review is given of the thickening mechanisms of three main groups of rheology modifiers, i.e. cellulose, acrylics and urethanes. These rheology modifiers act by means of hydrophilic or hydrophobic groups (or both). Measurements on two coatings are presented. The results indicate several factors which influence the coatings rheology and performance. According to Kastner [2001], HEC and alkali swellable emulsions (ASE thickeners) are the best modifiers for dispersion paints for indoor or outdoor application when flow and

levelling are not very important. For higher-performance coatings flow and levelling become more important and hydrophobically modified ethylene urethane rheology modifiers and hydrophobically modified alkali swellable emulsions (HEUR and HASE respectively) are effective rheological additives. Often the combination of HEUR with cellulose derivatives will combine the advantages of both systems. The effect of the rheology modifiers is investigated by looking mainly at the viscosity curves and the thixotropy of the water-borne coatings.

Rohm and Haas® supplied data sheets with all their rheology modifiers. According to the data sheets, the rheology modifiers used have the following advantages:

1. Acrysol ASE-60:
 - Outstanding in-can stability;
 - Resistance to syneresis (phase separation);
 - Good application properties;
 - Good paint stability and consistency.

2. Acrysol RM-5:
 - Good high-shear viscosity;
 - Excellent spatter resistance;
 - Superior film build;
 - Excellent flow and levelling.

3. Acrysol RM-2020:
 - Excellent film build;
 - Excellent flow and levelling.

4. Acrysol RM-8W:
 - Excellent spatter resistance.

Rheology modifiers are used to improve various aspects of the flow and deformation behaviour of coatings. Prideaux [1993] studied the properties that rheology modifiers wish to optimise. They are:

- Flow;
- Structure;
- Sag resistance;
- Spatter resistance;
- Film build;
- Brush drag;
- Brush loading.

Thorp [1993] also studied the effect of rheology modifiers on spatter, application rheology, and levelling and sagging behaviour. Rheology modifiers are formulated by manipulation of the chemical structure. Prideaux [1993] examined the chemistry of HEUR and HASE rheology modifiers and their interaction with other paint components in detail. A comparison is also drawn between properties of ASE, HASE and HEUR rheology modifiers with regards to:

- Formulating cost;
- Film properties;
- Microbial attack;
- Environmental aspect;
- Exterior durability;
- Ease of incorporation;
- Ease of handling.

Prideaux [1993] concluded that an understanding of the associative interactions that occur is necessary to control the viscosity over a wide shear-rate range. By careful choice of product type and grade, a correct balance of properties can be achieved cost effectively in almost every formulation type.

The behaviour of rheology modifiers in the presence of other chemical agents was examined by Kraus et al. [1998] and Knoef et al [1992] in the following manner:

- Kraus et al. [1998] states that instability in latex paints can be caused by interactions between dispersants and associative thickeners. Generally speaking, HEUR rheology modifiers function best with acid copolymer dispersants and HASE rheology modifiers with poly-acid dispersants. This paper discusses the chemistry of the rheology modifiers and

explains the interactions with other components in paint so that formulation can be made easier.

- Knoef et al. [1992] examines a qualitative model for the thickening action of urethane polymeric thickeners. The model is based on the formation of micelles and the bridging between micelles of urethane polymeric thickeners. The fundamental rheological characteristics of the thickeners are discussed in terms of their effect on paint rheology. Interactions with other components used in paint such as surfactants and solvent are discussed. Behaviour of the paint during application and the influence of the urethane thickener on several paint film properties are also discussed. A prediction for the optimum paint rheology with the urethane polymeric thickeners and surfactant is given.

The study done by Murakami et al. [1995] is of great importance in this specific study, because it addressed the influence of HASE rheology modifiers on the rheology profiles of coating formulations containing conventional all-acrylic binders. All HASE thickeners provide viscosities at high shear rates that are higher than observed with the HEC thickener, while at lower shear rates there are distinct differences among HASE and HEUR thickeners. It is an important study due to the fact that the effect of rheology modifiers on paint was investigated by using an all-acrylic paint, PE-free paint, with the all-acrylic binder AE-748.

2.8 Modelling

Existing models can be used to model the flow and viscosity behaviour of coatings (and the flow behaviour of the raw materials of coatings such as vesiculated beads). These existing models were reviewed by Mezger [2002]. The following were existing models reviewed by him:

- Ostwald de Waal;
- Bingham;
- Casson;
- Herschel-Bulkley;
- Cross;
- Philips-Deutsch.

As can be seen, there are a number of models, but not every model can be used for every kind of flow behaviour. Therefore Mezger [2002] also indicated which models are best to fit specific types of flow behaviour.

Modelling can also be performed on certain rheological characteristics other than the flow and viscosity behaviour of a substance. These models are regression models and are used to predict a specific property.

Details on the different models are included in the chapter on modelling (chapter 8).

CHAPTER 3 Experimental

3.1 Test Instrumentation

Tests are carried out by means of a rheometer. One distinguishes between a rheometer and a viscometer in the following way:

According to Ferguson et al [1991], the name *rheometer* itself implies that something more is measured than a mere measurement of viscosity, while a *viscometer* measures only the viscosity of the test sample. A *rheometer* could be seen as an instrument that will provide quantitative data on the rheology of a fluid.

3.1.1 Rheometer

The rheometer used for most of the tests is the Physica MCR 300 (Modular Compact Rheometer). The technical specifications are given in the table below.

Table 3-1: Technical specifications of MCR 300

Specifications	MCR 300
Bearing type:	Air bearing
Minimum torque [μ Nm]:	0.02
Maximum torque [mNm]:	150
Torque resolution [μ Nm]:	< 0.001
Normal force range [N]:	0.01 to 50
Normal force resolution [N]:	0.001
Axial force [N]:	0.01 to 50
Speed range [1/min]:	10^{-5} to 3000
Frequency range [Hz]:	10^{-4} to 100
Angular resolution [μ rad]:	< 0.01
Temperature range [$^{\circ}$ C]:	-30 to 150
Dimensions [mm]:	530*335*405
Weight [kg]:	45

The rheometer is capable of performing tests in the rotational mode as well as the oscillatory mode. Temperature control is carried out by means of a TEK 150P temperature control unit which can operate in the range mentioned above. Its heating and cooling rate is 13° C per minute, with tap water used as counter cooling for the Peltier. A Peltier is a small solid-state device that functions as

a heat pump by means of a DC current passing through two ceramic plates. An illustration of the Physica MCR 300 is given below.



Figure 3-1: Photo of Physica MCR 300 (Modular Compact Rheometer) with power supply unit

This type of rheometer is ideal for testing samples in the coating industry. A fast controlling rheometer with a highly dynamic measuring drive is required for structural recovery tests in order to obtain a result coming close to reality, since the jumps between the different speeds have to be performed very rapidly [Mezger, 1999].

3.1.2 Measuring Systems

Different measuring systems exist. The nature of the sample and the type of test determine the ideal measuring system. The measuring system used in the rheometer can be seen in the photo below. It fits into the rotating part of the rheometer by means of a high-precision coupling system, which makes cleaning of the bob between tests very easy.

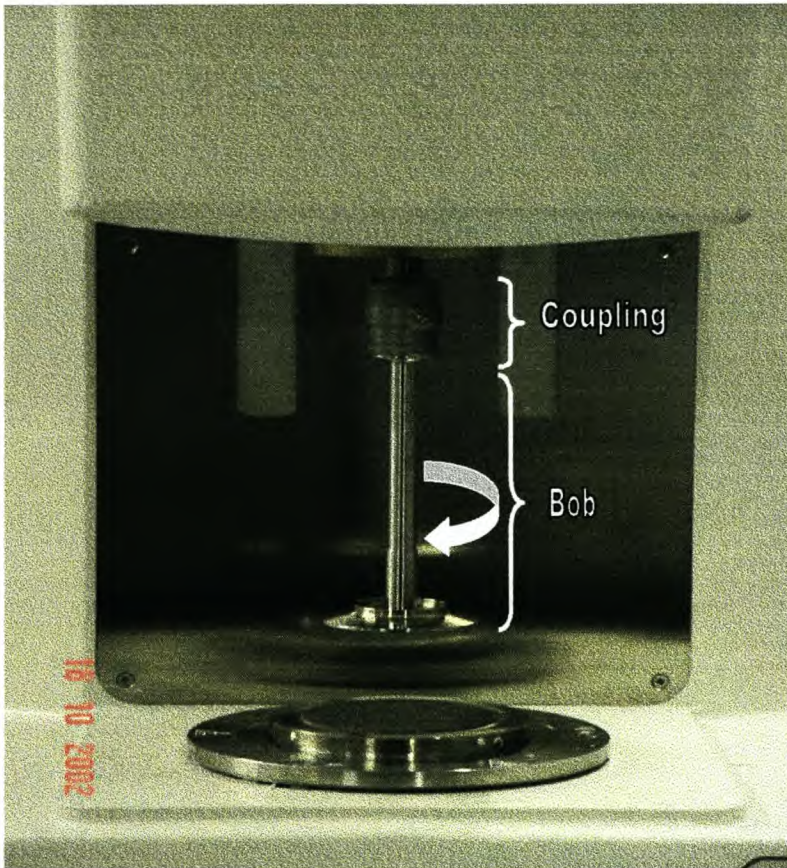


Figure 3-2: Photo of measuring system

The plate can be seen below the bob in Figure 3-2.

The measuring systems available, along with their advantages and disadvantages, are given below.

3.1.2.1 Cone-and-Plate Measuring Systems

This measuring system consists of a bob with a conical surface and a fixed plate with a flat surface. An illustration of the cone and plate measuring system is given in Figure 3-3.

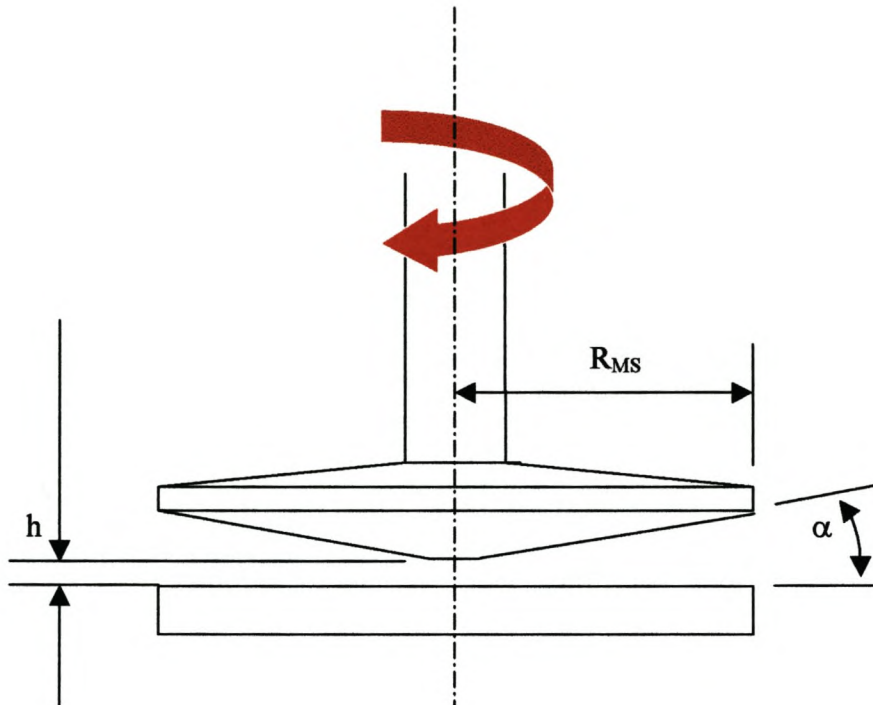


Figure 3-3: The cone-and-plate measuring system

The geometrical dimensions of importance are the cone radius R_{MS} , the cone angle α and the cone tip truncation, h .

- Cone radius $R_{MS} = 25 \text{ mm}$
- Cone angle $\alpha = 1^\circ$
- Cone tip truncation $h = 50 \text{ }\mu\text{m}$.

The cone tip is truncated in order to:

- Prevent abrasion on the surfaces of the cone and the plate;
- Prevent friction between the cone and the plate;
- Make it possible to measure samples with small-sized particles.

The following rule of thumb is given for samples with small particles:

It is recommended that $d_{max} \leq h/5$

Advantages and disadvantages are given below.

Advantages:

- Homogenous shear conditions exist because the shear rate is constant in the entire conical gap. Therefore, if possible, it is advantageous to carry out most of the tests with the cone-and-plate measuring system.
- A very small amount of the sample is required.
- Most of the air bubbles are pressed out of the conical shear gap before the test starts.
- Cleaning is very easy.

Disadvantages:

- The particle size is limited for dispersions
- The following can happen at the edge of the upper plate:
 - Emptying of the gap;
 - Flowing of and spreading of the sample;
 - Evaporation of solvents (can be reduced with solvent trap and a cover such as low-viscous silicon oil);
 - Skin formation.

3.1.2.2 Parallel-Plate Measuring System

The parallel-plate measuring system consists of two plates. An illustration of the plate-and-plate measuring system is given in Figure 3-4.

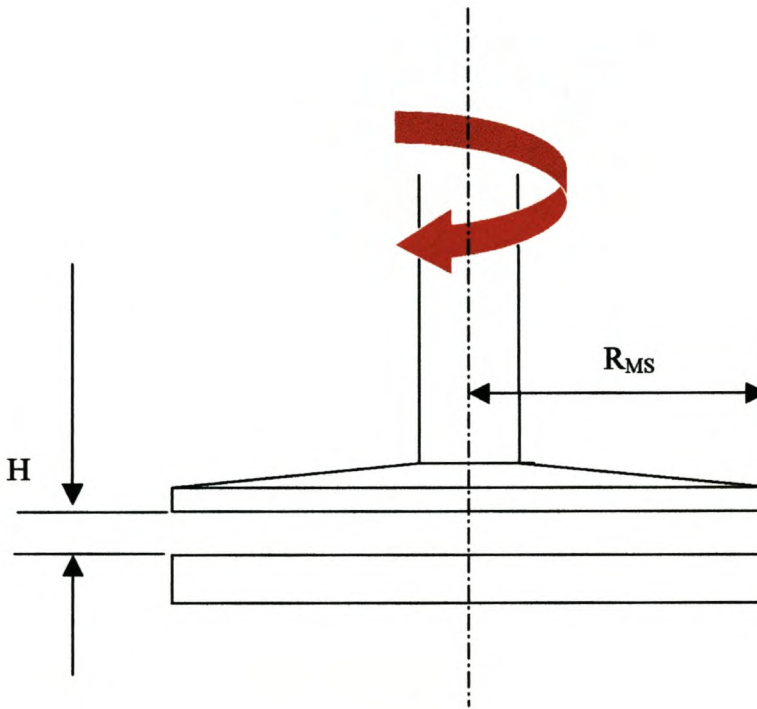


Figure 3-4: Plate-and-plate measuring system

The geometry of the plate is determined by the plate radius and the following rule of thumb should be adhered to [Mezger, 2002]:

The distance between the two parallel plates must be $H \ll R_{MS}$ with $H \leq 1\% R_{MS}$.

Therefore with plate radius of $R_{MS} = 25$ mm, it is safe to operate at gaps of 250 μ m.

This rule of thumb is especially important for rotational tests, where the sample flows nonhomogeneously across the entire gap. Therefore, if possible, the plate-and-plate measuring

system should be used only when performing oscillatory tests within the LVER, where the samples are deformed homogeneously throughout the entire gap.

It should be stated clearly that the shear rate value is not constant in the parallel plate system. Therefore, references to the shear rate used during measurements will refer to the shear rate at the edge of the plate, where it is the highest.

Once again the following rule of thumb is given for samples with small particles:

It is recommended that $d_{max} \leq H/5$

Advantages and disadvantages are given below.

Advantages:

- It is possible to measure dispersions with relatively large particles.

Disadvantages:

- There is no constant shear gradient in the gap, because the shear rate increases in value from zero at the centre of the plate to the maximum at the edge.
- The following can happen at the edge of the upper plate:
 - Emptying of the gap;
 - Flowing of and spreading of the sample;
 - Evaporation of solvents (can be reduced with solvent trap and a cover such as low-viscous silicon oil).
- Skin formation.

3.2 Test Types

The rheometer is able to perform rotational and oscillatory tests.

3.2.1 Rotational Tests

Two basic alternatives are available in the rotational mode.

3.2.1.1 Controlled Shear-Rate Tests (CSR)

The shear rate is set and controlled and the shear stress is measured. This test method is selected when specific shear rates have to be simulated, e.g. sedimentation of particles, surface levelling of coating, sagging of a coating on a vertical wall, flow in pipes, roller/brush application of paint, etc.

- The CSR test type is used to determine the flow and viscosity curves. Flow curves are the data obtained from rotational tests with the shear stress (τ) on the y-axis and the shear rate ($\dot{\gamma}$) on the x-axis. Viscosity curves are plotted with the viscosity (η) on the y-axis and the shear rate ($\dot{\gamma}$) on the x-axis.
- The CSR test type is also used to determine the viscosity/time curve at a constant shear rate. The result is the viscosity as a function of time, $\eta = f(t)$.

The following parameters must be considered when presetting the test method when a test is performed in the CSR mode:

- Shear rate profile: ramp, linear or constant;
- Data point profile: ramp or linear (usually the same as the shear rate profile);
- Min/max shear rate (depending on measuring system);
- Total test duration;
- Time duration for collecting data point;
- Temperature control.

The time duration for collecting the data points is very important, especially when measuring at low shear rates (e.g. $\dot{\gamma} < 1 \text{ s}^{-1}$). It is important to ensure that the measuring point duration is long enough to measure the steady-state viscosity and not the transient viscosity.

3.2.1.2 Controlled Shear-Stress Tests (CSS)

The shear stress is set and controlled and the shear rate determined. In nature all flow processes are shear-stress controlled and therefore the CSS test type is useful to test fluids that act under natural forces such as the sagging behaviour of paint under gravity. And therefore the CSS test type is also a classic method for the determination of the apparent yield point. The CSS test method is also used to determine:

- The flow curves, $\dot{\gamma} = f(\tau)$ and viscosity curves $\eta = f(\tau)$
- The viscosity/time curve, $\eta = f(t)$.

Once again, the same parameters as mentioned in section 3.2.1.1 must be considered when presetting the test method.

3.2.2 Oscillatory Tests

The substance to be measured is exposed to an oscillation frequency. The oscillations are mostly performed at very low shear loads in order not to destroy the internal structure of the sample while the test is running. Oscillatory tests are used to determine the viscoelastic behaviour of samples by means of a frequency-dependent, controlled sinusoidal strain/stress function.

The oscillatory tests can be preset as strain in terms of the sine function:

$$\text{i. } \gamma(t) = \gamma_A \sin(\omega t) \tag{3-1}$$

or as stress as the sine function:

$$\text{ii. } \tau(t) = \tau_A \sin(\omega t) \tag{3-2}$$

These preset functions result in the following measurements:

iii. $\gamma(t) = \gamma_A \sin(\omega t + \delta)$ (3-3)

or in terms of stress values:

iv. $\tau(t) = \tau_A \sin(\omega t + \delta)$ (3-4)

In equations 3.3 and 3.4 the phase shift angle, δ ($^\circ$), is the difference between the preset and the measuring values. Therefore, for an ideally elastic fluid, $\delta = 0^\circ$ (in-phase) and for an ideally viscous fluid, $\delta = 90^\circ$ (out-of-phase).

CHAPTER 4 Rheological Properties of Vesiculated Beads

4.1 Background

Vesiculated beads (Figure 4-1) are used, in addition to titanium dioxide (TiO_2), as cost effective opacifiers for latex paints to increase the amount of light scattered by microvoids, thereby achieving the required level of opacity. The vesiculated beads have been commercially available under the trademark Spindrifit® [Ritchie, 1993]. The Spindrifit process was developed by Dulux Australia in the 1970s and fully commercialised in the 1980s. The vesiculated beads are currently also being manufactured by Plascon South Africa. The vesiculated beads are spherical polymer beads (polyester cross-linked with styrene) that contain stable microvoids and encapsulated TiO_2 dispersed within them, produced as a slurry in water and therefore convenient to be used in water-borne paints. The vesiculated beads are currently manufactured by means of three different processes:

- the Cowles reactor;
- the emulsion reactor;
- the homogenisation process.

About two-thirds of the beads are air by volume and therefore cost less compared to the equivalent volumes of TiO_2 , resulting in a reduced formula cost. Savings are generally in the order of 10-20% on the raw material cost per litre [Ritchie, 1993]. A reduction in paint weight per litre is also a benefit.

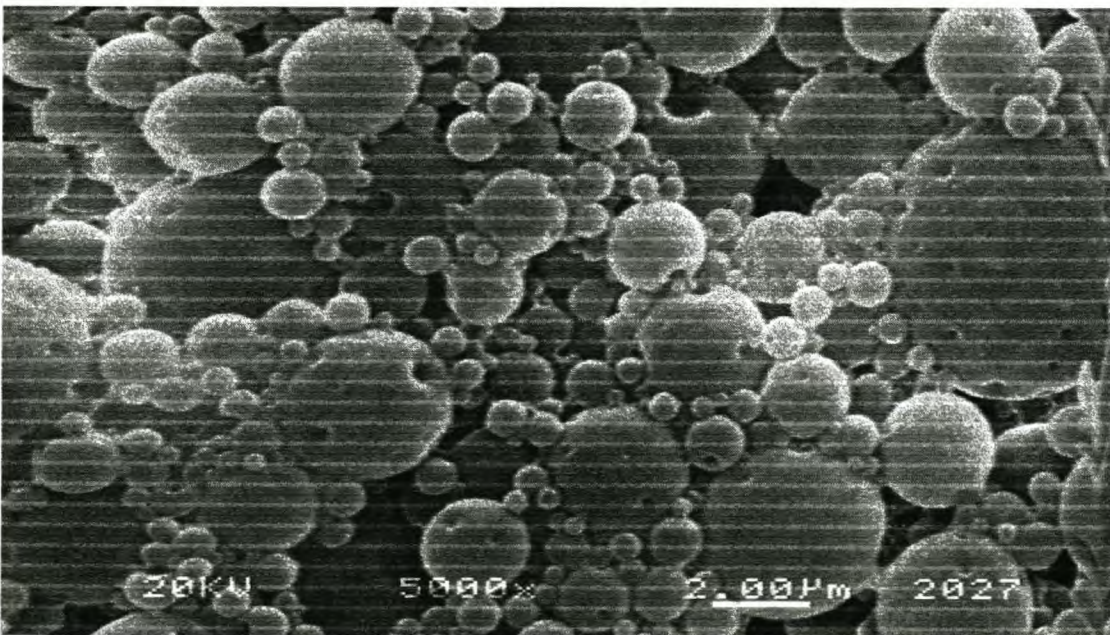


Figure 4-1: A SEM photograph of the vesiculated beads (× 5000 times)

The vesiculated beads dispersion is considered to have a complex structure, as there are many parameters that influence the characterisation. Some paints, e.g. PE-free (Pigment and Extender free) paints (see Chapter 5), are formulated with up to 75% of the vesiculated beads as raw material.

Due to the complex structure of the vesiculated beads and the large amounts used in coatings, it is essential to understand the rheology of the vesiculated beads, as a raw material, in order to be able to develop predictive strategies for stability of the final coating.

4.2 Chemical and Physical Composition of the Vesiculated Beads Dispersion

Before attempting to examine the rheological behaviour of the vesiculated beads dispersion, the chemical and physical composition need to be well understood so that rheology can be used successfully as a method to explain the flow and deformation behaviour.

The vesiculated beads dispersion typically has the following composition [Gous, 2002]:

Table 4-1: Chemical and physical composition of the vesiculated beads dispersion

Material name	Percentage [%]
Water:	74.54
Polyester:	14.67
Styrene:	6.39
Polyvinyl alcohol (PVOH):	1.39
Hydroxy ethyl cellulose (HEC):	0.26
Titanium dioxide (TiO ₂):	0.84
Cumene hydroperoxide (CHP):	0.12
Diethylene triamine (DETA):	0.27
Ferrous sulfate (FeSO ₄):	0.01
Acticide 14:	0.17
Disponil SUS 87:	0.85
Tween 80:	0.50
Physical character	
Solids [%]:	24 – 28
Particle size ¹ [micron]:	1 – 30
Density [kg/m ³]:	~ 1000
Viscosity ² [Pa.s]:	0.1 – 1000 (shear thinning)

¹ Process sensitive

² Determined by means of MCR 300 rheometer (T=25°C)

The vesiculated beads dispersion can be viewed as two basic parts with different physical characteristics - the one part which is the hard, undeformable polymer latex consisting mainly of a cross-linked polymer (polyester) with a copolymerised monomer (styrene); and the other part, which is the aqueous phase with thickening and dispersing agents consisting mainly of PVOH, HEC and water. Elastic (solid-like) and viscous (liquid-like) properties are therefore present, which affects the rheological behaviour.

A suspension with a solid content as high as in the case of the vesiculated beads dispersion (24% – 28%) is considered to be a concentrated suspension. The effective solids concentration is even higher because of the water trapped within the vesicles of the beads. The following definition is given for a concentrated suspension by Tadros [1986]:

Concentrated suspensions are suspensions where particle interactions are many-body in nature and the translational motion of the particles is restricted.

Chander [1997] reviews the challenges in characterisation of concentrated suspensions and states that the stability of concentrated suspensions depends on the ability to predict correctly the system response from characteristics of the solids and the suspending medium.

The following physical properties of the vesiculated beads will also affect the rheological measurements:

- Particle-particle interaction;
- Sterical stabilisation;
- Degree of flocculation;
- Particle size distribution;
- Slip near the walls during measurements.

Therefore, due to the complex structure of the vesiculated beads dispersion, rheological characterisation is very difficult.

4.3 Manufacturing Processes for Vesiculated Beads

As mentioned in section 4.1, vesiculated beads are currently manufactured by means of three different processes:

- The Cowles reactor;
- The emulsion reactor;
- The homogeniser.

In each of these processes the shear rates differ significantly due to the difference in degree of agitation, which is considered to have an effect on the final product.

The effect of the shear rate during the manufacturing process of the vesiculated beads has been examined briefly by Gunning [1975]. He observed that the rate of agitation is critical and plays an important role in the final product. He defines a critical shear rate as *the maximum shear rate which will not cause any significant irreversible formation or agglomeration of two or more particles in a dispersion*. It was also observed that the shear rate is characteristic of the particular equipment used for the manufacturing purposes and, at higher shear rates than the critical shear rate, distorted clusters of granules are formed.

4.3.1 The Emulsification Process in an Emulsion Reactor

The emulsification process makes use of the impeller illustrated in Figure 4.2. Three of these four-bladed, 45° pitched-blade-turbine (PBT) impellers are used on a single impeller axis.



Figure 4-2: PBT impeller blade for emulsification process

The equation given by Gray [1986] is used to determine the order of magnitude of shear rate that the impeller forces on the liquid medium. The average shear rate in the impeller zone is proportional to the rotational speed of the impeller.

$$\dot{\gamma}_{av} = K_I N \quad (4-1)$$

where $K_I \approx 12$ for open impellers and N for pitched-blade turbine impellers given as follows:

$$ND = \frac{Q_{eff}}{0.43} \left(\frac{T}{D} \right)^{3/2} \frac{1}{T^2} \quad (4-2)$$

with Q_{eff} the effective volumetric pumping rate from the impeller determined by:

$$Q_{eff} = N_Q ND^3 \quad (4-3)$$

and N_Q determined at a D/T ratio of 0.52 and the impeller Reynolds number given by the following equation:

$$N_{Re} = \frac{1480D^2NS_g}{\eta} \quad (4-4)$$

with S_g and η values taken as the specific gravity and the viscosity of water respectively. The pumping number is obtained from a graph that gives the pumping number, N_Q , as a function of impeller Reynolds number N_{Re} and D/T ratio [Gray, 1986].

Therefore, substituting the values for:

the impeller diameter, $D = 9.2$ cm,

the tank diameter, $T = 17.4$ cm,

the impeller rotating speed, $N = 350$ rpm,

and the pumping number, $N_Q = 0.6$ (determined from a figure given by Gray [1986])

into equations 4-1 to 4-3, the shear rate is estimated to be in the order of 100 s^{-1} .

4.3.2 The Cowles Process

The Cowles process makes use of the impeller blade illustrated in Figure 4.3. A single disc-turbine type of agitator is used to ensure radial mixing at high shear rates.

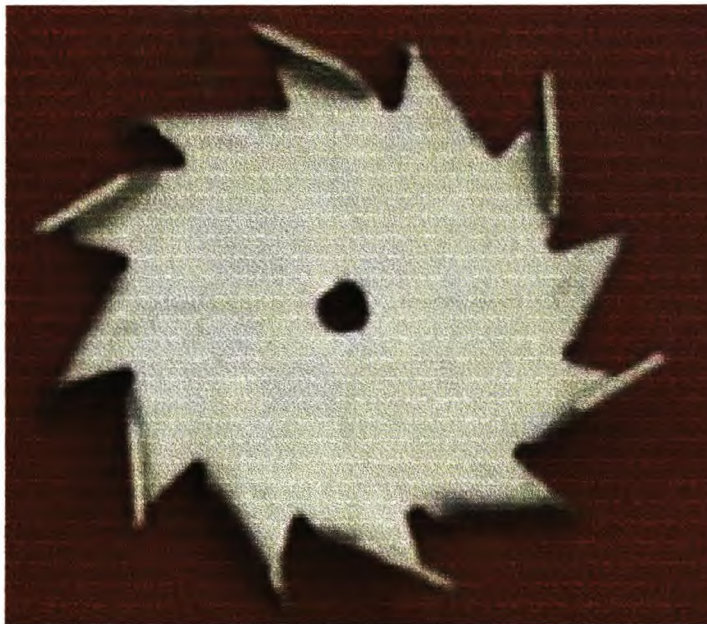


Figure 4-3: Disc turbine impeller blade for Cowles process

These types of impellers are used to enhance mixing in a radial direction due to high shear rates caused by a large surface area, as can be seen in Figure 4-3. No published literature for determining the shear rate induced by the Cowles type of disperser could be found. A report by Plascon

Research Centre [Various, 2001], however, states that '*the Cowles disperser has a higher mixing intensity than the impeller used for the emulsification process in the emulsification reactor*'; in other words, it has a higher effective volumetric pumping rate, Q_{eff} . It can therefore be assumed that the Cowles blade produces significantly higher shear rates than the emulsion reactor.

4.3.3 The Homogenisation Process

Flow through the homogeniser can be modelled as flow through a set of small circular tubes. The shear rate through a small circular tube is given by Chiu et al. [1998] as:

$$\dot{\gamma} = \frac{4Q}{\pi a^3} \quad (4-5)$$

and therefore the shear rates present in the homogeniser is estimated to be in the order of $5\,000\text{ s}^{-1}$.

It can therefore be concluded that there are large differences in the shear rates and that:

$$\dot{\gamma}_{\text{emulsion}} \ll \dot{\gamma}_{\text{cowles}} \ll \dot{\gamma}_{\text{homogeniser}}$$

4.3.4 Discussion of Results

The effect of the different shear rates during each process was examined by means of the rheology curves.

Samples for each of the processes were prepared with properties for particle size, particle size distribution and total solids percentage given in the table below.

Table 4-2: Physical properties of vesiculated beads samples

Process	Particle Size [μm]	Particle Size Distribution ³ [μm]	Percentage Solids [%]
Cowles:	3.12	1.78	23.87
Emulsion:	3.34	1.87	23.94
Homogeniser:	2.98	1.70	23.77

From Table 4-2 it can be seen that samples were prepared in such a manner that the physical properties were very similar and therefore did not play a major role in the differences in rheological properties. This ensures that only the effect of the amount of shear in each process is examined.

4.3.4.1 Viscosity Curves

The viscosity curves for the samples produced by each of the three different processes are given in Figure 4-4 below.

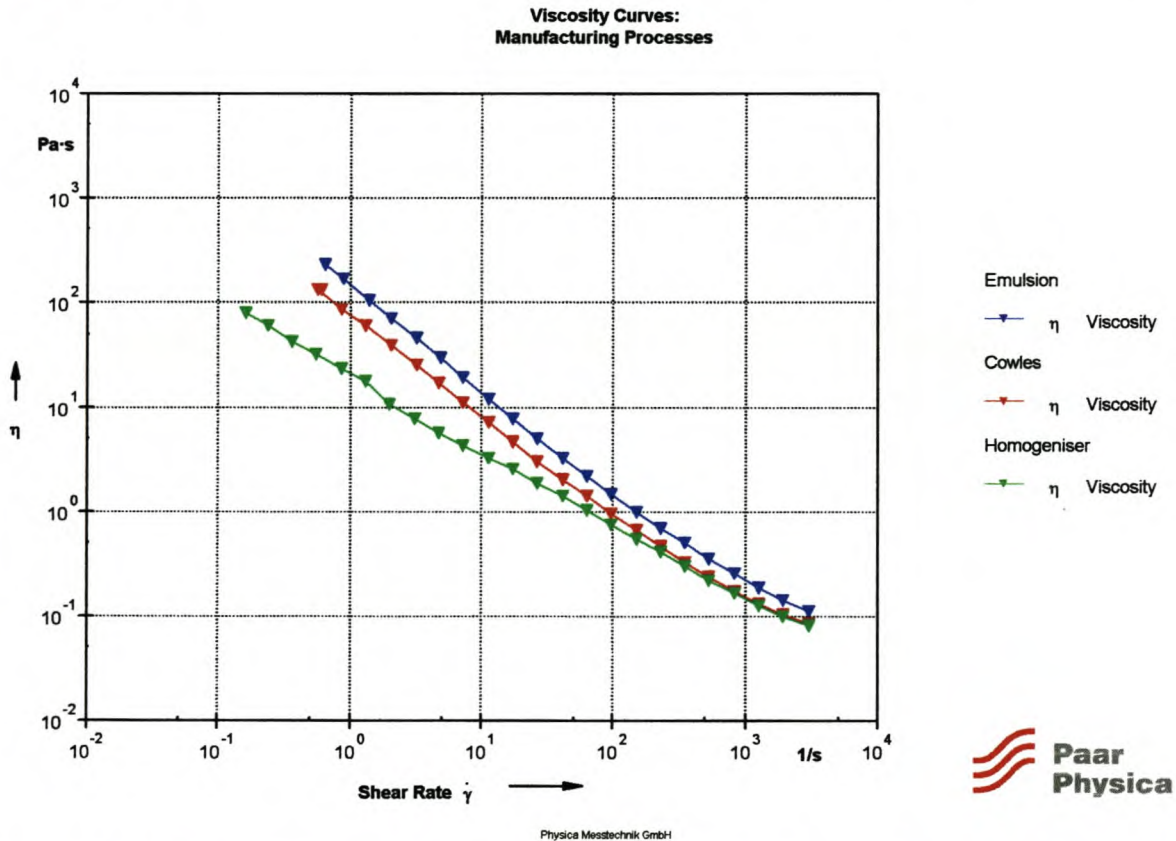


Figure 4-4: Viscosity curves for vesiculated beads dispersion produced by each of the three different processes

³ Particles size distribution is based on a 95% standard deviation. Therefore, 95% of the particles fall within x μm of the average particle size.

Figure 4-4 gives an indication of the following flow behaviour of the vesiculated beads:

- There are variations in the shear viscosities of the three samples exist. The differences are even greater in the low-shear-rate range, while the viscosities are almost similar at the high-shear-rate range. In other words, the pseudoplasticity of the samples increases from the homogeniser, to the emulsion process and therefore differences in the structure of the samples exist. Prideaux [1993] states that the higher the molecular weight of the HEC, the more pseudoplastic the viscosity curves become, because entanglements are broken down by shear forces. This observation by Prideaux [1993] gives rise to the possibility that the difference in shear rates during manufacturing processes causes the polymer chains (mostly thought to be HEC polymer chains due to the high molecular weight in comparison with other polymers) to break up in different degrees of chain lengths, resulting in different degrees of pseudoplasticity. At higher shear rates all the polymer chains are aligned in the direction of flow, whether short or long, and therefore little difference in high-shear viscosity is observed.
- Whether this is the reason or not, is not as important as the fact that there are differences in the viscosity behaviour, which are caused by the differences in the manufacturing process.

4.3.4.2 Amplitude Sweeps

The amplitude sweeps for the samples produced by each of the three different processes are given in Figure 4-5 below.

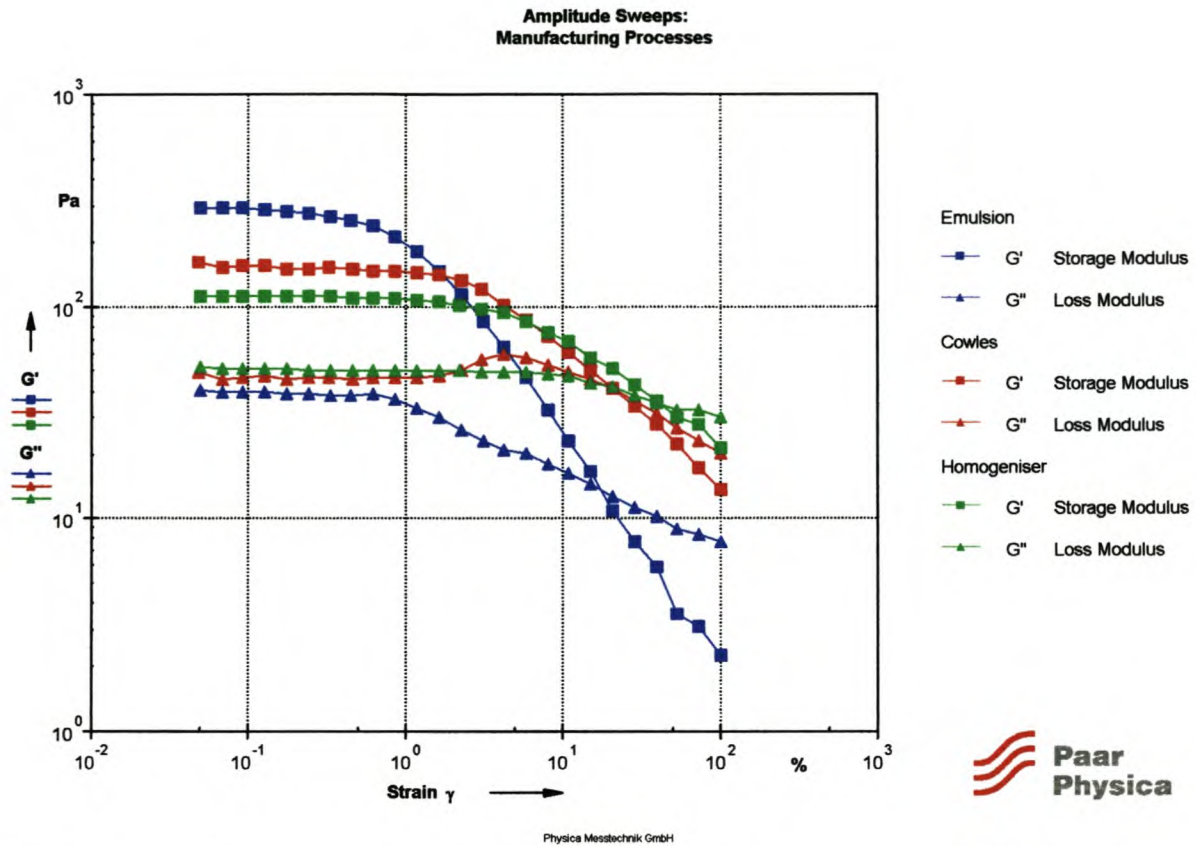


Figure 4-5: Amplitude sweeps for the three different vesiculated bead samples

The following information concerning the character of the vesiculated beads samples is obtained from Figure 4-5:

- $G' > G''$ in the LVER for all the samples and therefore the solid-like behaviour predominates over the liquid-like behaviour and the samples show some form of rigidity.
- G' increase from the sample manufactured on the homogeniser (high shear) to the sample manufactured on the emulsion reactor (low shear). It is possible that the longer HEC polymer chains behave more elastically than the shorter polymer chains due to the higher number of entanglements. The relationship between the molecular weight of the HEC and the value of G' in the LVER has also been examined by Liang et al. [1993] for a polystyrene latex in the presence of HEC and by Kiratzis et al [1998] for alumina and polystyrene latexes in the presence of HEC. Liang et al. [1993] observed an increase in the G' values as the molecular weight of the HEC increased and Kiratzis et al. [1998] gives the following relationship between G' and the molecular weight of the HEC:

$$G' \propto M_R^{1.3}$$

The difference in the amplitude sweep curves for the three samples is thought to be related to the difference in shear rates in each process. The following figure illustrates the relationship between G' and the shear rate.

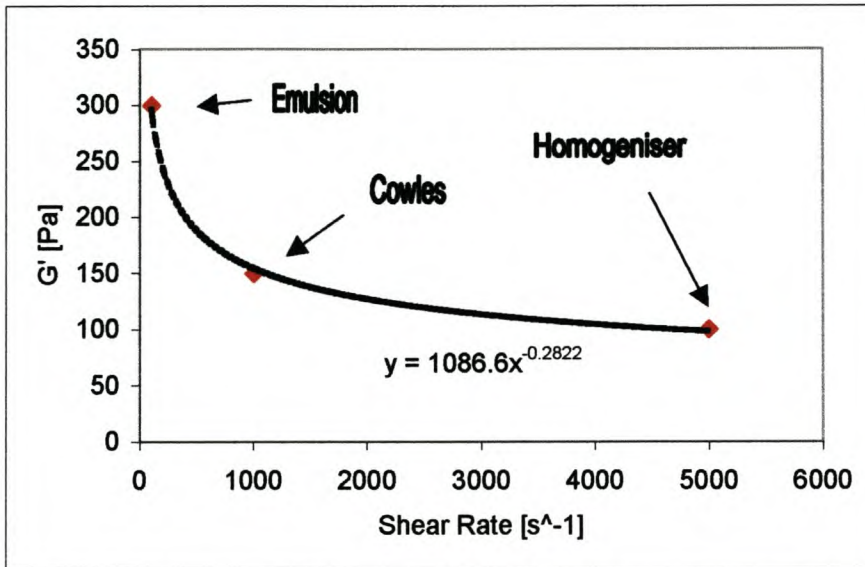


Figure 4-6: Relationship between G' and shear rate for vesiculated beads⁴

Therefore the relationship between G' and the shear rate is as follows:

$$G' \propto \dot{\gamma}^{-0.28 \pm 0.01}$$

The ± 0.01 allows for variations in the shear rate of the Cowles process ($500 \text{ s}^{-1} < \dot{\gamma} < 1500 \text{ s}^{-1}$) due to the fact that it could not be determined accurately. However, only three data points were used for this correlation and therefore it must be remembered that a considerable degree of uncertainty remains.

It is therefore clear that the structural strength of the vesiculated beads decreases in a power-law manner with an increase in shear of the process.

- In the LVER larger differences in the values of the storage modulus (G') exist than differences in the loss modulus (G'') of the samples. This confirms the fact that the

⁴ Shear rates obtained from equation 4-1 and 4-5 for emulsion reactor and homogeniser respectively. Shear rate for Cowles reactor is an estimation.

differences in the structure of the three samples are mainly due to the differences in elastic behaviour (G') and not the viscous behaviour (G'').

The amplitude sweeps can also be illustrated with the stress values on the x-axis, as in Figure 4-7 below.

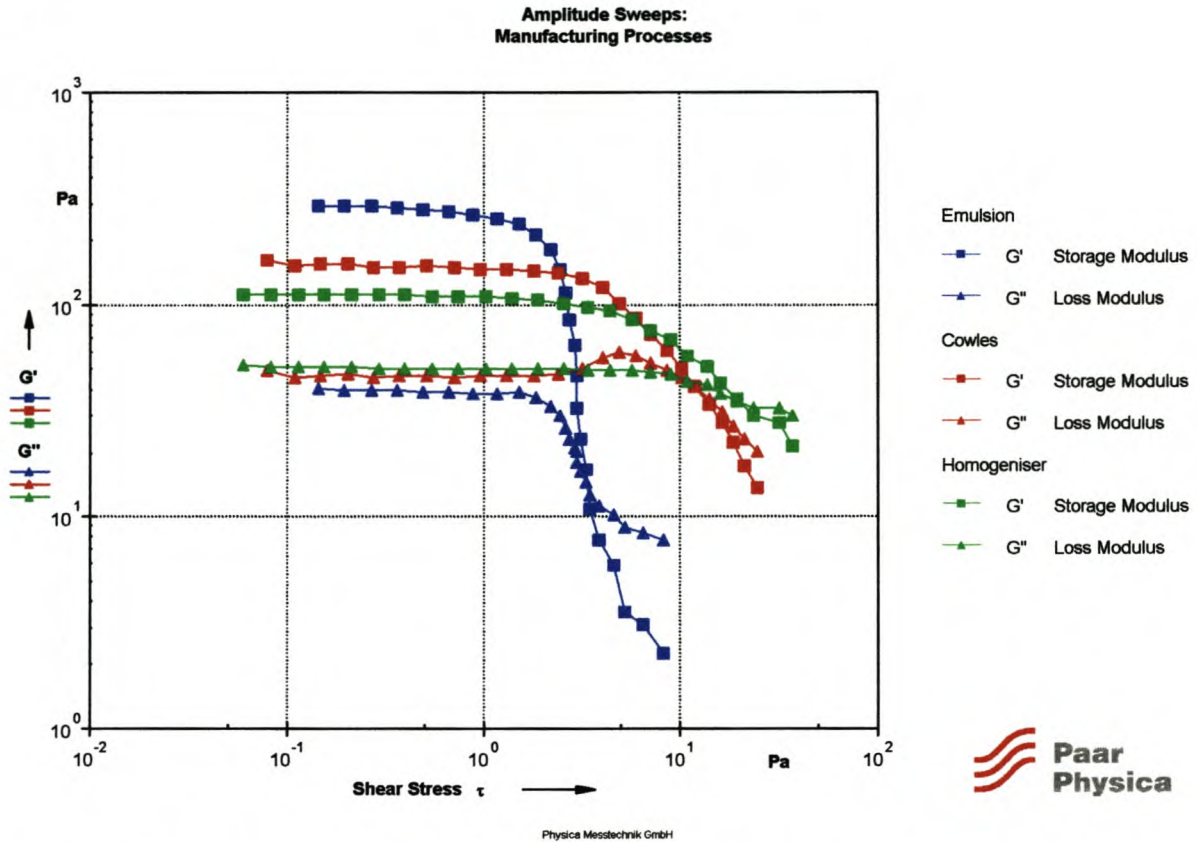


Figure 4-7: Amplitude sweep with stress on x-axis for vesiculated beads

The following information is obtained from Figure 4-7:

- Although the sample manufactured on the emulsion process has the highest structural strength (G'), it also has the smallest yield point ($\tau_y = \pm 0.7$ Pa obtained from the data table), and vice versa for the sample manufactured on the homogeniser ($\tau_y = \pm 3.2$ Pa obtained from the data table). Kiratzis et al. [1998] tried to explain the behaviour of G' and the yield point by investigating a sterically stabilised polyester latex in the presence of HEC, which therefore closely resembles the vesiculated beads dispersion. According to him, the following holds true:

- $G' \propto$ number of bonds between particles and elasticity of each bond;
- Yield stress \propto number of bonds between particles and strength of the bonds.

While G' is primarily determined by the *number* of particle bonds, the yield stress is predominantly determined by the *strength* of the particle bonds. One can therefore conclude that, if the vesiculated beads dispersion behaves in the same manner as the polyester latex, the increased G' value in the LVER is due to an increase in the number of particle bonds and that the increase in yield point is due to the increase in the strength of the particle bonds.

- A much more sudden breakdown in the structural strength occurs at the yield point for the sample manufactured on the emulsion process. In other words, if it is true that $G' \propto$ number of bonds, then it must be true that more bonds are broken down, which seems to be more likely with the longer polymer chains.

4.3.4.3 Frequency Sweeps

The frequency sweeps are given in Figure 4-8 below. The complex viscosity, $|\eta^*|$ is given on the y-axis instead of G' and G'' as in the conventional way. This is done in order to obtain the 'viscosity' behaviour in the LVER.

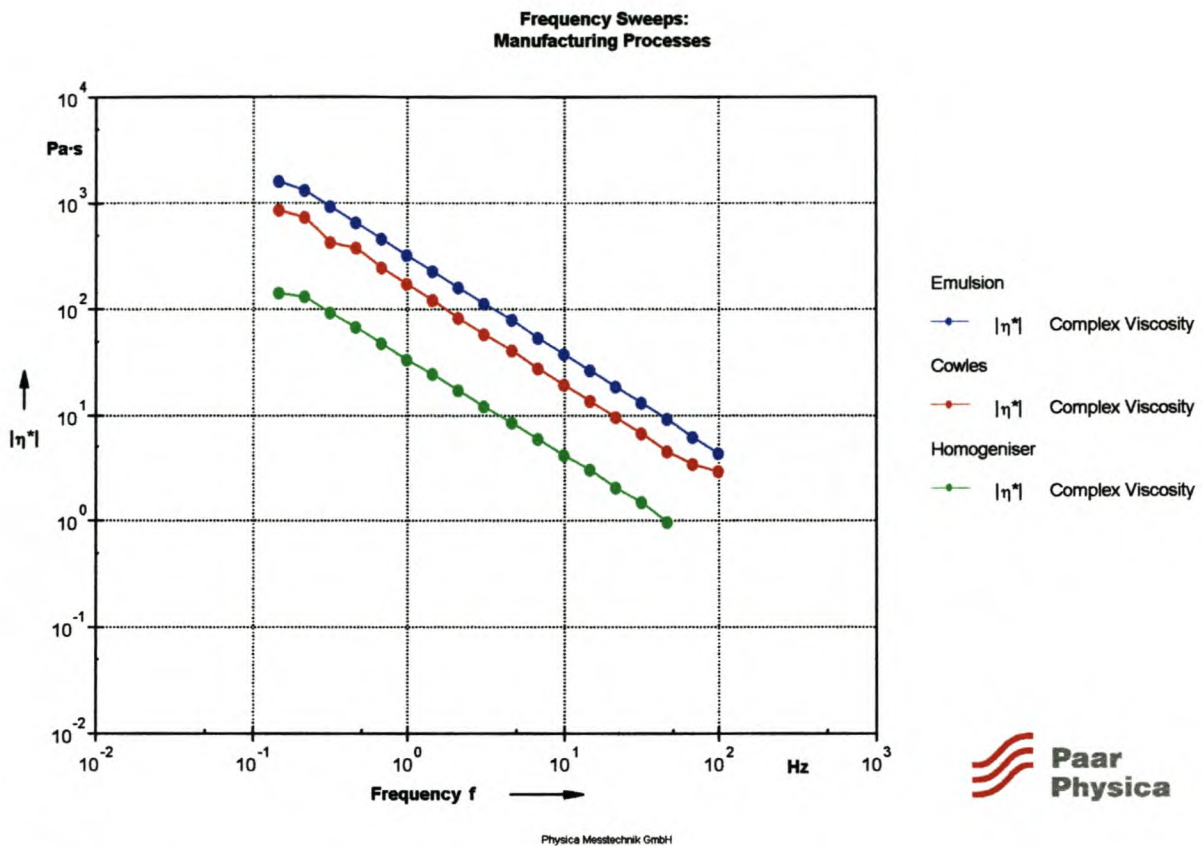


Figure 4-8: Frequency sweeps with complex viscosity on y-axis

Figure 4-8 gives the following information of the vesiculated beads in the LVER:

- Once again the difference in internal structure can be observed by means of the complex viscosity, which is an indication of the ‘viscosity’ in the LVER or when the sample is at rest (observed at low frequencies). The possible cause for the lower viscosity behaviour for the sample from the homogenisation process was discussed earlier in sections 4.3.4.1 and 4.3.4.2 in terms of the length of HEC chains.
- The curves for the complex viscosity of each sample do not converge at higher frequencies but tend to stay parallel to each other over the whole frequency range. With the viscosity curves (see section 4.3.4.1), the samples *flow* at high shear rates and the molecules and particles are aligned in the direction of flow resulting in almost the same viscosity behaviour. For the complex viscosity the samples are tested within the LVER and therefore do not *flow* because the molecules and particles are not aligned.

4.3.5 Conclusions

- Differences are observed in the:
 - Low-shear-rate viscosity;
 - Structural strength in the LVER, G' ;
 - Yield points, τ_y ;
 - $\tan \delta$ -values, $\tan \delta = G''/G'$;
 - Complex viscosity, $|\eta^*|$,for samples prepared according to different methods.

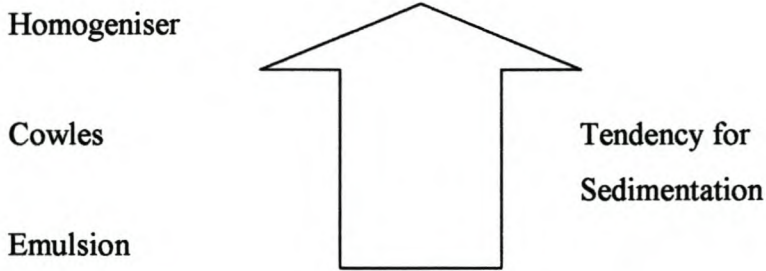
Therefore the various manufacturing processes result in the vesiculated beads having different rheological behaviour.

- The differences in rheological behaviour are thought to be a result of differences in shear rates in each process.
- The differences in rheological behaviour have an effect on the stability of the samples. The stability of a dispersion decreases with decreasing G' values and therefore it would appear that the homogeniser produces vesiculated beads with the lowest stability, while the emulsion reactor produces beads with the highest stability.
- The solid-like behaviour (G') predominates over the liquid-like (G'') behaviour for all the samples and therefore all the samples have structures with a certain degree of rigidity. This assists in creating anti-sedimentation properties.

4.3.6 Implications of Differences in Manufacturing Processes

- Different degrees of structural strengths exist and therefore the samples will have different degrees of stability. Higher structural strength in these samples is advantageous as the samples consist of high solid loads and may therefore tend to sedimentate if the structural strength at low frequencies (state of rest) is not high enough.

According to the rheological behaviour, the tendency of the vesiculated beads to sedimentate increases in the following order:



- According to Prideaux [1993], high molecular weight HEC tends to cause an unacceptably high degree of spattering on roller application. Therefore coatings formulated with vesiculated beads from different manufacturing processes might tend to spatter in different degrees. That is, a coating manufactured from beads produced by the homogeniser might spatter less than a coating with beads produced by the emulsion reactor due to lower molecular weight HEC.
- Ease of recovery increases with decreasing structural strength and therefore the beads produced on the homogeniser are the easiest to recover the next day.

4.3.7 Concluding Remarks

It will be possible to control the rheological behaviour of the vesiculated beads by means of variation of the molecular weight of the HEC. For example, if too low viscosities and structural strengths start to become a problem in the high-shear processes such as the homogeniser, a higher molecular weight HEC can be used to obtain the desired viscosities.

4.4 Effect of Raw Materials on Rheology of Vesiculated Beads

The raw materials that were most likely to play a big role on the rheology of the dispersion were investigated.

4.4.1 Effect of Hydroxy-Ethyl-Cellulose (HEC)

In order to obtain the proper viscosity to maintain the suspension of vesiculated beads and pigment in the dispersion, the addition of a cellulosic thickener to adjust the rheological characteristics is required [Karickhoff, 1984]. The amount of thickener need only be sufficient to impart the desired viscosity behaviour.

Three samples with varying amounts of HEC were prepared. The amount of HEC ($M_R = 400\ 000$ g/mol), along with other properties of the vesiculated beads samples, are given in Table 4-3.

Table 4-3: Properties of vesiculated beads samples with different levels of HEC

Sample	Amount of HEC in sample [%]	Average Particle Size [μm]	Particle Size Distribution ⁵ [μm]	Total Solids Content [%]
HEC1:	0.18	2.28	1.68	23.75
HEC2:	0.25	2.37	1.81	24.07
HEC3:	0.31	2.67	1.53	23.30

Cellulosic thickeners such as HEC occupy a large volume in the water phase and therefore act by thickening the water. HEC has little interaction with other ingredients [Whitton et al., 2001]. According to Prideaux [1993], HEC tend to impart a higher low-shear viscosity than is sometimes desirable (brush marks, poorer flow and levelling) and lower high-shear viscosities (poorer film build) and therefore have the tendency to be more pseudoplastic than the ideal.

According to Karickhoff [1984], HEC thickeners are especially useful in thickening aqueous systems consisting of water and a polymer latex, and are particularly useful in lower solids coatings which contain vesiculated beads as part of the coating pigmentation.

⁵ Particles size distribution is based on a 95% standard deviation. Therefore, 95% of the particles fall within x μm of the average particle size.

4.4.1.1 Viscosity Curves

The effect of HEC on the viscosity curves is given in Figure 4-9 below.

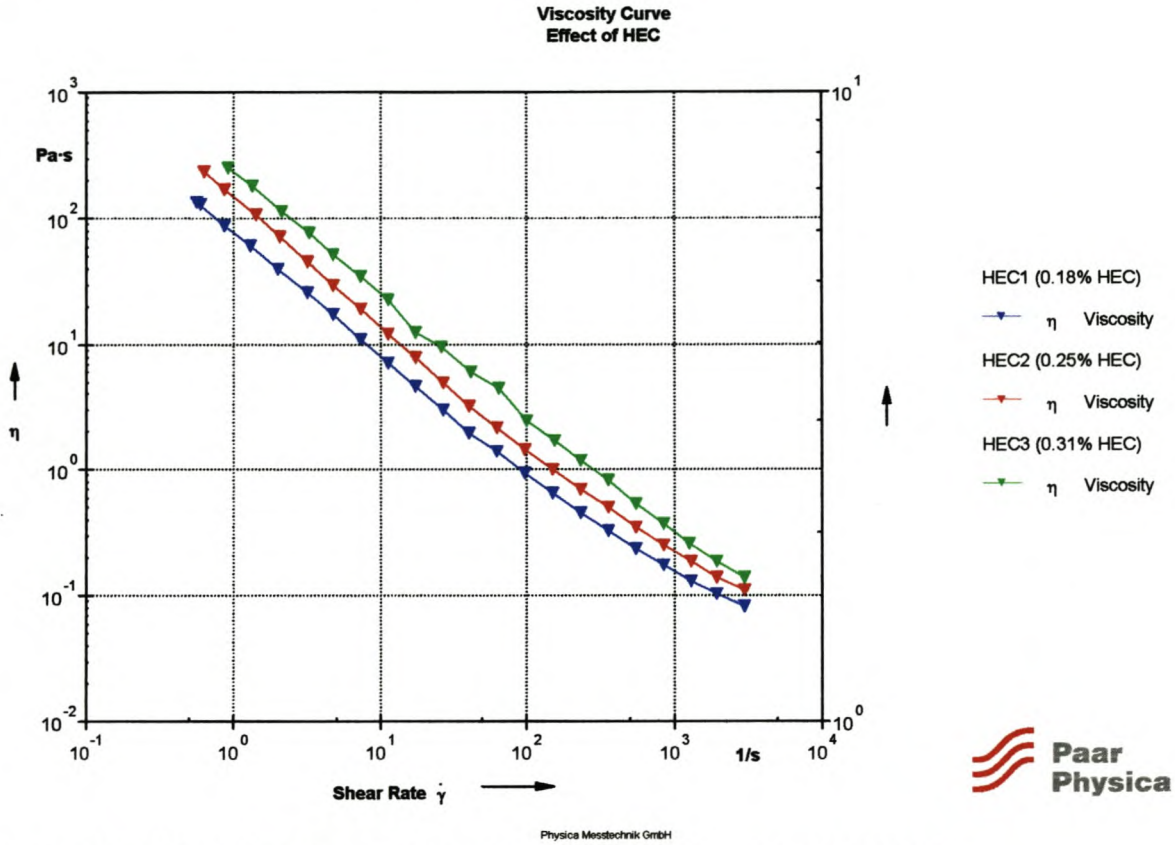


Figure 4-9: Effect of HEC content on viscosity curves for vesiculated beads

Figure 4-9 gives the following information on the flow behaviour of the vesiculated beads:

- The viscosity over the whole shear-rate range increases as the amount of HEC increases. The HEC is not associative in the system, because it affects the whole viscosity curve in more or less the same manner.

4.4.1.2 Amplitude Sweeps

The effect of HEC on the amplitude sweeps is given in Figure 4-10 below.

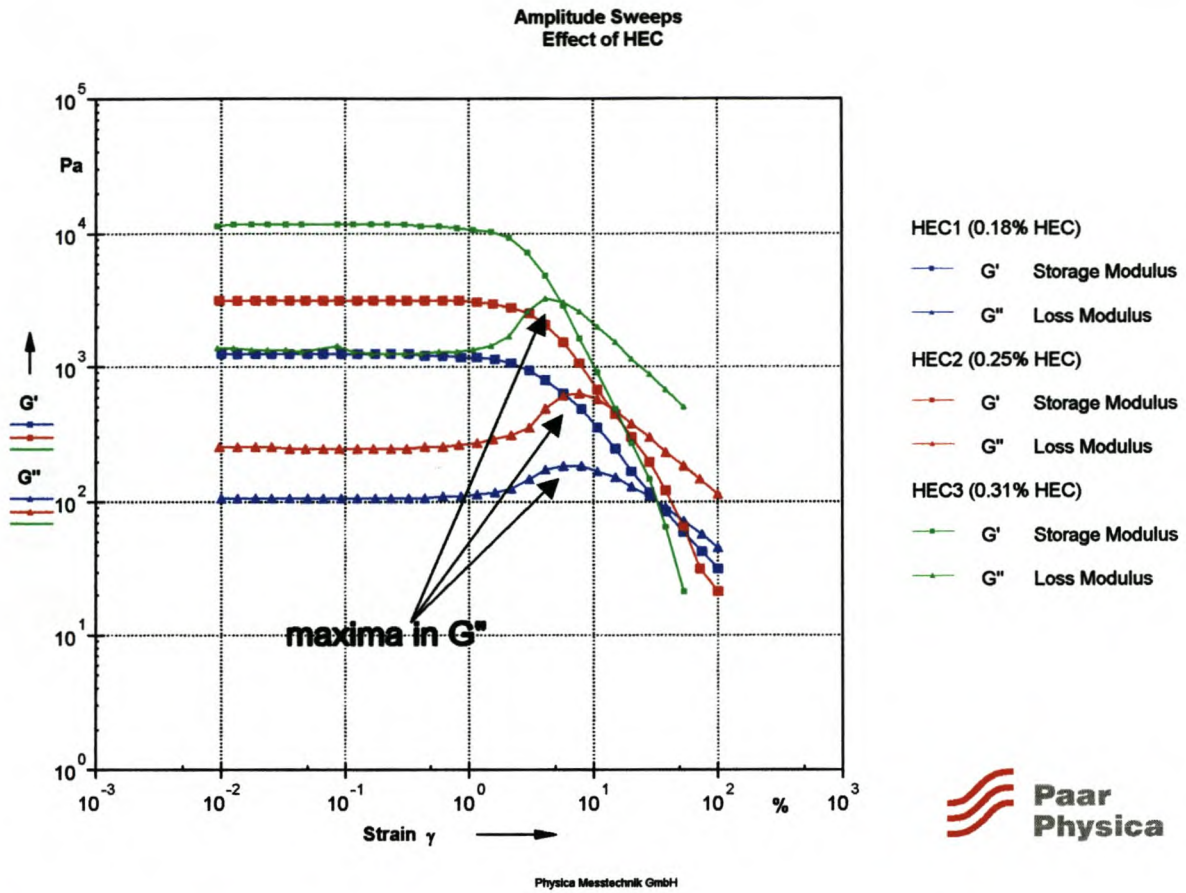


Figure 4-10: Effect of HEC content on the amplitude sweeps for vesiculated beads

Figure 4-10 gives the following information about the character of the vesiculated beads:

- $G' > G''$ in the LVER for all the samples and therefore the solid-like part of all the samples predominates over the liquid-like part and the structures have a certain degree of rigidity.
- The value of the storage modulus (G') in the LVER increases as the amount of HEC increases and therefore an increase in the structural strength of the sample occurs. The relationship between the G' values in the LVER and the amount of HEC is given in Figure 4-11 below.

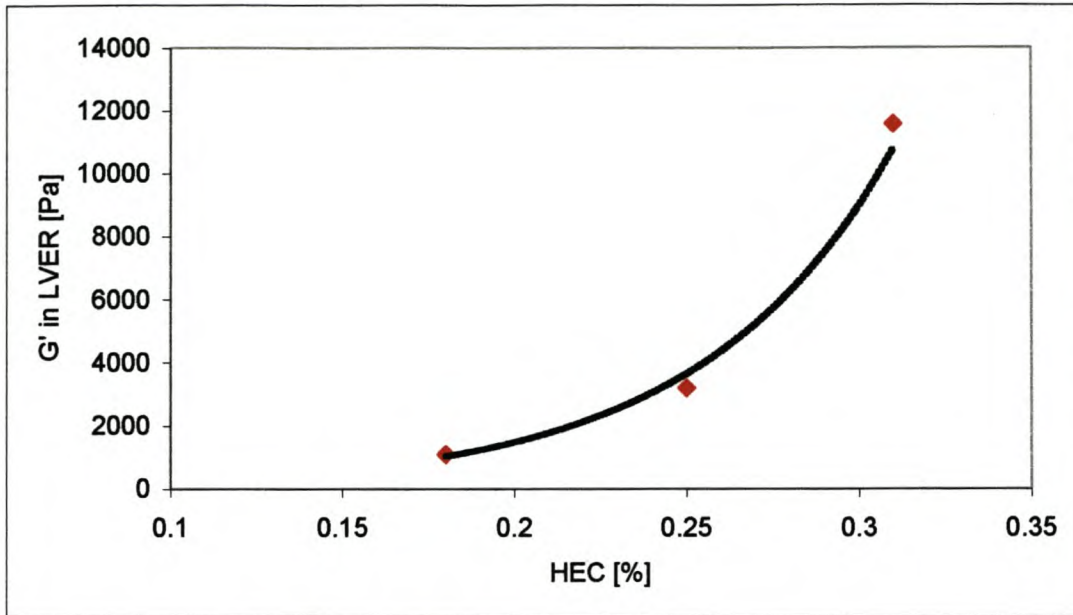


Figure 4-11: Relationship between amount of HEC and G' values in the LVER

Figure 4-11 illustrates that the G' values in the LVER increase with an increase in the amount of HEC.

This behaviour was also observed by Liang [1993] for a polystyrene latex in the presence of HEC and by Kiratzis et al. [1999] for a suspension of alumina particles in the presence of HEC.

- At strain values above the yield point, both G' and G'' are amplitude dependent, with G' decreasing monotonically and G'' going through a maximum at a strain value of $\pm 5\%$ (indicated with arrows in Figure 4-11). Kiratzis et al. [1999] found the same behaviour for an aqueous alumina suspension in the presence of HEC and ascribed this type of behaviour to a well-known entanglement theory that indicates the existence of topological restraints that delay the long-range configurational rearrangements of the molecules.

To examine the effect of an increasing amount of HEC on the yield point of the samples, the amplitude sweeps are illustrated in Figure 4-12 below, with the stress on the x-axis.

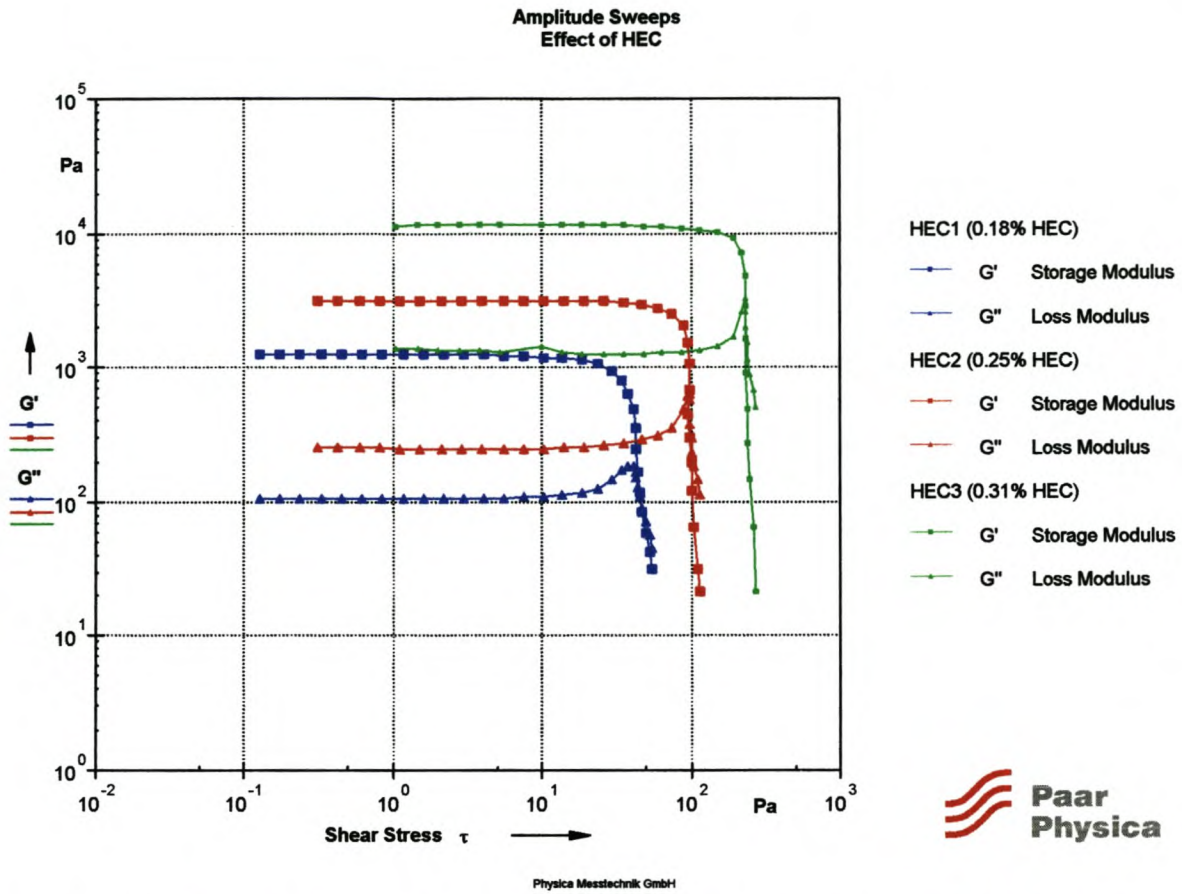


Figure 4-12: Effect of HEC content on amplitude sweeps for vesiculated beads (stress on x-axis)

Figure 4-12 reveals the following information about the yield points of the vesiculated beads:

- There is an increase in the yield point as the amount of HEC increases. The following figure illustrates this relationship.

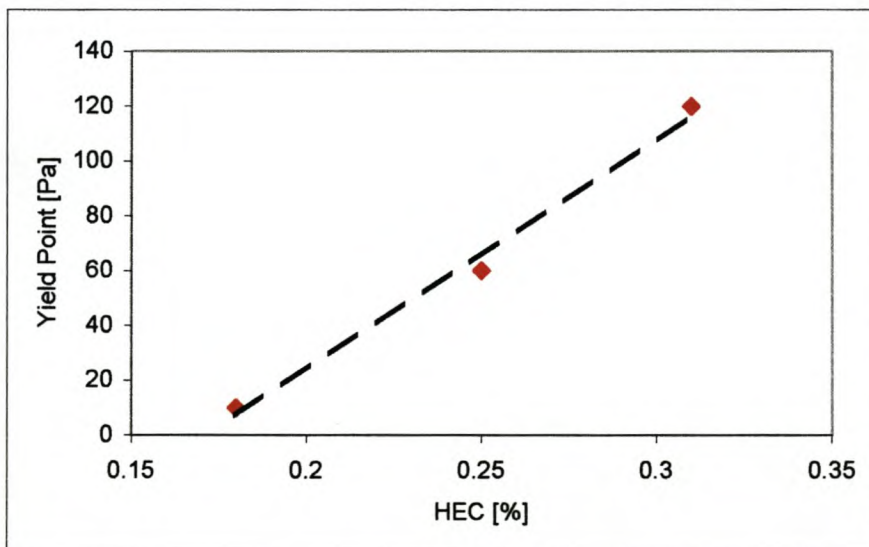


Figure 4-13: Relationship between yield point and the amount of HEC

Figure 4-13 illustrates a linear relationship between the yield point and the amount of HEC.

- The G' values increase exponentially, while the yield points increase linearly with increasing amounts of HEC. This difference is attributed to the fact that G' is a measure of the *number* of bonds that are formed, while the yield point is directly related to the total *strength* of the bonds [Liang et al., 1993]. It therefore seems that, as the amount of HEC increases, the entanglements increase exponentially, while the total strength of the bonds between the molecules increases linearly.

4.4.1.3 Frequency Sweeps

The effect of the amount HEC on the frequency sweeps is given in Figure 4-14 below.

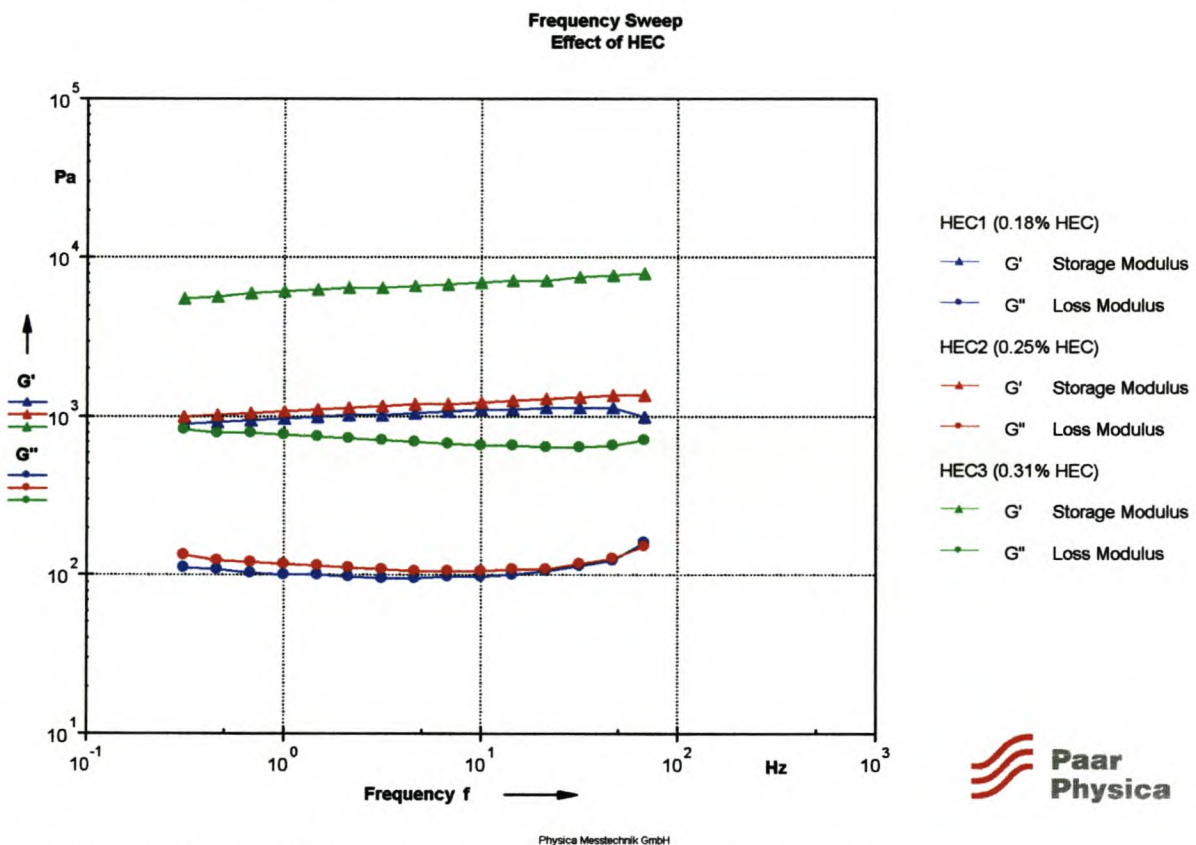


Figure 4-14: Effect of HEC content on frequency sweeps for vesiculated beads

Figure 4-14 gives the following information of the behaviour of the beads in the LVER:

- The shape of the curves looks more or less the same; the only difference is that the values of G' and G'' seem to increase with an increase in the amount of HEC.

- $G' \gg G''$ for all the samples over the whole frequency range and are almost parallel to each other with little slope, indicating a stable structure.
- The G' and G'' curves for the HEC1 and HEC2 samples are almost similar, while there is a large increase in the G' and G'' curves at higher levels of HEC (HEC3). This behaviour cannot be explained entirely, but might be an indication of a possible critical HEC concentration. Liang et al. [1993] also found a sudden increase in G' values for latex particles in the presence of HEC at a critical volume fraction of HEC, ϕ_c . He states further that this critical volume fraction may be taken as the gelation point, i.e. the volume fraction of HEC at which a continuous network structure is produced.

The ratio between G' and G'' ($\tan \delta$) is illustrated in Figure 4-15 below.

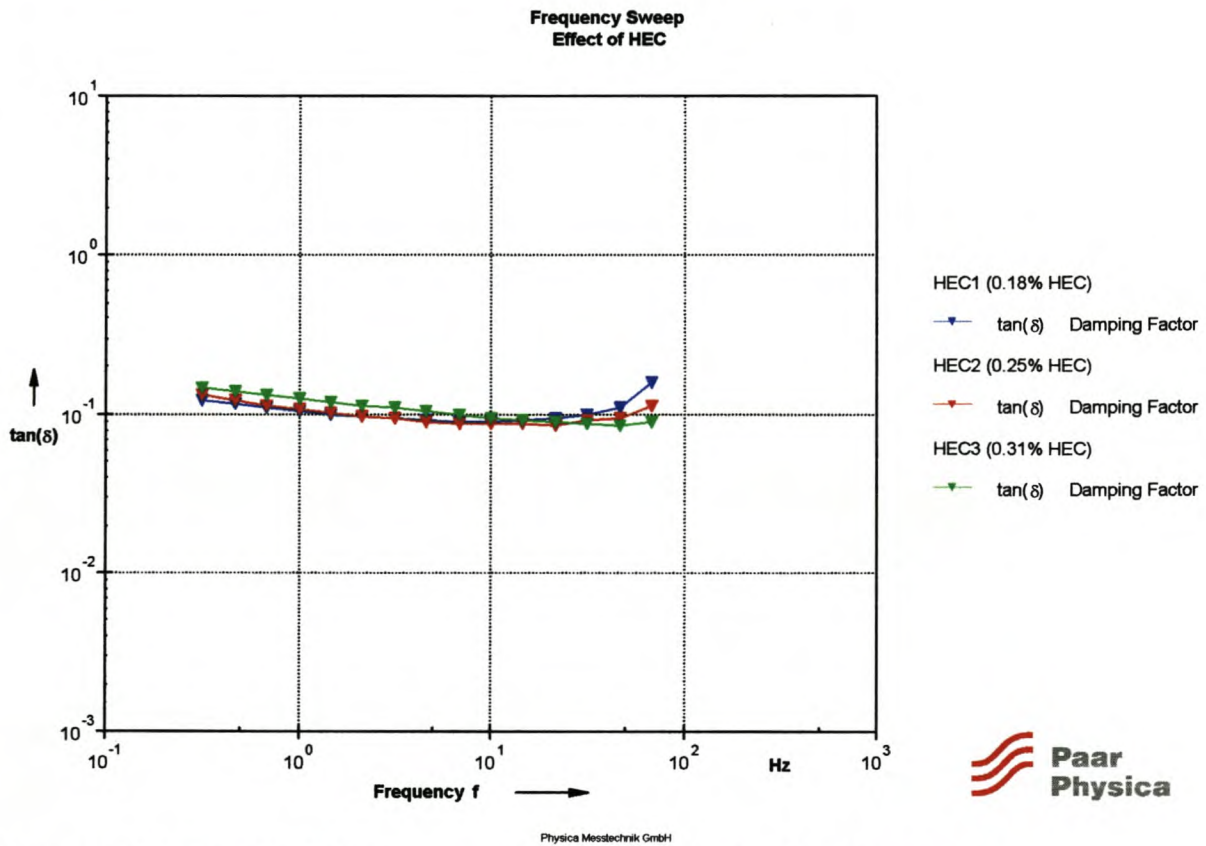


Figure 4-15: Effect of HEC content on frequency sweeps ($\tan \delta$ vs. frequency)

The following information is obtained from Figure 4-15:

- At lower frequencies ($f < 20$ Hz) the $\tan \delta$ values indicate that G' is ± 10 times larger than G'' ($\tan \delta = G''/G' = 0.1$) for all the samples and therefore the structures are stable and should not tend to separate or sedimentate, because a three-dimensional network exists that keeps the polymer particles intact.
- At low to medium frequencies (0.1 Hz – 10 Hz) the curves also indicate that the ratio of G''/G' does not increase with increasing levels of HEC. This may be an indication that 0.18% of HEC is sufficient to keep the vesiculated beads in suspension and that higher levels of HEC result in an excess.
- At higher frequencies (10 Hz – 100 Hz) G'' gets larger with respect to G' for decreasing levels of HEC. In other words, $\tan \delta$ increases. This may be the onset of possible detanglements of the HEC molecules at higher frequencies. At the lowest amount of HEC (HEC1), the molecules detangle the 'easiest' due to steric reasons and the increase in $\tan \delta$ value starts at a lower frequency than for those of higher levels of HEC (HEC2 and HEC3).

It can be seen that $\tan \delta$ tends to increase at:

- HEC1 @ 10 Hz
- HEC2 @ 21 Hz
- HEC3 @ 46 Hz.

This behaviour illustrates an increase in the structural stability as the amount of HEC increases, because 'flow' starts at higher frequencies.

4.4.1.4 Three-Interval-Thixotropy-Test (3-ITT)

The effect of the amount HEC on the structural recovery is given in Figure 4-16 below.

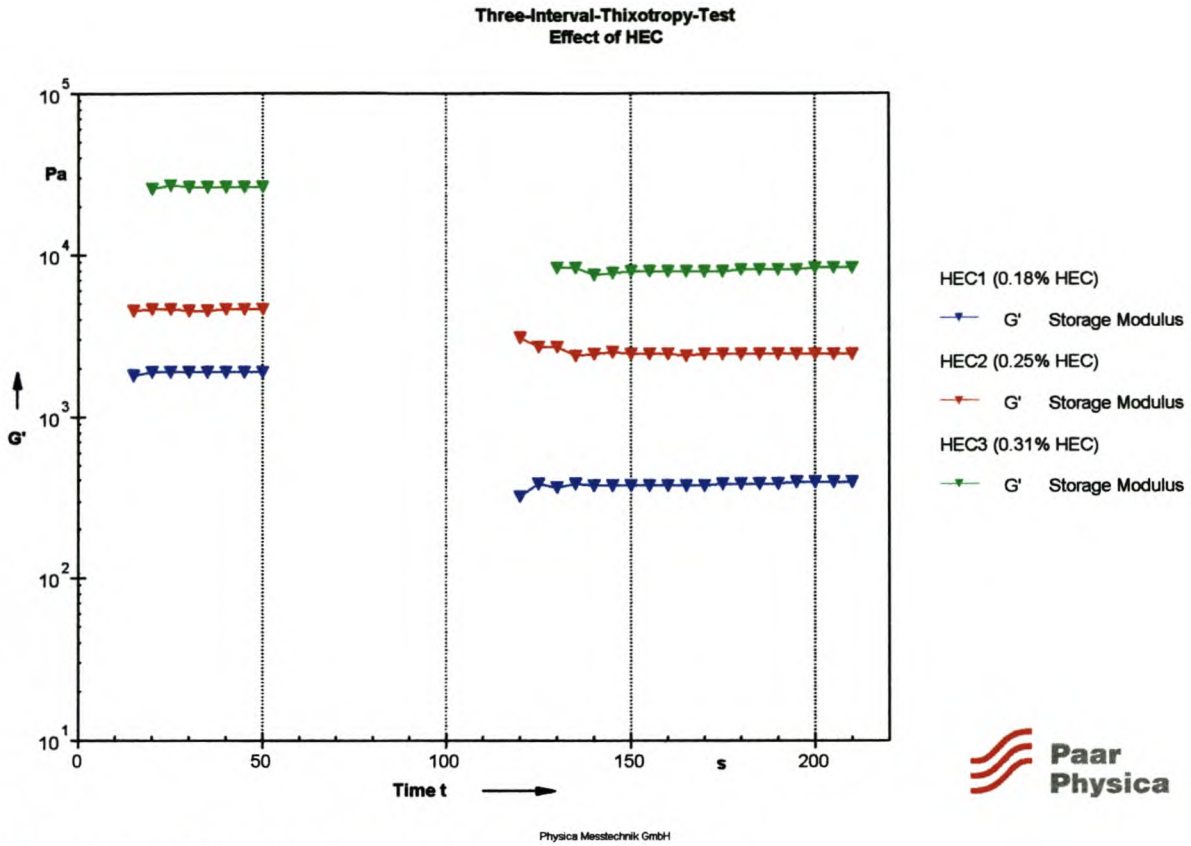


Figure 4-16: Effect of HEC content on structural recovery

Whitton et al. [2001] examined the structural recovery in HEC systems after high shear has been applied. He observed that, at rest, the viscosity of a system containing HEC is very high and in some cases the system at rest approaches a gelled state. As higher shear is applied to the system, the viscosity drops considerably. After the high shear is removed, the system *rapidly returns to its original* high viscosity or semi-gelled state.

Figure 4-16 gives the following information about the structural recovery of the vesiculated beads after high shear:

- After a high shear load the structure does not recover *rapidly to its original state* as observed by Whitton et al. [2001], even after 2 minutes. In other words, an irreversible change in the structure has occurred or the recovery process is very slow. It is therefore possible that the recovery of the structure is not governed by the amount of HEC, but rather by some other factor such as the particle size distribution.
- The structural recovery after high shear does not follow a linear relationship with the amount of HEC. The degree of structural recovery (obtained from the data tables of the 3-ITT) after 1 minute is as follows:

0.18% HEC	-	20.7% recovery of G'
0.25% HEC	-	52.3% recovery of G'
0.31% HEC	-	31.7% recovery of G'

This behaviour once again illustrates the fact that the degree of structural recovery has a complex dependency related to the amount of HEC in the system.

4.4.1.5 Conclusions

The following are the most important conclusions:

- An increase in the amount of HEC results in the following behaviour:
 - An increase in the overall viscosity indicating that HEC is not associative in this system [Prideaux, 1993];
 - An exponential increase in the structural strength (G') and therefore an increase in the stability of the vesiculated beads dispersion;
 - A linear increase in the yield points;
 - An increase in the stability of the dispersion over the whole frequency range (long and short-time scales);
 - An increase in the onset point (lower frequencies) of 'flow' in the LVER, indicating an increase in the stability.
- Different values of HEC do not affect the shape of the frequency curves and this therefore indicates that a variation in the amount of HEC within the experimental values does not lead to instability of the dispersion.
- The structural recovery of the dispersions after a high shear load has a complex dependency related to the amount of HEC.

4.4.1.6 Practical Implications of Varying the Amount of HEC

- A large increase in the amount of HEC might cause the dispersion to transform into a gelled state in the state of rest due to the increase in structural strength and yield point. This will also cause brush marks in the final coating and may result in poor flow and levelling properties.
- An increase in the amount of HEC will also result in more difficult mixing and pumping due to an increase in the viscosity at higher shear rates.
- An increase in the amount of HEC makes the dispersion more stable, which assists in prevention of phase separation and sedimentation, resulting in good storage behaviour.

4.4.1.7 Concluding Remarks

It is therefore clear that the dispersion must contain the optimum amount of HEC to ensure stability of the dispersion but must not make mixing, pumping, etc. more difficult due to a too high structural strength. It seems that the current level of HEC (0.25%) is sufficient in providing both stability and appropriate workability.

4.4.2 Effect of Polyvinyl-Alcohol (PVOH)

In order to obtain the proper viscosity to maintain the suspension of vesiculated beads and pigment in the paint and to improve application characteristics, the water-based paints require the addition of a polymer such as PVOH to adjust the rheological characteristics. The PVOH acts as a non-ionic surfactant for the polymer beads and stabilises the suspension of particles by means of steric hindrance. If insufficient (too little/too much) dispersion stabiliser is used, the suspension may become unstable [Gunning, 1975].

The PVOH used is a surface-active agent, which is partially (88%) hydrolysed polyvinyl acetate. The presence of the surface-active agent assists in the formation of a stable emulsion [Tioxide, 1981].

Larson [2000] states that polymer chains such as PVOH can be grafted onto the surfaces of particles to stabilise them by producing a steric barrier to flocculation. If the chains are long enough and interact favourably, the particles are kept at an arm's length from each other and cannot flocculate.

Three samples with varying amounts of PVOH were prepared. The amount of PVOH in each sample was as follows.

Table 4-4: Amount of PVOH in each sample

Sample	Amount of PVOH in sample [%]	Average Particle Size [μm]	Particle Size Distribution ⁶ [μm]	Total Solids Content [%]
PH1:	1.00	2.40	1.83	23.65
PH2:	1.45	2.33	1.55	23.36
PH3:	1.69	2.13	1.44	23.47

4.4.2.1 Viscosity Curves

The effect of PVOH content on the viscosity curves is illustrated in Figure 4-17 below.

⁶ Particles size distribution is based on a 95% standard deviation. Therefore, 95% of the particles fall within $x \mu\text{m}$ of the average particle size.

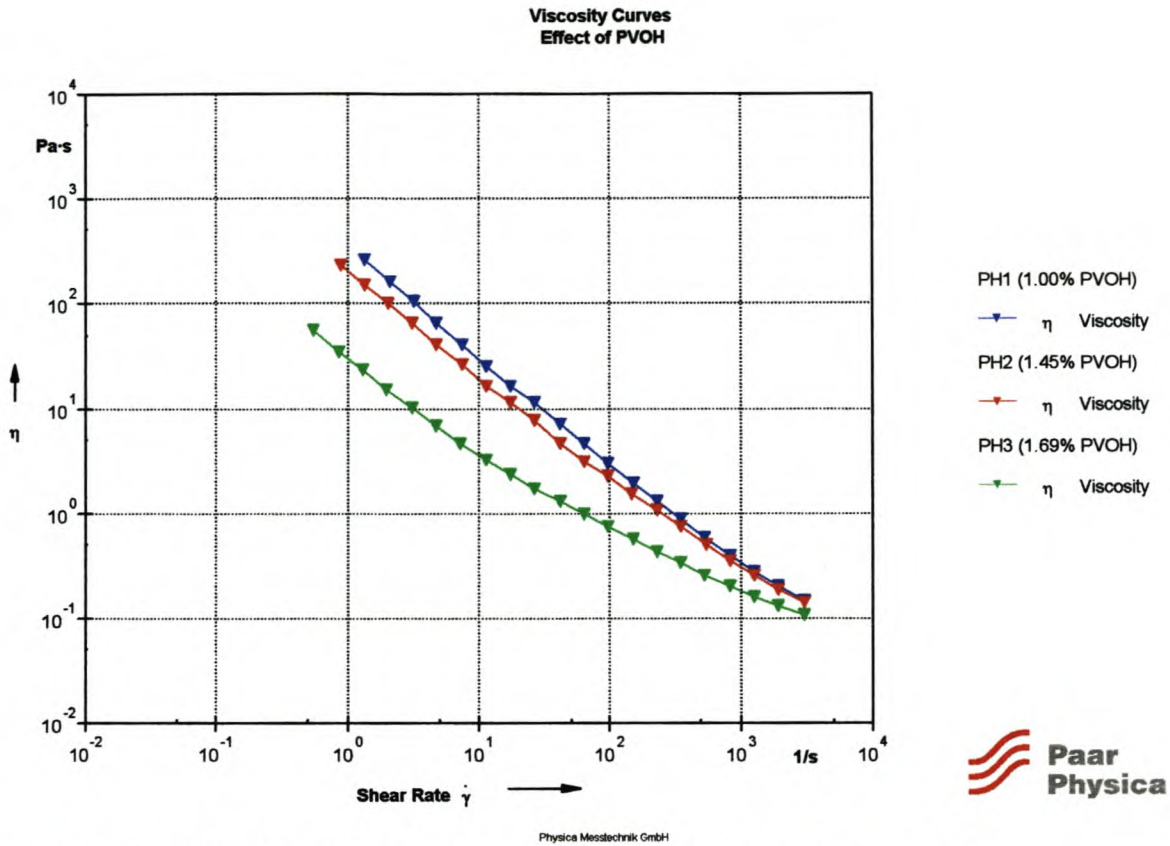


Figure 4-17: Effect of PVOH content on viscosity curves for vesiculated beads

Figure 4-17 shows the following concerning the flow behaviour of the vesiculated beads:

- The viscosity decreases as the amount of PVOH increases. The effect is greater at the low-shear viscosities than at the high-shear viscosities. Nommensen et al. [1999] gives a possible explanation. He describes the polymer layer as a ‘lubrication’ layer which is a permeable medium through which solvent can flow and therefore influences the hydrodynamic behaviour of the particles. He calculated the lubrication force (the force required to push two particles together) as a function of the amount of ‘lubricating’ polymer for hard spheres. He finds that the lubrication force increases exponentially with increasing amounts of polymer. Particle-particle interaction will therefore become less with an increase in the lubrication force, in other words with an increase in the amount of PVOH.

4.4.2.2 Amplitude Sweeps

The effect of PVOH on the amplitude sweeps is illustrated in Figure 4-18 below.

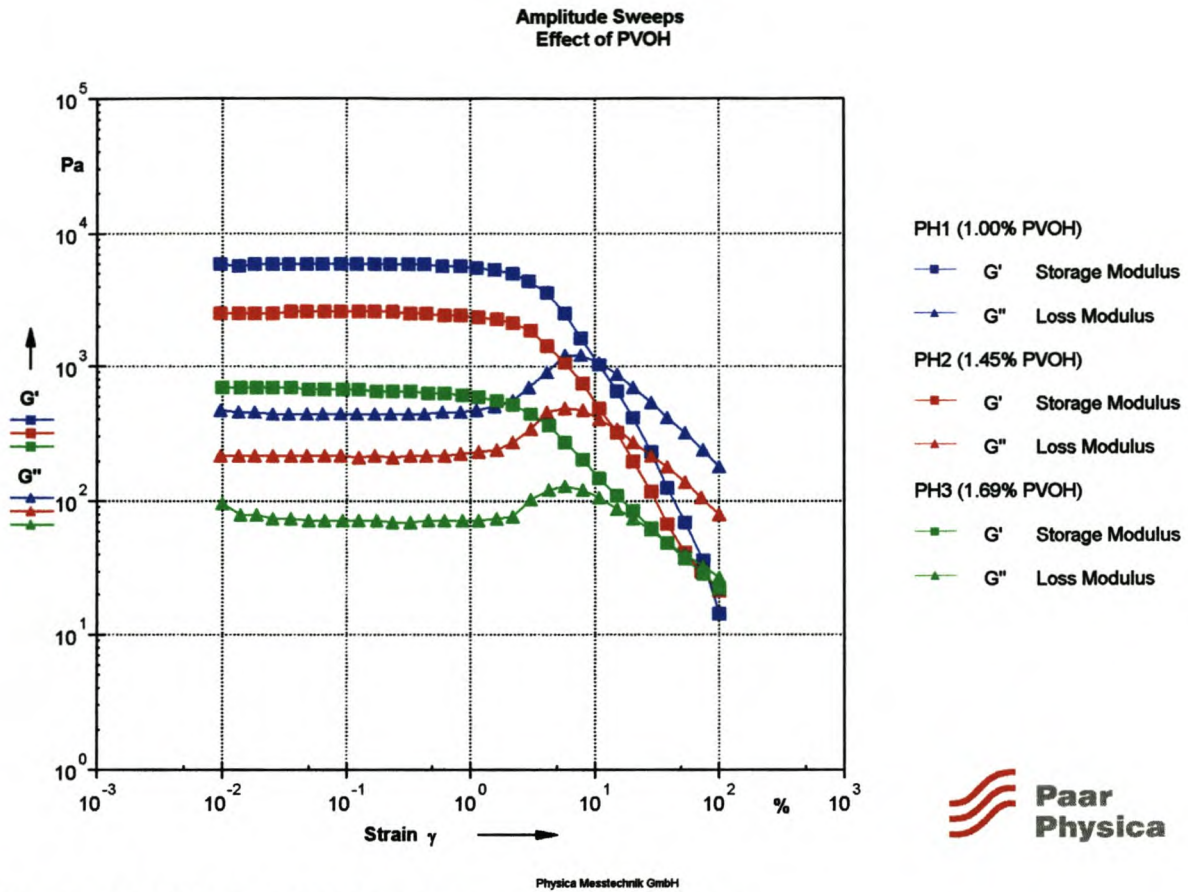


Figure 4-18: Effect of PVOH content on amplitude sweeps

Figure 4-18 reveals the following information about the character of the vesiculated beads:

- $G' > G''$ for all the samples in the LVER and therefore the solid-like behaviour predominates over the liquid-like behaviour and the samples show some degree of rigidity.
- The structural strength (G') decreases with an increase in the level of PVOH. An explanation for this has already been given by Nommensen et al. [1999] in terms of the 'lubrication' force (see section 4.4.2.1). The dependency of G' on the amount of PVOH is given in the following figure.

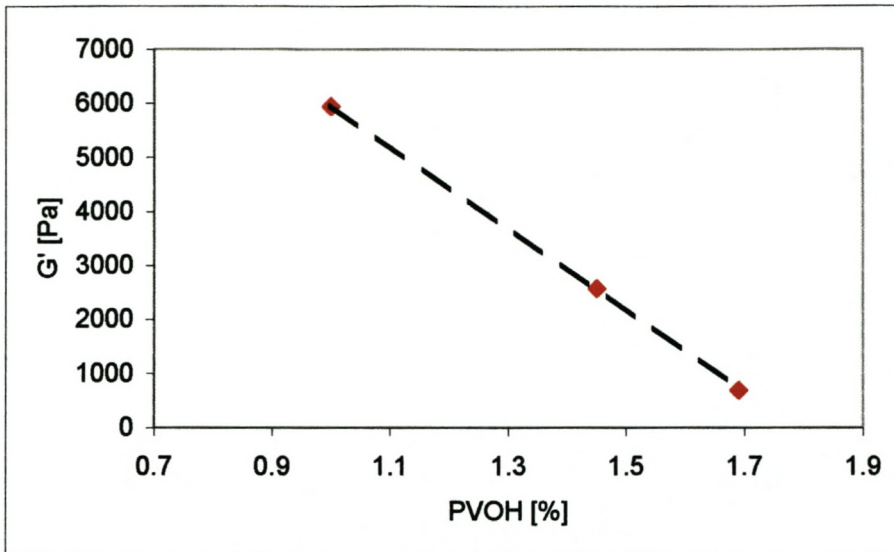


Figure 4-19: Relationship between G' and amount of PVOH

Figure 4-19 shows that G' decreases with increasing amounts of PVOH.

To determine what the dependency of the yield stress is on the amount of PVOH, the amplitude sweep is illustrated in Figure 4-20 with the stress values on the x-axis.

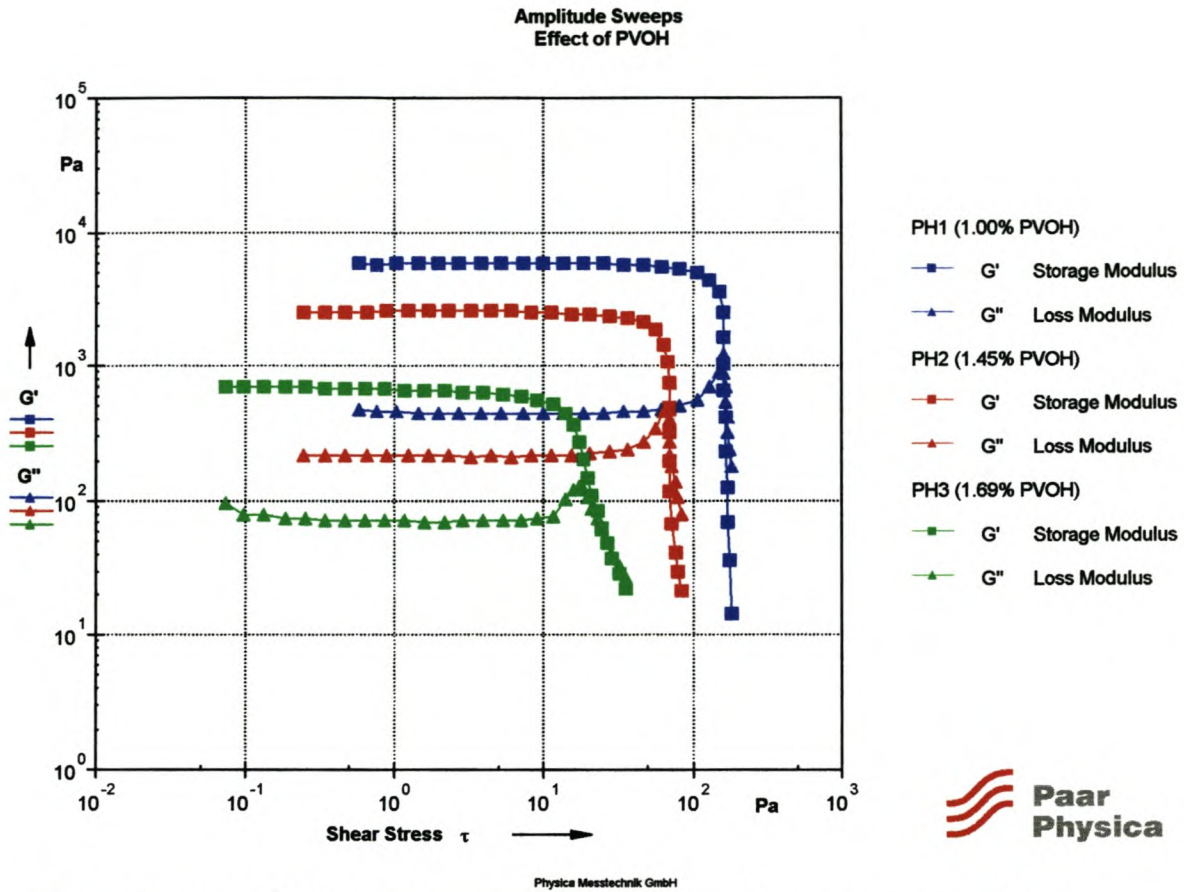


Figure 4-20: Effect of PVOH content on amplitude sweep (stress values on x-axis)

The following information is obtained from Figure 4-20:

- The LVER and yield stress decrease with an increase in the amount of PVOH. This can possibly once again be ascribed to the ‘lubrication theory’ given by Nommensen et al. [1999]. The dependency of the yield point on the amount of PVOH is given in the figure below.

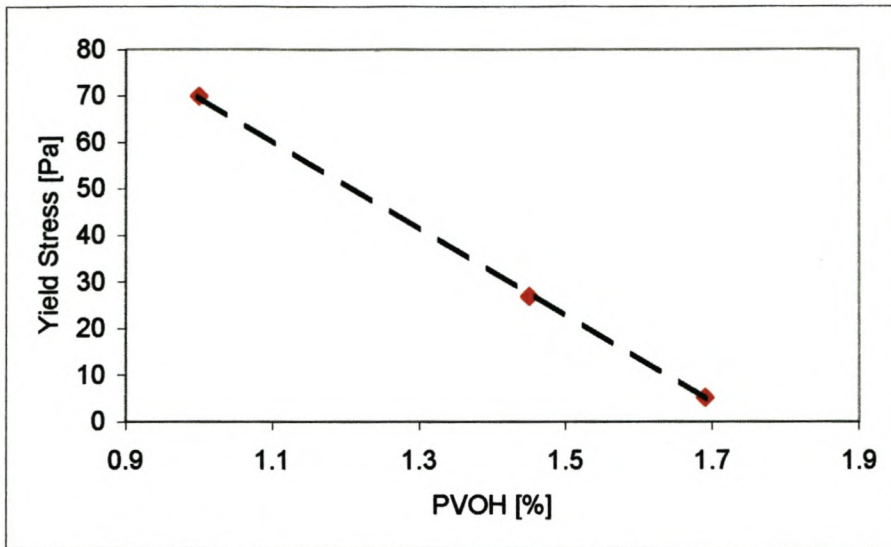


Figure 4-21: Relationship between yield stress and amount of PVOH

Figure 4-21 shows that the yield stress decreases with increasing amounts of PVOH.

4.4.2.3 Frequency Sweeps

The amplitude sweeps indicate that the degree of ‘lubrication’ increases with an increase in the amount of PVOH. Therefore at high levels of PVOH the possibility for the samples to sedimentate exists due to an increase in the degree of ‘lubrication’. In order to investigate whether sedimentation will occur or not, the $\tan \delta$ (G''/G') values are illustrated on the frequency sweep. Higher $\tan \delta$ values indicates a greater tendency to sedimentate because G'' gets larger.

The effect of PVOH on the $\tan \delta$ values is illustrated in Figure 4-22 below.

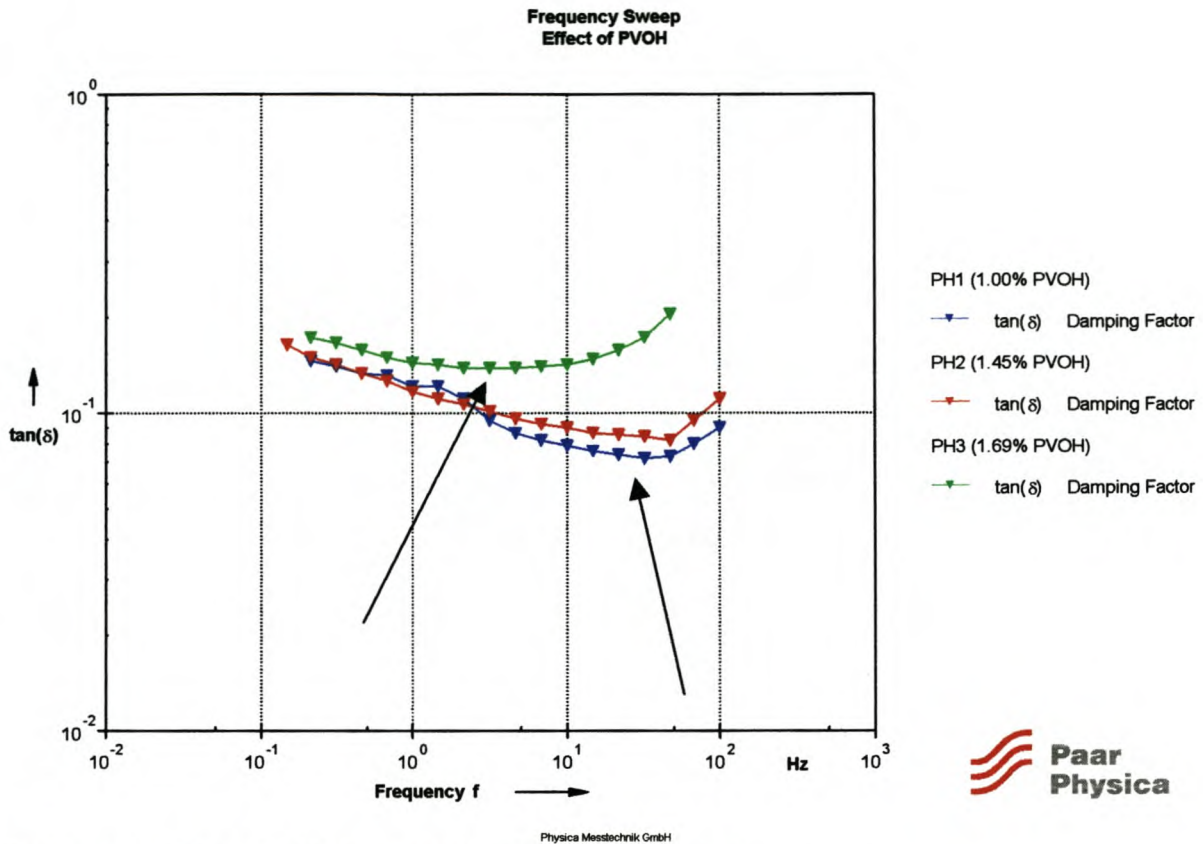


Figure 4-22: Effect of PVOH content on frequency sweeps

Figure 4-22 gives the following information about the sedimentation behaviour of the vesiculated beads:

- The sample with the largest amount of PVOH (PH3) has the highest $\tan \delta$ values at small frequencies and therefore suggests, as suspected, that this sample is most likely to show some degree of sedimentation, although $\tan \delta$ is still smaller than 1 and therefore should not tend to sedimentate.
- An increase in the amount of PVOH causes the sample to ‘flow’ sooner in the high-frequency area. This onset of flow occurs when G'' starts to increase with respect to G' , in other words where the $\tan \delta$ values start to increase (illustrated by arrows). This phenomenon was also observed with a decrease in the amount of HEC (see section 4.4.1.3). Therefore an increase in the amount of PVOH can lead to instability of the dispersion.

4.4.2.4 Three-Interval-Thixotropy-Test (3-ITT)

The effect of PVOH on the structural recovery is illustrated in Figure 4-23.

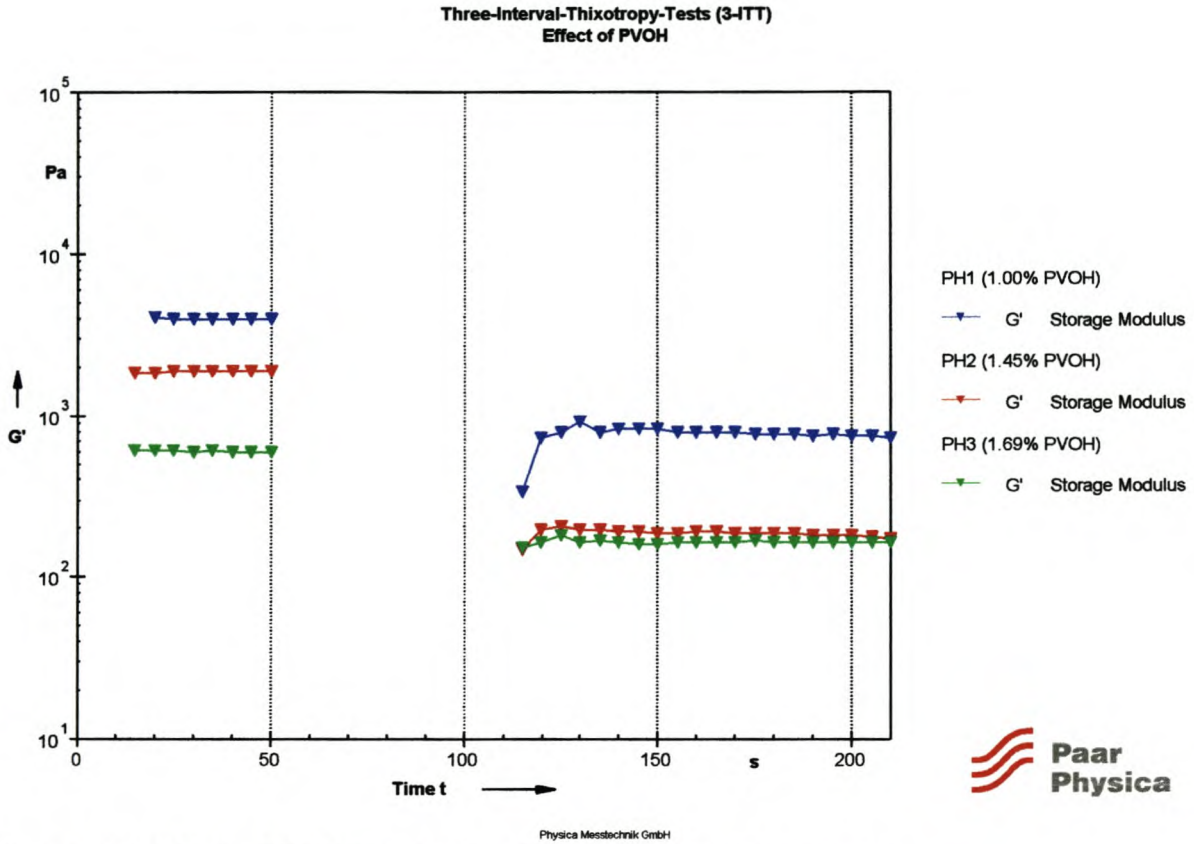


Figure 4-23: Effect of PVOH content on the structural recovery curves

Figure 4-23 gives the following information about the structural recovery of the vesiculated beads after high shear:

- The degree of structural recovery after 1 minute into the recovery phase is given as follows:

1.00% PVOH – 4.39% recovery

1.45% PVOH – 9.26% recovery

1.69% PVOH – 27.77% recovery

From the above data it is clear that an increase in the amount of PVOH results in an increase in the amount of structural recovery. This once again supports the ‘lubrication’ theory - the higher the percentage of PVOH present in the sample, the better ‘lubricated’ the beads are and the easier they recover into a state of lowest energy.

- This also supports the theory that the recovery of the dispersion is not a function of the aqueous phase (water and HEC), but rather of the polymer particles and its surface-active agent, PVOH.

4.4.2.5 Conclusions

The following are the most important conclusions that can be drawn:

- The viscosity decreases as the amount of PVOH increases;
- The structural strength (G'), the LVER and the yield point decrease linearly with an increase in the amount of PVOH and therefore indicate a decrease in the stability of the sample;
- The $\tan \delta$ values of the frequency sweep indicate that the tendency of the solid particles to sedimentate become higher as the amount of PVOH increases;
- The degree of structural recovery tends to increase as the amount of PVOH increases;
- The stability of the dispersion decreases with an increase in the amount of PVOH.

4.4.2.6 Practical Implications

The most important practical implications are as follows:

- A large decrease in the amount of PVOH might cause the dispersion to transform into a gelled state at the state of rest due to the increase in structural strength and yield point. This will make pouring and stirring very difficult.
- A decrease in the amount of PVOH will also result in more difficult mixing and pumping due to an increase in the viscosity at higher shear rates.

- An increase in the amount of PVOH makes the dispersion more unstable and therefore more likely to sedimentate. The storage stability therefore decreases with an increase in the PVOH.

4.4.2.7 Concluding Remarks

It is evident that the level of PVOH plays an important role in the hydrodynamic behaviour of the particles. The beads seem to follow the 'lubrication theory' where particle-particle interactions become less with an increase in the lubrication force (increase in PVOH).

4.4.3 Effect of Diethylene Triamine (DETA)

It is of help to look at what role DETA plays in the bead formation process in order to be able to explain the rheological behaviour. Microvoids are formed in the swellable core polymer containing carboxylic acid groups by means of a volatile amine, DETA. The particles are subjected to the DETA in the aqueous dispersion to swell the core. The dispersion is dried to remove the swellant and provide a microvoid within the polymer [Sikorski et al., 1984]. Therefore DETA plays a role in the degree of vesiculation which is proportional to the amount of water absorbed into the polymer particle to form the vesicles.

Geoffrey [1982] also states that when the amount of amine of the promoter system is increased, the viscosity of the emulsion may be adversely affected. It is known that organic amines such as DETA may cause excessive thickening and/or general instability of the emulsion when present in excessive amounts.

The amounts of DETA in each sample are as follows:

Table 4-5: Amount of DETA in each sample

Sample	DETA [%]	Average Particle Size [μm]	Particle Size Distribution ⁷ [μm]	Total Solids Content [%]	pH
DETA1 ⁸ :	0.27	2.11	1.46	23.42	6.71
DETA2 ⁹ :	0.34	2.10	1.42	23.19	7.26

4.4.3.1 Viscosity Curves

The effect of DETA on the viscosity curves can be seen in Figure 4-24 below.

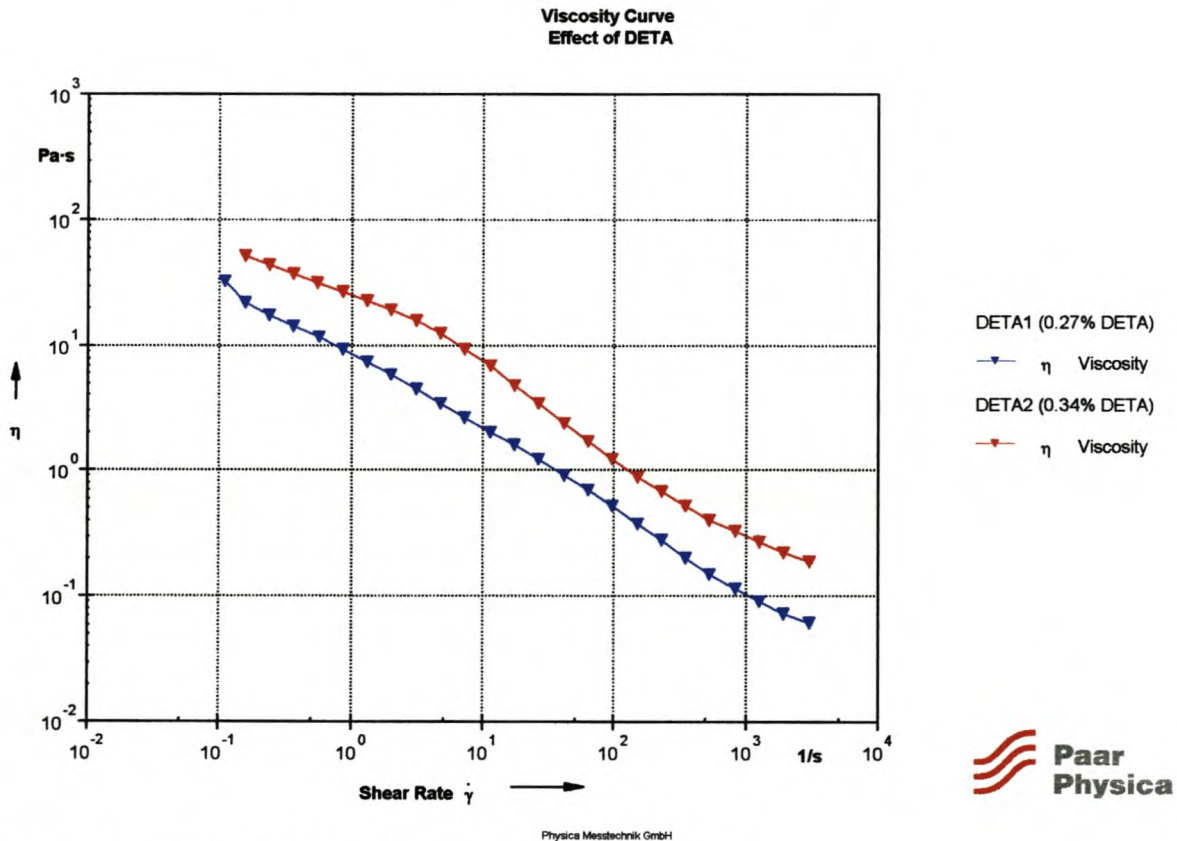


Figure 4-24: Effect of DETA content on the viscosity curves

⁷ Particles size distribution is based on a 95% standard deviation. Therefore, 95% of the particles fall within $x \mu\text{m}$ of the average particle size.

⁸ Standard level of DETA used in beads formulation (50 % more than required for neutralisation of acid groups of polyester).

⁹ 100 % more than required for neutralisation of polyester acid groups

Figure 4-24 shows that:

- The viscosity increases dramatically over the whole shear rate range with an increase in the amount of DETA.

These observations correspond to the findings of Geoffrey et al. [1982] that an increase in the amount of DETA may have a drastic effect on the thickening of the dispersion. A 32% increase in the amount of DETA has the following effect on the low- and high-shear viscosities:

Table 4-6: Effect of DETA on low- and high-shear viscosity

	Low-shear viscosity @ 1 s^{-1} [Pa.s]	High-shear viscosity @ 3000 s^{-1} [Pa.s]
DETA1:	7.32	0.06
DETA2:	22.7	0.19
Viscosity increase: [%]	± 300	± 300

Therefore, increasing the amount of DETA by 1%, results in an increase in the viscosity of $\pm 10\%$, which indicates that the system is very sensitive to changes in the levels of DETA.

4.4.3.2 Amplitude Sweeps

The effect of DETA on the amplitude sweeps can be seen in Figure 4-25 below.

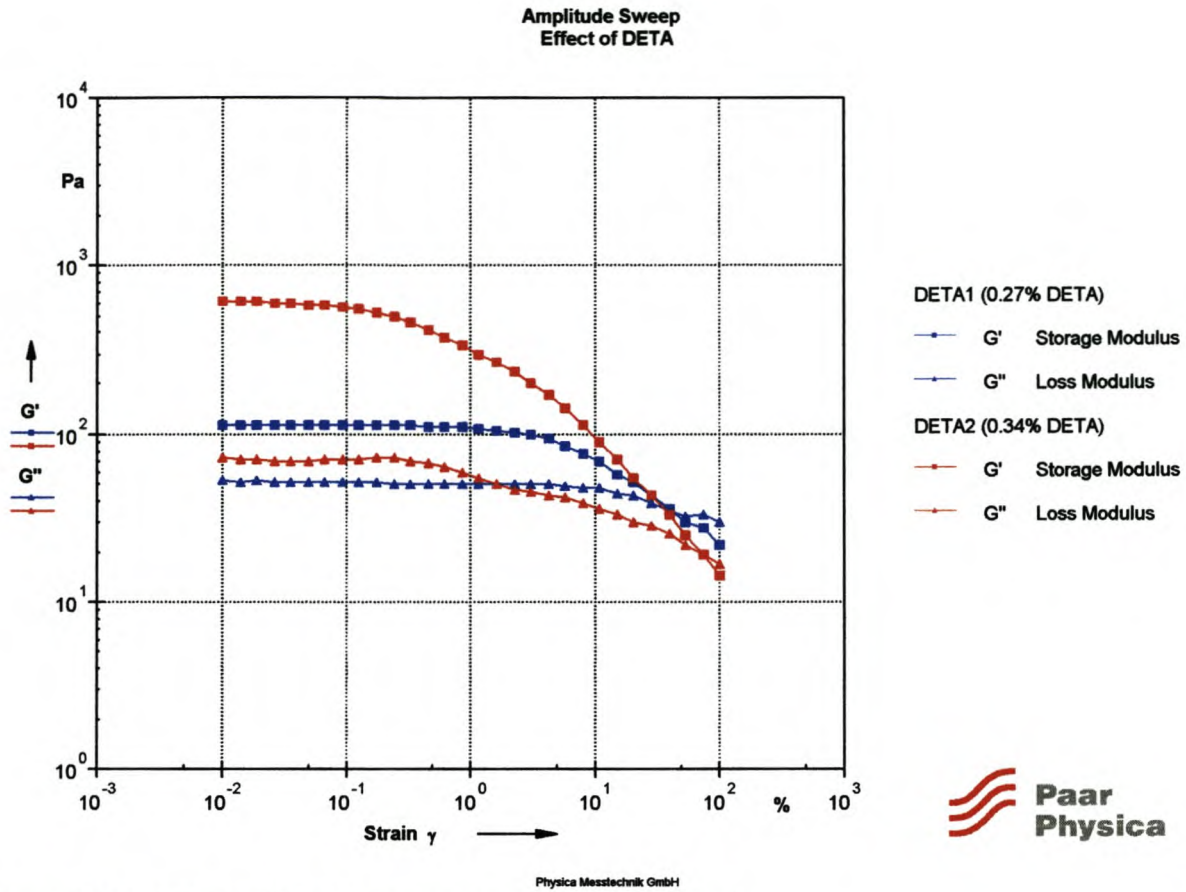


Figure 4-25: Effect of DETA content on amplitude sweeps

Figure 4-25 reveals the following information about the character of the vesiculated beads:

- The solid-like character (G') in the LVER increases significantly (± 6 times) with an increase in the amount of DETA;
- A large increase in the $\tan \delta$ values (G''/G') occurs with an increase in DETA.

According to the proposed mechanism for the formation of the beads, increasing the amount of DETA will result in a decrease in the amount of water in the aqueous phase on the ‘outside’ of the polymer particles because more water is absorbed *into* the polymer particle. Therefore, examining the ratio of the liquid- to solid-like (G''/G') behaviour will result in a clearer picture.

The ratio between the liquid- and solid-like behaviour ($\tan \delta = G''/G'$) is given in Figure 4-26 below.

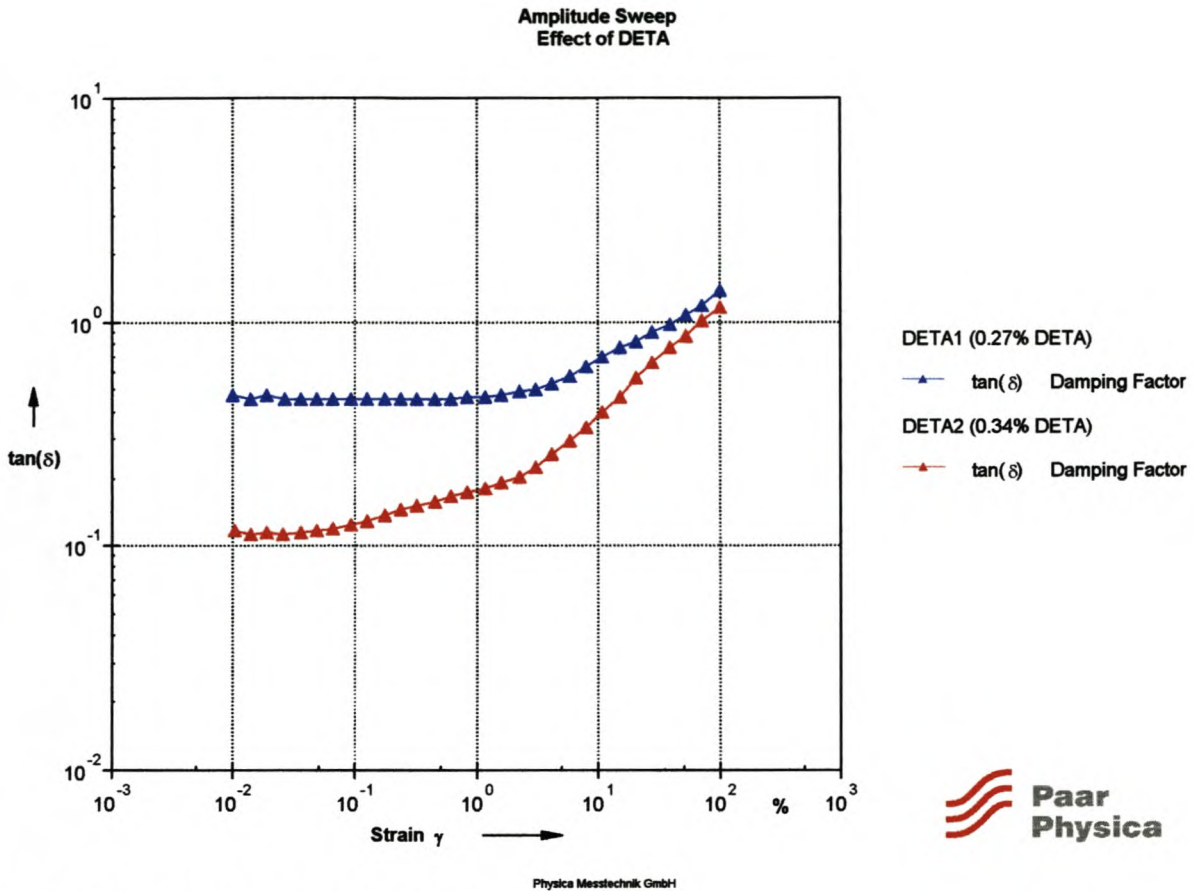


Figure 4-26: Liquid-/solid-like behaviour in LVER

Figure 4-26 gives the following information about the liquid/solid-like behaviour of the vesiculated beads:

- The $\tan \delta$ value in the LVER decreases with an increase in the amount of DETA. That is, G''/G' decreases with an increase in the amount of DETA and therefore G'' decreases with respect to G' . This corresponds with the proposed mechanism that an increase in the amount of DETA results in more water being absorbed into the polymer particle and therefore there is less water in the aqueous (viscous) phase, which results in more solid-like behaviour.

4.4.3.3 Frequency Sweeps

The effect of DETA on the frequency sweeps is given in Figure 4-27 below.

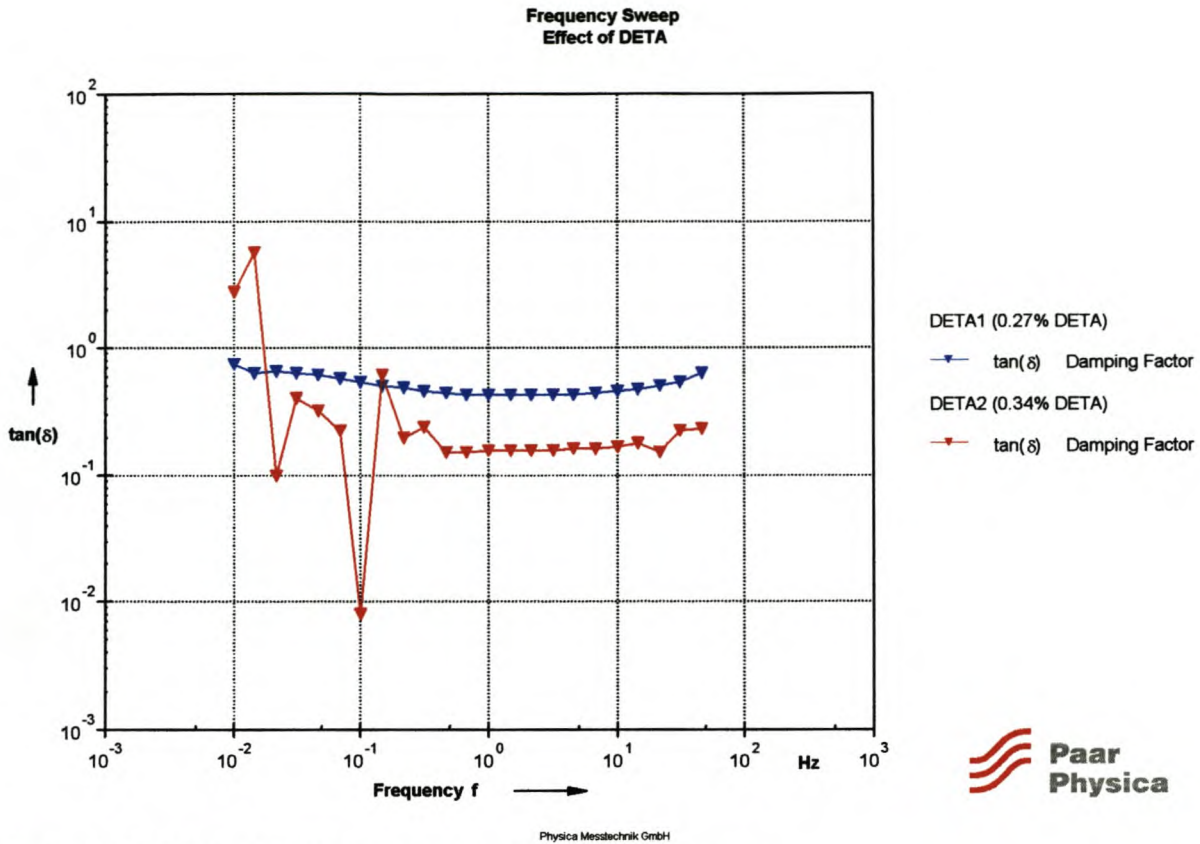


Figure 4-27: Effect of DETA content on the frequency sweeps

Figure 4-27 reveals the following information about the vesiculated beads in the LVER:

- The $\tan \delta$ -values for the dispersion with the normal amount of DETA (DETA1) seem to be constant over the whole frequency range, including the low frequencies. The dispersion with the higher amount of DETA (DETA2) seems to be unstable at low frequencies (< 0.5 Hz). This may be due to the higher apparent ‘solid content’ in the dispersion. Inter-particle actions become more frequent at higher apparent ‘solids content’, which results in a jagged response, which is illustrated in the frequency sweep at low frequencies. The measuring system ‘struggles’ to measure the properties at low frequencies due to the higher solid-like character.

4.4.3.4 Three-interval-thixotropy-test (3-ITT)

The effect of DETA on the structural recovery is given in Figure 4-28 below.

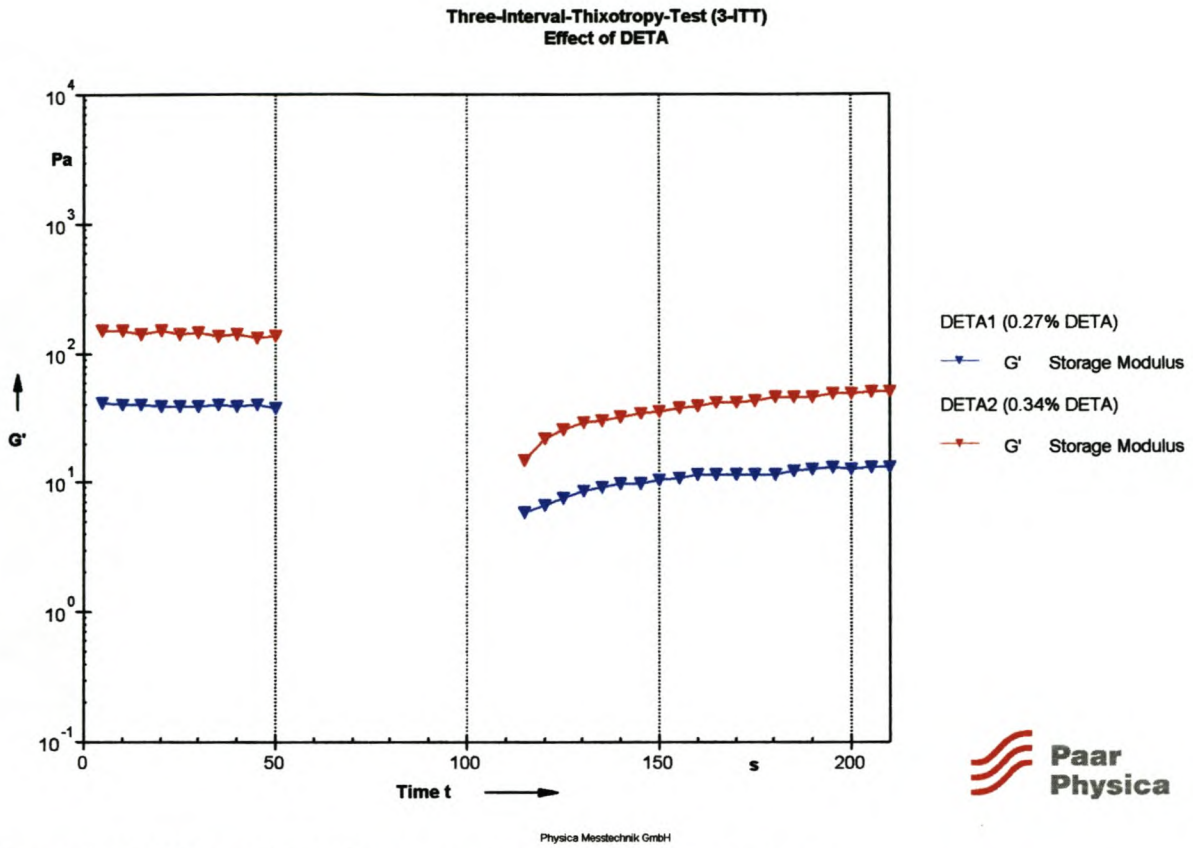


Figure 4-28: Effect of DETA content on structural recovery curves

The degree of structural recovery is given in the table below.

Table 4-7: Degree of structural recovery after 80 seconds

Sample	Degree of structural recovery [%]
DETA1:	36.5
DETA2:	33.8

From Table 4-7 it is apparent that the difference in the degree of structural recovery is not significant and therefore the addition of DETA does not have such a big effect on the recovery as it does on the character of the sample.

4.4.3.5 Conclusions

- An increase in the amount of DETA causes a large viscosity increase over the whole shear rate range.

- An increase in the amount of DETA results in a drastic increase in the structural strength G' of the dispersion. But the structural strength can very easily increase too much, so that the dispersion has a gel-like character which makes workability (pumping, mixing, pouring) impossible.
- An increase in the amount of DETA results in a sharp decrease in the $\tan \delta$ values, therefore indicating a sharp increase in the solid-like character from liquid-like character.
- An increase in the amount of DETA does not have a great effect on the degree of structural recovery.

4.4.3.6 Practical Implications

Not only does DETA have a great effect on the degree of vesiculation, but also on the rheological behaviour of the dispersion. A large increase in the viscosity behaviour and the structural strength is observed with small increases in the amount of DETA. This thickening effect by increasing the amount of DETA may cause the sample to become gel-like and therefore make handling (stirring, mixing, pumping, etc.) difficult.

Care must therefore be taken to add exactly the correct amount of DETA. Currently, 0.27% (by mass) of DETA is added to the vesiculated beads formulation for neutralisation of the polyester acid groups, resulting in DETA levels which are in excess of 50%.

4.4.4 Effect of LMA

Laurel methacrylate (LMA) is added to the vesiculated beads dispersion in order to make the beads water resistant. The LMA makes up 0.32 % of the dispersion. Original literature, such as the patents on producing vesiculated beads, does not describe a component that makes the beads water resistant and therefore there is no literature which describes the effect of LMA on the rheology of the vesiculated beads. There is, however, a preliminary patent application for vesiculated beads with

additional LMA. Rheological tests are used to investigate the dependency of various rheological properties on the addition of LMA.

4.4.4.1 Viscosity Curves

The effect of LMA on the viscosity curves is illustrated in Figure 4-29 below.

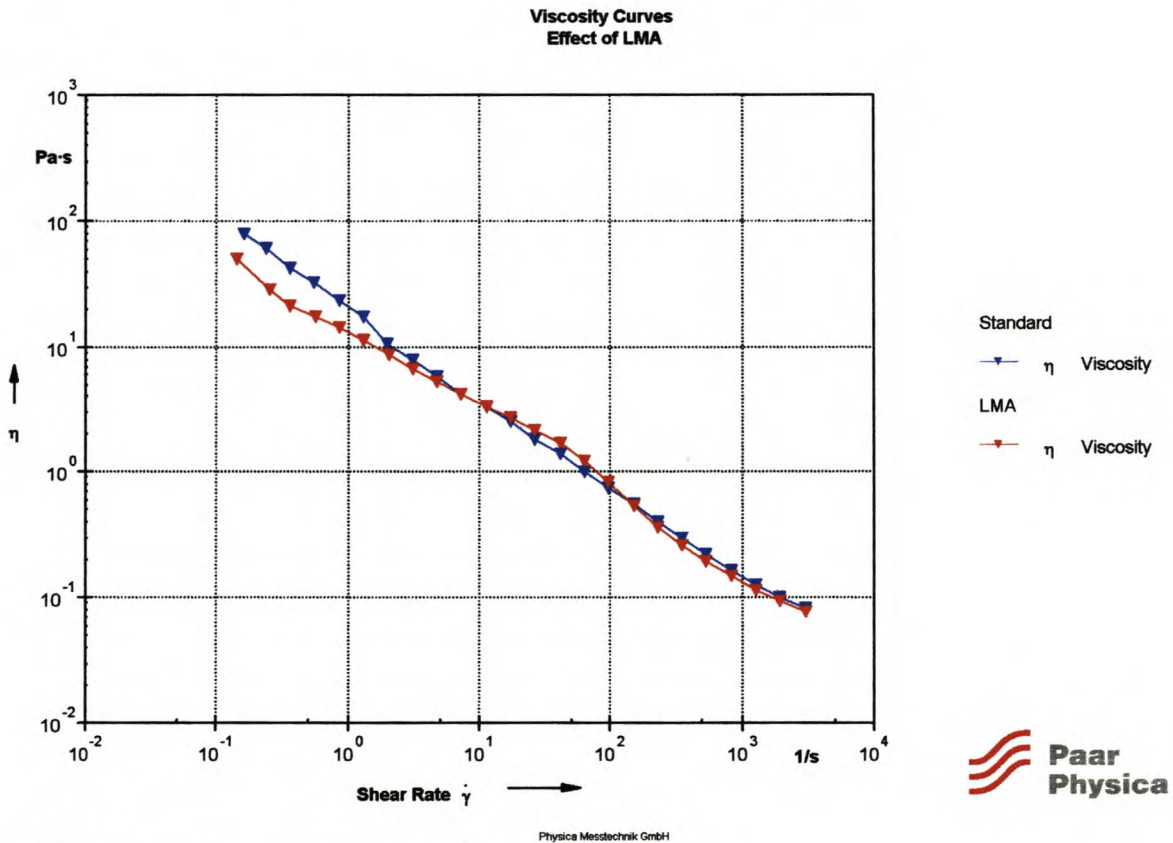


Figure 4-29: Effect of LMA on viscosity curves

Figure 4-29 shows what effect the addition of LMA has on the flow behaviour of the vesiculated beads:

- It appears as if the viscosity of the dispersion is unaffected by the addition of LMA. Tests carried out in the LVER will indicate whether the addition of LMA changes the internal structure of the sample.

4.4.4.2 Amplitude Sweeps

The effect of LMA on the amplitude sweeps is illustrated in Figure 4-30.

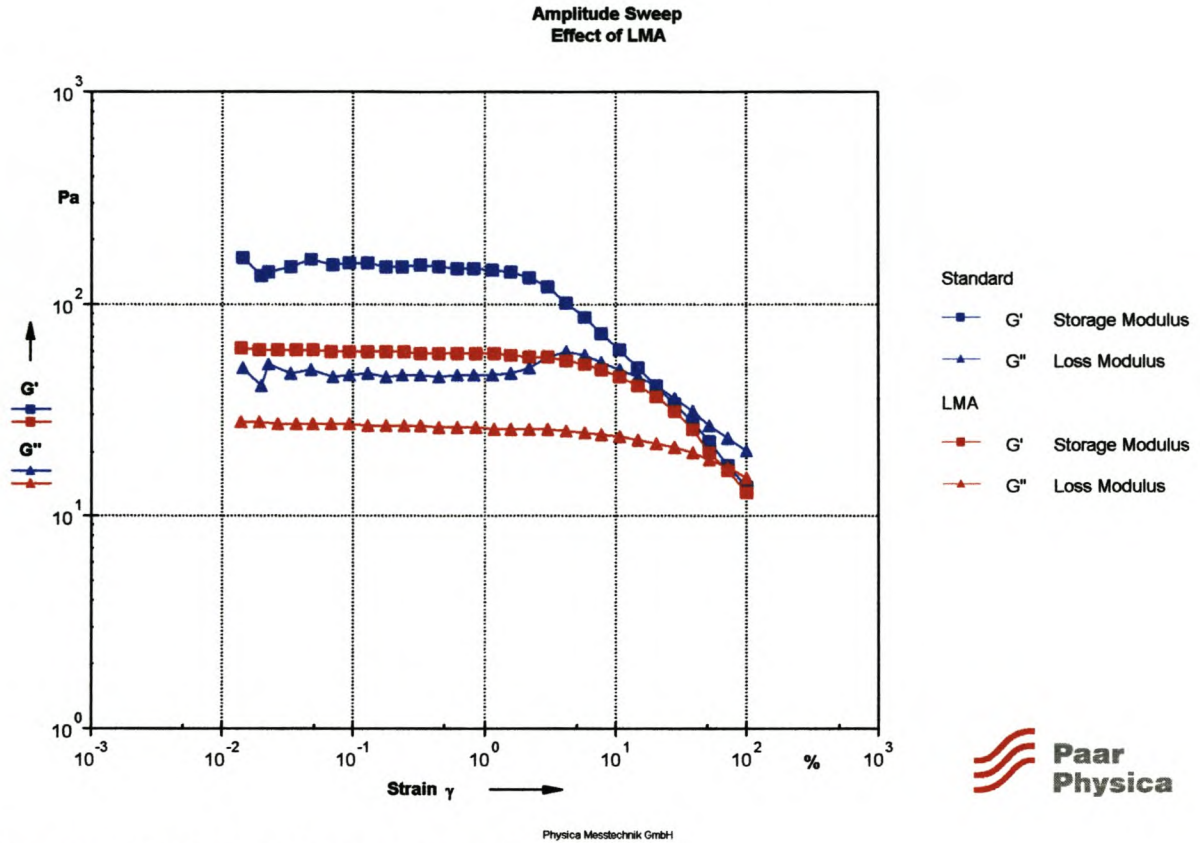


Figure 4-30: Effect of LMA on the amplitude sweeps

Figure 4-30 illustrates what effect the addition of LMA has on the character of the vesiculated beads:

- The addition of LMA results in a change in the internal structure of the sample. LMA causes the G' and G'' values in the LVER to decrease and hence there is a decrease in the degree of structural strength.

4.4.4.3 Frequency Sweeps

The effect of LMA on the frequency sweeps is illustrated in Figure 4-31 below.

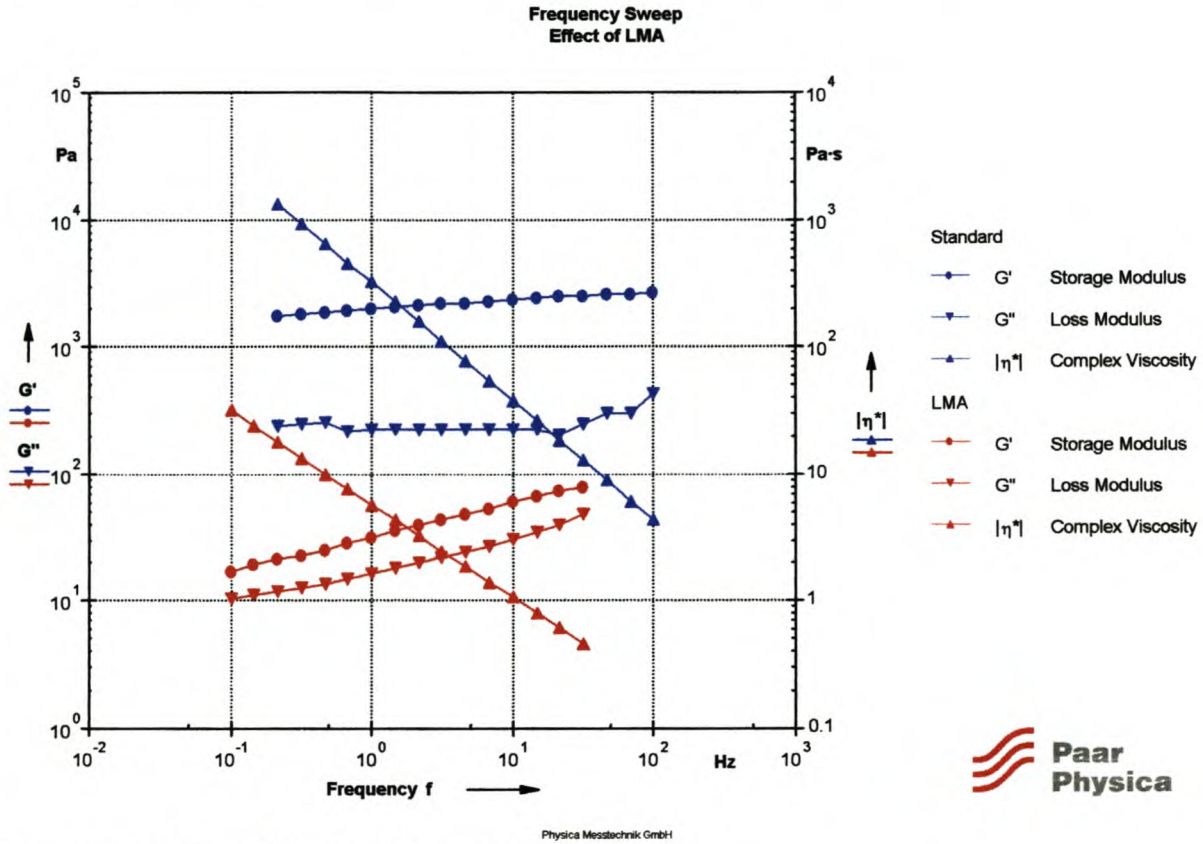


Figure 4-31: Effect of LMA on frequency sweeps

Figure 4-31 shows how addition of LMA affects the character of the vesiculated beads in the LVER:

- Although the viscosity curves in section 4.4.4.1 do not illustrate the difference in the flow behaviour, the complex viscosity $|\eta^*|$ measured in the LVER does illustrate the difference in the deformation properties of the sample;
- The G' and G'' values of the sample without the LMA (standard) run almost parallel to each other, with only a very slight slope, indicating a relative strong structural strength. The G' and G'' values of the sample with the LMA also run parallel to each other, but at a steeper slope and therefore indicate a lower degree of structural stability;
- $G' \gg G''$ for the sample without the LMA (standard), while $G' > G''$ for the sample with the LMA and therefore addition of LMA causes a decrease in the structural stability over the whole frequency range.

4.4.4.4 Conclusions

- The first impression one gets from the viscosity curves is that the addition of LMA does not change the flow and deformation properties of the sample - there appears to be no difference in the viscosity behaviour of the samples.
- By investigating the structure of the sample further by means of tests in the LVER, it becomes apparent that the addition of LMA does have an effect on the rheological properties of the samples, causing a decrease in the degree of structural strength and the dispersion stability.

4.4.4.5 Practical implications

Addition of LMA will have the following practical implications:

- Addition of LMA has a decreasing effect on the structural strength of the sample as well as the dispersion stability. This may lead to possible sedimentation or phase separation behaviour.

4.5 Effect of Physical Properties – Particle Size

The Cowles process was used to investigate the effect of particle size and particle size distribution on the rheology of the vesiculated beads dispersion. Three different samples were produced with the following properties (28% solids content):

Table 4-8: Particle size with corresponding Cowles impeller speed

Sample	Stirring Speed [rpm]	Particle Size [μm]	Particle Size Distribution ¹⁰ [μm]
Cowles 1:	619	3.12	1.52
Cowles 2:	498	4.82	2.40
Cowles 3:	389	7.64	4.39

¹⁰ Particles size distribution is based on a 95% standard deviation. Therefore, 95% of the particles fall within x μm of the average particle size.

4.5.1 Viscosity Curves

The effect of particle size on the viscosity curves is illustrated in Figure 4-32 below.

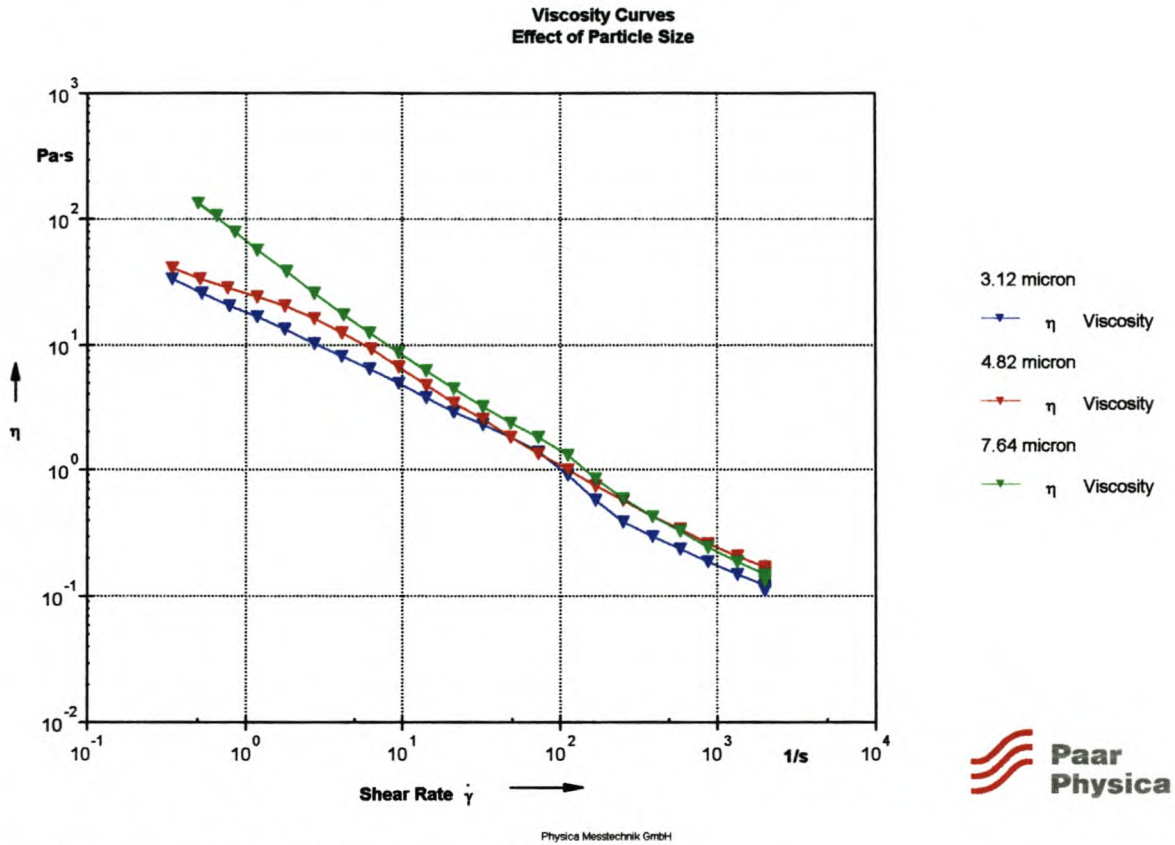


Figure 4-32: Effect of particle size on viscosity curves

Figure 4-32 gives the following information about the flow behaviour of the vesiculated beads:

- A decrease in the stirrer speed has the effect of increasing the particle size and particle size distribution, which results in an increase in the viscosity, especially in the low-shear rate range. Mewis et al. [2000] studied the effect of particle size distribution on the rheology of sterically stabilised dispersions and lattices. He states that the particle size distribution can have a profound effect on the rheology. The maximum packing is an important characteristic parameter. A mixture of different sizes can be packed more densely than monodisperse particles, which increase the maximum packing. Larson [2000] also states that the viscosity of high solid-load dispersions becomes very sensitive to small variations in particle properties such as surface roughness, size and shape, polydispersity, etc.

The dependency of low-shear viscosity on the stirrer speed is given in the figure below.

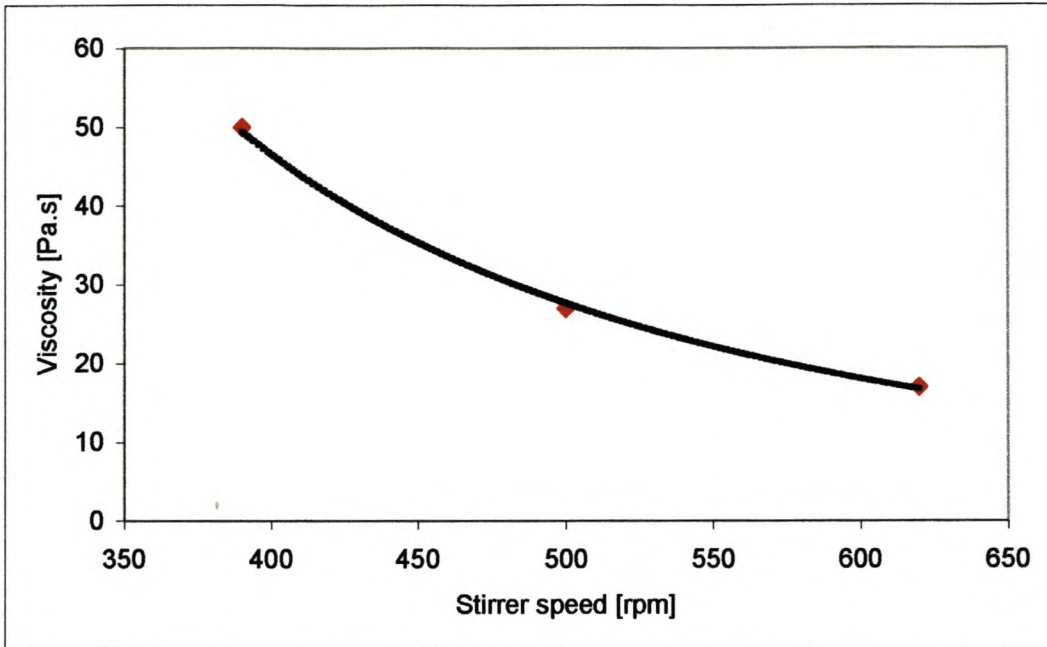


Figure 4-33: Relationship between low-shear viscosity ($\dot{\gamma} = 1 \text{ s}^{-1}$) and the stirrer speed

The dependency of the particle size (PS) and particle size distribution (PSD) is given in the figure below.

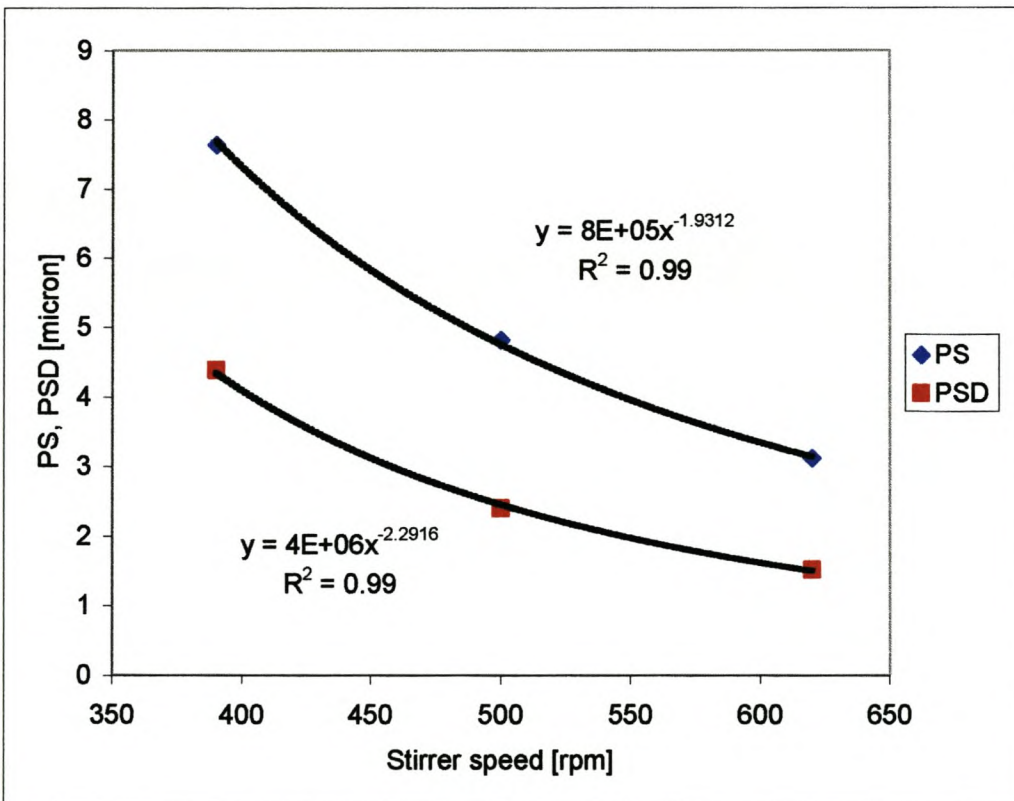


Figure 4-34: Correlation between particle size (PS), particle size distribution (PSD) and stirrer speed

The particle size distribution curve in Figure 4-34 and the viscosity curve in Figure 4-33 have very similar trends, because their power-law indexes are very similar (-2.29 and -2.33 respectively). Therefore it is possible that the particle size distribution has a greater effect on the viscosity than the actual particle size (power-law index is -1.93). However, only three data points were used for this correlation and therefore it must be remembered that a considerable degree of uncertainty remains;

- The sample with larger particle size and particle size distribution is more pseudoplastic. Mewis et al. [2000] also states that the particle size distribution can give rise to a very broad shear-thinning region.

4.5.2 Amplitude Sweep

The effect of particle size on the amplitude sweeps is illustrated in Figure 4-35 below.

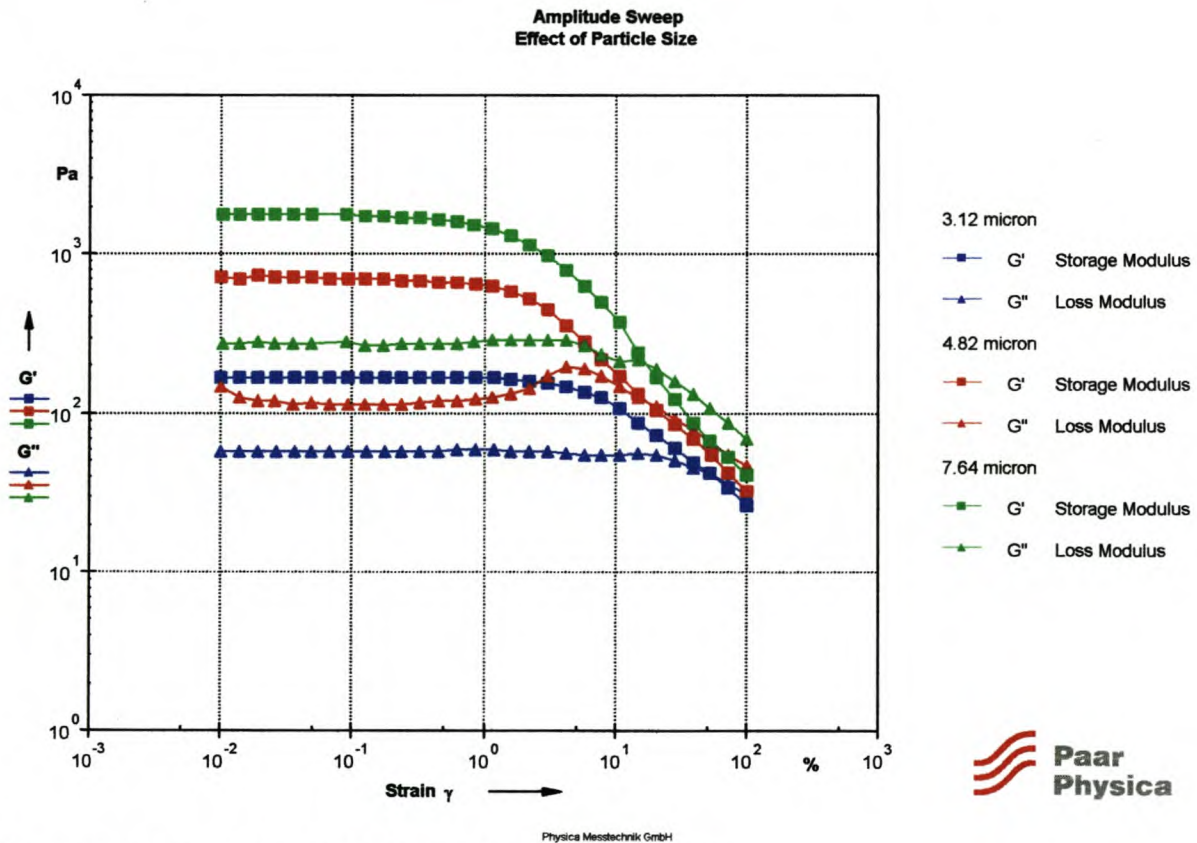


Figure 4-35: Effect of particle size on the amplitude sweep

Figure 4-35 shows what effect the particle size has on the character of the vesiculated beads:

- $G' > G''$ for all the samples in the LVER and therefore the solid-like behaviour predominates over the liquid-like behaviour and the samples show some form of rigidity;

- The structural strength (G') increases with an increase in the particles size. This may be due to the wider particle size distribution, which results in a more densely packed structure and therefore a higher structural strength. The relationship between G' , G'' and the stirrer speed is given in the figure below.

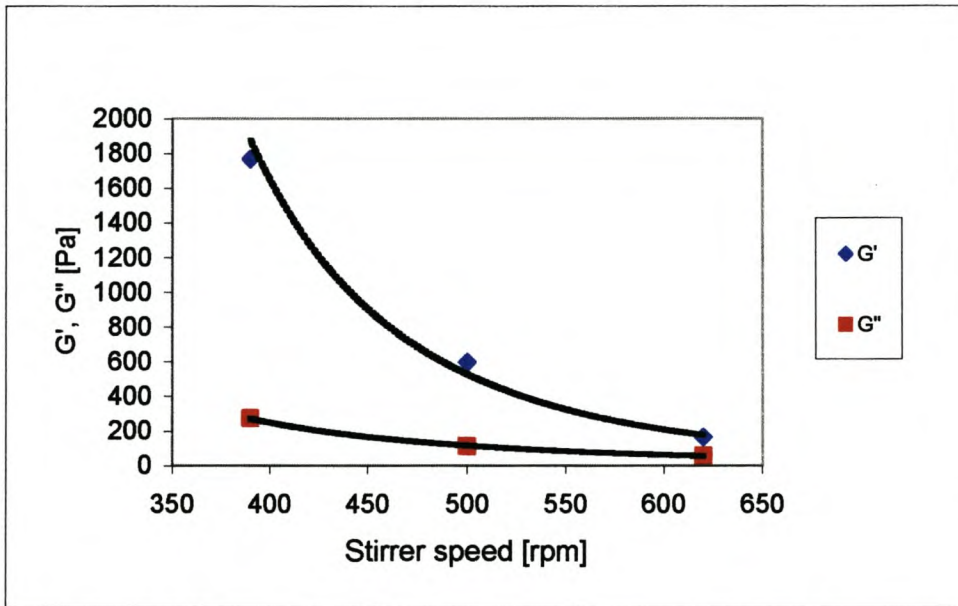


Figure 4-36: Relationship between G' , G'' in the LVER and the stirrer speed

The graph reveals that G' is affected more by the stirrer speed than G'' and decreases faster than G'' with an increase in stirrer speed (decrease in particle size). Therefore one can assume that an increase in the stirrer speed results in a decrease in the structural strength.

4.5.3 Frequency Sweeps

The effect of particle size on the frequency sweeps is illustrated in Figure 4-37 below.

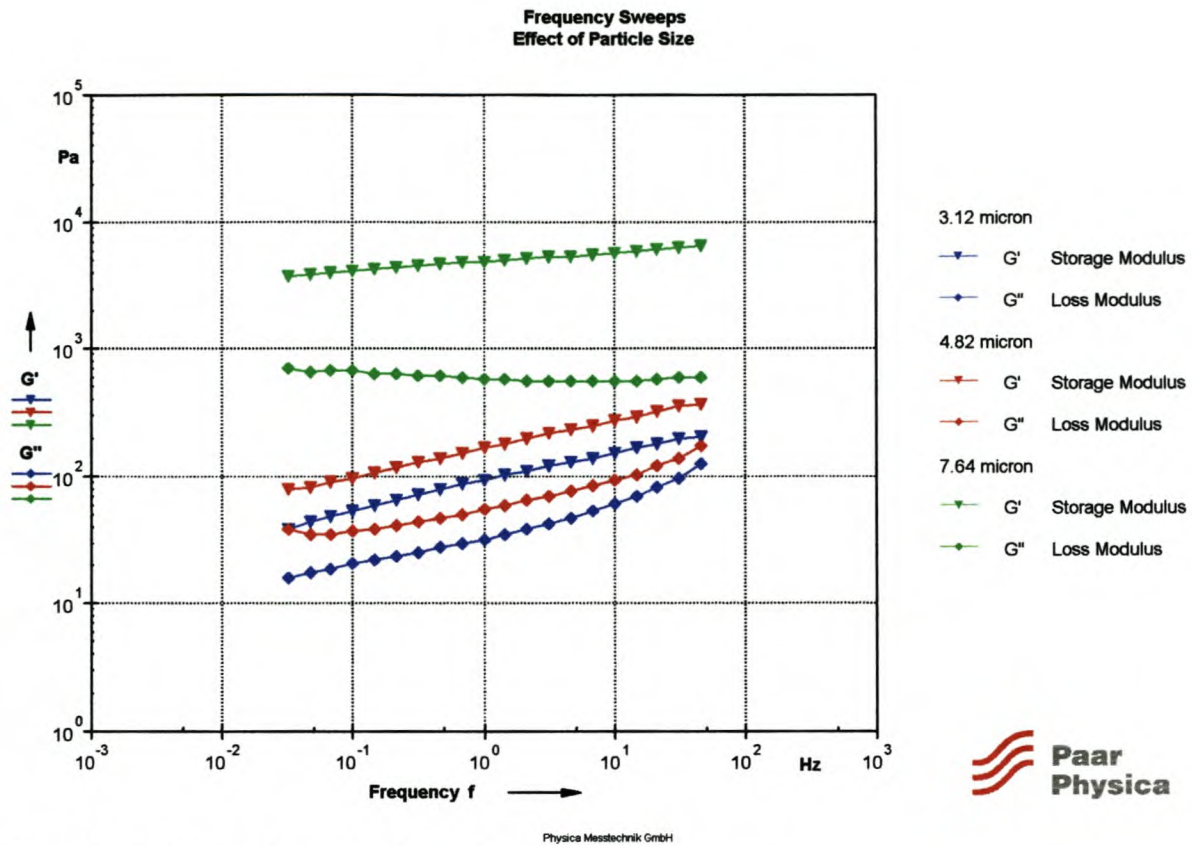


Figure 4-37: Effect of particle size on frequency sweeps

Figure 4-37 gives the following information about the character of the vesiculated beads in the LVER:

- It is clear that the G' and G'' values increase as the average particle size increases;
- The shape of the curves also changes as the average particle size increases. The G' and G'' curves run almost parallel to each other showing very little slope, which is an indication of high structural strength;
- The G' curve of the 7.64 micron beads has a relatively steep slope compared to the G'' curve, which has almost no slope. This indicates that the behaviour of this vesiculated beads sample is highly dependent on the solid-like character and not so much on the liquid-like character;
- $G' \gg G''$ for the sample with the largest particle size, while $G' > G''$ for the samples with the smaller particle sizes. In other word, an increase in the particle size results in an increase in the G' values with respect to the G'' values. This has also been illustrated in Figure 4-36 for the character of the vesiculated beads in terms of G' and G'' in the LVER.

4.5.4 Conclusions

The following conclusions can be drawn:

- A variation in particle size has a large effect on the rheological behaviour of the dispersions;
- An increase in the particle size results in an increase in the viscosity of the dispersion especially the low-shear rate viscosity;
- An increase in the particle size results in a more shear-thinning dispersion;
- G' and G'' increase with an increase in the particle size, but G' is affected more by the variation in particles size than G'' ;
- An increase in the particle size results in an increase in the structural strength of the sample and therefore results in a more stable structure;
- An increase in the particle size results in an increase in stability of the dispersion due to the G' and G'' curves that run almost parallel to each other with little slope in the frequency sweep;
- It appears as if the particle size distribution has a great effect on the rheology of the dispersion. A larger particle size also results in a wider particle size distribution, which seems to be the cause of the increase in the structural strength.

4.5.5 Practical Implications

- The increase in viscosity as the particle size increases will result in more viscous flow behaviour, making workability (mixing, stirring and pumping) more difficult.
- The increase in the structural strength as the particle size increases will result in a more stable dispersion, which assists in acting against sedimentation and phase separation behaviour.

4.6 Effect of Manufacturing Parameters

The homogeniser can operate with different processing parameters. Two of these parameters are examined to determine the effect on the rheology of the dispersion.

4.6.1 Effect of Number of Passes¹¹

A change in the number of passes affects the shear in the homogeniser, with the following analogy in mind:

increase in number of passes = increase in total duration of shear.

The effect of the number of passes is investigated by using 1, 2 and 3 passes respectively. Only amplitude and frequency sweeps are performed on these samples in order to obtain the character of the sample in the LVER.

4.6.1.1 Amplitude Sweeps

The effect of the number of passes on the amplitude sweeps is illustrated in Figure 4-38 below.

¹¹ One pass is the equivalent of flow once through the homogeniser.

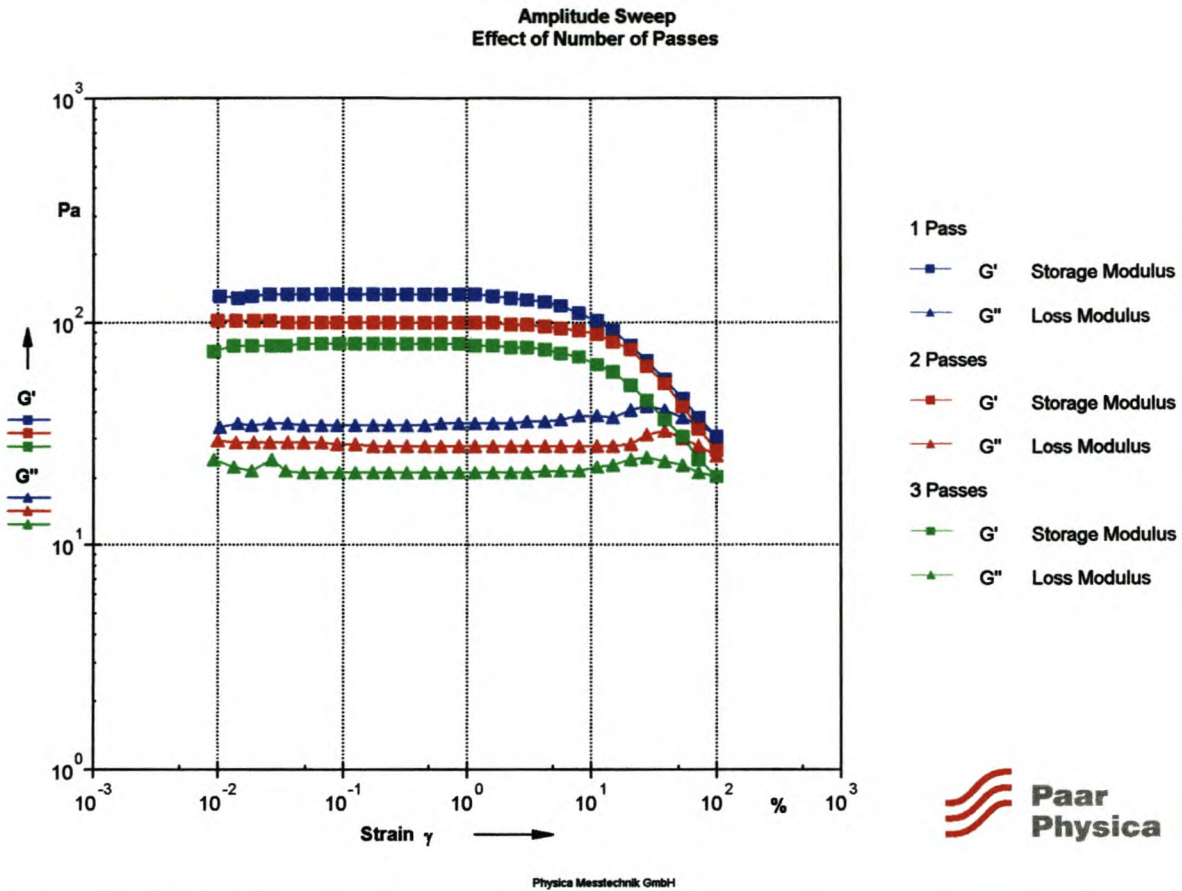


Figure 4-38: Effect of number of passes on the amplitude sweep

Figure 4-38 reveals the following information about the character of the vesiculated beads:

- G' and G'' values in the LVER decrease with an increase in the number of passes. This is analogous to results obtained earlier in section 4.3 – an increase in the amount of shear results in a decrease in the solid-like behaviour (G') of the sample. It must, however, also be mentioned that an increase in the number of passes also results in a decrease in particle size as mentioned in section 4.5.1. A decrease in particle size also results in a decrease in the solid-like behaviour. This makes it difficult to investigate *only* the effect of the number of passes on the solid like (storage modulus G') behaviour in terms of the amount of shear.

4.6.1.2 Frequency Sweeps

The effect of the number of passes is illustrated in Figure 4-39 below. G' is on a linear y-axis in order to see the effect of the number of passes more clearly.

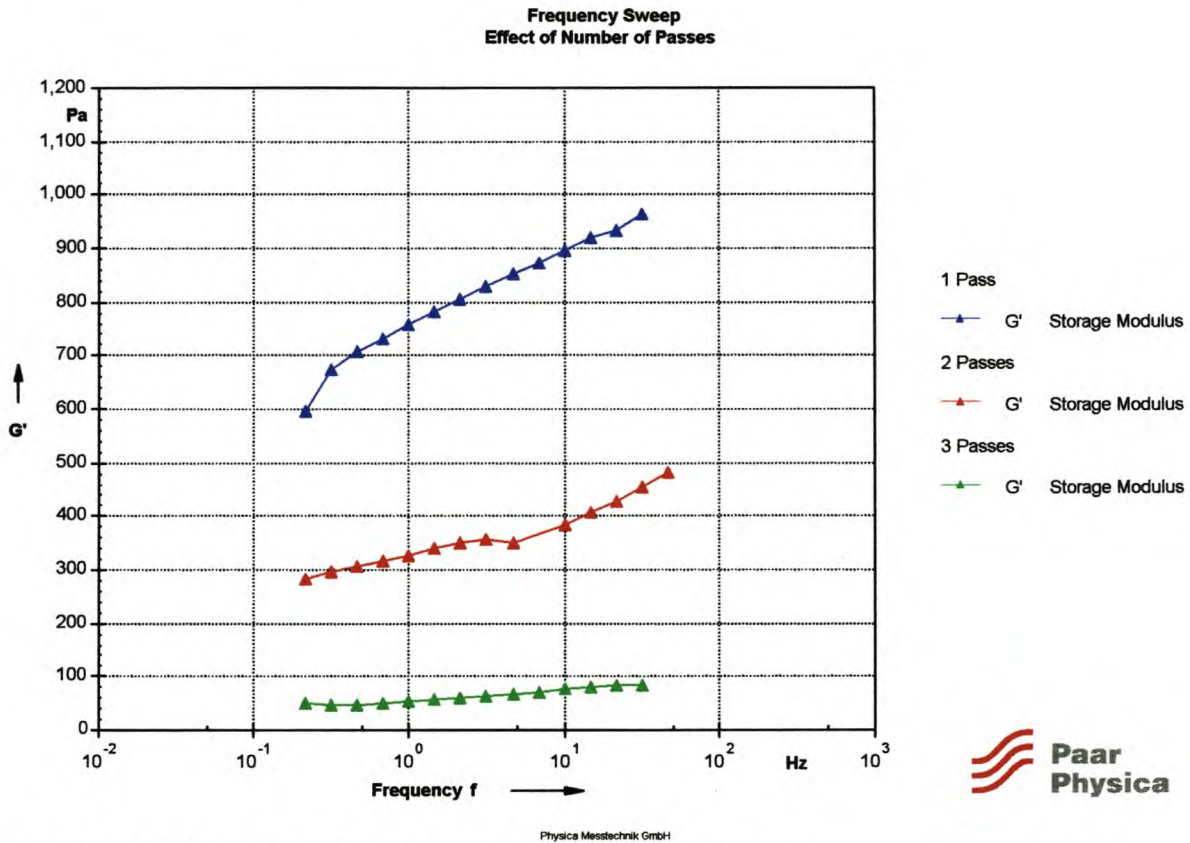


Figure 4-39: Effect of number of passes on the frequency sweep

Figure 4-39 shows that:

- G' decreases with an increase in the number of passes. In other words, the structural strength of the sample decreases as the amount of shear increases. This is the same phenomenon that was observed when examining the different processes to investigate the effect of shear (see section 4.3) - an increase in the shear results in a decrease in the stability of the dispersion;
- But there is also an increase in the gradient of the G' curves as the number of passes decreases, indicating that the network is less stable at lower frequencies. With a very steep slope for the G' curve, as with the beads manufactured with only one pass, there is a possibility of the G' curve crossing the G'' curve at lower frequencies, therefore resulting in liquid-like character ($G'' > G'$), which may lead to possible instability.

4.6.1.3 Conclusions

- An increase in the number of passes results in a decrease in the particle size as well as an increase in the total shear and it has been proven previously that both these factors have an effect on the rheology of the dispersion. Therefore it is difficult to determine exactly what the effect of increasing shear is on the rheology of the vesiculated beads by increasing the number of passes.
- Increasing the number of passes does, however, have an overall effect of decreasing the structural strength (G' values), but making the sample less susceptible to breakdown of the network and therefore in a way makes the dispersion more stable over a wide frequency range.

4.6.2 Effect of Geometry of Plungers

The effect of shear in the homogeniser was also investigated by using two different geometries for the plungers that resulted in two different levels of shear. The plungers differ in groove depth and equation 4-5 is used to determine the degree of shear in each.

Plunger 1:

- groove depth = 1.7 mm
- resulting shear = $\pm 7000 \text{ s}^{-1}$

Plunger 2:

- groove depth = 4.43 mm
- resulting shear = $\pm 1\,000 \text{ s}^{-1}$

Therefore the plunger with the deeper grooves (plunger 2) results in lower shear rates. It must, however, also be kept in mind that the grooves of each plunger are only 25 mm in total length, resulting in very short durations of shear in the grooves.

4.6.2.1 Amplitude Sweep

The effect of the plunger geometry on the amplitude sweeps is illustrated in Figure 4-40 below.

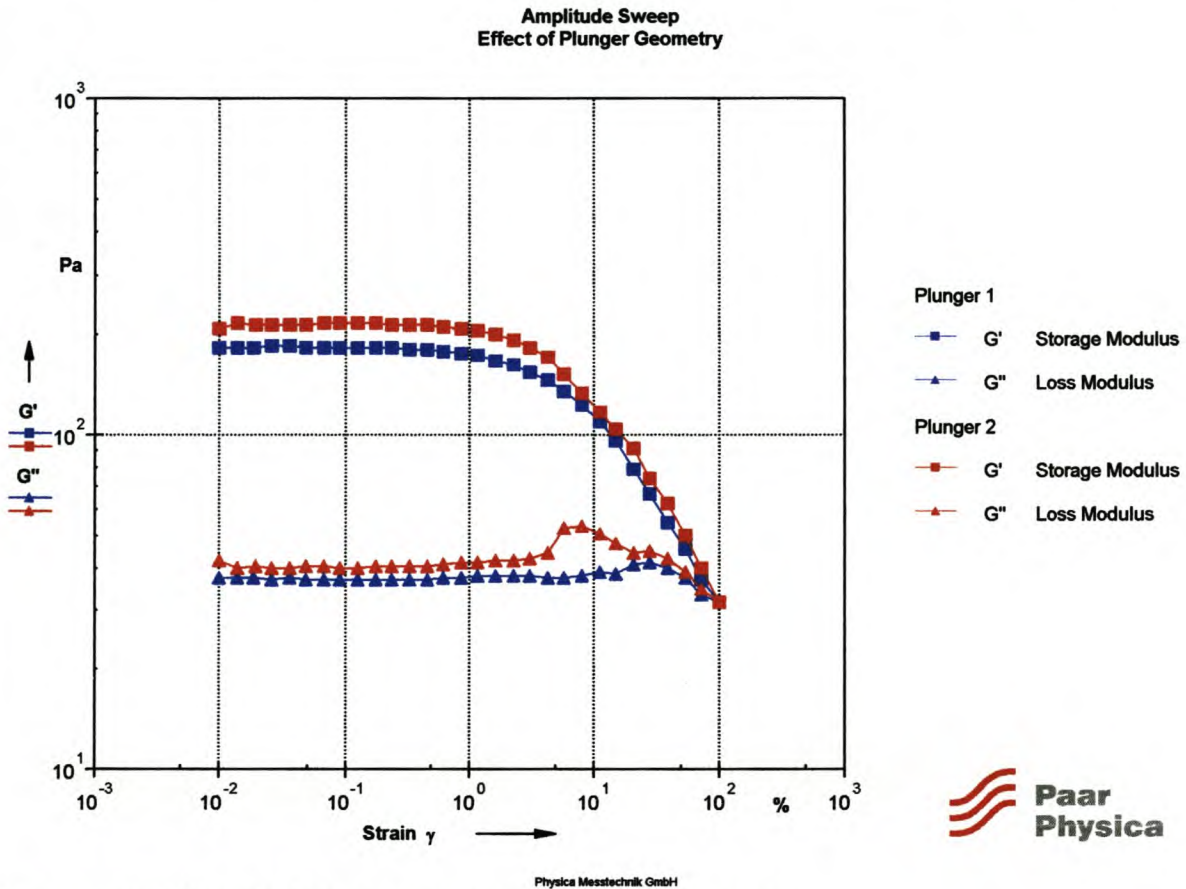


Figure 4-40: Effect of plunger geometry on amplitude sweeps

Figure 4-40 gives the following information about the character of the vesiculated beads:

- There is a slight increase in the storage modulus (G') when plunger 2 (lower shear) is used. The differences in G' curves are not significant in having an effect on the rheology of the samples. One almost expected a larger difference in the G' curves due to the large difference in shear between the two plungers (7000 s^{-1} vs. 1000 s^{-1}), but the short duration of shear might be the reason for the small differences in rheological behaviour;
- The low-shear plunger (plunger 2) causes the G'' curve to have a peak at strain values of $\pm 5\%$ while the other curve does not. As stated earlier, this indicates the existence of

topological restraints that delay the long-range configurational rearrangements of the molecules. This is an indication that there are small differences in the liquid-like character of the samples.

4.6.2.2 Frequency Sweep

The effect of the plunger geometry is illustrated in Figure 4-41 below.

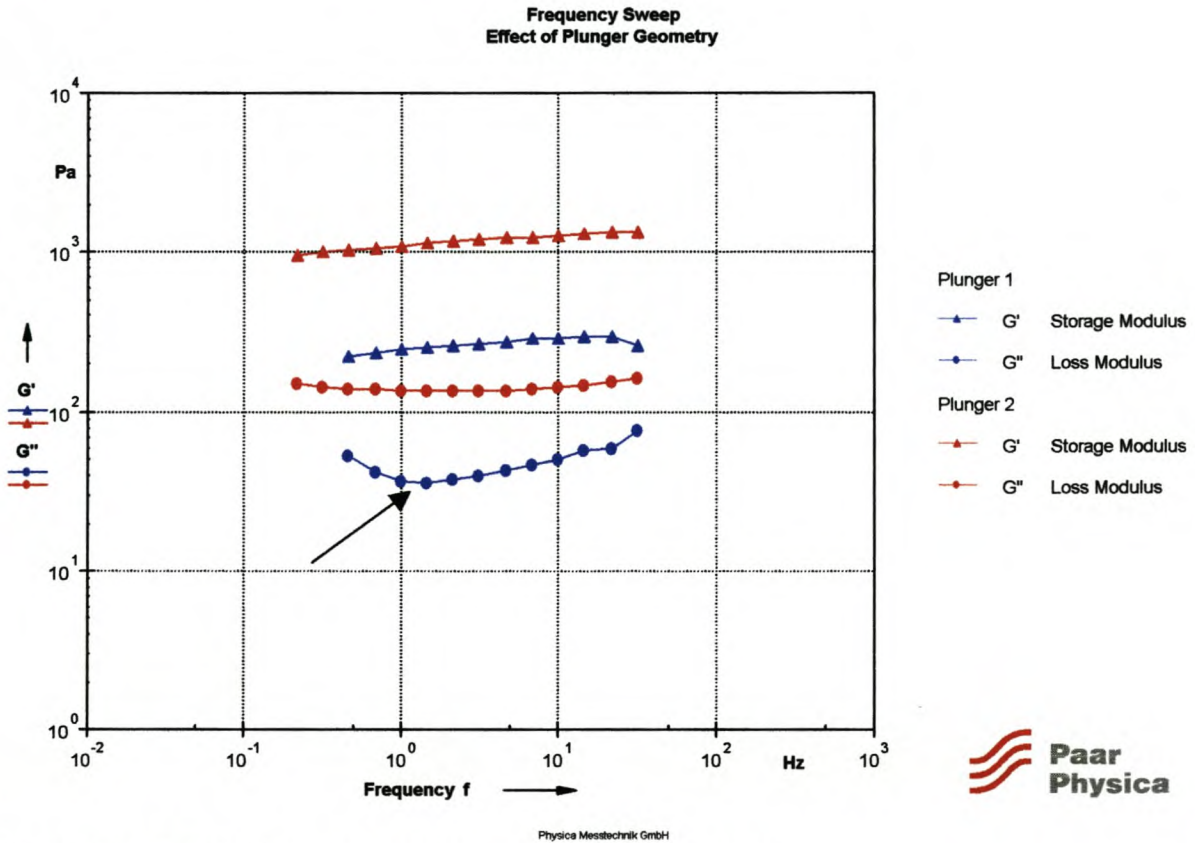


Figure 4-41: Effect of plunger geometry on frequency sweeps

Figure 4-41 reveals the following information:

- The sample produced on plunger 1 (high shear) has a lower structural strength than the sample produced on plunger 2 (low shear);
- $G' > G''$ for both samples and run more or less parallel to each other with little slope, indicating a stable structure;
- The cause/implications of the phenomenon indicated by the arrow in Figure 4-41 is not known.

4.6.2.3 Conclusions

- It appears as if plunger 1 causes a decrease in the structural strength of the dispersion without affecting the stability of the dispersion.

4.7 Curing of the Beads

Curing starts as soon as the initiator system is added. Rheological properties of the sample were measured while the reaction was taking place in the measuring system. In other words, the time-dependent behaviour of the sample while a chemical reaction was taking place was measured. The response is illustrated in the figure below.

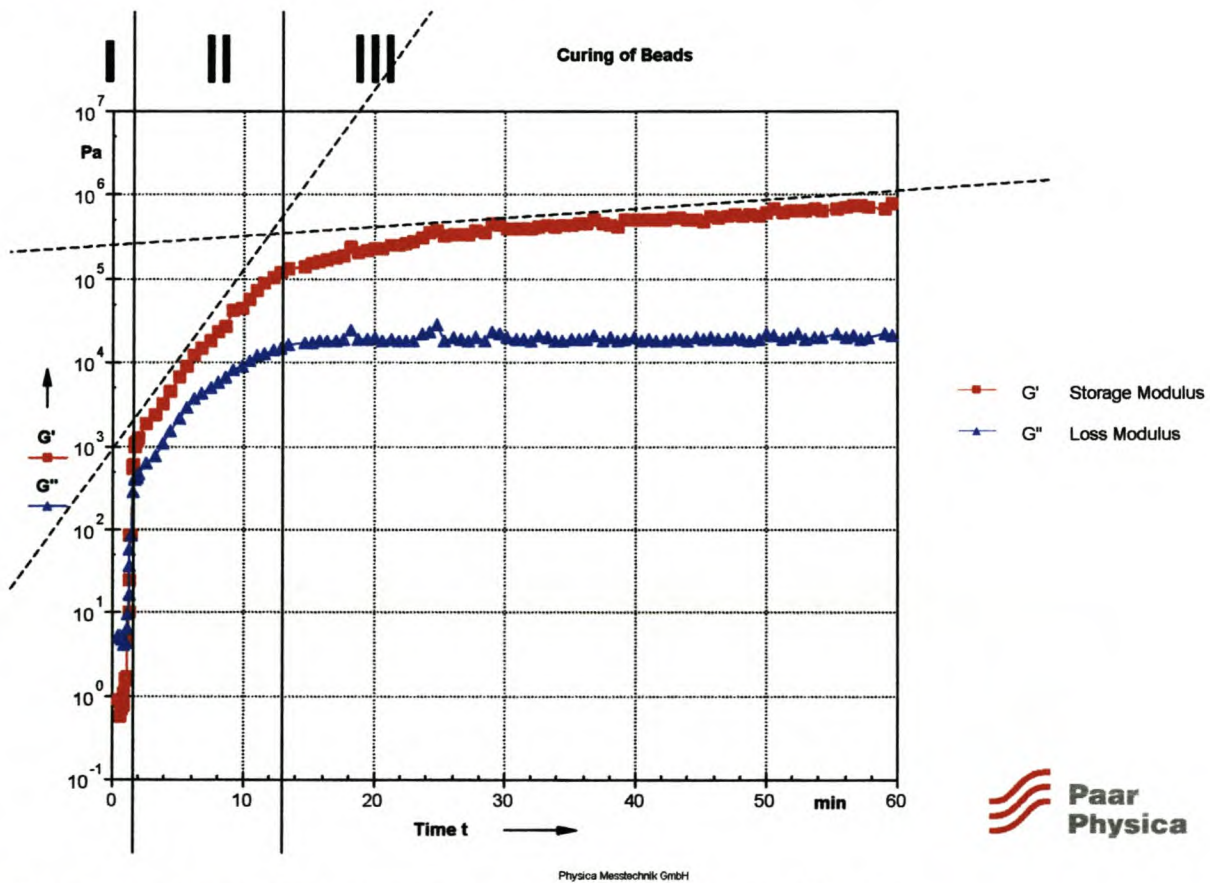


Figure 4-42: Rheological parameters during curing reaction at 70°C

Figure 4-42 can be divided into three main regions, I, II and III (see above):

- Region I: $G'' > G'$ and therefore the liquid-like behaviour predominates over the solid-like behaviour;
- Region II: $G' > G''$ and therefore the solid-like behaviour predominates over the liquid-like behaviour;

- Region III: G' still predominates over the liquid-like behaviour, but the slopes of G' and G'' are different from those of region II. At $t = 15$ min it is clear that there is an inflection point in both G' and G'' . It is also known that the curing reaction reaches an exotherm after 15 minutes. The inflection point can therefore indicate the point where the exotherm is reached and the reaction then takes place at a different rate, resulting in different G' and G'' curves;
- According to Mezger [2002], two time points are of importance during the curing reaction:
 1. The gel-point $G'=G''$
 2. The minimum viscosity.

But he also states that some users refer to the cure time as the tangent lines of the constant, high-plateau value after curing and the previously rapid increase in the curve due to the curing reaction (see dashed lines in Figure 4-42). One can see that the dashed lines cross where the third interval starts at $t=15$ min.

The actual curing of the vesiculated beads is illustrated in Figure 4-43 below [Gous, 2002].

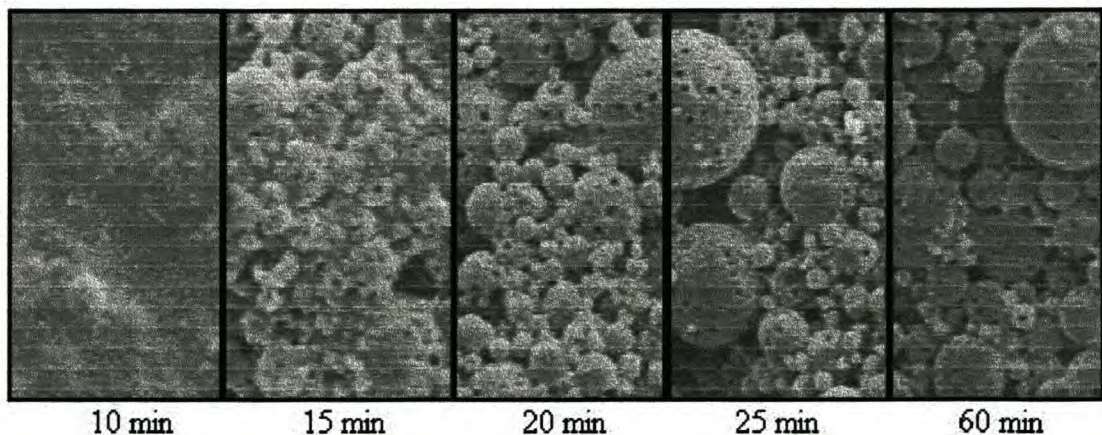


Figure 4-43: SEM photos taken at different stages during the curing of the vesiculated beads

At 10 minutes into the curing reaction one cannot distinguish between the solid-like and liquid-like parts of the sample. Figure 4-42 illustrates that below 10 minutes, the solid-like and liquid-like character are still relatively similar. However, at 15 minutes into the curing reaction one can start to see the formation of the beads and this corresponds to the inflection point in the G' and G'' curves in Figure 4-42. At 20 minutes into the curing reaction the beads are formed, but are still not very discrete. Figure 4-42 illustrates the constant plateau of the G'' curve, which also starts at 20 minutes. Therefore, the liquid-like character of the sample does not change any more and it may be at this point where all the water is already absorbed into the beads to have formed the vesicles. After 20

minutes into the curing reaction the discreteness of the beads improves, which corresponds to the increasing values of the G' curve.

One can focus on region I of Figure 4-42 to examine the first few minutes of the curing reaction in more detail. The first 3 minutes of the curing reaction are given in Figure 4-44 below.

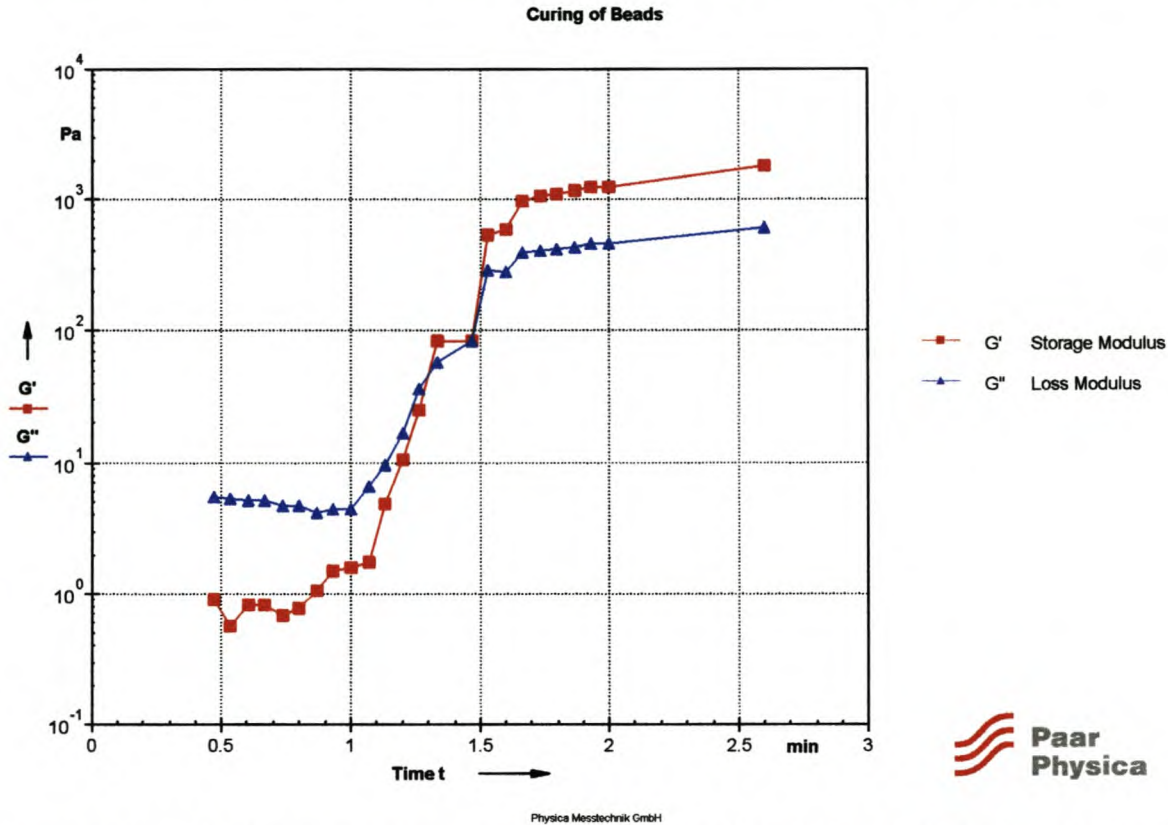


Figure 4-44: Initial changes in character of the vesiculated beads during the curing reaction at 70°C

Figure 4-44 gives the following information about the initial stages of the curing reaction:

- Initially, the curing starts off at $t = 0$ with $G'' > G'$ and therefore the viscous part of the sample predominates over the elastic part;
- G' and G'' start to increase at $t = 1$ minute. The slope of the G' curve is steeper than the slope of the G'' curve and at $t = 1.3$ minutes a cross-over between the G' and G'' curves occurs. In other words, the gel point is reached;
- At $t > 1.3$ minutes, $G' > G''$ and therefore the solid-like behaviour predominates over the viscous behaviour.

Rheology can therefore be used as a useful tool to investigate the curing reaction *as* it is taking place. Properties such as G' and G'' can give valuable information on a possible mechanism for the formation of the beads; however, determining this was not part of this study.

4.8 Conclusions

The following are the most important conclusions that can be drawn regarding vesiculated beads:

- Differences in the character of the beads exist due to differences in the manufacturing processes. These differences in the character of the samples result in different rheological behaviour that can affect the stability of the final product. The differences are thought to be a result of differences in the levels of shear in each process;
- An optimum amount of HEC exists that ensures the stability of the vesiculated beads dispersion and at the same time allows for sufficient flow and deformation behaviour;
- The beads seem to follow the ‘lubrication theory’, where particle-particle interactions become less with an increase in the lubrication force (increase in PVOH). Therefore an optimum amount of PVOH exists that ensures stability of the polymer beads and at the same time allows for sufficient flow and deformation behaviour;
- Excessive amounts of DETA may lead to severe instability and excessive thickening of the beads. The vesiculated beads formulation is very sensitive to changes in the amount of DETA;
- Addition of LMA to the formulation may lead to possible instability of the dispersion without affecting the flow properties;
- An increase in the particle size affects the rheology significantly and also results in an increase in the stability of the dispersion;
- The numbers of passes used in the homogeniser have an effect on the structural strength and the stability of the dispersion. Increasing the number of passes results in a decrease in the structural strength, but makes the dispersion more stable over a wider frequency range;
- The plunger geometry used in the homogeniser affects the structural strength of the dispersion, but does not affect the stability of the dispersion;

- **Rheological test methods can be used to investigate the curing reaction of the vesiculated beads.**

CHAPTER 5 Rheological Properties of Pigment & Extender-Free Paint (PE-Free Paint)

The increase in the cost of pigment (TiO_2) has forced paint-developing companies into the use of alternative opacifying agents in order to reduce the amount of pigment used in the paint, thereby reducing the manufacturing costs. The rheology of vesiculated beads as a raw material (opacifying agent) has been examined in the previous chapter (Chapter 4 – Rheological Properties of Vesiculated Beads). In this chapter the rheological behaviour of a paint formulated with the vesiculated beads as an opacifying agent is determined. Vesiculated beads are produced as a slurry in water and are therefore convenient to be used in water-borne paints. The microvoids of the beads are filled with water and diffuse out when the paint film dries. The particle size of the beads make them ideal to be used in low-sheen to flat paints [Ritchie, 1993], which are compared to existing low-sheen/flat paints.

5.1 Concept of the New Paint

The incorporation of vesiculated beads into commercial paint will have great advantages in terms of cost savings. The new paint is developed mainly to be used as a ‘contractor’s paint’ – a low-cost paint that is used by builders as a first coating for a newly constructed building.

5.2 Chemical Properties of New Paint

The new paint is formulated so that it consists mainly of vesiculated beads, resulting in great cost savings. According to Ritchie [1993], it has been found useful to formulate paints at 35 - 40% volume solids to optimise application properties. Eight different PE-free paint samples were prepared, varying in:

1. Amount of vesiculated beads;
2. Amount of emulsion;
3. Type of coalescent.

The chemical composition of the PE-free paint is given in Table 5-1 below.

Table 5-1: Chemical composition of PE-free paint given as % of total mass

PE-free Paint	Vesiculated Beads [%]	Emulsion [%]	Coalescent Type @ 1.1 % [-]	Pigment [%]	NH ₃ [%]	Rheology Modifier [%]
JE4/Ucar:	74.36	12.93	Ucar	9.70	0.97	0.97
JE4/Coasol:	74.36	12.93	Coasol	9.70	0.97	0.97
JE5/Ucar:	77.59	9.70	Ucar	9.70	0.97	0.97
JE5/Coasol:	77.59	9.70	Coasol	9.70	0.97	0.97
JE5.1/Ucar:	80.83	6.47	Ucar	9.70	0.97	0.97
JE5.1/Coasol:	80.83	6.47	Coasol	9.70	0.97	0.97
JE5.2/Ucar:	71.13	16.17	Ucar	9.70	0.97	0.97
JE5.2/Coasol:	71.13	16.17	Coasol	9.70	0.97	0.97

From Table 5-1 it can be seen that all the samples consist mainly of vesiculated beads and emulsion (A-296D) and therefore the chemical formulation is indeed very simple and easy to formulate in comparison with other existing ‘contractor’s paints.

5.3 Rheology of New Paint

The following properties of the new paint were investigated by means of rheology:

- Flow properties
- Spatter
- Settling
- Sag
- Levelling.

These properties were compared to those of existing paint that also fall within the ‘low-sheen’ type of paint manufactured by the same company.

5.3.1 Viscosity Curves

The viscosity curves are given in Figure 5-1 below.

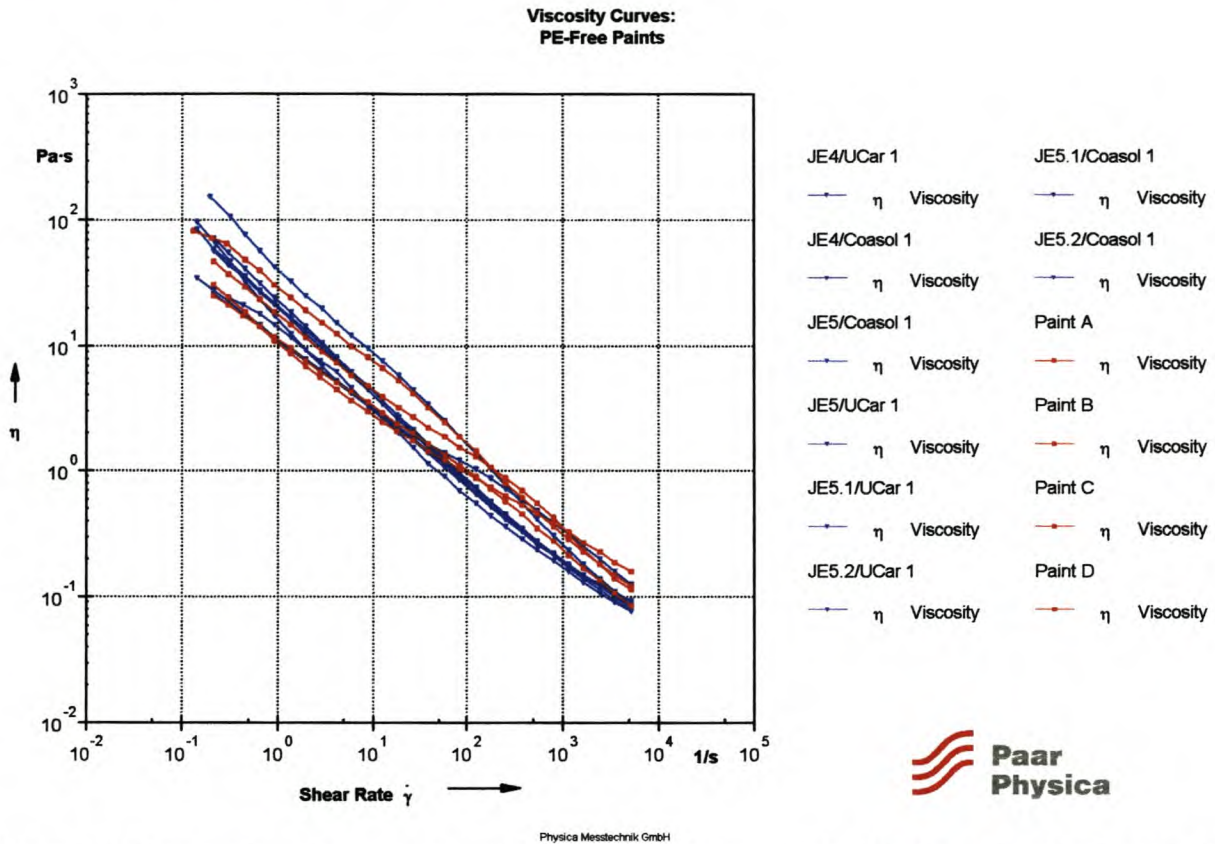


Figure 5-1: Comparison between viscosity curves of PE-free paints (blue) and standard paints (red)

The idea of Figure 5-1 is to compare the viscosity curves of the PE-free paints (blue) as a group to the standard paints (red).

Figure 5-1 shows the following flow behaviour for the PE-free paints:

- In general it can be seen that the two sets of curves (PE-free paints in blue, standard paints in red) have more or less the same shape for viscosity behaviour. It can therefore be assumed that the PE-free paints have the same degree of pseudoplasticity as the standard paints. Whitton et al. [2001] found that paint systems containing cellulosic thickeners such as HEC have high viscosities and the paint at rest almost approaches a gelled state. As higher shear is applied to the paint, the viscosity drops considerably, allowing easy application. He also states that HEC does not provide a completely acceptable combination of low- and high-shear rate viscosities. The viscosity curves, however, indicate that the PE-free paints have acceptable low- and high-shear rate viscosities resulting in good in-can

stability due to the high low-shear viscosity and will also have good application properties due to the relatively low high-shear viscosities.

- To compare the flow properties of the PE-free paints to that of the standard paints in a quantitative manner, the power-law model is fitted to all the viscosity curves. The power-law model is given by the following mathematical equation [Barnes et al., 1989]:

$$\eta = K\dot{\gamma}^{n-1} \tag{5-1}$$

where n is the power-law index which gives an indication of the degree of shear thinning. From equation 5-1 it can be seen that the smaller n becomes, the more pseudoplastic the substance becomes. K is the consistency index, which gives an indication of the low-shear viscosity. The n and K values can therefore give an indication of the application properties at high shear rates (degree of shear thinning) and the degree of in-can stability, respectively.

The power-law parameters are given in Table 5-2 below.

Table 5-2: Power-law parameters, K and n for PE-free and standard paints with R²-values

Paint Type	K [Pa.s ⁿ]	n [-]	R ² [-]
JE4/Ucar:	20.13	0.3236	0.9988
JE4/Coasol:	19.66	0.3320	0.9987
JE5/Coasol:	21.72	0.3189	0.9980
JE5/Ucar:	11.48	0.4883	0.9908
JE5.1/Ucar:	14.73	0.3132	0.9910
JE5.2/Ucar:	42.86	0.2751	0.9982
JE5.1/Coasol:	10.90	0.4250	0.9986
JE5.2/Coasol:	11.45	0.4175	0.9987
<i>Average:</i>	19.12	0.3617	
Paint B:	11.27	0.4472	0.9975
Paint A:	27.54	0.3706	0.9932
Paint C:	10.81	0.4881	0.9943
Paint D:	17.25	0.4341	0.9953
<i>Average</i>	16.72	0.4350	

From the values listed it is calculated that the PE-free paints have on average a consistency index (K) that is 14.4% higher than that of the standard paints and a power-law index, n, that is 16.9% lower than the standard paints. Before drawing conclusions from these values, one

must examine what effect JE5.2Ucar has on the average value of the consistency index, K and the power-law index, n , of the PE-free paints.

By omitting JE5.2/Ucar, which is more representative of the set of PE-free paints, a consistency index, K , that is 5.9% lower (was 14.4% higher) than that of the standard paints and a power-law index which is 14% lower (was 16.9% lower), is obtained. JE5.2/Ucar is therefore considered to be an outlier.

A 5.9% decrease in the low-shear viscosity of the PE-free paint is not large enough to indicate a significant difference in the low-shear-viscosity behaviour, while the higher degree of pseudoplasticity (14%) is considered to be a significant difference. Therefore the PE-free paints are considered to be more pseudoplastic than the standard paints. However, a statistical analysis is required to confirm these findings.

- As a first observation, the higher degree of shear thinning indicates that PE-free paints may perhaps not have the same degree of structural strength as the standard paints, but Mezger et al. [1998] has indicated that the viscosity curve *alone* is not sufficient in paint rheology for quality assurance.

5.3.2 Amplitude Sweeps

The amplitude sweeps of the PE-free paints are given in Figure 5-2 (Ucar as coalescent) and Figure 5-3 (Coasol as coalescent) below.

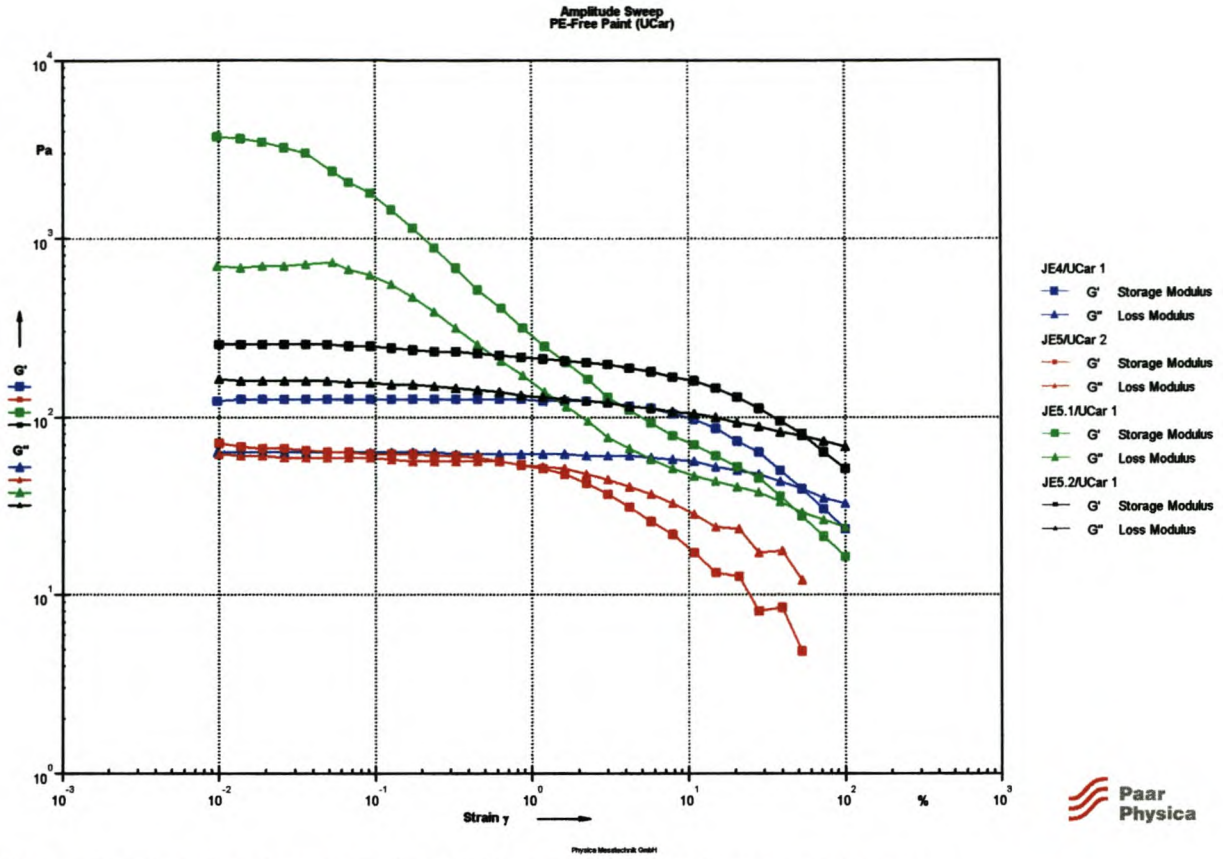


Figure 5-2: Amplitude sweeps for PE-free paints with Ucar as coalescent

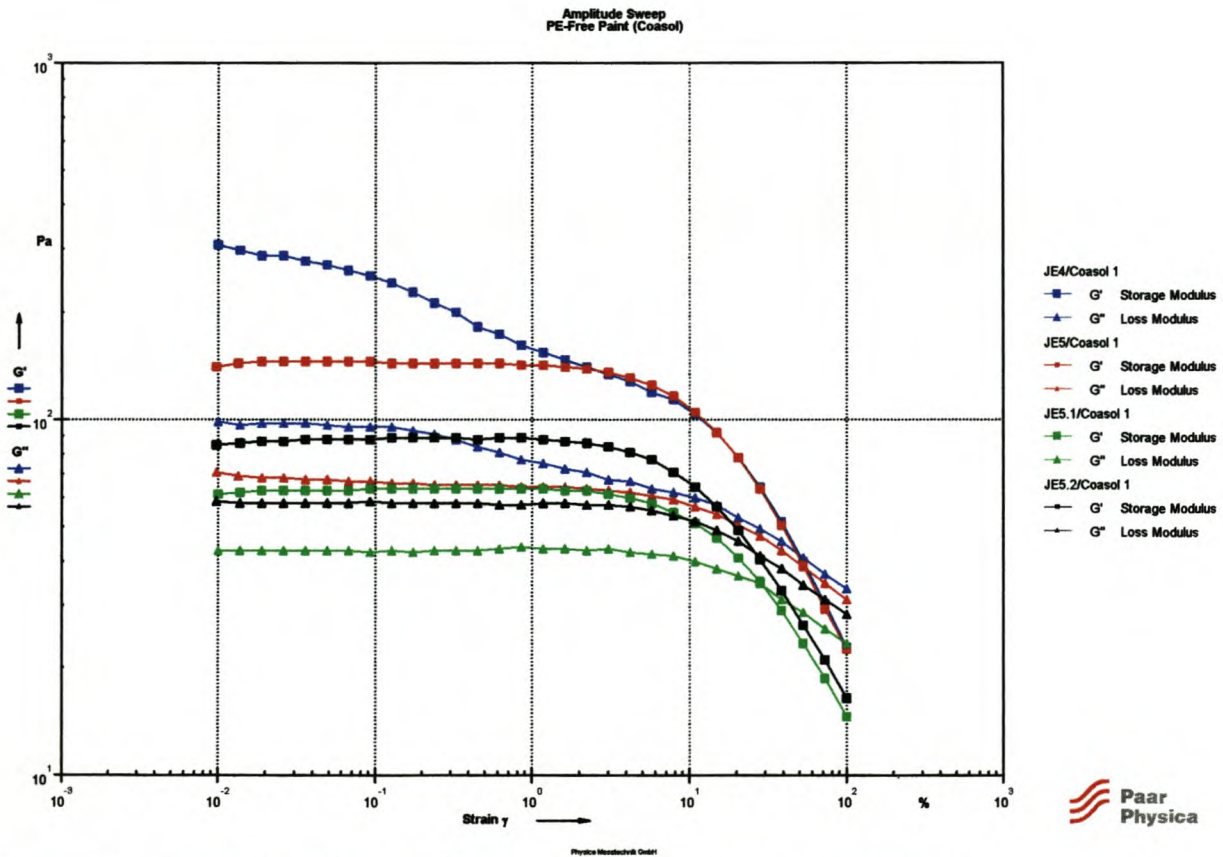


Figure 5-3: Amplitude sweeps for PE-free paints with Coasol as coalescent

Figures 5-2 and 5-3 give the following information about the character of the paints:

- $G' > G''$ for all the PE-free paints in the LVER. Therefore the solid-like behaviour predominates over the liquid-like behaviour and the PE-free paints show some degree of rigidity;
- Rheological properties at different ratios of beads to emulsion are examined. The beads to emulsion ratios are given in the table below.

Table 5-3: Beads/emulsion ratio

PE-free paint sample:	Beads/Emulsion [-]
JE5.2:	4.39
JE4:	5.75
JE5:	8.00
JE5.1:	12.5

The following figure illustrates the relationship between G' and the beads/emulsion ratios.

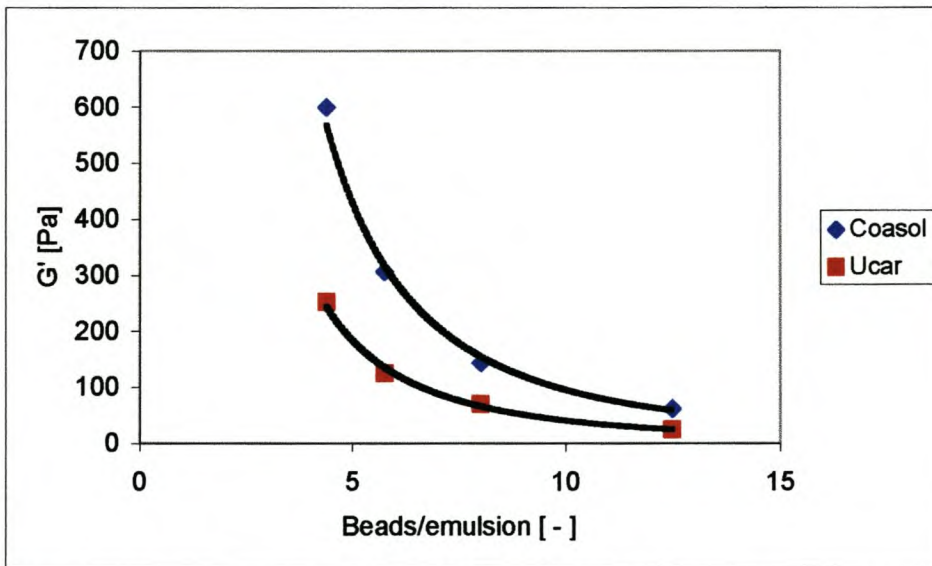


Figure 5-4: Relationship between G' and beads/emulsion ratio.

The effect of beads/emulsions ratio can clearly be seen in Figure 5-4. For both Coasol and Ucar samples, the structural strength decreases with an increase in the beads/emulsion ratio. Therefore, the structural strength can be increased by increasing the level of emulsion or by decreasing the level of beads.

The figure also reveals that the samples with Coasol as the coalescent results in a stronger structural strength in comparison to the samples with Ucar as a coalescent. Therefore, using Coasol as the coalescent can also increase the structural strength.

- The yield points for the PE-free paints and the standard paints obtained from the amplitude sweeps are given in Figure 5-5 below:

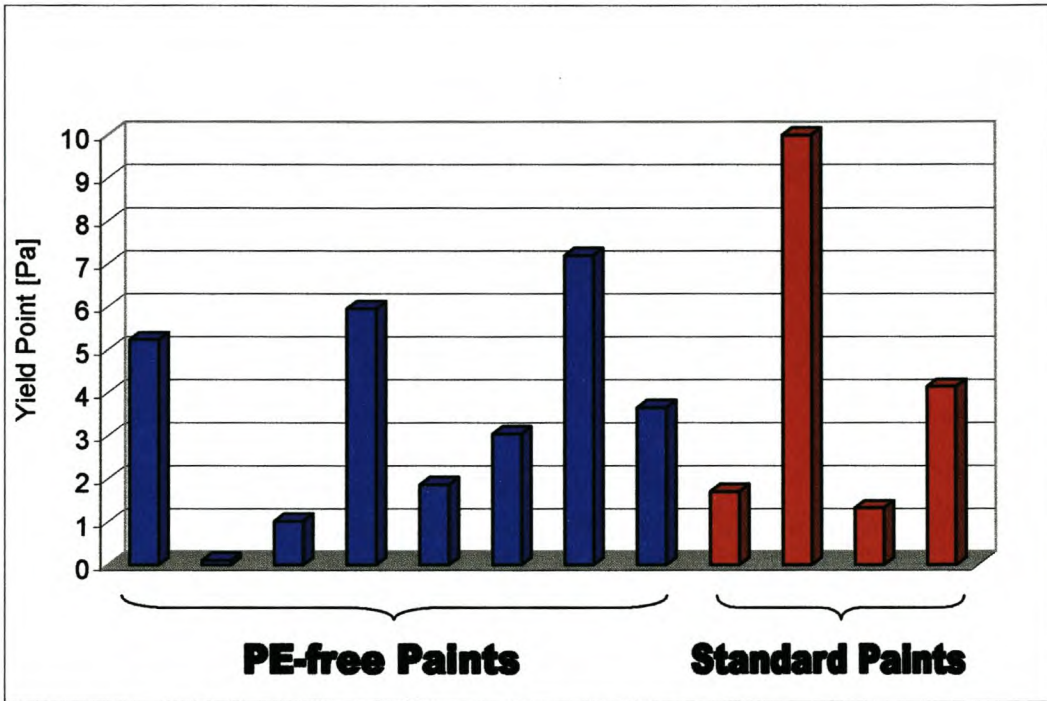


Figure 5-5: Apparent yield points obtained from amplitude sweeps.

Figure 5-5 reveals that most of the PE-free paints have acceptable yield points in comparison to those of the standard paints, except for two of the PE-free paints for which the yield point is below 1 Pa. Therefore these two PE-free paints are the mostly likely to show sagging behaviour on a vertical wall and this is an indication of possible poor in-can stability. The yield point also affects the levelling behaviour.

5.3.3 Frequency Sweeps

The frequency sweeps are illustrated in Figure 5-6 (Ucar as coalescent) and Figure 5-7 (Coasol as coalescent) below.

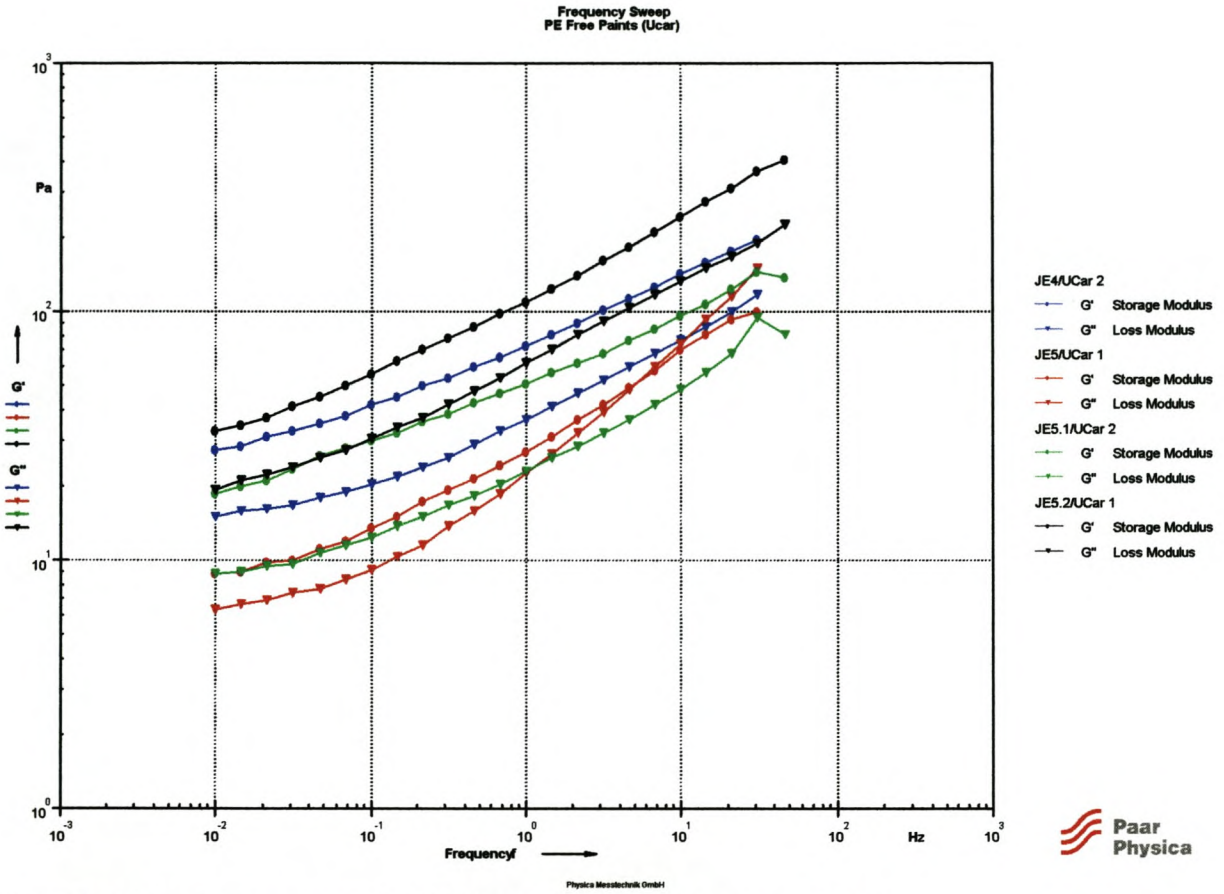


Figure 5-6: Frequency sweep for PE-free paints with Ucar as coalescent

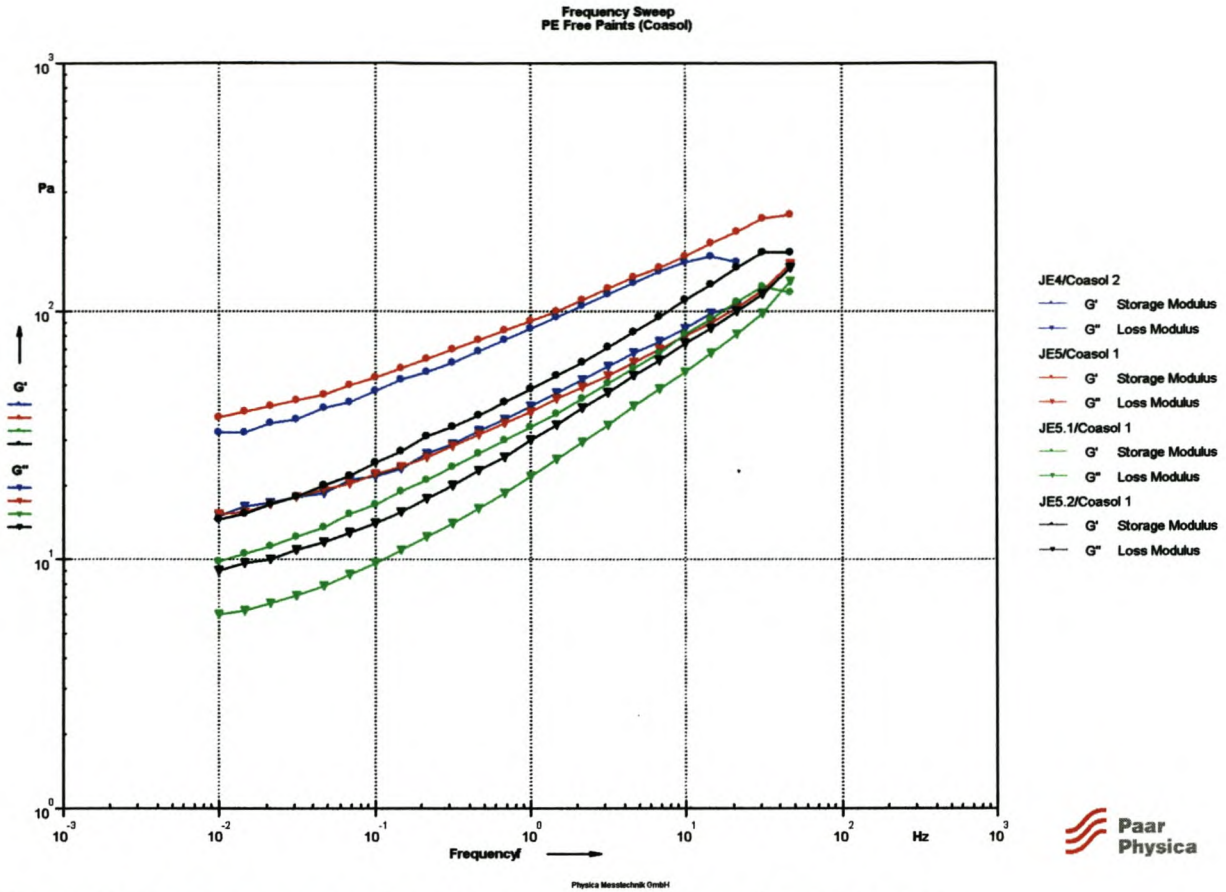


Figure 5-7: Frequency sweep for PE-free paints with Coasol as coalescent

Figures 5-6 and 5-7 give the following information about the behaviour of the PE-free paints in the LVER:

- $G' > G''$ over the whole frequency range and therefore the solid-like behaviour predominates over the liquid-like behaviour and there is a certain degree of stability.
- A more detailed investigation is done on each sample at the high- and low-frequency areas respectively. Trendlines can be fitted to the G' and G'' curves in the high frequency range, e.g.:

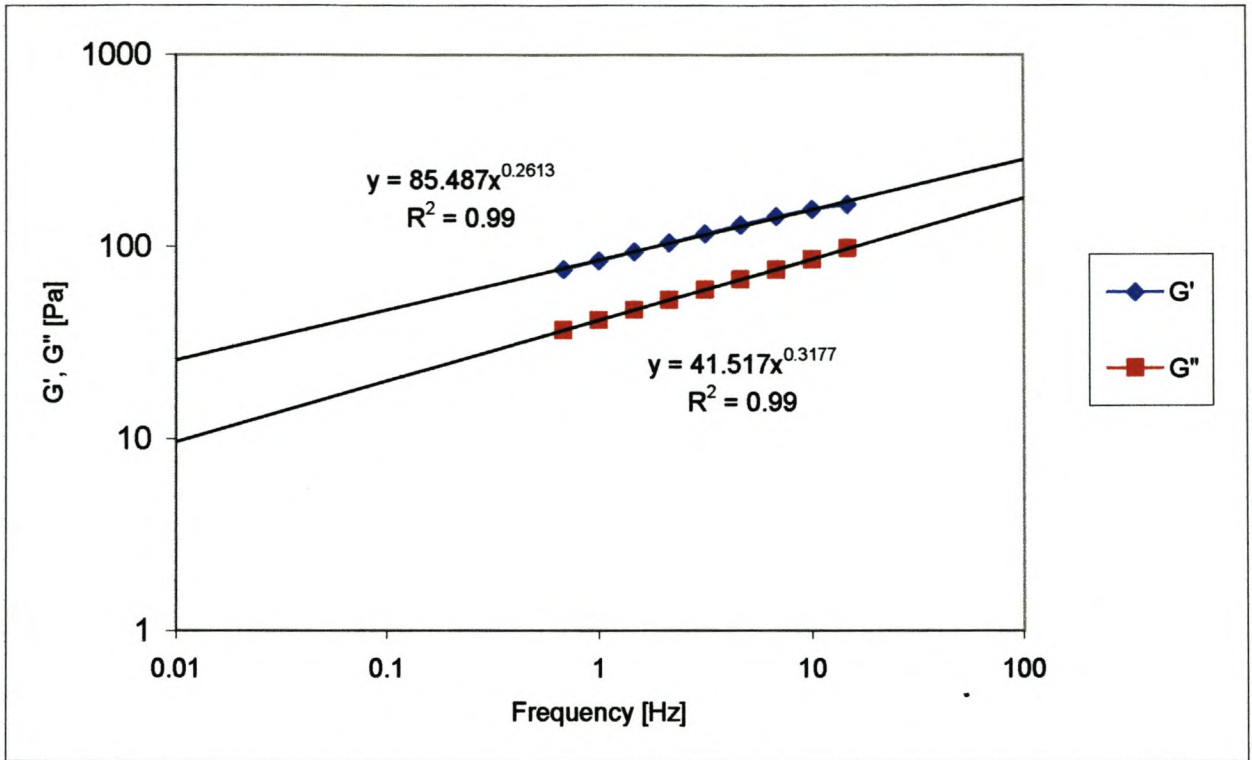


Figure 5-8: Trendlines for G' and G'' in high-frequency range for JE4/Coasol.

The same can be done for another sample, e.g.:

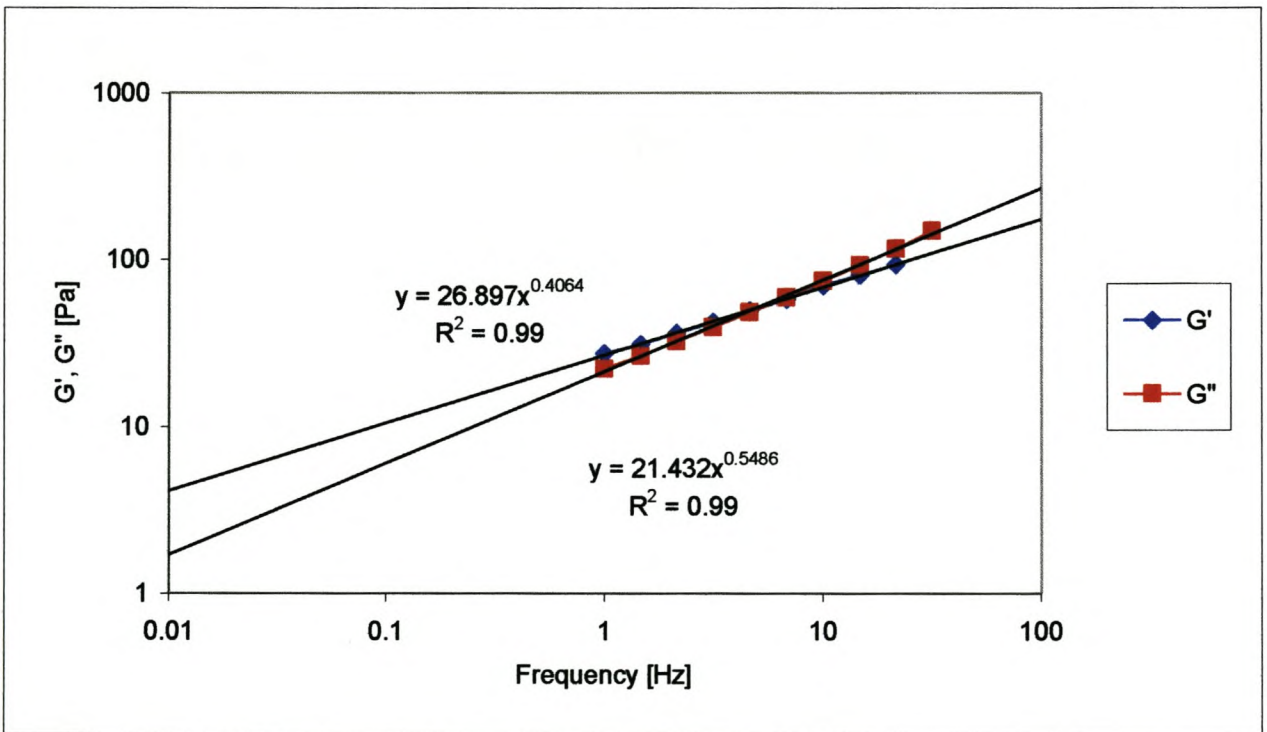


Figure 5-9: Trendlines for G' and G'' at high-frequency range for JE5/Ucar.

The difference in the trendlines of Figure 5-8 and Figure 5-9 is obvious – the trendlines of G' and G'' in Figure 5-9 have a cross-over point, while there is no cross-over point for the trendlines in Figure 5-8. Both figures indicate that a power-law model fits well to both G' and G'' with R^2 -values larger than 0.99.

The power-law index, n , is the gradient of the curve when expressed in linear terms. As described in the Appendix B, a paint will spatter when $G'' > G'$ in the high-frequency range and therefore the gradients of the curves can be used to determine whether G'' will be larger than G' and therefore whether spatter will occur or not. Expressed mathematically:

$G''_{\text{gradient}} > G'_{\text{gradient}}$ – more likely to spatter

$G'_{\text{gradient}} > G''_{\text{gradient}}$ – less likely to spatter

Therefore spatter will occur when:

$$G'_{\text{gradient}} - G''_{\text{gradient}} < 0$$

These values, $G'_{\text{gradient}} - G''_{\text{gradient}}$, for the standard paints and the PE-free paints are given in Figure 5-10 below.

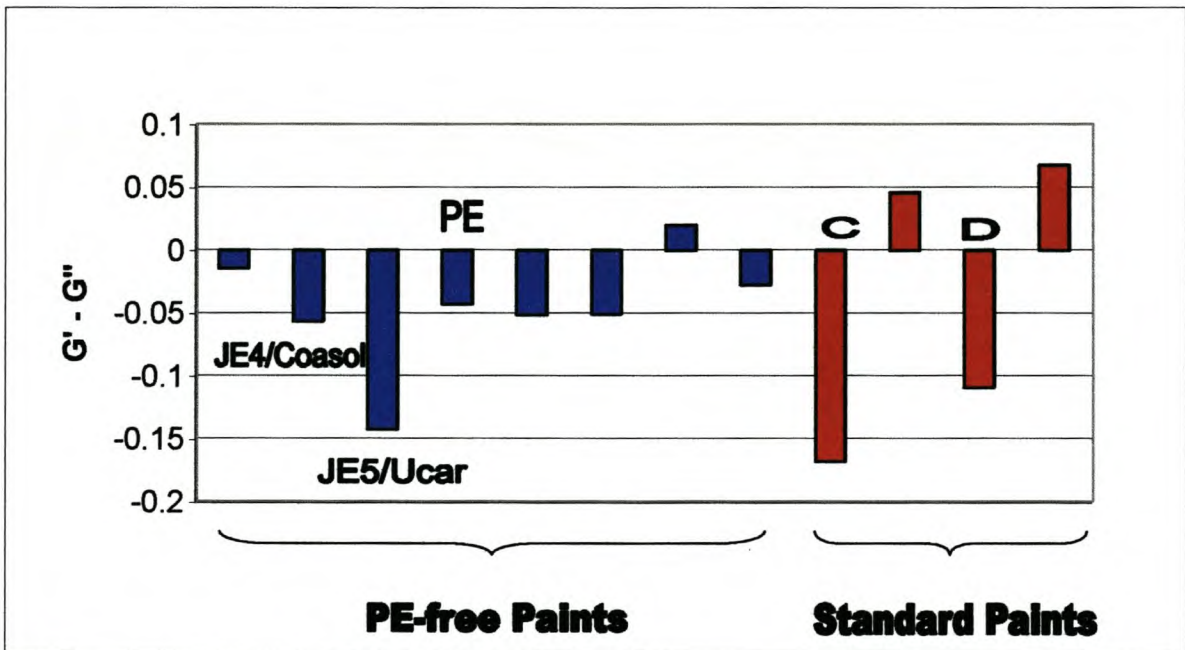


Figure 5-10: Degree of spatter

From Figure 5-10 it can be seen that most of the paints have a negative difference in the values of $G'_{\text{gradient}} - G''_{\text{gradient}}$ and therefore will tend to spatter, as paints tend to do. However, it can

also be seen that the PE-free paints, in general, have smaller negative values and will therefore tend to spatter less than, for example, paint C and paint D of the standard paints. Therefore spatter should not be a problem during roller application of the PE-free paints. The following photos illustrate the spatter behaviour.

Paint C:



vs.

Paint PE:



Figure 5-11: Comparison between spatter of standard paint (paint C) and PE-free paint (paint PE)

The differences in spatter can clearly be seen. Figure 5-10 predicts that the PE-free paint (paint PE) will spatter a lot less than the standard paint (paint C), which is in fact the case as can be seen by looking at the photos in Figure 5-11.

Measurements of degree of spatter have also been done in the laboratory using standard test methods. The results obtained from these standard methods are compared to those obtained from rheological test methods in order to determine whether there is a direct correlation between the degree of spatter and the data obtained from the frequency sweep.

- In the laboratory values are given for different degrees of spatter. The value of 4 is assigned to a paint that spatters a lot and the value of 1 is assigned to a paint that spatters minimally. The following values have been assigned to the PE-free paints and standard paints as a result of their tendency to spatter (the table also includes $G'_{\text{gradient}} - G''_{\text{gradient}}$ values):

Table 5-4: Laboratory values for spatter

Paint sample	Laboratory values for spatter	$G'_{\text{gradient}} - G''_{\text{gradient}}$	Confidence Level (Upper 95%)	Confidence Level (Lower 95%)	Within Limits
JE4/Ucar:	1	- 0.014	-0.004	-0.024	✓
JE4/Coasol:	2	- 0.056	-0.043	-0.069	✓
JE5/Ucar:	3	- 0.142	-0.129	-0.136	✗
JE5/Coasol:	1	- 0.043	-0.037	-0.048	✓
JE5.1/Ucar:	2	- 0.051	-0.054	-0.065	✓
JE5.1/Coasol:	2	- 0.051	-0.049	-0.052	✓
JE5.2/Ucar:	2	+ 0.020	0.022	0.016	✓
JE5.2/Coasol:	2	- 0.027	-0.018	-0.036	✓
Paint C:	4	- 0.168	-0.133	-0.201	✓
Paint A:	4	+ 0.046	0.055	0.037	✓
Paint D:	4	- 0.109	-0.095	-0.123	✓
Paint B:	3	+ 0.068	0.063	0.012	✗

Table 5-4 illustrates that for all the paints, except for JE5/Ucar and Paint B, the values for $G'_{\text{gradient}} - G''_{\text{gradient}}$, fall within a 95% confidence limit.

The values for the degree of spatter obtained from the laboratory tests are scaled down in order to be able to compare them with the results obtained from the frequency sweep. The comparison is given in the following figure.

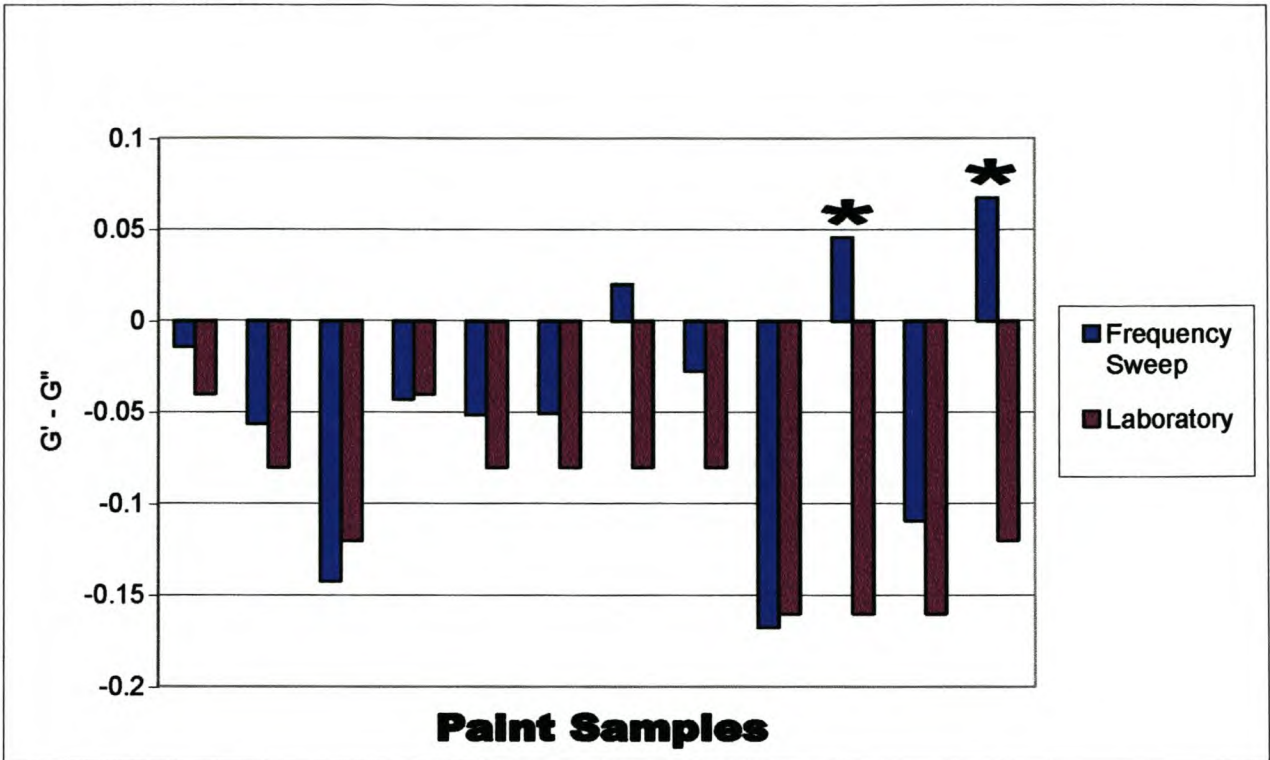


Figure 5-12: Comparative results for degree of spatter (laboratory vs. frequency sweep)

Figure 5-12 reveals that there is a good correlation between results obtained from the laboratory tests and the frequency sweeps for the degree of spatter. This method of determining the degree of spatter by means of the frequency sweep can be used as a valuable method in quantifying the degree of spatter instead of relying on the human factor for which each test result may be subjective and therefore not exact. This fact that two paints do not show a good correlation (indicated with ‘*’ in Figure 5-12) between laboratory tests and the frequency sweep may therefore be due to human error.

The same can be done at the low-frequency range by fitting trendlines to the G' and G'' curves in order to determine the tendency of the samples to settle. A sample with a loss factor (G''/G') larger than 1 in the low-frequency range of the frequency sweep will tend to settle because $G'' > G'$ and vice versa. The following figure is an indication of the loss factors obtained in the low-frequency range for the PE-free paints and the standard paints.

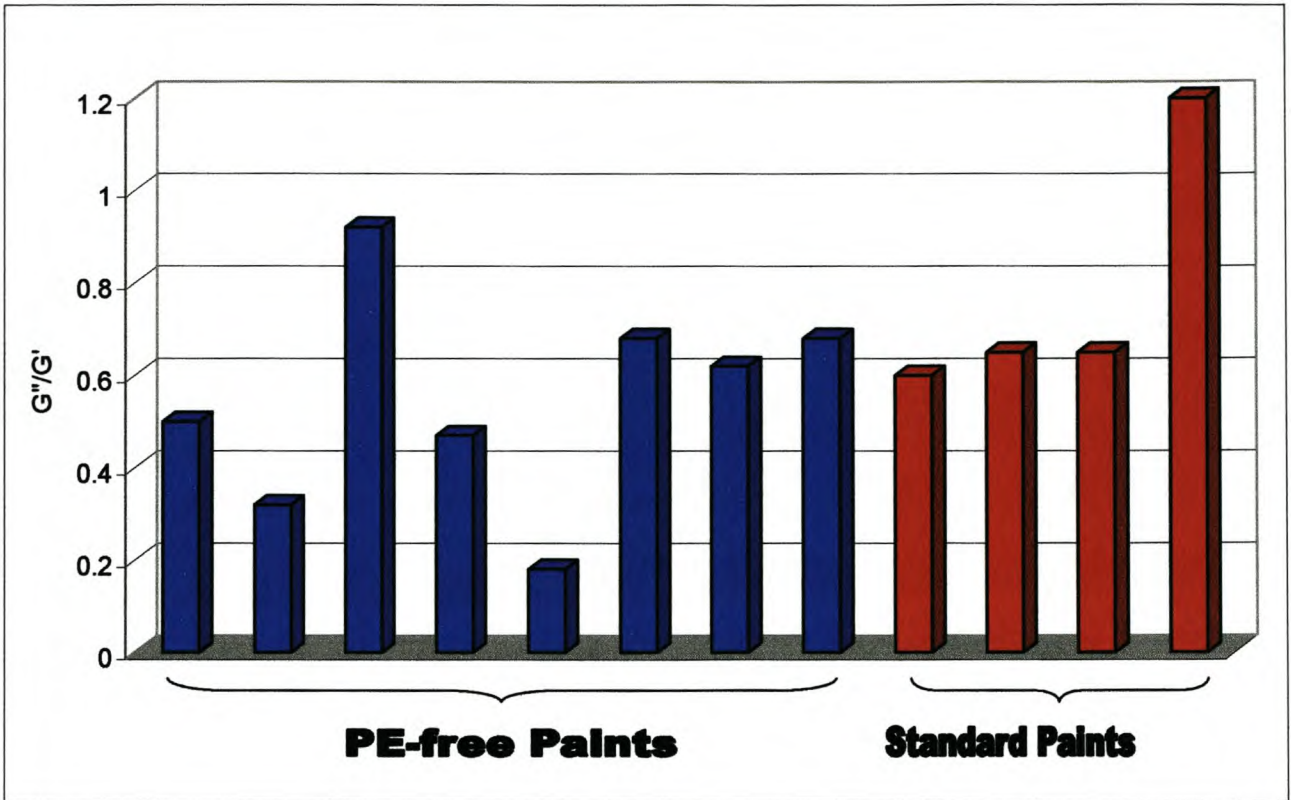


Figure 5-13: Loss factor in low-frequency range

Figure 5-13 reveals that PE-free paints all have $\tan \delta$ values < 1 and are therefore not likely to sedimentate or become unstable at low frequencies or during long time-scale behaviour and therefore show good in-can stability.

5.3.4 Three-Interval-Thixotropy-Test (3-ITT)

The rate of structural recovery of a sample after a high-shear load has been applied affects the following properties of the final coating:

- Levelling – too fast structural recovery results in poor levelling;
- Sagging – too slow structural recovery results in sagging;
- Layer thickness – too fast/too slow structural recovery can result in unwanted layer thicknesses.

The rate of structural recovery is obtained by performing a three-interval-thixotropy test on each of the samples. The rate of structural recovery after high shear is given by the rheological parameters of G' and G'' . For a start, a power-law trendline is then fitted to the G' -structural recovery curves to

determine the recovery of the elastic part. The recovery of the elastic part (G') is investigated as opposed to the viscous part (G'') of the sample as G' predominates during the structural recovery phase for all the samples. The power-law parameter, n , is an indication of the rate of structural recovery.

5.3.4.1 Effect of Structural Recovery Rate on the Levelling Behaviour

Once again, values of 1 (desired levelling behaviour) to 4 (undesired levelling behaviour) have been assigned to samples showing acceptable and unacceptable levelling behaviour respectively. The following table illustrates these assigned values, along with the power-law parameter, n .

Table 5-5: Laboratory values for levelling and the power law parameter, n

Paint sample	Laboratory values for levelling	n
JE4/Ucar:	3	0.143
JE4/Coasol:	3	0.144
JE5/Ucar:	3	0.285
JE5/Coasol:	2	0.163
JE5.1/Ucar:	2	0.287
JE5.2/Ucar:	2	0.147
JE5.1/Coasol:	2	0.125
JE5.2/Coasol:	3	0.202
Paint C:	2	0.153
Paint A:	2	0.158
Paint D:	1	0.106
Paint B:	3	0.077

Again, as was done for the spattering behaviour, the values obtained in the laboratory are scaled down in order to compare them with the power-law parameter, n . The comparison of these values is given in the following figure.

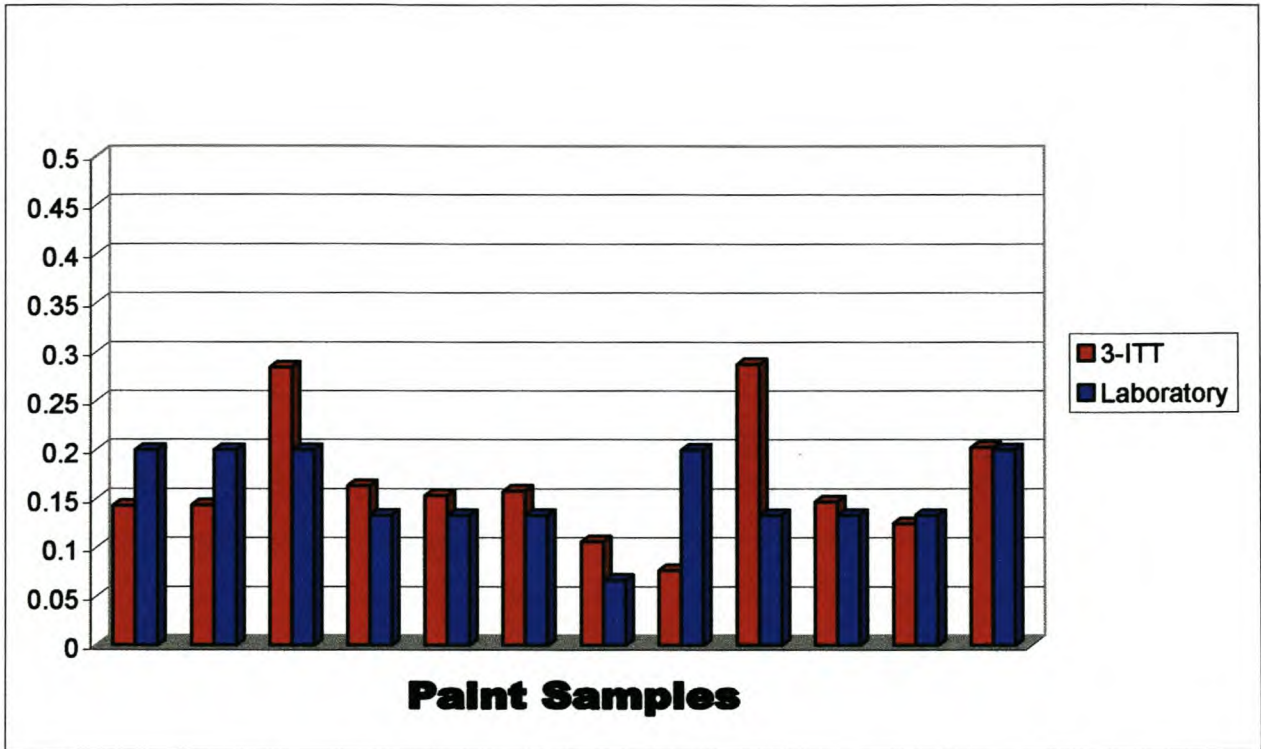


Figure 5-14: Comparison between laboratory results and the power-law parameter, n , obtained from the 3-ITT for the levelling behaviour of the PE-free paints and the standard paints.

The figure reveals that there is a good correlation between the results obtained from the three-interval-thixotropy test (3-ITT) and the tests performed in the laboratory. Therefore the 3-ITT method is useful in quantifying the degree of levelling. What makes this test method very attractive for determining the levelling behaviour is the fact that it is independent of human assessment.

The structural recovery curves not only indicate the rate of structure recovery, but also whether $G' > G''$ or vice versa, which is an important criterion for investigation of the levelling behaviour directly after application. If the structural recovery curves indicate that $G'' > G'$ directly after high shear, then the sample behaves in a liquid-like manner and is able to flow and can fill cracks and produces a smooth surface, etc. If the structural recovery curves indicate that $G' > G''$ directly after the high shear load, then the sample behaves in a solid-like manner and therefore does not flow and cannot level out properly.

As stated earlier, G' predominates over G'' for all the samples directly after a high-shear load has been applied and therefore all the samples will show relatively poor levelling behaviour, as indicated by the laboratory values given to the levelling behaviour (see Table 5-5).

Whitton et al. [2001] also investigated the structural recovery of paint systems containing cellulosic thickeners and found that after high shear has been applied to these paints, the paint rapidly returns to its original high viscosity or semi-gelled state and therefore, although cellulosic thickeners are virtually non-reactive in the paint, are often deficient in providing some basic application requirements. Because of the fast recovery rate of the paint system, paints containing cellulose have poor levelling and flow behaviour. This fast structural recovery behaviour is also observed in the PE-free paints. Karickhoff [1984] states that this is especially true in latex paints containing vesiculated beads as part of the pigmentation. It is especially difficult to obtain the required film build properties upon brush and roller application of these coatings.

5.3.4.2 Effect of Structural Recovery on Layer Thickness

As stated earlier, G' predominates over G'' directly after the high-shear load has been applied. The paint sample therefore does not have the opportunity to flow and level out after application, which will result in a relatively thick layer. The rate of structural recovery, measured in terms of G' , is therefore used to estimate the layer thickness.

The following figure illustrates the relationship between the layer thickness measured in the laboratory and the rate of structural recovery obtained from three-interval-thixotropy tests (3-ITT) performed on the rheometer.

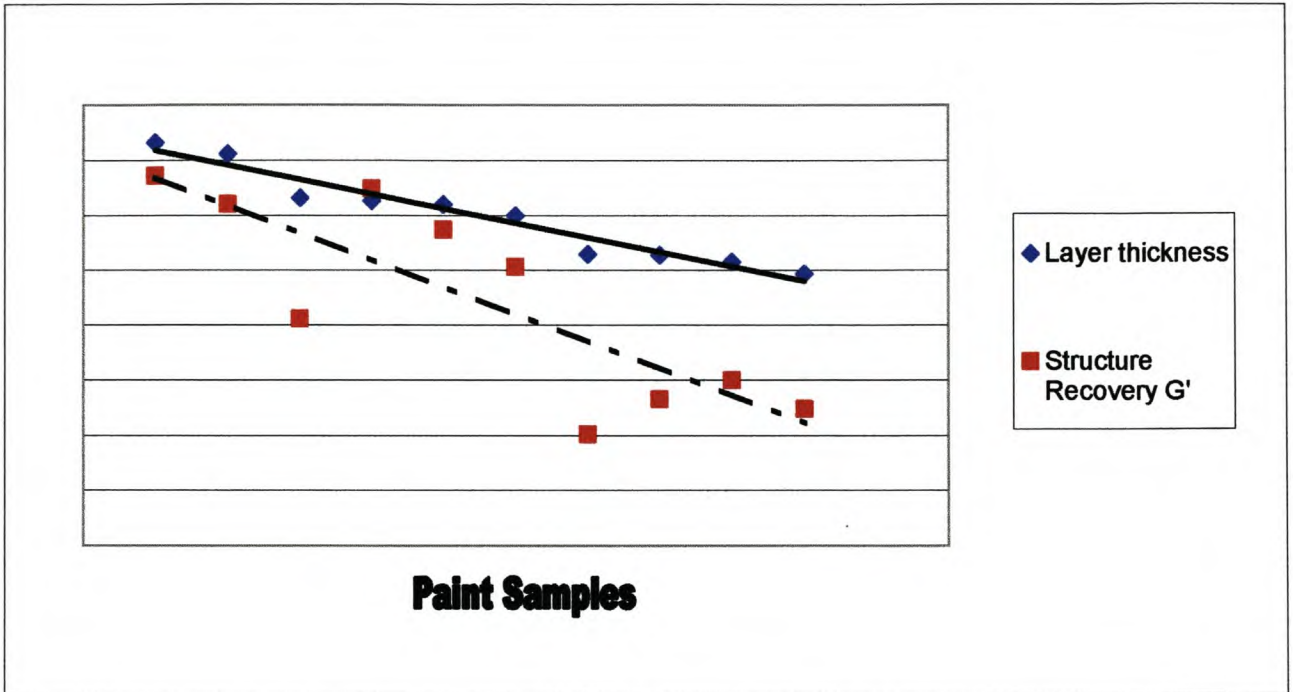


Figure 5-15: Correlation between layer thickness and the structural recovery (G')

Figure 5-15 reveals that there is a direct correlation between the layer thickness and the rate of structural recovery. That is, the faster the rate of structural recovery, the larger the layer thickness. Therefore, the three-interval-thixotropy test can once again be used as a quantitative method for predicting the layer thickness.

5.3.4.3 Effect of Structural Recovery on Sagging Behaviour

The solid-like behaviour predominates over the liquid-like behaviour ($G' > G''$) after the high-shear load has been applied and therefore the samples do not flow after application and sagging should not be a problem. The yield points obtained from the amplitude sweeps also indicate this behaviour (see Figure 5-5).

It is difficult to quantify the sagging behaviour by means of standard laboratory test methods and therefore no laboratory data exist to be compared to the rheological data. Again the value of the 3-ITT can be seen in quantifying the sagging behaviour.

5.4 Conclusions

The following conclusions can be drawn from the previous tests:

- In general, the PE-free paints have comparable viscosity behaviour to that of existing paints in the same class. The PE-free paints indicate in general that they are 14% more shear-thinning in behaviour, with more or less the same low-shear viscosities as existing paints. Therefore, the PE-free paints should show acceptable in-can stability (at low shear rates) and application behaviour (at high shear rates);
- According to the amplitude sweeps, the solid-like behaviour (G') predominates over the liquid-like behaviour (G'') and therefore shows some degree of rigidity and a certain degree of structural stability, because the particles are kept intact in the network;
- Different ratios of beads to emulsion (beads/emulsion) affect the stability of the PE-free paints. For both Coasol and Ucar PE-free type paints, the structural strength decreases with an increase in the beads/emulsion ratio;
- Coasol as the coalescent results in a stronger structural strength in comparison to the samples with Ucar as a coalescent. Therefore, using Coasol as the coalescent can also increase the structural strength;
- Most of the PE-free paints have acceptable yield points in comparison to those of the standard paints, except for two of the PE-free paints for which the yield point is below 1 Pa. Except for these two, the PE-free paints will show good in-can stability and anti-sag behaviour;
- The frequency sweeps also indicate that, in general, the PE-free paints are stable over the whole frequency range;
- PE-free paints, in general, have smaller negative values for $G'_{\text{gradient}} - G''_{\text{gradient}}$ and will therefore tend to spatter less than some of the standard paints. PE-free paints therefore show good anti-spatter behaviour and should not be a problem during roller application;

- The tendency of the PE-free paints not to spatter, according to rheological data, correlates well with spatter tests in the laboratory;
- PE-free paints all have $\tan \delta$ values < 1 and are therefore not likely to sedimentate or become unstable at low frequencies or during long time-scale behaviour and therefore show good in-can stability;
- The structural recovery curves of the PE-free paints indicate that they are prone to poor levelling and flow behaviour directly after application;
- Once again, the levelling behaviour obtained from the rheological data correlates well with levelling tests performed in the laboratory;
- The PE-free paints result in relatively thick films;
- It was found that there is a direct correlation between layer thickness and structural recovery behaviour obtained from the rheological data;
- The structural recovery curves also indicate that the PE-free paints are not prone to sagging behaviour.

CHAPTER 6 Rheological Properties of Paint

This chapter examines the rheological properties of commercially available paints. The rheological properties of the paint *as a final product* are examined. As we all know, not only are there different paint manufactures, but each paint manufacturer also manufactures a variety of paints for different application purposes and paints that fall into different quality bands. The paints are then also further classified as matt, sheen, gloss, etc. It is therefore clear that a specific paint is *designed* with a specific end-use in mind, to which the rheological properties should conform as well. Some of these properties for indoor and outdoor paints are listed below.

- Indoor (walls and ceilings):
 - Ease of application
 - Good in-can stability
 - Thin layer thickness (mostly)
 - Little or no spatter
 - Little or no sagging
 - Smooth surface
 - Be able to fill small cracks and holes.

- Outdoor (walls and roofs):
 - Ease of application
 - Good in-can stability
 - Thick layer thickness
 - Some degree of spatter allowed
 - Some degree of sag allowed
 - Rough surface
 - Be able to fill large cracks and holes.

The rheological properties of the coatings will be examined, with the end-use of the coating kept in mind. In other words, rheological tests are carried out in order to determine whether the rheological properties correlate with the specific application it is designed for.

6.1 Rheological Characterisation of Commercial Paints of Company ABC

Table 6-1 lists the type of commercial paints that are rheologically examined.

Table 6-1: Description of paints

Paint	Base	Quality ¹	Use	Description
Paint A:	Water	High	Exterior	Sheen/semi-gloss
Paint B:	Water	High	Interior	Sheen/semi-gloss
Paint C:	Water	High	Interior	Dead matt
Paint D:	Water	Low	Interior/exterior	Matt
Paint E:	Water	Medium	Interior/exterior	Matt
Paint F:	Water	High	Exterior	Textured*
Paint G:	Water	High	Interior (ceiling)	Dead matt
Paint H:	Water	High	Exterior (roof)	Durable
Paint I:	Solvent	High	Interior	Sheen

* High flexibility (elasticity)

Expressing all the coatings on one graph will defeat the purpose of illustrating the differences between the paints because there are too many curves. Therefore the paints are grouped in order to compare them properly. They are grouped as follows:

Group I:

Matt/dead-matt paints will be compared on the basis of their *quality* and also to a sheen/semi-gloss paint. The paints of group I are:

- Paint A - High quality, sheen/semi-gloss
- Paint C - *High quality*, dead-matt
- Paint D - *Low quality*, matt
- Paint E - *Medium quality*, matt

Therefore:

- A and C (sheen/semi-gloss vs. dead-matt)
- A, C, D and E (*low* vs. *medium* vs. *high* quality)

¹ Quality as defined by paint manufacturing company ABC

Group II:

Paints of group II are compared on the basis of their main end-use properties. The paints of group II are:

- Paint A – Sheen/gloss (*water-based*)
- Paint F – Textured
- Paint G – Dead matt, ceiling paint
- Paint H – Roof paint
- Paint I – Sheen/gloss (*solvent-based*)

Therefore:

- A and I (*water-based sheen/gloss vs. solvent-based sheen/gloss*)
- A, F, G and H (based on their end-use properties as above)

6.1.1 Group I

6.1.1.1 Viscosity Curves

The viscosity curves are given in Figure 6-1 below.

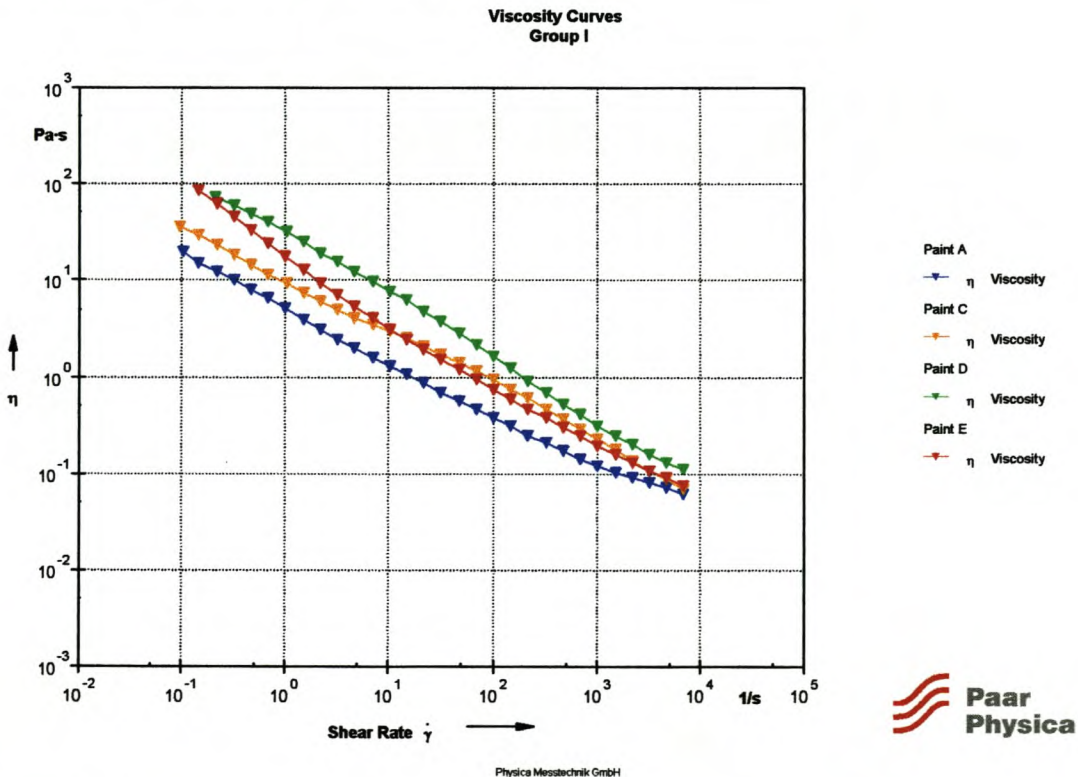


Figure 6-1: Viscosity curves for paints of group I

Figure 6-1 gives the following flow behaviour for the group I paints:

- All the paints behave in a pseudoplastic manner. The power-law parameter, n , gives an indication of the degree of pseudoplasticity.

Table 6-2: Power-law parameter, n , for viscosity curves of group I paints

Paint	n	R^2
Paint D:	0.35	0.9984
Paint E:	0.34	0.9930
Paint C:	0.45	0.9975
Paint A:	0.47	0.9952

It appears from the viscosity curves and the power-law parameter n that the higher-quality paints, paints C and A, have higher n values and therefore lower degrees of pseudoplasticity. The lower-quality paints, paints D and E, have lower n values and therefore higher degrees of pseudoplasticity. In other words, it appears as if the structure of the lower quality paints is broken down easier under shear than that of the higher quality paints. But coatings have complex flow behaviour due to complex structures and therefore examination of the structural strength must be carried out in the LVER (see sections 6.1.1.2 and 6.1.1.3 for the amplitude and frequency sweeps respectively) to determine the character of the paint.

- The low-quality matt paint, paint D, has the highest apparent viscosity over the whole shear-rate range, therefore resulting in poor flow and levelling behaviour, which will result in brush marks in the final coating. Paint D even has the highest viscosity in the high-shear rate range, although it behaves in the most pseudoplastic manner of all the paints.
- It can be seen that the high-quality paints have relatively low low-shear viscosities, making handling easier, not causing brush marks and illustrating better levelling behaviour. The lower low-shear viscosity does not necessarily imply that a paint is of a higher quality. The ideal top-quality paint behaves in the following manner - it will have a relatively low low-shear viscosity to allow for ease of workability and good levelling behaviour, but at the same time it will have a high degree of structural strength and stability to prevent the sample from settling and therefore ensures good in-can behaviour. In other words, there is a trade-

off between ease of workability and good levelling behaviour, and the degree of structural strength in the low-shear rate range. Once again one can see that examining the character of the sample in the LVER is also important and that information from *only* the viscosity curve is not sufficient to determine the character of the coating.

- A certain degree of stiffness (semi-gelled state) was observed when opening a can of paint E, which made it very difficult to stir. Paint E shows a high degree of shear thinning between the shear rates of 0.1 s^{-1} and 10 s^{-1} . The steep gradient of the viscosity curve indicates a high degree of structural strength at even lower shear rates than what is measured ($< 0.1 \text{ s}^{-1}$). This is unwanted low-shear behaviour.

6.1.1.2 Amplitude Sweeps

The amplitude sweeps are given in Figure 6-2 below.

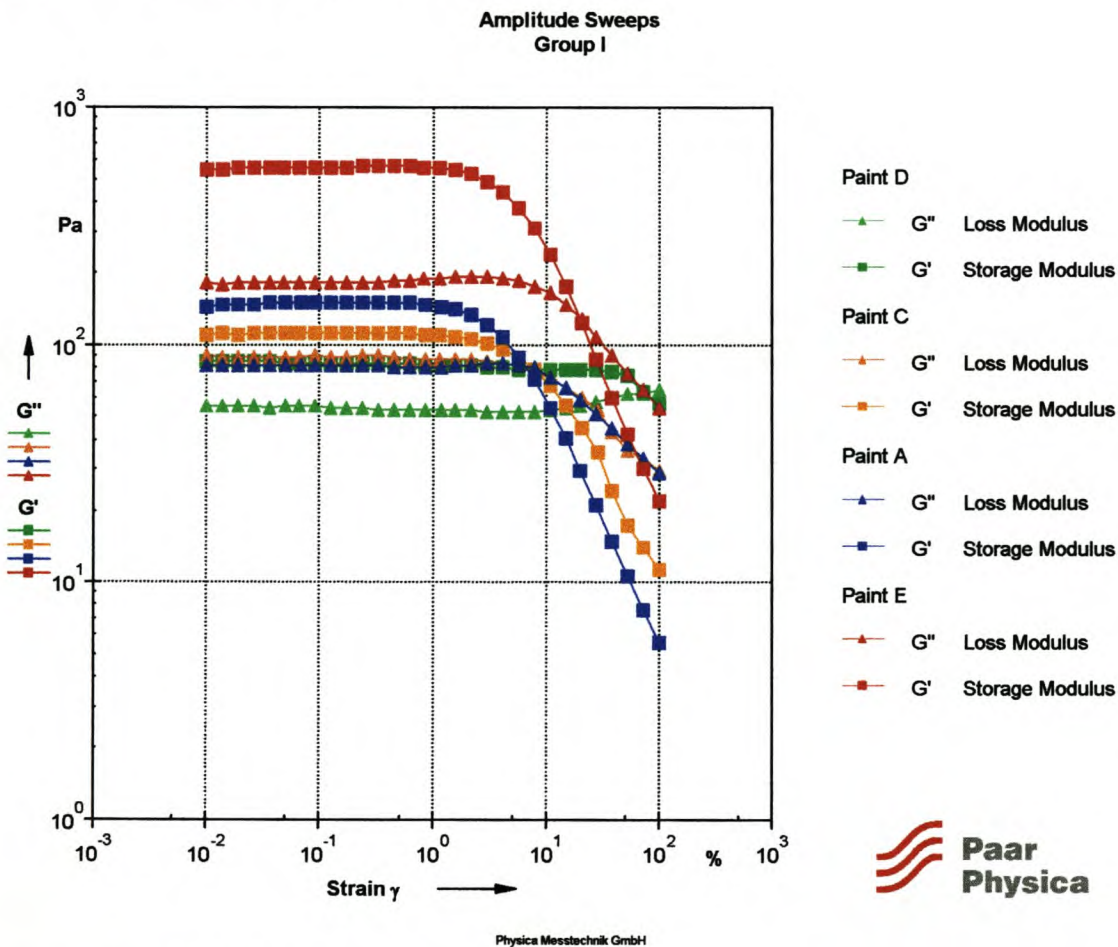


Figure 6-2: Amplitude sweeps for group I paints

Figure 6-2 gives the following information about the character of the group I paints:

- All the samples show some degree of rigidity due to the fact that the solid-like behaviour predominates over the liquid-like behaviour ($G' > G''$) in the LVER.
- The amplitude sweep of paint E illustrates its high degree of structural strength in the LVER as was expected from examination of the viscosity curves. The storage modulus of paint E is ± 4 times higher than that of the high-quality sheen paint, paint A, and it is clear why paint E is in a semi-gelled state in the can. The small $\tan \delta$ (G''/G') values in the LVER for paint E also indicate the tendency of the paint to be in a semi-gelled state.

Table 6-3: $\tan \delta$ values in the LVER for group I paints

Paint	$\tan \delta$ [-]
Paint A:	0.56
Paint C:	0.81
Paint D:	0.65
Paint E:	0.32

The table shows that the $\tan \delta$ value for paint E is almost 2 times smaller than that of the next higher $\tan \delta$ value, that of paint A.

- On the other side of the spectrum, Figure 6-2 illustrates that paint D (low quality) has the lowest degree of structural strength (G') in the LVER.
- By omitting the G' and G'' curves of paint E, Figure 6-2 shows that a decrease in the structural strength occurs, which is in accordance with the quality of the paint. The structural strengths are as follows:

Table 6-4: Structural strength (G') and quality for group I paints

Paint	Quality	G' [Pa]
Paint A:	High	150
Paint C:	High	112
Paint D:	Low	84

- The yield points obtained from the data tables of the amplitude sweeps are given in Table 6-5 below.

Table 6-5: Yield points for group I paints obtained from amplitude sweeps

Paint	Quality	Yield Point [Pa]
Paint A:	High	3.2
Paint C:	High	4.0
Paint D:	Low	52
Paint E:	Medium	16

The difference in yield points is clear. Paints A and C (high quality) have far smaller yield points than paints D and E (low/medium quality). Mezger [2002] gives the following relationship between layer thickness and the yield point:

$$\text{layer thickness} \propto \text{yield point}$$

It can therefore be seen that the paints with very high yield points, paints D and E, will result in excessively thick films. However, the film thickness of the wet layer also depends a lot on its time-dependent behaviour during structural regeneration after a high-shear load (see section 6.1.1.4 – Three-Interval-Thixotropy-Test) as well as other factors such as wall roughness, etc. In general it can be seen that the low-quality paints have much higher yield points than those of the high-quality paints.

- The high yield points of the low-quality paints, paints D and E, will also result in poor levelling behaviour, leaving brush marks and an uneven surface.

6.1.1.3 Frequency Sweeps

The frequency sweeps are given in Figure 6-3 below.

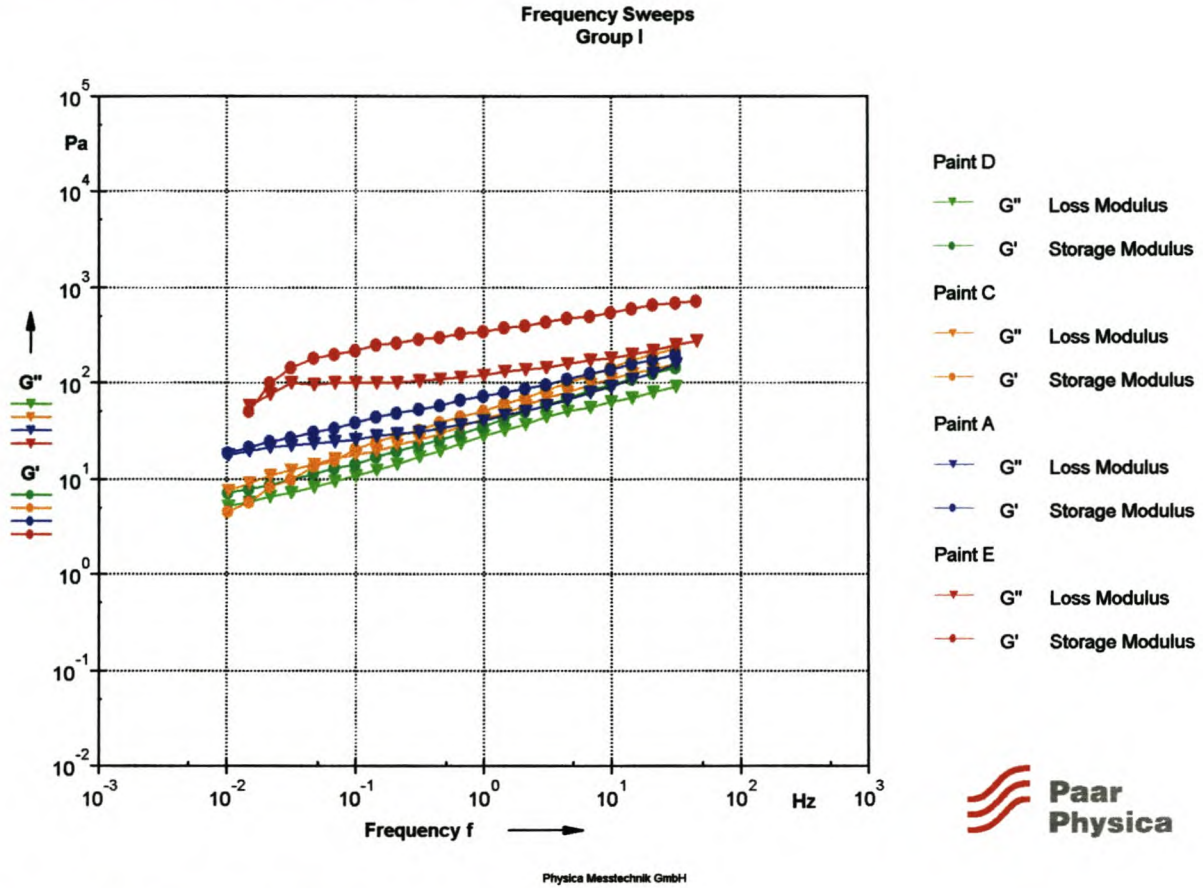


Figure 6-3: Frequency sweeps for the group I paints

Figure 6-3 gives the following information about the behaviour of the group I paints in the LVER:

- All the paints of group I are stable in the high-frequency range, because the solid-like behaviour predominates over the liquid-like behaviour ($G' > G''$).
- The G' and G'' curves for all the paints are almost parallel straight lines throughout the entire frequency range with only a slight slope which is an indication of a stable dispersion.
- The fact that $G' > G''$ in the high-frequency range will also assist against spattering behaviour during roller application.

- In the low-frequency range ($f < 1$ Hz) both paints A and C behave in a manner in which the liquid-like behaviour (G'') predominates over the solid-like behaviour (G') and therefore the sample is allowed to gradually spread under its own weight and flow as a highly viscous liquid. This enables the paint to flow and the film to spread out and will result in good levelling behaviour without any brush marks.
- This liquid-like behaviour usually results in poor in-can stability, but paints A and C both have high structural strengths, G' (see Table 6.4), which assists against sedimentation and therefore illustrates ideal long time-scale behaviour.

6.1.1.4 Three-Interval-Thixotropy-Test (3-ITT)

The 3-ITT curves are given in Figure 6-4 below.

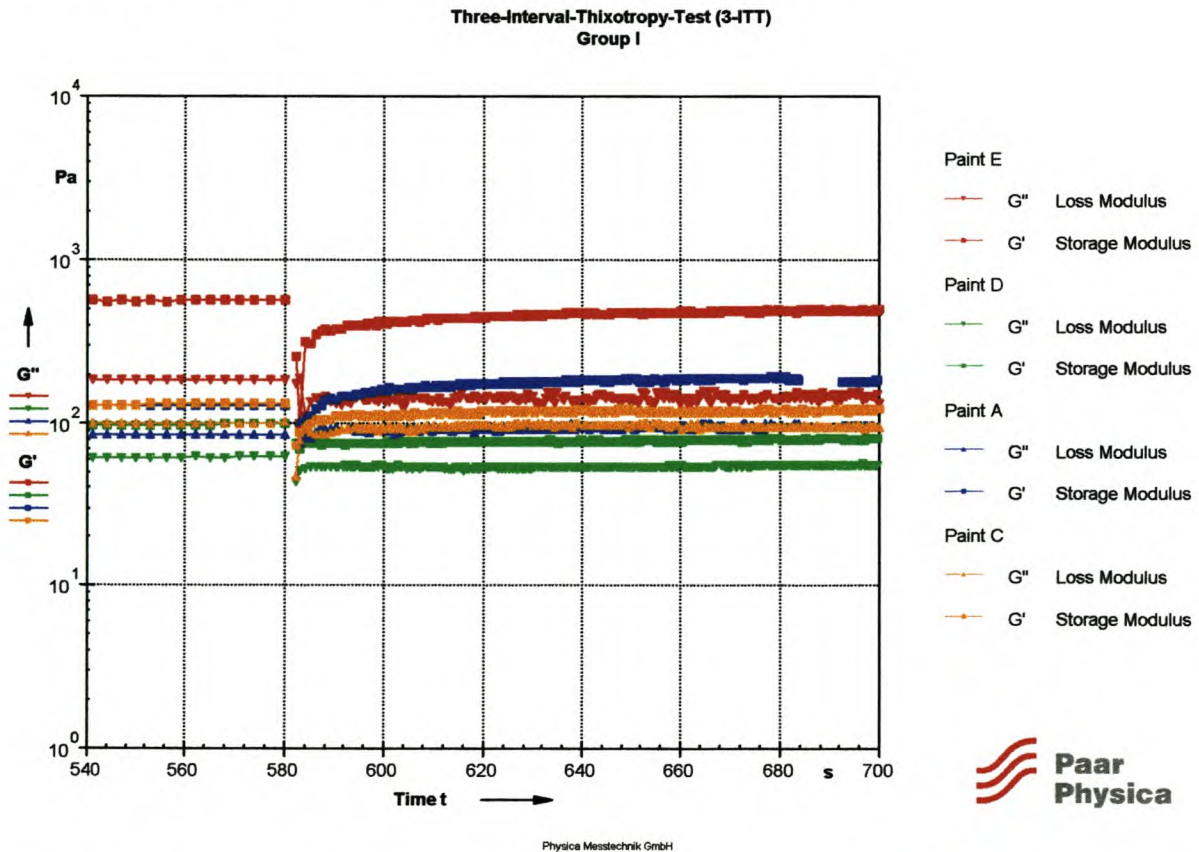


Figure 6-4: 3-ITT curves for group I paints

Figure 6-4 shows the following behaviour for the group I paints after high shear:

- $G' > G''$ for all the paints directly after the high-shear load and therefore the solid-like behaviour of the samples predominates almost immediately over the liquid-like character, therefore not allowing any flow (levelling) to take place. The following table illustrates the amount of structural recovery for each paint.

Table 6-6: Percentage structural recovery for paints of group I

Paint	% recovery after 5 sec.	% recovery after 10 sec.	% recovery after 20 sec.	% recovery after 60 sec.	% recovery after 100 sec.
Paint E:	55	67	72	83	86
Paint D:	75	75	76	78	80
Paint A ² :	80	108	125	143	148
Paint C:	75	84	84	90	90

From the table it is clear that all the paints recover very quickly, with paints D, A and C recovering to at least 75% of their original structural strength after only 5 seconds, therefore recovery is very quick and levelling behaviour not at an optimum.

6.1.1.5 Conclusions

The following are the most important conclusions that can be drawn:

- The higher-quality paints have lower degrees of pseudoplasticity and therefore indicates that their structures are not broken down as easily as that of the lower-quality paints. This is a first indication that the high-quality paint has a higher structural strength, resulting in better stability of the paint.
- The low-quality matt paint is prone to poor flow and levelling behaviour, resulting in possible brush marks due to the high viscosity over the whole shear-rate range. It is interesting, because this paint also has the highest degree of pseudoplasticity, but still has the highest viscosity in the high-shear rate range.

² Structural recovery greater than 100% occurs when the structure is broken down during high shear, which allows for a new arrangement of molecules resulting in a higher structural strength than before the shear load was applied.

- The high-quality paints have lower low-shear viscosities than the low-quality paints. The advantages of this behaviour are that it allows for good flow and levelling behaviour to ensure that no brush marks are left behind on the final coating. However, a possible disadvantage is that the lower low-shear viscosities indicate that the paints might have lower structural strengths and therefore should show poor structural stability and possible sagging behaviour. However, the structural strengths (G') of the high-quality paints obtained from the amplitude sweeps indicate that these paints have in fact high structural strengths and therefore will show good in-can stability. The amplitude sweeps also indicate that these paints have acceptable yield points and therefore show acceptable sagging behaviour.
- The low-shear viscosity and the structural strength of paint E indicates a very high low-shear viscosity and structural strength, respectively, and is therefore likely to be in a semi-gelled state in the state of rest, which it indeed seems to be. This gelled state makes workability (pumping, mixing, pouring) difficult.
- All the paints, whether low or high quality, have a solid-like character that predominates over the liquid-like behaviour and therefore all the paints show some degree of rigidity and therefore some stability.
- The structural strength of the paints seems to increase with increasing quality.
- The lower-quality paints have excessively high yield points, which can cause the paints to result in a too-thick layer thickness and poor flow and levelling behaviour resulting in brush marks.
- None of the paints shows a tendency towards excessive spatter behaviour.
- All the paints of group I have solid-like character directly after high shear and therefore none of the paints shows entirely ideal flow and levelling behaviour, because the paints are not allowed to flow directly after application. This may result in possible brush marks and poor flow and levelling behaviour of the final coating.

6.1.2 Group II

6.1.2.1 Viscosity Curves

The viscosity curves for the paints of group II are given in Figure 6-5 below.

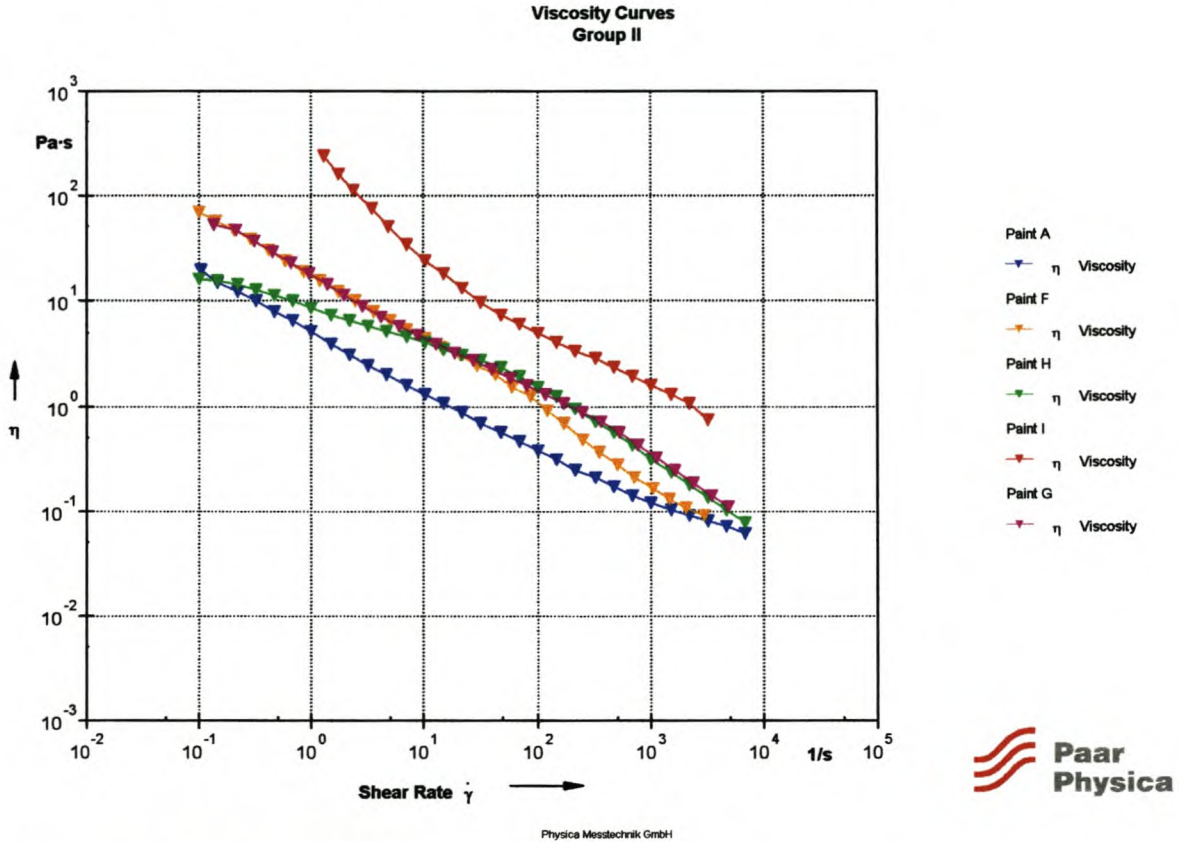


Figure 6-5: Viscosity curves for group II paints

Figure 6-5 indicates the following flow behaviour for the group II paints:

- It becomes clear, when the viscosity curves of group II are compared to those of group I, that the curves are much more diverse in behaviour over the whole shear-rate range in terms of shear-thinning behaviour and general viscosity behaviour, therefore indicating very different flow behaviour. For example, when comparing the sheen paints (water-based vs. solvent based), the water-based sheen paint (paint A) follows a power-law model with R^2 values of 0.9952 in contrast to the solvent-based sheen paint (paint I) that has a R^2 value of only 0.9002 for the power-law model. In other words, the viscosity behaviour of the two sheen paints differs a lot. In addition to the difference in the shape of the viscosity curves,

the solvent-based paint has viscosity behaviour of almost one decade higher than the water-based paint over the whole shear-rate range.

- The high low-shear viscosity of the solvent-based paint can result in problematic workability behaviour.
- Paint H, the roof paint, is less pseudoplastic in the low shear-rate range ($\dot{\gamma} < 10 \text{ s}^{-1}$) and, although still pseudoplastic in behaviour, tends to be more Newtonian. This already illustrates the liquid-like character of the paint.
- Paint F, the textured paint with solid particles, shows a lot of pseudoplastic behaviour in the high shear-rate range ($\dot{\gamma} > 100 \text{ s}^{-1}$). This behaviour is ideal for a paint that is textured – the particles in the paint are allowed to *flow* and orientate themselves during application due to the low viscosity behaviour in the high shear-rate range.

Although a lot of information on the character of the paints was obtained from the viscosity curves, only the tests performed in the LVER give information about the character of the samples that is entirely accurate (see sections 6.1.2.2 and 6.1.2.3 for the amplitude and frequency sweeps for the paints of group II).

6.1.2.2 Amplitude Sweeps

The amplitude sweeps are given in Figure 6-6.

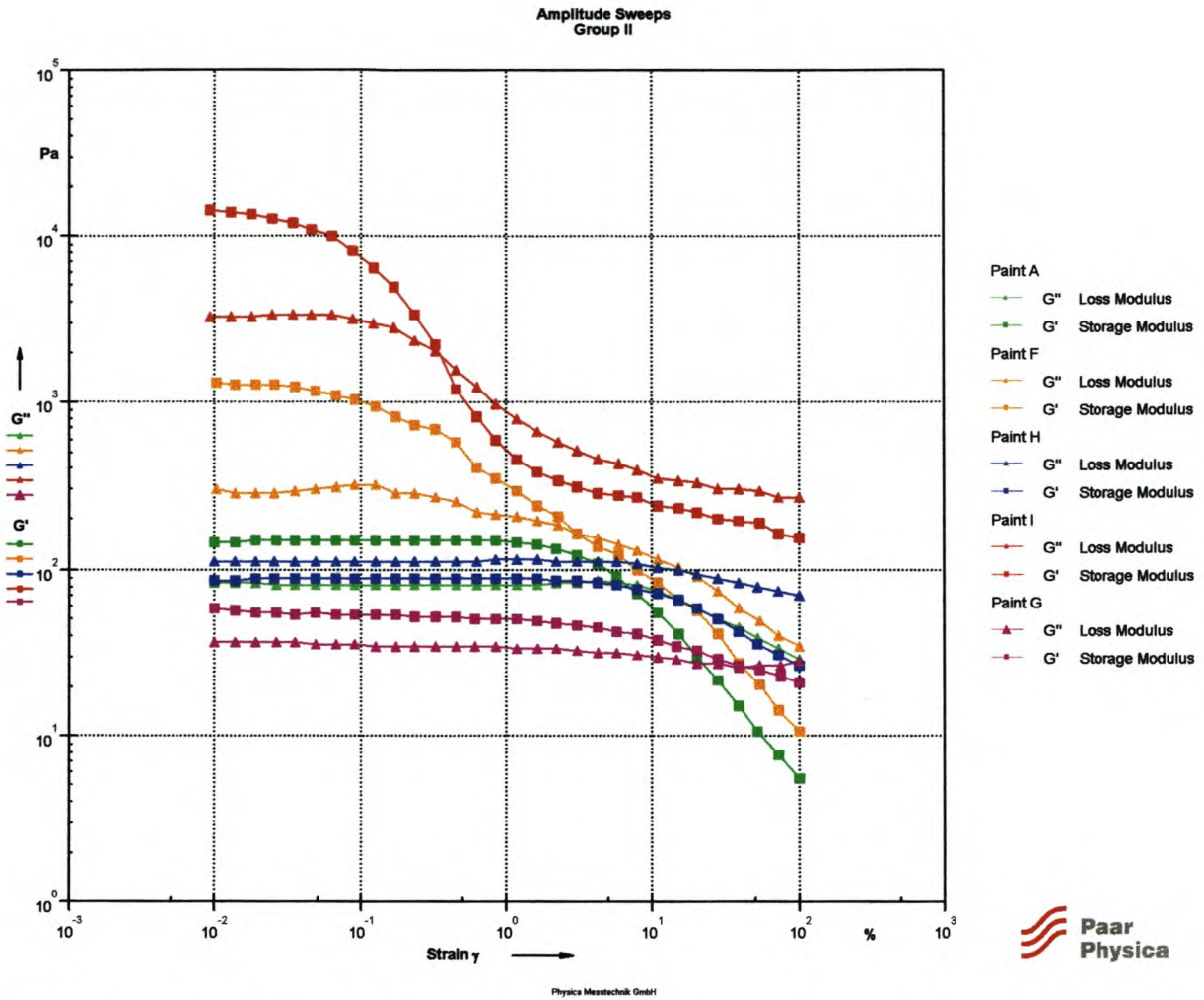


Figure 6-6: Amplitude sweeps for group II paints

The following information about the character of the group II paints are given in Figure 6-6:

- $G' > G''$ in the LVER for all the paint samples except for paint H, the roof paint, and therefore the solid-like behaviour predominates over the liquid-like character; the samples also show some rigidity and therefore a certain form of stability. However, paint H has a liquid-like character in the LVER and therefore has a lower degree of stability.
- Different degrees of structural strengths (G') exist for the various paints of group II.

Table 6-7: Structural strengths (G') of group II paints

Paint	Description	G' [Pa]
Paint I:	Sheen (solvent-based)	1420
Paint F:	Textured	1330
Paint A:	Sheen (water-based)	150
Paint H:	Roof	87
Paint G:	Ceiling	57

The difference in structural strengths is apparent from the table. The difference in the structural strength between the ceiling paint and the solvent-based sheen paint is more than 20 times. It is almost as if one can correlate the structural strength with the durability of the paint (except the roof paint). A solvent-based sheen paint is used as an all-surface paint and a textured paint as a durable outdoor paint, especially for harsh weather conditions, while a ceiling paint will hardly ever have to be very durable as it experiences no wear and tear.

- The yield points are given in the table below.

Table 6-8: Yield points of group II paints

Paint	Yield Point [Pa]
Sheen (solvent-based):	3.2
Textured:	0.6
Sheen (water-based):	3.5
Roof:	8.2
Ceiling:	0.3

The following yield point information is obtained from Table 6-8:

- The sheen paints (water- and solvent-based) have more or less the same yield points and will therefore have very similar sagging behaviour on a vertical wall.
- The textured paint has a very low yield point. If the yield point is used as an indication of the layer thickness of the final coating, then it is quite surprising for an outdoor paint to have such a thin layer thickness. However, the yield point is only an indication of what the layer thickness might be, as the layer thickness also depends on the structural strength of the paint and the rate of structural recovery of the paint after high shear (see section 6.1.2.4. - Three-Interval-Thixotropy-Test).

- The roof paint, although the liquid-like behaviour predominates over the solid-like behaviour, has a very high 'yield point'. This will result in poor levelling behaviour leaving possible brush marks, which is not too problematic because the roof paint is a protective paint and not a decorative one. The high yield point will also result in a thick film that helps to protect the roof.
- The ceiling paint has a surprisingly low yield point for a paint that should not be allowed to sag. Such low yield points are also an indication of possible spatter during roller application, although this needs to be investigated in the frequency sweep (see section 6.1.2.3 – Frequency Sweeps).

6.1.2.3 Frequency Sweeps

The frequency sweeps are given in Figure 6-7 below.

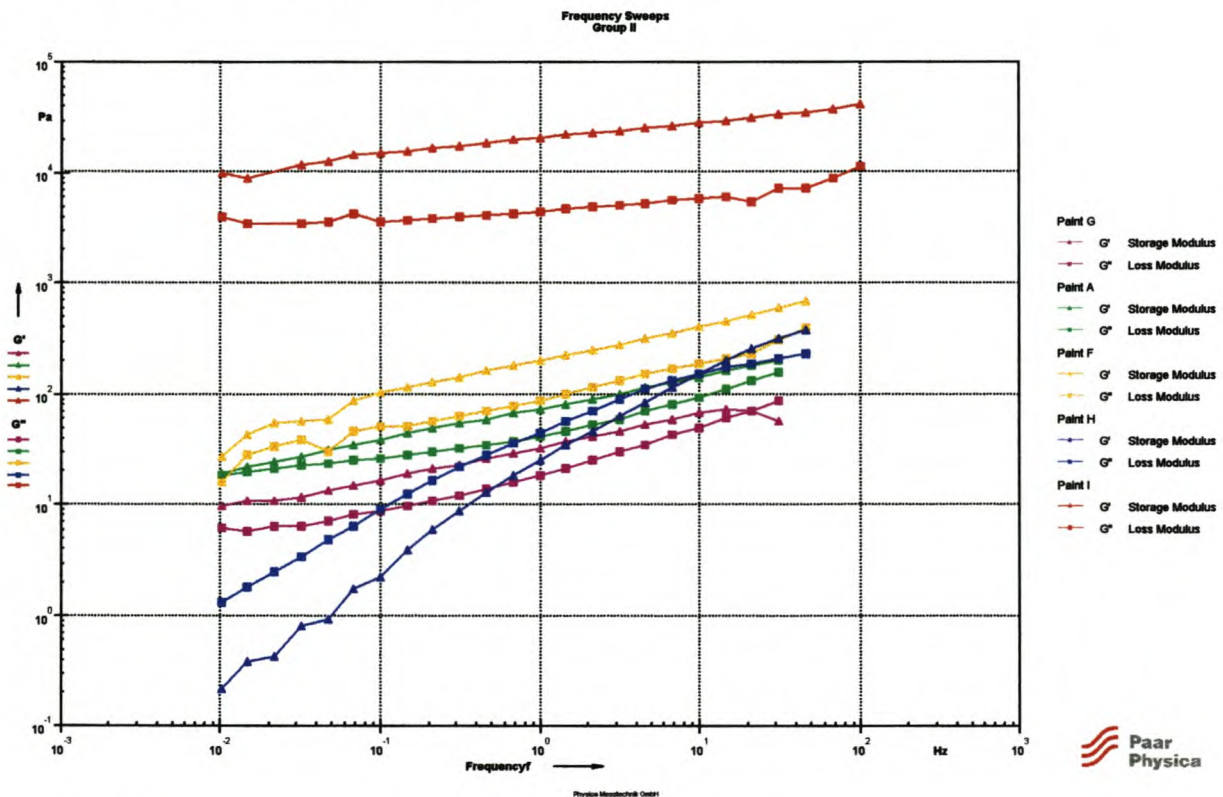


Figure 6-7: Frequency sweeps for group II paints

Figure 6-7 gives the following information about the behaviour of the group II paints in the LVER:

- All the paints, except paint H, behave in a predominantly solid-like way over the whole frequency range, with the G' and G'' curves running almost parallel, with only a slight slope; therefore there is a certain degree of stability.
- Once again, the high structural strength of paint I (solvent-based/sheen) stands out above the rest. It is also observed that this paint behaves in a semi-gel-like manner in the can.
- Paint H behaves in a viscous manner in the low-frequency range, with the curves not running parallel and with very steep gradients. This may lead to instability in the long time-scale behaviour such as in-can storage, resulting in possible sedimentation or phase separation.
- Paint G, the ceiling paint, indicates that that it will have a tendency to spatter during roller application due to the G'' modulus having the tendency to be larger than G' in the high-frequency range of the frequency sweep (as was suspected with the very low yield point). Laboratory tests also indicate that the ceiling paint indeed spatters excessively (see Figure 6-8).

Ceiling paint:



vs.

High-quality matt paint:



Figure 6-8: Spatter behaviour for the ceiling paint and a high-quality matt paint.

This is quite strange behaviour for a ceiling paint, which is designed specifically for anti-spatter behaviour.

6.1.2.4 Three-Interval-Thixotropy-Test (3-ITT)

The 3-ITT curves are given in Figure 6-9 below.

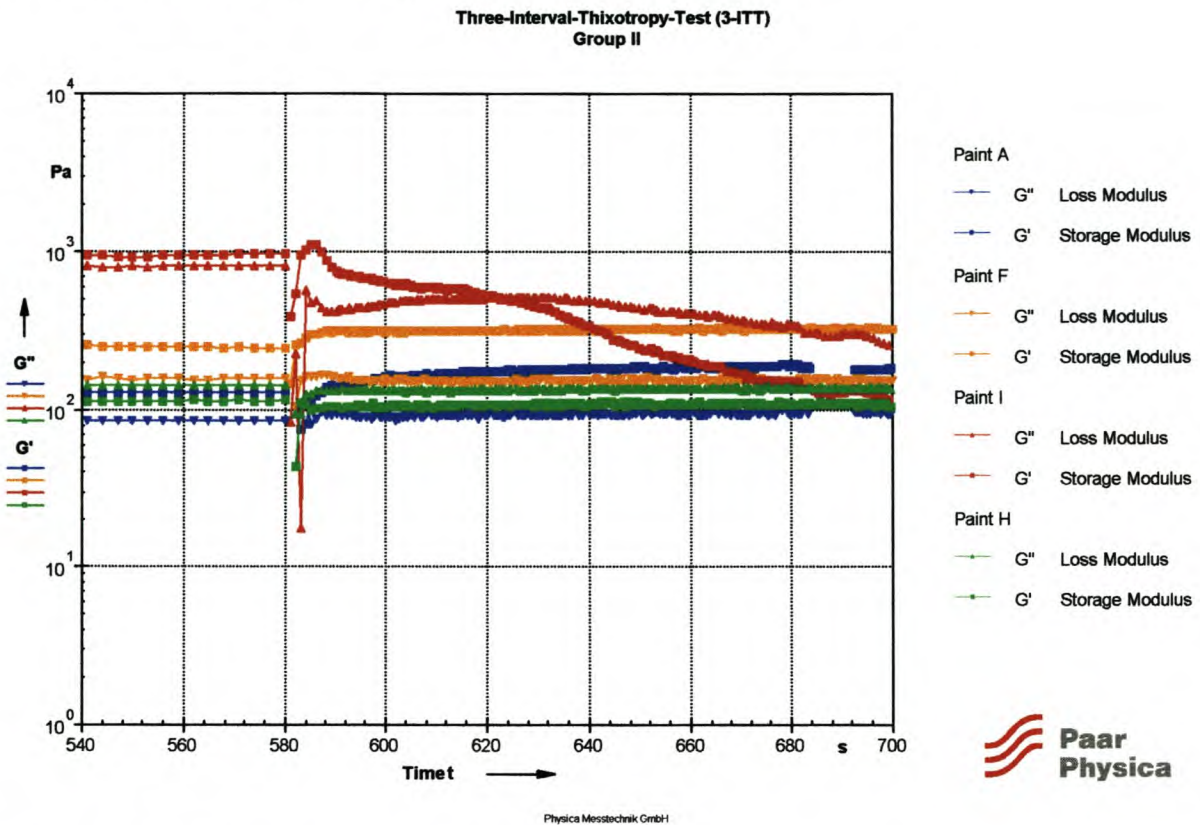


Figure 6-9: 3-ITT curves for group II paints

Figure 6-9 reveals the following information:

- Once again, as with group I, most of the structures recover immediately, with $G' > G''$ except for paint H, which has liquid-like behaviour after the high-shear load (as it does before the high-shear load). Therefore the paints do not flow directly after application and this may result in poor levelling behaviour such as brush marks and an inability to fill cracks and holes.
- Paint F recovers to even higher G' values immediately after the high-shear load and therefore has almost no time to flow and level out on the surface. Previously (section 6.1.2.2 – Amplitude sweeps) it was found that this paint has a very low yield point value and that this might result in possible sagging behaviour; however, the 3-ITT shows different behaviour and indicates that the paint will not tend to sag too much after application. Paint

F is the textured paint which is designed for high durability and therefore recovers quickly to form a relatively thick film, but will not be able to fill large cracks and holes ideally.

- Paint I recovers in a very strange manner. G' recovers immediately to be higher than G'' , but then decreases so that after 40 seconds G'' is greater than G' and therefore behaves in a liquid-like manner. The instructions on the can state: “*Stir and let stand for 8 hours before use*”.

Paint I is a solvent-based paint. Therefore this test is not ideal for testing the behaviour directly after application, because the measuring system does not allow for the same rate of evaporation of the solvent as happens when the solvent based-paint is spread in a thin film on the surface. However, this test method is reliable in determining the structural recovery after it has been stirred and left to stand for 8 hours, because then the same conditions are simulated (very little evaporation of solvent). It will be interesting to see how the structure recovers during the entire 8 hours after mixing.

- The recovery of paint A was already discussed in section 6.1.1.4.

6.1.2.5 Conclusions

- The viscosity behaviour of the two sheen paints differs completely, not only in viscosity levels but also in shear-thinning behaviour. The water-based sheen paint can be modelled accurately with the power-law model ($R^2 = 0.9952$), while the solvent-based sheen paint can not be modelled *that* accurately with the power-law model ($R^2 = 0.9002$).
- The high structural strength (G') and high low-shear viscosity of the solvent-based paint might lead to possible poor workability.
- The paints of group II show diverse flow behaviour.
- The solid-like character (G') of all the paints (except the roof paint) predominates over the liquid-like character (G'') and therefore a certain degree of rigidity/stability exists.

- There seems to be a correlation between the structural strength (G') and the durability of the paint (except the roof paint).
- The textured and ceiling paints have low yield points, which does not seem to correlate with the end-use they are designed for.
- All the paints in group II seem to be stable except paint H, the roof paint, which seems to show poor long time-scale behaviour, resulting in poor in-can stability.
- The ceiling paint might tend to spatter, which is especially unacceptable for a ceiling paint.
- All the group II paints, except the roof paint (paint H), recover, with the solid-like behaviour predominating over the liquid-like behaviour directly after high shear. Therefore the paints are not allowed to flow and this may result in poor flow and levelling behaviour of the paints, resulting in brush marks and the inability to fill cracks in the surface.

6.2 Rheological Comparison of Paints From Company ABC and XYZ

Paints that fall within the same categories, but from two different companies, were examined. The four paints are all top of their range. The details of the paints are given in the table below.

Table 6-9: Description of paints manufactured by two different companies

Paint	Company	Base	Quality	Use	Description
Paint ABC1:	ABC	Water	High	Interior	Sheen/semi-gloss
Paint XYZ1:	XYZ	Water	High	Interior	Sheen/semi-gloss
Paint ABC2:	ABC	Solvent	High	Interior	Sheen/gloss
Paint XYZ2:	XYZ	Solvent	High	Interior	Sheen/gloss

From the table it can be seen that two water-based paints and two solvent-based paints, all of high quality, have been chosen for the rheological comparison.

6.2.1 Water-Based Paints

6.2.1.1 Viscosity Curves

The viscosity curves of the two water-based paints, paints ABC1 and XYZ1, are given in Figure 6-10 below.

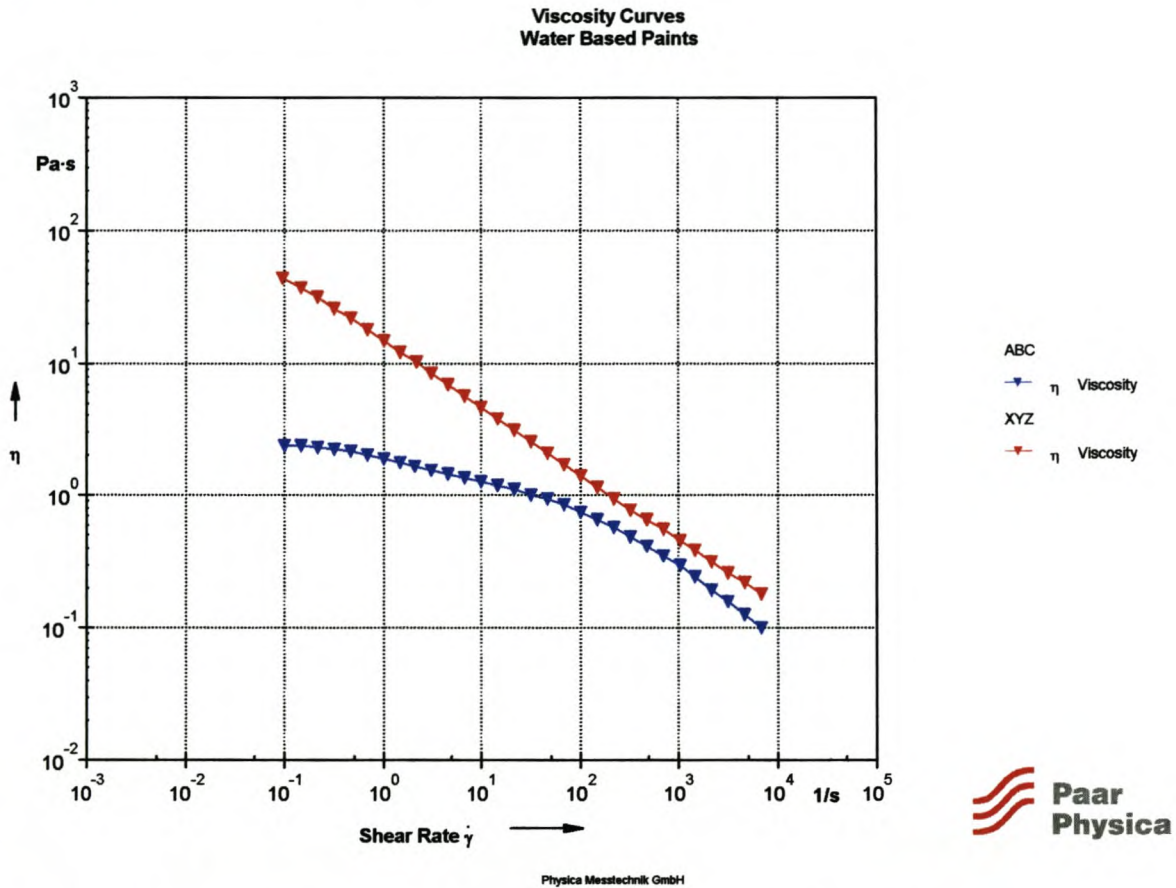


Figure 6-10: Viscosity curves for water-based paints of companies ABC and XYZ

The following flow behaviour is indicated by Figure 6-10:

- The differences in the viscosity curves can clearly be seen. The viscosity curve for the paint manufactured by company XYZ is higher over the whole shear-rate range than that of the paint manufactured by company ABC.
- The paint manufactured by XYZ is much more shear-thinning than that of the paint manufactured by ABC.

- The difference in the viscosity behaviour in the low shear-rate range is especially noticeable in contrast to the high shear-rate range, where the difference in viscosity is not that great. The following table gives the values for the high- and the low-shear viscosities.

Table 6-10: High and low-shear viscosities of water-based paints

Paint company	Low-shear viscosity @ 0.1 s^{-1} [Pa.s]	High-shear viscosity @ 10^4 s^{-1} [Pa.s]
ABC:	2.4	0.102
XYZ:	43.5	0.180

The values in the table indicate the large difference in low-shear viscosities and the smaller difference in high-shear viscosities. The power-law model is not fitted to the different curves as it is apparent that the power-law model will not give a good fit for the paint manufactured by company ABC and will therefore not be comparable on model parameters.

The high value of the low-shear viscosity of the paint manufactured by company XYZ will lead to good in-can stability, but will lead to poor flow and levelling behaviour, which may result in brush marks. Difficult roller and brush application can also be expected due to the high high-shear viscosity. The low low-shear viscosity of the paint manufactured by ABC will possibly lead to less satisfactory in-can stability compared to the paint of company XYZ, but better flow and levelling behaviour with fewer brush marks on the final film.

The degree of in-can stability observed from the viscosity curves by means of low-shear viscosities, is only a preliminary finding; the amplitude sweep and the frequency sweep will give more informative results (see sections 6.2.1.2 and 6.2.1.3 respectively).

- The paint manufactured by ABC is almost Newtonian in the low shear-rate range. In other words, the paint almost behaves like a purely viscous liquid. This already gives an indication of the liquid-like behaviour in the LVER at very low deformations (e.g. low yield point, sagging behaviour, etc). This is investigated further in the oscillatory tests.

6.2.1.2 Amplitude Sweeps

The amplitude sweeps of the two water-based paints, paints ABC1 and XYZ1, are given in Figure 6-11 below.

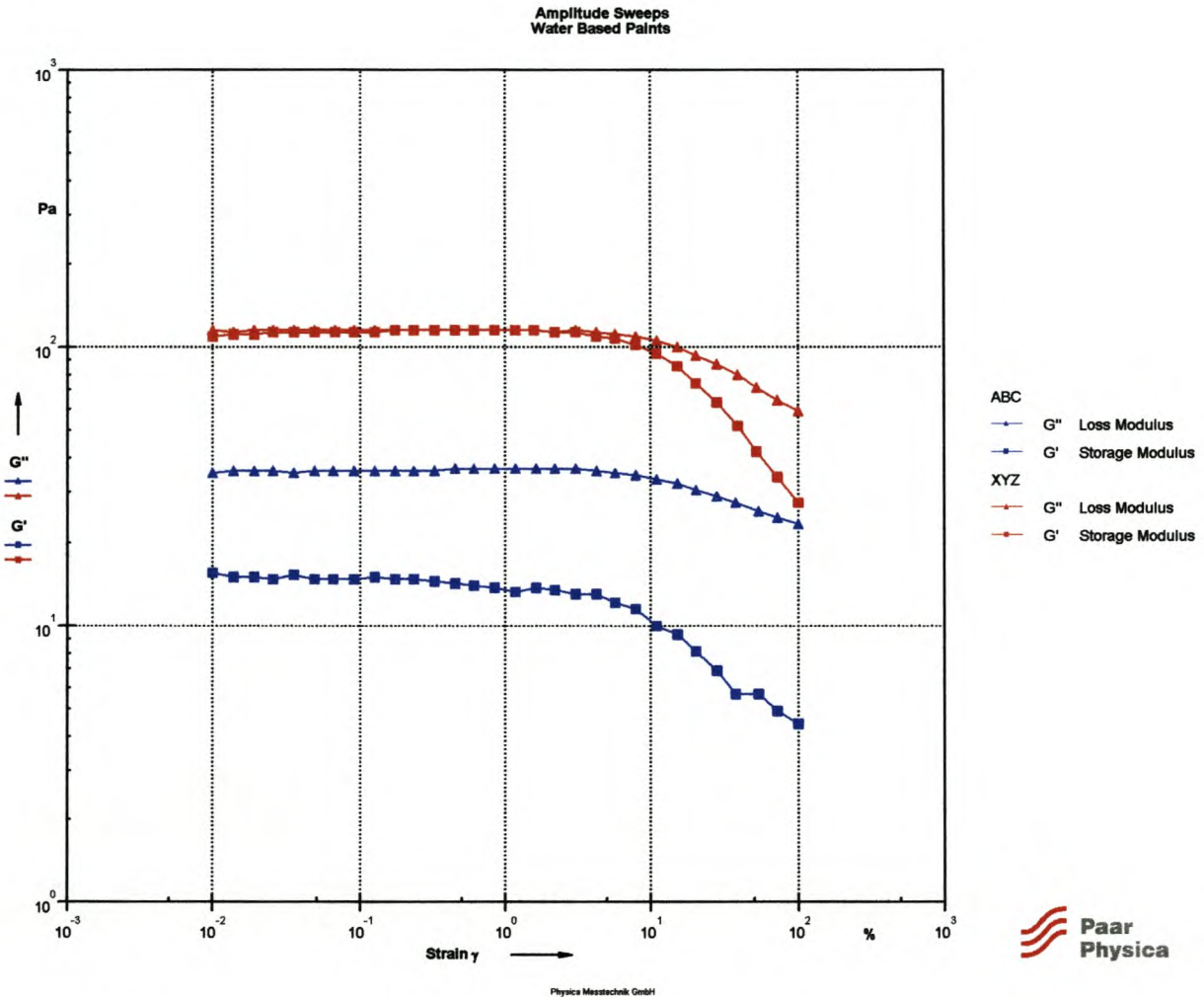


Figure 6-11: Amplitude sweeps for water-based paints of companies ABC and XYZ

Figure 6-11 reveals the following information about the character of the two water-based paints:

- It is clear from the figure that differences exist in the character of the two paints manufactured by the two companies.
- $G' < G''$ for the paint manufactured by paint company ABC, in contrast to the paint manufactured by XYZ, where $G' = G''$ in the LVER. Therefore, the liquid-like behaviour predominates over the solid-like behaviour for the paint manufactured by ABC and very

little degree of a structure exists. This also confirms the near-Newtonian (viscous) behaviour in the low shear-rate range of the viscosity curves.

- Both the paints show a largely liquid-like character in the LVER and therefore both will have low yield points due to the liquid-like character. The low yield points are also an indication of possible spatter during roller application.
- To examine the yield points of the samples, the stress values are expressed on the x-axis.

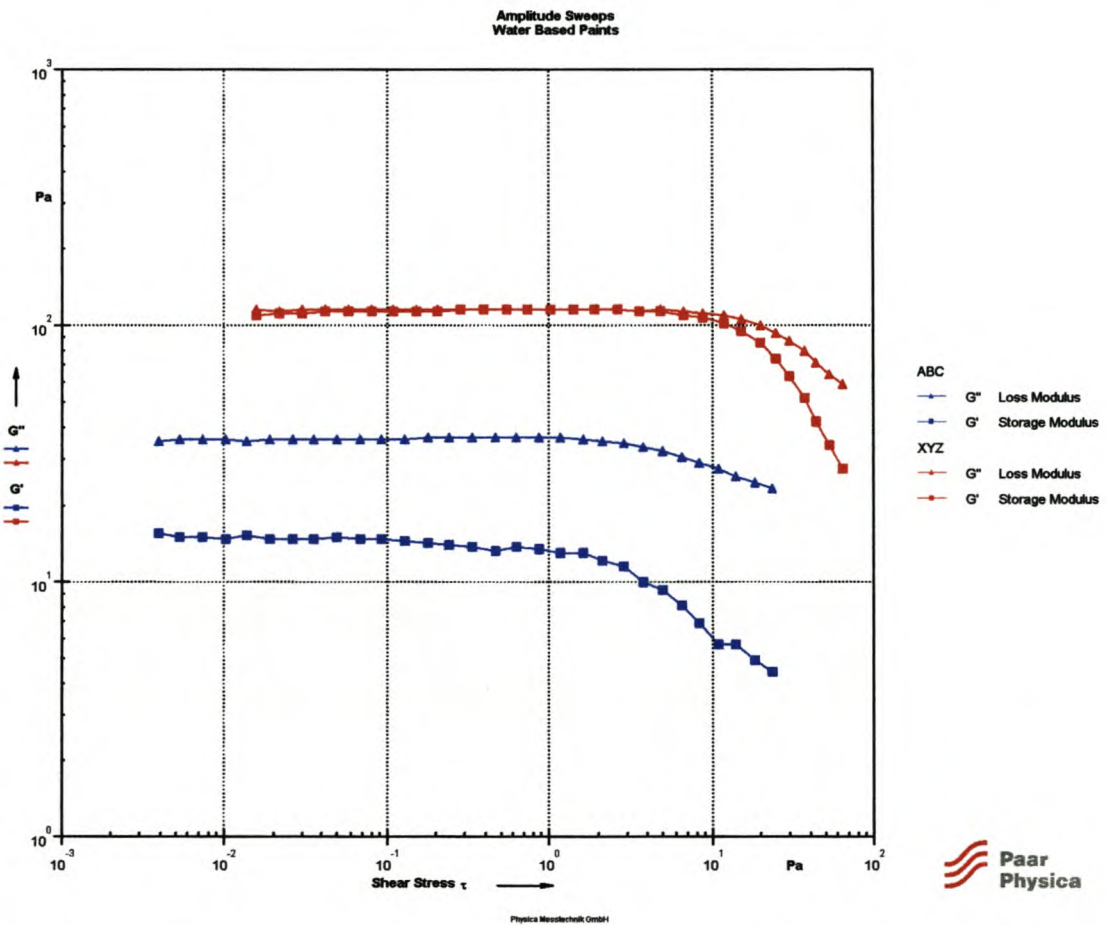


Figure 6-12: Amplitude sweeps for water-based paints of companies ABC and XYZ (shear stress on x-axis)

If the yield point is determined where $G'' > G'$, then both samples have very small yield points, because both have a largely liquid-like character in the LVER, with $G'' \geq G'$ (a long discussion can follow on what the yield point of a sample exactly is – whether it is the point where $G'' > G'$, or whether it is the point where the constant plateau values of G' or G'' starts to deviate from the values in the LVER is still not entirely clear). However, the fact

remains that both paints have a predominantly liquid-like character. This is already an indication of what the paint is designed for - the low yield point will result in very good levelling, resulting in the sheen/gloss paint it is designed to be. However, sagging and spattering might be a problem. The time-dependent tests will lead to a better understanding of the long and short time-scale behaviour.

- The paint manufactured by XYZ has a higher structural strength in terms of G' and may therefore tend to sag less. Further tests are required to determine sagging behaviour (see section 6.2.1.4 – Three-Interval-Thixotropy-Test)

6.2.1.3 Frequency Sweeps

The frequency sweeps of the two water-based paints, paints ABC1 and XYZ1, are given in Figure 6-13 below.

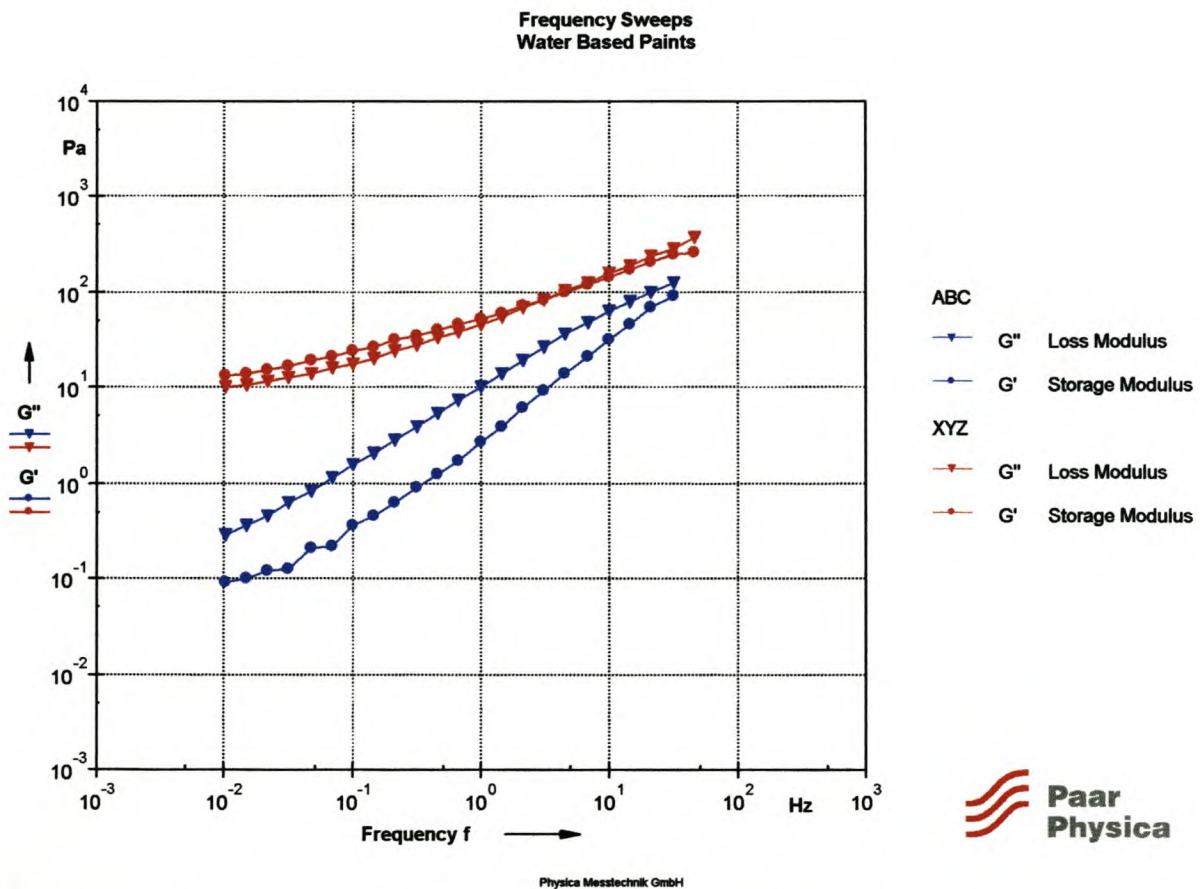


Figure 6-13: Frequency sweeps for water-based paints of companies ABC and XYZ

Figure 6-13 shows the following behaviour of the two water-based paints in the LVER:

- $G'' > G'$ in the low-frequency range for the paint manufactured by ABC and therefore the liquid-like behaviour predominates over the solid-like behaviour. This may lead to possible sedimentation or phase separation and therefore might show poor in-can stability. The gradients of the G' and G'' curves are also very steep and therefore the paint is less stable.
- $G' > G''$ in the low-frequency range for the paint manufactured by XYZ and therefore the solid-like behaviour predominates over the liquid-like character (although G' predominates over G'' only marginally). This paint will have a smaller tendency towards sedimentation and phase separation and therefore show better in-can stability than the paint manufactured by ABC. The gradients of the G' and G'' curves are also shallower and therefore the paint has higher stability.
- The liquid-like behaviour of both paints is very evident in the low-frequency range. The low-frequency range simulates changes in the structure that takes place at long time-scales, like levelling and sagging of the paint. As mentioned earlier, both these paints are sheen/gloss paints, which explains their viscous behaviour in the low-frequency range, allowing for good levelling and degassing, resulting in a sheen/gloss coating.
- $G'' > G'$ in the high-frequency range and therefore the liquid-like behaviour predominates over solid-like behaviour and both samples will tend to spatter to a certain extent during roller application.

6.2.1.4 Three-Interval-Thixotropy-Test (3-ITT)

The 3-ITT curves of the two water-based paints, paints ABC1 and XYZ1, are given in Figure 6-14.

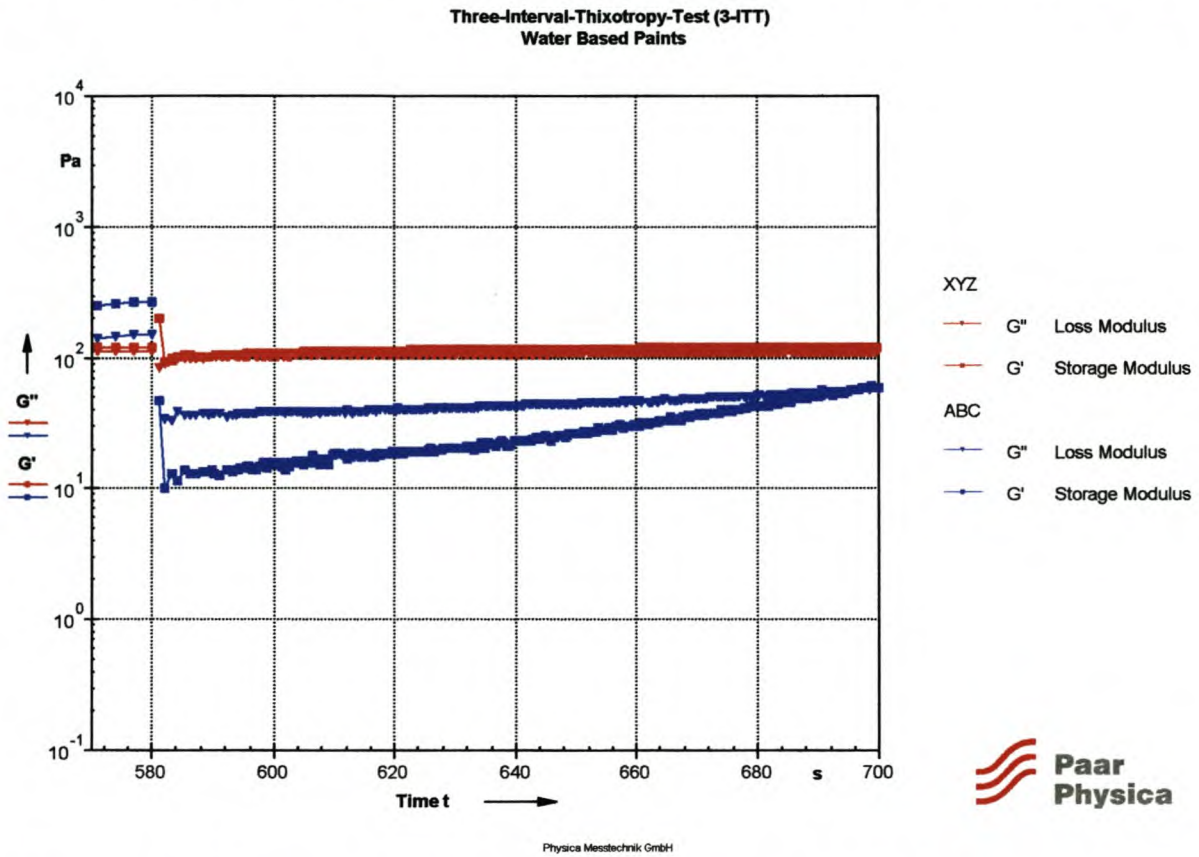


Figure 6-14: 3-ITT curves for water-based paints of companies ABC and XYZ

Figure 6-14 shows the following behaviour for the structural regeneration of the two water-based paints after high shear:

- $G' = G''$ directly after the shear load for the paint manufactured by XYZ and therefore the solid and liquid-like behaviour have equal weight on the recovery of the structure of the paint. This type of recovery behaviour is probably the best for a sheen/gloss type of paint with a very low yield point – the sample is allowed to flow directly after the high-shear load, but not too much to prevent unwanted layer thickness and sagging behaviour due to the low yield point. The structural recovery of both G' and G'' might, however, be too fast to allow for optimal levelling behaviour. In contrast, the paint manufactured by ABC has a liquid-like character directly after a high-shear load and therefore the sample is allowed to flow. But the time period that $G'' > G'$ is also very important. $G'' > G'$ for almost two minutes and therefore the paint sample has liquid-like character for a very long duration of time after

application. This will result in excellent sheen/gloss properties, but poor layer thickness and possible sagging behaviour.

6.2.1.5 Conclusions

The following comparison between the water-based paints can be made:

Table 6-11: Comparison between water-based paints from companies ABC and XYZ

	Company ABC	Company XYZ
In-can stability:	x	✓
Spatter:	xx	x
Ease of application:	✓	✓✓
Levelling:	✓✓	✓
Sag:	x	✓
Mixing/stirring:	✓	✓

From a rheological point of view, Table 6-11 shows that the paint manufactured by company XYZ is in general of a higher quality. However, the paint manufactured by company ABC will have better sheen/gloss properties (end-use it is specifically designed for) due to better levelling behaviour after application.

6.2.2. Solvent-Based Paints

6.2.2.1 Viscosity Curves

The viscosity curves for the two solvent-based paints, paints ABC2 and XYZ2, are given in Figure 6-15 below.

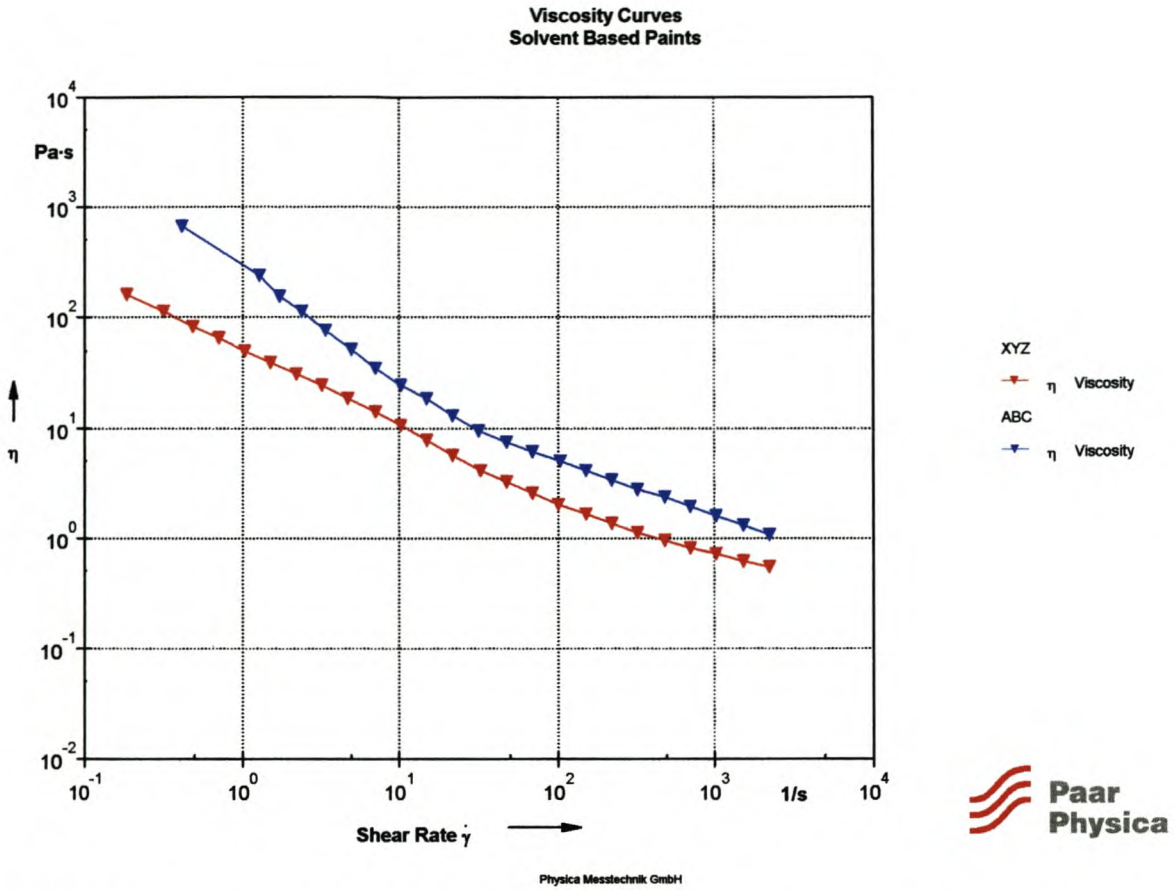


Figure 6-15: Viscosity curves for solvent-based paints of companies ABC and XYZ

Figure 6-15 illustrates the following flow behaviour for the two solvent-based paints:

- Both paints have more or less similar flow behaviour over the whole shear-rate range. In other words, both paints show almost equal shear-thinning behaviour. The paint manufactured by ABC tends to show a little bit more pseudoplasticity in the low shear-rate range.
- The paint manufactured by ABC has a higher viscosity over the whole shear-rate range. Therefore, the paint manufactured by ABC will tend to have better in-can stability and a higher yield point (although this is only a preliminary conclusion), but poorer application behaviour due to its higher high-shear viscosity and workability will also be more difficult due to higher medium-shear viscosities.

6.2.2.2 Amplitude Sweeps

The amplitude sweeps for the two solvent-based paints, paints ABC2 and XYZ2, are given in Figure 6-16 below.

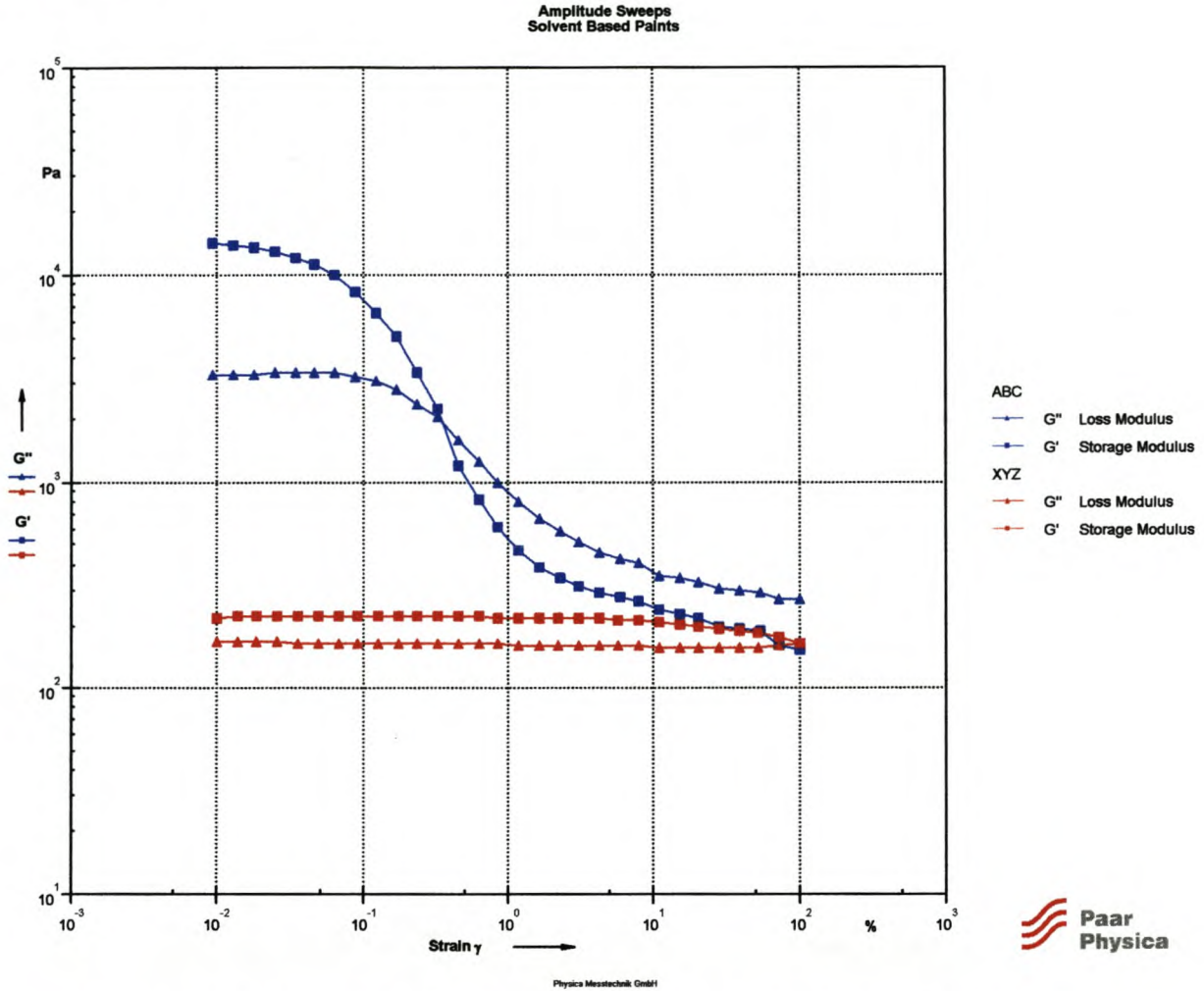


Figure 6-16: Amplitude sweeps for solvent-based paints of companies ABC and XYZ

The following information about the character of the paints is obtained from Figure 6-16:

- Clear differences exist in the character of the paints by examination of the G' and G'' curves in the LVER. Both paints have a solid-like behaviour ($G' > G''$) in the LVER, therefore showing some form of rigidity. $G' \gg G''$ for the paint manufactured by ABC in contrast to the paint manufactured by XYZ, where G' is not that much greater than G'', indicating a possible semi-gelled state during storage.

- Not only does the paint manufactured by ABC have higher G' values in relation to G'' values (lower $\tan \delta$ values), but the paint manufactured by ABC also has a higher internal structural strength because of the higher G' values. Therefore it is possible that the paint manufactured by ABC almost reaches a semi-gelled state in the state of rest.
- To investigate the yield point, the shear stress is presented on the x-axis.

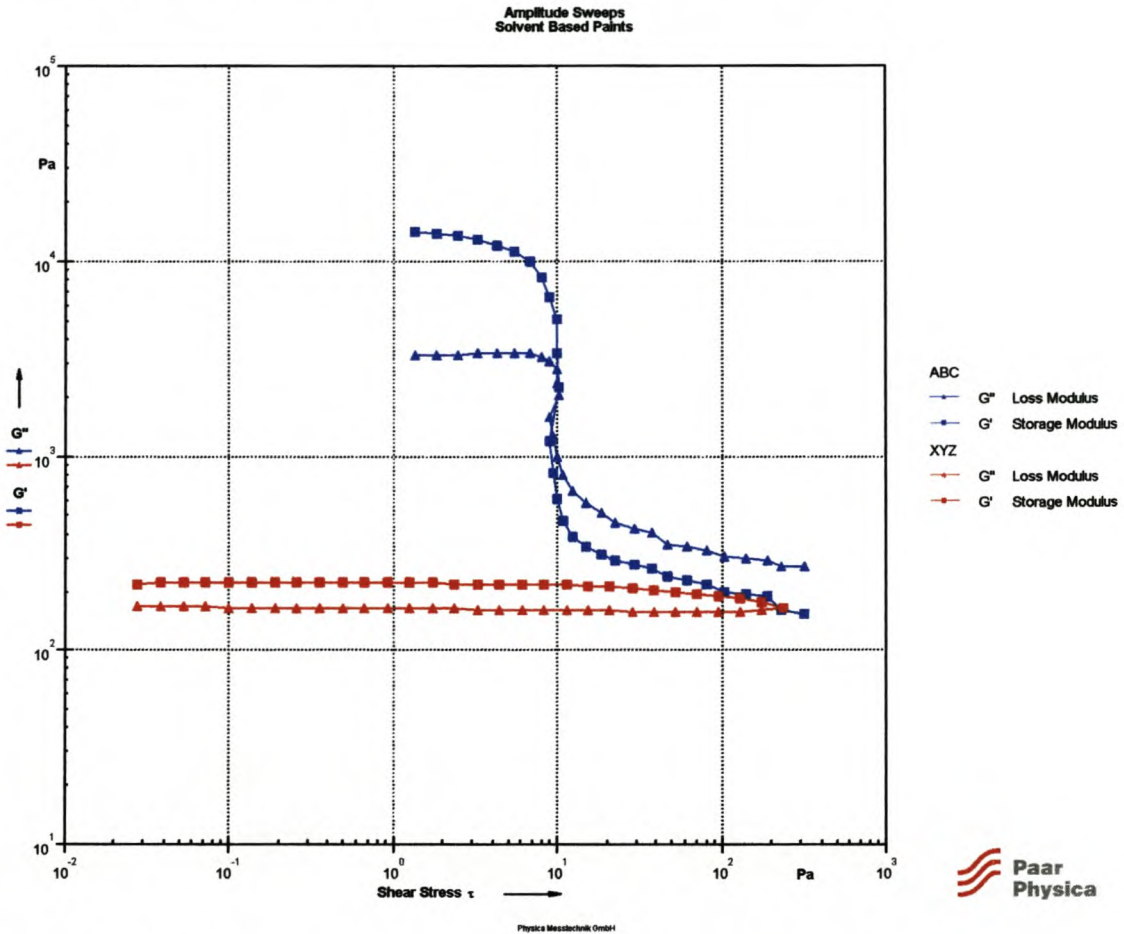


Figure 6-17: Amplitude sweep for solvent-based paints expressed in terms of shear stress

The paint manufactured by ABC has a much lower yield point than the paint manufactured by XYZ. The excessively high yield point of the paint manufactured by XYZ may result in poor levelling behaviour with brush marks. It may also result in a much thicker film.

6.2.2.3 Frequency Sweeps

The frequency sweeps for the two solvent-based paints, paints ABC2 and XYZ2, are given in Figure 6-18 below.

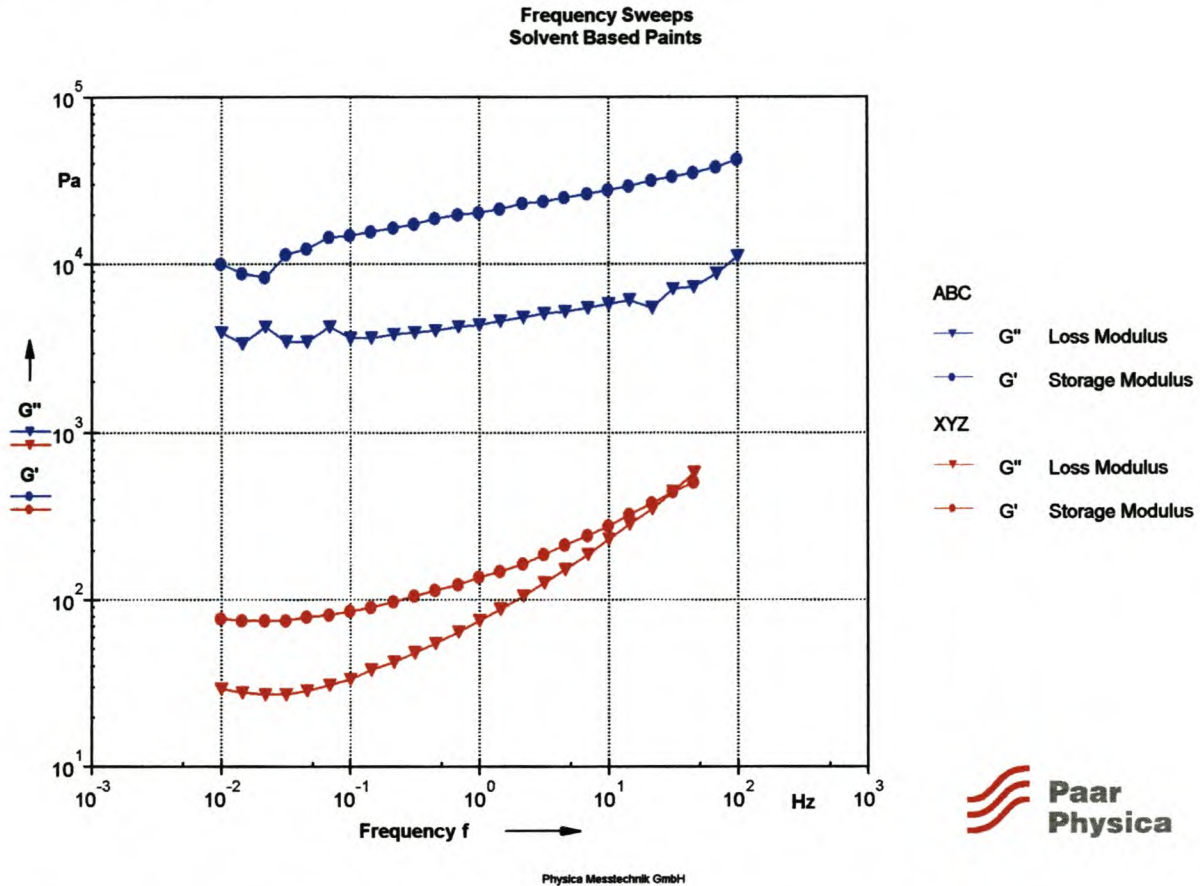


Figure 6-18: Frequency sweeps for solvent-based paints of companies ABC and XYZ

Figure 6-18 shows the following behaviour of the solvent-based paints in the LVER:

- $G' > G''$ for paint manufactured by ABC over the whole frequency range, running almost parallel to each other with little slope, an indication of a stable structure. The solid-like behaviour therefore predominates over the liquid-like behaviour over the whole frequency range. $G' > G''$ for paint manufactured by XYZ, but only up to a certain frequency where the G' and G'' curves converge and a cross-over point occurs where $G'' > G'$. Therefore, the solid-like behaviour predominates over the liquid-like character below the cross-over point, but the liquid-like behaviour predominates above the cross-over point at higher frequencies. The G' and G'' curves of company XYZ are not parallel to each other over the whole frequency range with a steeper slope, an indication of a less stable structure.

- The paint manufactured by ABC has a higher overall structural strength due to higher G' values.
- Both paints demonstrates solid-like behaviour ($G' > G''$) in the low-frequency range (long time-scale behaviour) with curves running parallel with only a slight slope, an indication of good long time-scale behaviour such as good in-can stability. Therefore sedimentation and phase separation should not be a problem for both paints.
- The liquid-like character predominates over the solid-like character for the paint manufactured by XYZ and therefore the paint is likely to spatter during roller application. The paint manufactured by ABC has solid-like behaviour in the high-frequency range and is therefore less likely to spatter.

6.2.2.4 Three-Interval-Thixotropy-Tests (3-ITT)

The 3-ITT curves of the two solvent-based paints, paints ABC2 and XYZ2, are given in Figure 6-19 below.

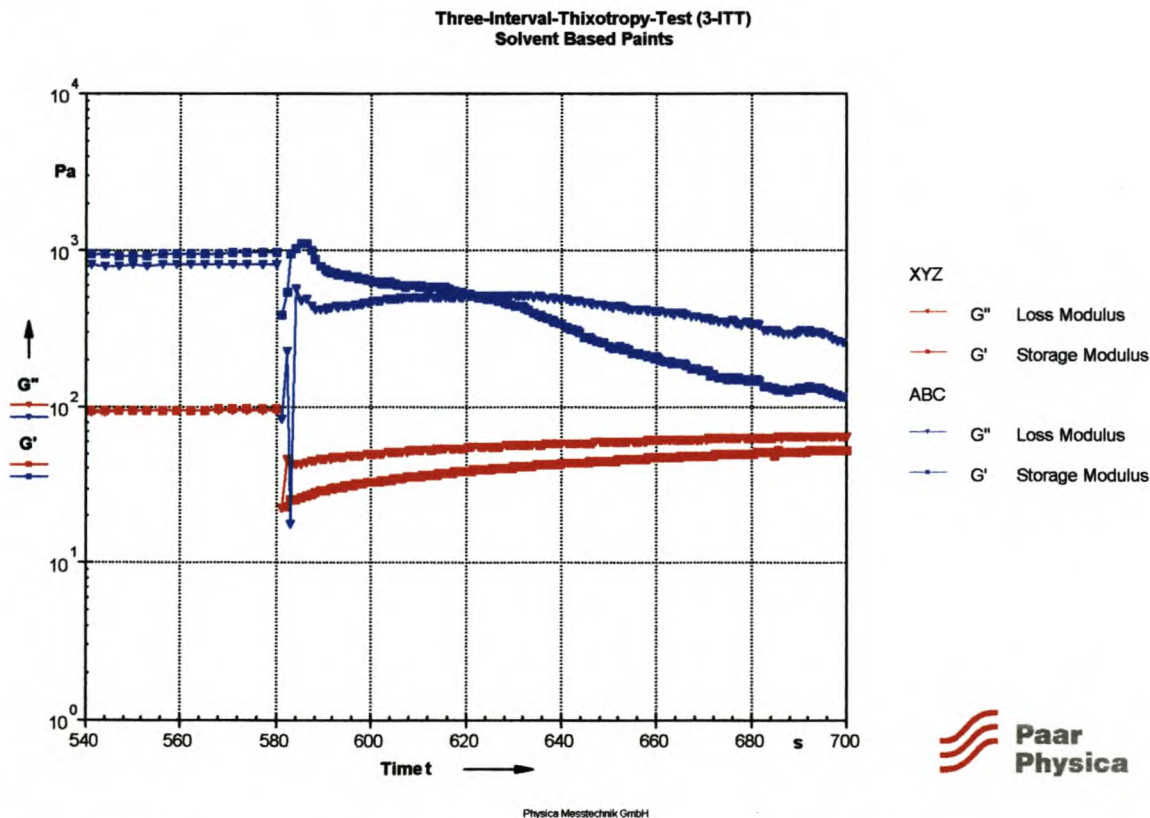


Figure 6-19: 3-ITT curves for solvent-based paints of companies ABC and XYZ

Figure 6-19 gives the following information about the structural regeneration of the solvent-based paints after high shear:

- Very different behaviour exists in the G' and G'' curves directly after the shear load. $G'' > G'$ for the paint manufactured by XYZ, allowing for the paint to flow and level out. It will therefore show good levelling properties, being able to fill cracks and small holes, but it might tend to sag after application. However, it has a very high yield point (see section 6.2.2.2), which will act against sagging behaviour. In contrast, the other paint immediately recovers with $G' > G''$ and the structural strength then decreases again. The instructions on the back of the can for this paint state: “*Stir and let stand for 8 hours before use*”. From the recovery curves it is evident why it must be left to stand for 8 hours after mixing, before it is applied – the structure must recover first.

6.2.2.5 Conclusions

The following comparison between the two solvent-based paints can be made:

Table 6-12: Comparison between solvent-based paints from companies ABC and XYZ

	Company ABC	Company XYZ
In-can stability:	✓✓	✓
Spatter:	✓	✗
Ease of application:	✓	✓
Levelling ³ :	-	-
Sag:	✓	✗
Mixing/stirring:	✓	✓

From a rheological point of view, Table 6-12 shows that the paint manufactured by company ABC is in general of a higher quality.

³ The levelling behaviour is omitted – the measuring system is not suitable for measurements of structural recovery after high shear for solvent-based paints, because it does not allow for the appropriate rate of solvent evaporation.

6.3 Comparison of a High-Quality (expensive) and a Low-Quality (inexpensive) Paint in Terms of Rheological Behaviour

Two paints that are both matt-type and low-sheen in behaviour are compared to each other in rheological terms.

Table 6-13: Cost of high- and low-quality paints⁴

Paint:	Price [Rand/litre]
High quality:	40
Low quality:	25

6.3.1 Viscosity Curves

The viscosity curves of the high- and low-quality paints are given in Figure 6-20 below.

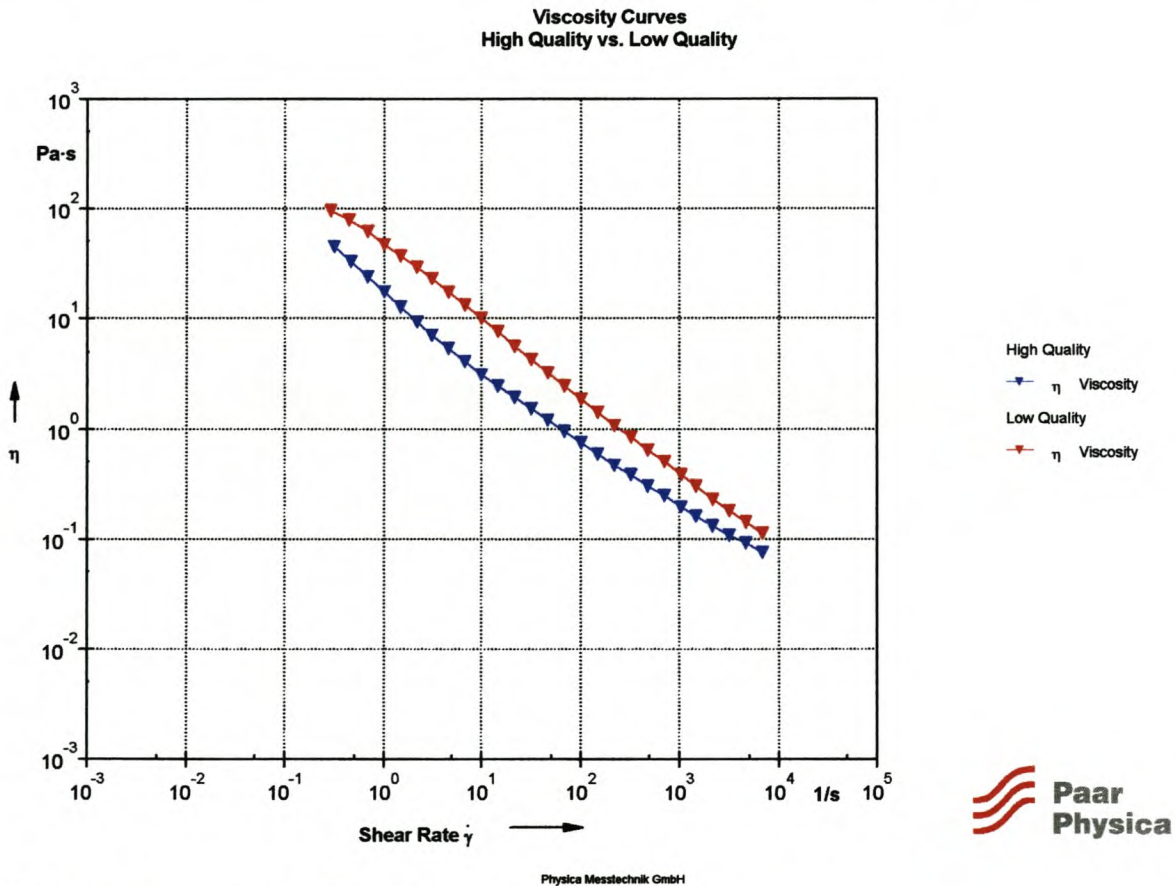


Figure 6-20: Viscosity curves for high- and low-quality paints

⁴ December 2002

The viscosity curves in Figure 6-20 show the following flow behaviour for the low- and high-quality paints:

- The viscosity of the low-quality paint is higher than the viscosity of the high-quality paint over the whole shear-rate range, but is especially noticeable in the low shear-rate range, where the low-shear viscosity of the low-quality paint is almost double that of the high-quality paint. The high low-shear viscosity of the low-quality paint will result in good in-can stability, but is excessively high. It will therefore result in brush marks in the final coating and result in poor flow and levelling behaviour with an inability to fill small cracks and holes. Roller or brush application of the low quality paint is also difficult due to the higher high-shear viscosity. This is typical behaviour of low-quality paint, where a large amount of thickener is added to the paint formulation to thicken it instead of the desired rheology modifier, which acts associatively. The thickener thickens the paint over the whole shear-rate range and does not adjust the viscosity behaviour associatively. The high-quality paint has a lower low-shear viscosity to allow for good levelling properties, but is still high enough to provide good in-can stability. At the same time, roller or brush application is easier due to the lower high-shear viscosity.
- Higher medium-shear rate viscosities of the low-quality paint will also result in difficulty in workability.

It is therefore apparent from the viscosity curves that the flow properties of the low-quality paint are insufficient.

6.3.2 Amplitude Sweeps

The amplitude sweeps of the high- and low-quality paints are given in Figure 6-21 below.

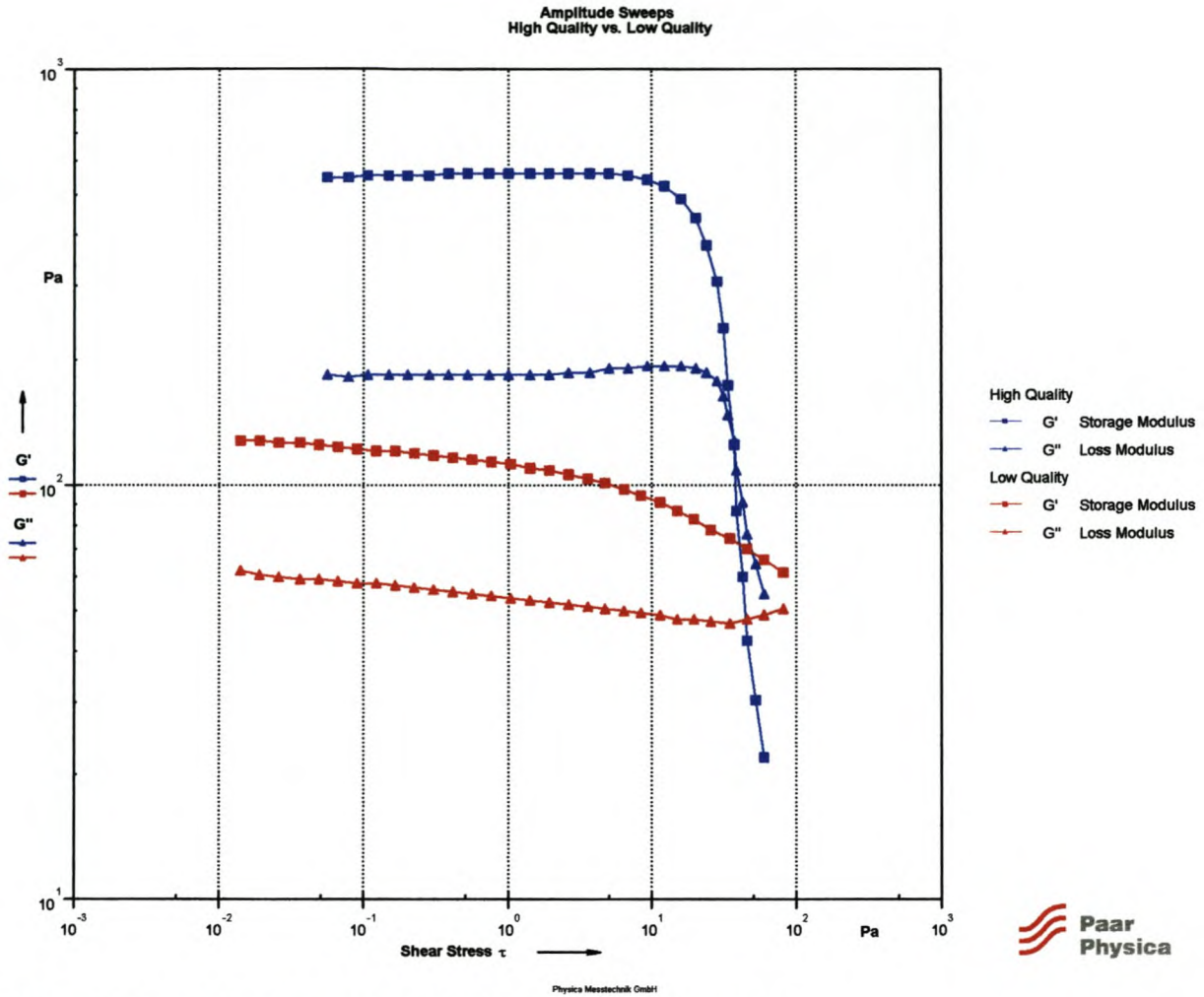


Figure 6-21: Amplitude sweeps for high- and low-quality paints

The following information about the character of the low- and high-quality paints was obtained from Figure 6-21:

- Both paints are stable in the LVER due to the fact that the paints are more solid-like ($G' > G''$).
- The structural strength (G') of the high-quality paint is almost 5 times higher than that of the low-quality paint. Therefore the high-quality paint has a much higher degree of structural strength.
- The low-quality paint does not have any clear LVER. In other words, the structure of the low-quality paint gets broken down even under the smallest of shear stresses and will therefore tend to sag.

- The high-quality paint has a clear yield value, whether it is measured by the sharp decrease in the structural strength or where $G'' > G'$. In other words, the high-quality paint demonstrates a certain degree of structural strength below its yield point, but also shows clear flow properties above its yield point. In contrast to the high-quality paint, the low-quality paint does not have a clear yield point and therefore does not have a specific structure at rest, nor flow properties above the yield point. One can clearly see that the high-quality paint is designed to have a definite yield point in contrast to the low-quality paint, which only has a steady decrease in the structural strength, but no clear yield point.
- The high yield point of the high-quality paint will result in good in-can behaviour and helps to act against sag; however, it might not have ideal levelling behaviour, resulting in brush marks and an inability to fill small cracks. The flow behaviour after a high shear load needs to be investigated (see section 6.3.4 – Three-Interval-Thixotropy-Tests).

6.3.3 Frequency Sweeps

The frequency sweeps for the high- and low-quality paints are given in Figure 6-22 below.

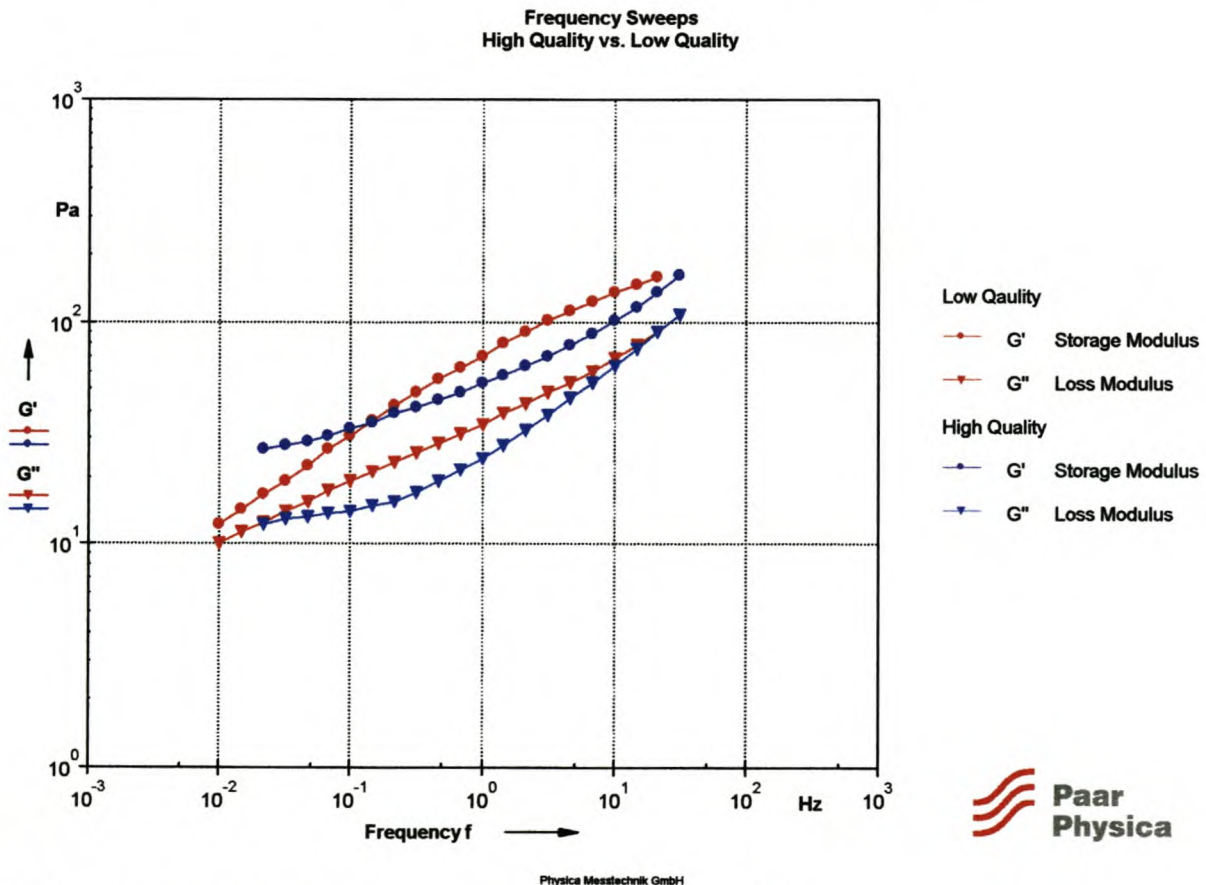


Figure 6-22: Frequency sweeps for low- and high-quality paints

Figure 6-22 reveals the following information about the behaviour of the low- and high-quality paints in the LVER:

- $G' > G''$ for the high-quality paint over the whole frequency range and therefore the solid-like behaviour predominates over the liquid-like behaviour and the paint shows some rigidity. The G' and G'' curves run almost parallel to each other with only a slight slope in the low-frequency range, an indication of dispersion stability. Therefore the solid-like behaviour predominates over the liquid-like behaviour in the low-frequency range showing stable long time-scale behaviour and therefore good in-can stability. The high-quality paint is therefore not likely to sedimentate or show phase separation.
- The solid-like behaviour of the high-quality paint also predominates over the liquid-like behaviour in the high-frequency range, or the short time-scale behaviour, and therefore the high-quality paint is not likely to spatter during roller application.
- $G' > G''$ for the low quality paint and therefore also illustrates solid-like behaviour, but the G' and G'' curves are steep and do not run parallel to each other, therefore showing a less stable structure.
- G'' tends to be larger than G' for the low-quality paint in the low-frequency range or the long time-scale behaviour and therefore the low-quality paint has liquid-like character in the state of rest which may lead to poor in-can stability (phase separation and sedimentation).

6.3.4 Three-Interval-Thixotropy-Test (3-ITT)

The structural recovery of the samples is illustrated in the three-interval-thixotropy-test given in Figure 6-23 below.

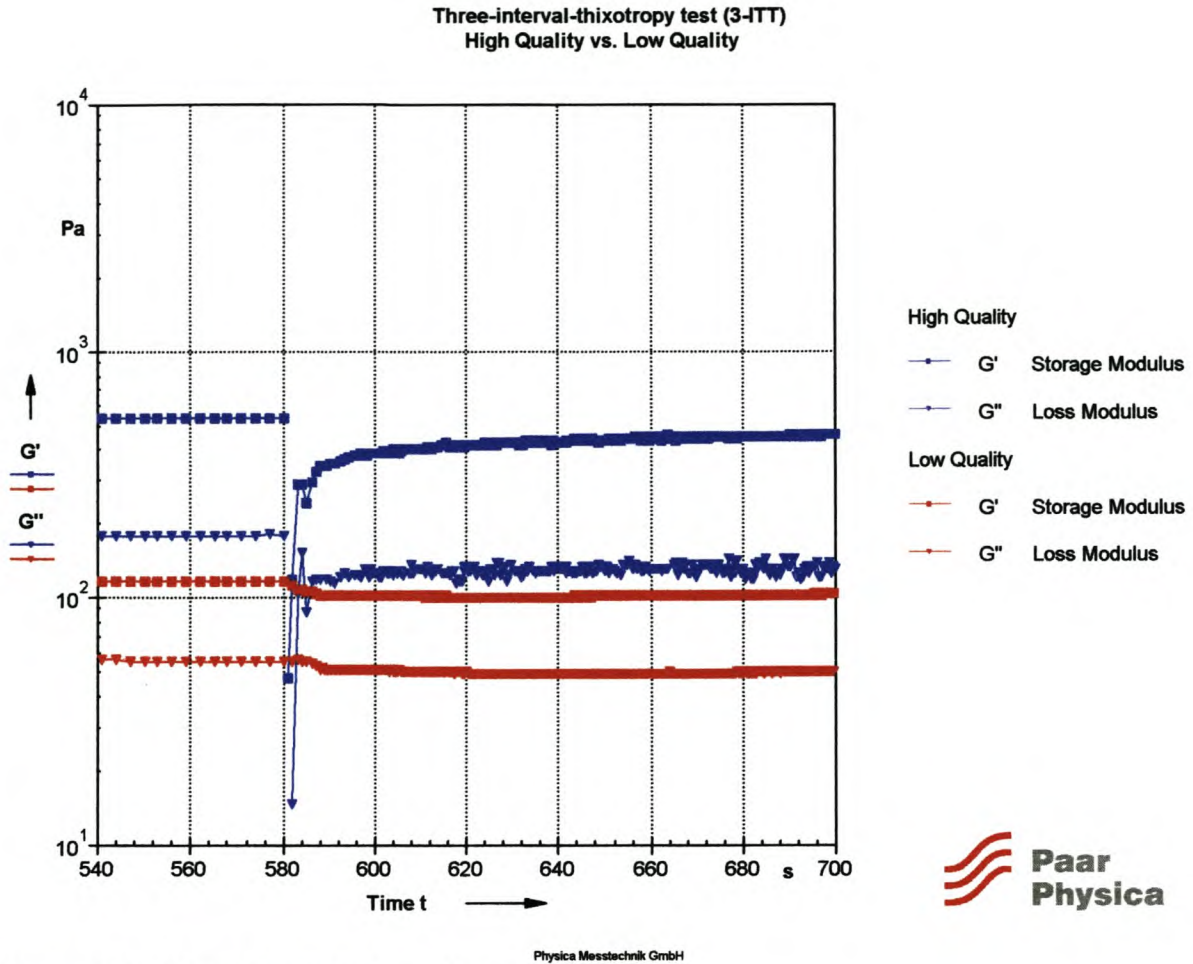


Figure 6-23: 3-ITT for the high- and low-quality paints

Figure 6-23 shows the following structural regeneration behaviour for the high- and low-quality paints:

- For both paints, $G' > G''$ directly after the high shear load and therefore the solid-like behaviour immediately predominates over the liquid-like behaviour and both paints are not allowed to flow and level due to viscous behaviour.
- The table below gives an indication of the rate of structural recovery.

Table 6-14: Structural recovery for high- and low-quality paints

Paint sample	% recovery after 10 seconds	% recovery after 20 seconds	% recovery after 40 seconds	% recovery after 60 seconds
High-quality paint:	66.5	72.7	78.4	79.5
Low-quality paint:	87.3	86.4	85.6	85.6

The values in the table illustrate that the high-quality paint takes longer for the structure to recover, allowing at least for some degree of levelling or orientation of particles. In contrast, the low-quality paint recovers very quickly (> 80% after 3 seconds) and does not allow any time for orientation of particles or some degree of ‘flow’.

- Both paints will have a thick layer due to the fact that $G' > G''$ directly after high shear and they therefore set quickly and do not level a lot. A thick layer is expected. According to the structural recovery curves, the high-quality paint will have a relatively thick film, but sufficient time is allowed for particles to orientate themselves and to fill small gaps in the surface. The low-quality paint will only result in a thick film as almost no time is allowed for the particles in the film to orientate themselves and to fill small cracks.
- As mentioned in the previous point, the low-quality paint is not allowed any time for the particles to orientate themselves in the film, leading to possible lower final film strength. This may lead to lower brushability and therefore a lower life span of the coating.

6.3.5 Conclusions

The following comparison between the high- and low-quality paints can be made:

Table 6-15: Comparison between high- and low-quality paint

	High Quality	Low Quality
In-can stability:	✓	✗
Spatter:	✓	✗
Ease of application:	✓	✗
Levelling:	✓	✗
Sag:	✓	✗
Mixing/stirring:	✓	✗

Table 6-15 illustrates that the high-quality paint really has better qualities than the low-quality paint in terms of the rheological behaviour.

6.4 The Consistency of the Paint Manufacturing Process

The consistency of the paint manufacturing process is determined by examining the rheological properties of a specific type of paint.

1. Manufactured at different times of the year (different batches)

The two paint samples (EPL-30) have the following codes:

- 2-E-033-C** - Manufactured in Cape Town (C), month of May (E), 33th batch (033) in the year 2002 (2).
- 2-G-044-C** - Manufactured in Cape Town (C), month of July (G), 44th batch (044) in the year 2002 (2).

These paints will be referred to merely as 'paint EPL-E' and 'paint EPL-G' respectively.

2. Manufactured at different factories

The same type of paint (EPL-30) is also manufactured at the Luipaardsvlei factory, Gauteng Province, as opposed to the two samples above, which are manufactured in Cape Town. The Luipaardsvlei sample is referred to simply as 'paint EPL-L'

6.4.1 Viscosity Curves

The viscosity curves for the three different paints are given in Figure 6-24 below.

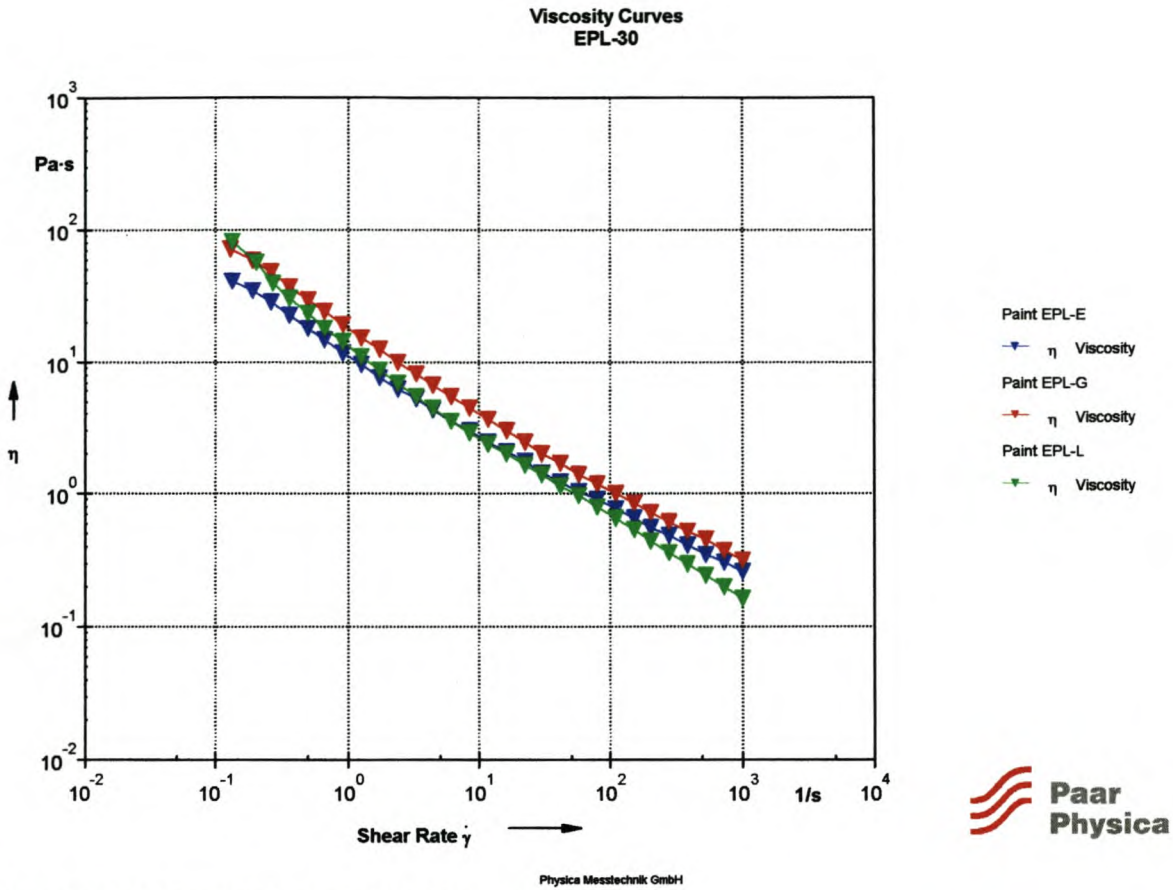


Figure 6-24: Viscosity curves for three different paints

- Paint EPL-E vs. paint EPL-G

Figure 6-24 shows that differences exist in the flow behaviour of the samples. Paint EPL-G has a higher viscosity than paint EPL-E over the whole shear-rate range. The following table gives an indication of the difference in viscosity at various shear rates:

Table 6-16: Viscosity values at various shear rates

Shear rate [s^{-1}]	Viscosity, paint EPL-G [Pa.s]	Viscosity, paint EPL-E [Pa.s]	Viscosity Difference [%]
1:	19.0	11.7	62
10:	4.41	2.97	48
100:	1.01	0.77	31
1000:	0.32	0.26	23

One can see that there is a large difference in the viscosity values in the low shear-rate range. The difference in viscosity values becomes smaller as the shear rate increases. Therefore, the two different paints should have more or less the same application properties

(at high shear rates), but different behaviour in the low shear-rate range such as in-can stability, yield point and levelling behaviour.

The power-law model is fitted to the viscosity curves in order to determine the power-law parameters, n and K . The parameters are given below.

Table 6-17: Power-law parameters for power law model

Paint	n [-]	K [Pa.s ^{n}]	R^2 [-]
Paint EPL-G:	0.39	18.14	0.9963
Paint EPL-E:	0.43	11.27	0.9958

Once again, the power-law index, n , indicates that paint EPL-G is more pseudoplastic than paint EPL-E, with a smaller value for the power-law index, n . The consistency index, K , of paint EPL-G is also higher than that of paint EPL-E, giving an indication of the higher low-shear viscosity.

- Paints EPL-E and EPL-G vs. paint EPL-L

Figure 6-24 also indicates the difference in flow behaviour of the samples produced in Cape Town (paint EPL-E and EPL-G) and the sample produced at Luipaardsvlei (paint EPL-L).

The degree of pseudoplasticity of the paint EPL-L is immediately noticed. One can see that the low-shear viscosity (at $\dot{\gamma} = \pm 0.1 \text{ s}^{-1}$) of paint EPL-L is higher than the low-shear viscosity for both samples manufactured at Cape Town. At the other end of the shear rate range, the high-shear viscosity of paint EPL-L is lower than that of both the Cape Town samples. In other words, the Luipaardsvlei sample is much more pseudoplastic than the samples manufactured in Cape Town. This can also be observed by looking at the power-law index, n , of the power law.

Table 6-18: Power law parameters, n and K

Sample	n [-]	K [Pa.s ^{n}]	R^2 [-]
Paint EPL-G:	0.39	18.14	0.9963
Paint EPL-E:	0.43	11.27	0.9958
Paint EPL-L:	0.33	14.30	0.9939

The power-law index, n , for the Luipaardsvlei sample (paint EPL-L) is lower than that of both the Cape Town samples (paint EPL-G and EPL-E) and is therefore more pseudoplastic.

The differences in the viscosity curves have the following practical implications:

- Due to the lower viscosity in the low shear-rate range, paint EPL-E has a lower degree of in-can stability, although oscillatory tests need to be performed to investigate the structure of the sample at rest.
- Due to the lower viscosity in the high shear-rate-range, paint EPL-L is easier to apply, although the high-shear viscosity is not much lower than that of paints EPL-E and EPL-G.
- The paint manufactured at Luipaardsvlei will have a higher in-can stability (higher low-shear viscosity) than the paints manufactured in Cape Town, but is still easier to apply to a surface (lower high-shear viscosity).

From the viscosity curves it is apparent that there are differences in the flow behaviour resulting from different manufacturing processes.

6.4.2 Amplitude Sweeps

The amplitude sweeps for the three different EPL-30 paints are given in Figure 6-25 below.

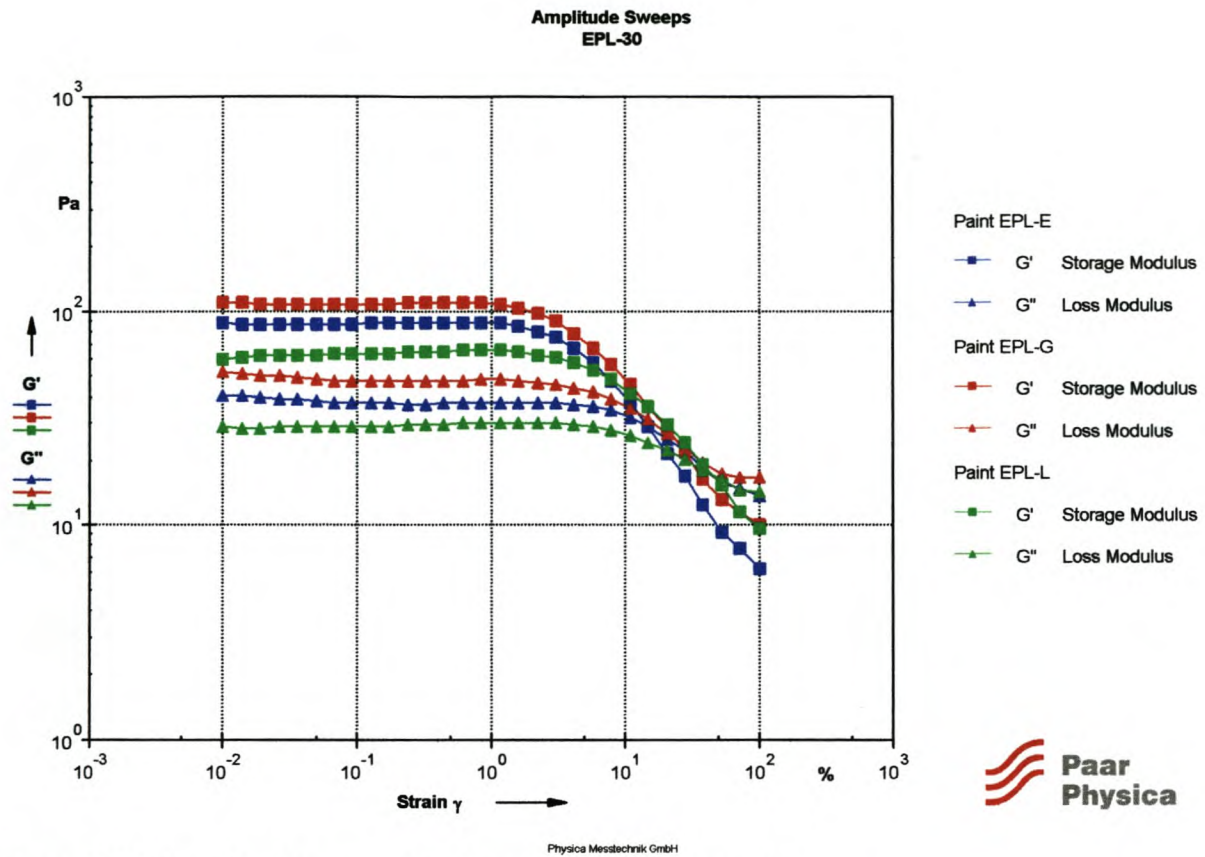


Figure 6-25: Amplitude sweeps for three EPL-30 paint samples

Figure 6-25 gives the following information about the character of the EPL-30 paints:

- $G' > G''$ for all the paint samples and therefore the solid-like behaviour predominates over the liquid-like behaviour and the paints all show a certain rigidity.
- Paint EPL-G has a higher structural strength (G') than paint EPL-E. This characteristic was already expected in section 6.3.1, where paint EPL-G has in general a higher viscosity than paint EPL-E.
- Paint EPL-L has the lowest structural strength. This was also expected in the viscosity curves, where paint EPL-L has the highest degree of pseudoplasticity; in other words, paint EPL-L's structure is broken down more easily.

- The yield points obtained from the data tables of the amplitude sweeps are as follows:

Table 6-19: Yield points

Paint	Yield Stress [Pa]
Paint EPL-E:	2.0
Paint EPL-G:	2.3
Paint EPL-L:	2.7

The yield points of the three paints are in the same order and therefore the sagging behaviour of the paints on a vertical wall will be more or less the same.

The amplitude sweeps can also be illustrated with the $\tan \delta$ values on the y-axis.

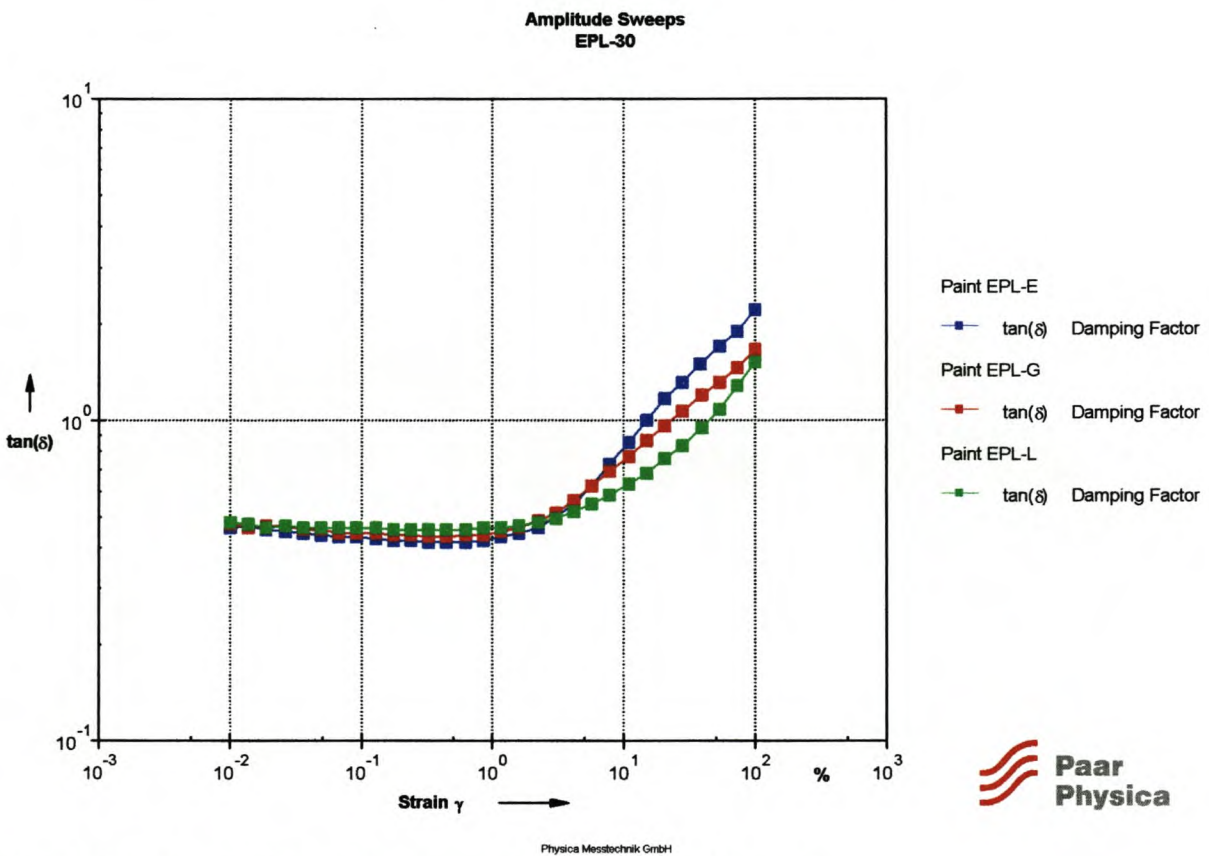


Figure 6-26: Amplitude sweeps expressed with $\tan \delta$ on the y-axis

Figure 6-26 reveals interesting information of the viscoelastic behaviour of the paints. All three samples have the same viscoelastic response to amplitude changes. In other words, they have the same viscoelastic behaviour in the LVER, although it was observed in Figure 6-25 that the

structural strengths, according to G' , are different. These same $\tan \delta$ values indicate that the ratio of the solid-like behaviour and liquid-like behaviour is the same for all the paints, which may be as a result of the identical composition of all three paints.

6.4.3 Frequency Sweeps

The frequency sweeps of the three different paints are given in Figure 6-27 below.

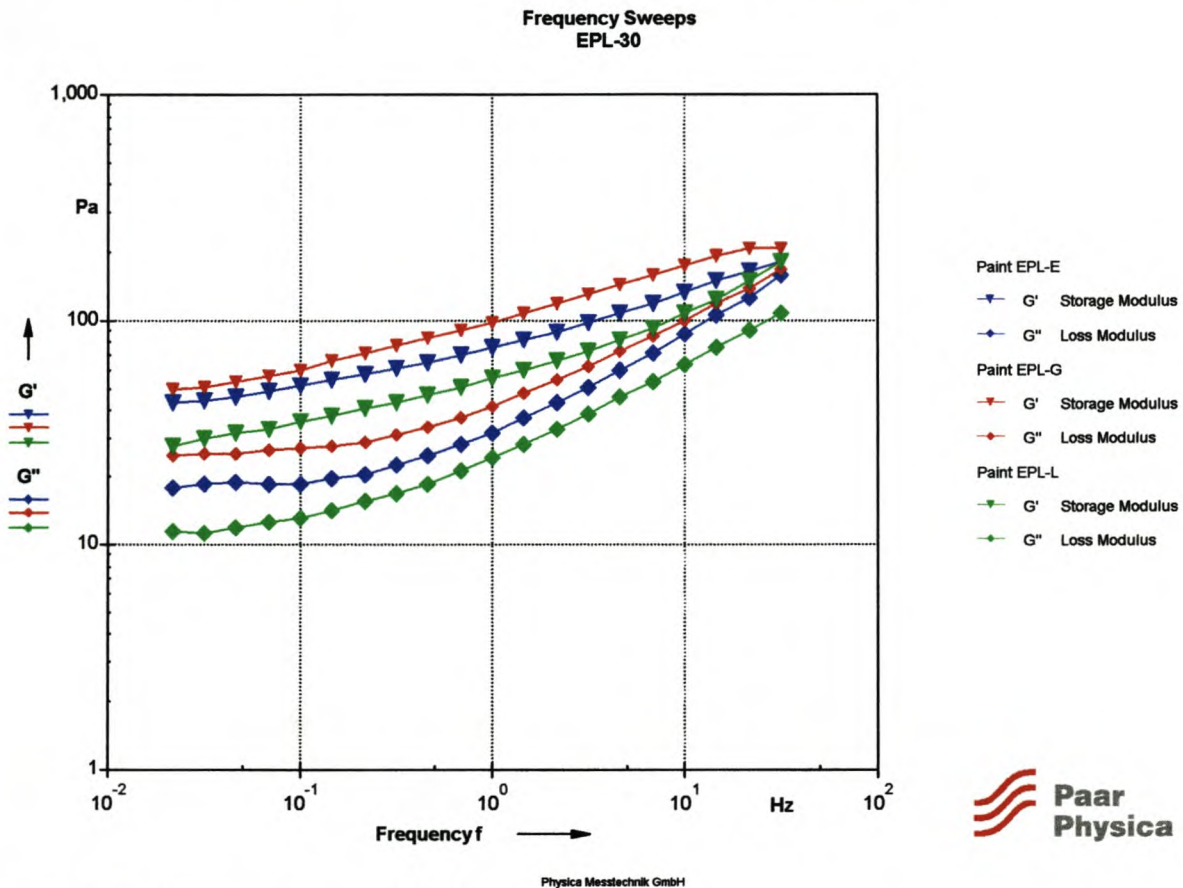


Figure 6-27: Frequency sweeps for the EPL-30 paints

Figure 6-27 gives the following information about the behaviour of the EPL-30 paints in the LVER:

- $G' > G''$ over the whole frequency range and therefore the paints are more solid-like than liquid-like.
- More specifically, the following indicates a high degree of structural stability for all three samples in the long time-scale behaviour (low frequency range):

- $G' > G''$ or in other words, the solid-like behaviour predominates over the liquid-like behaviour and therefore the three samples should display stable behaviour in the state of rest, e.g. not likely to sedimentate, settle and phase separate;
 - the curves of G' and G'' are almost parallel to each other with only a slight slope, an indication of a stable dispersion. Therefore G'' will not be larger than G' at even lower frequencies and the paints will not become unstable.
- While, in the high shear-rate range, G' and G'' for paints EPL-E and EPL-G tend to have different gradients with the $G''_{\text{gradient}} > G'_{\text{gradient}}$ and therefore according to Wollny [2002] may tend to show spatter behaviour during roller application. In contrast, G' and G'' for paint EPL-L are still parallel to each other and therefore $G'_{\text{gradient}} > G''_{\text{gradient}}$ and hence will tend not to spatter during roller application. This is illustrated mathematically by fitting a power-law model to the high-frequency range of the G' and G'' curves as explained earlier in Chapter 5 (Rheological Properties of PE-Free Paints). The differences in gradients of the G' and the G'' curves are then determined by subtraction of the power-law exponent, n , which is an indication of the gradient of the curve.

Table 6-20: Difference in slopes of G' and G'' curves in high-frequency range of frequency sweep

Paint sample	$G'_{\text{gradient}} - G''_{\text{gradient}}$	R^2 of G'	R^2 of G''
Paint EPL-E:	-0.21	0.9929	0.9921
Paint EPL-G:	-0.13	0.9982	0.9928
Paint EPL-L:	-0.05	0.9901	0.9998

From this table, it can be seen quantitatively that paints EPL-E and EPL-G are three to four times more likely to spatter than paint EPL-L (larger negative values). As mentioned previously, this method seems to be highly representative of the actual spatter behaviour.

6.4.4 Time Sweeps

The time sweeps for the three paints are given in Figure 6-28 below.

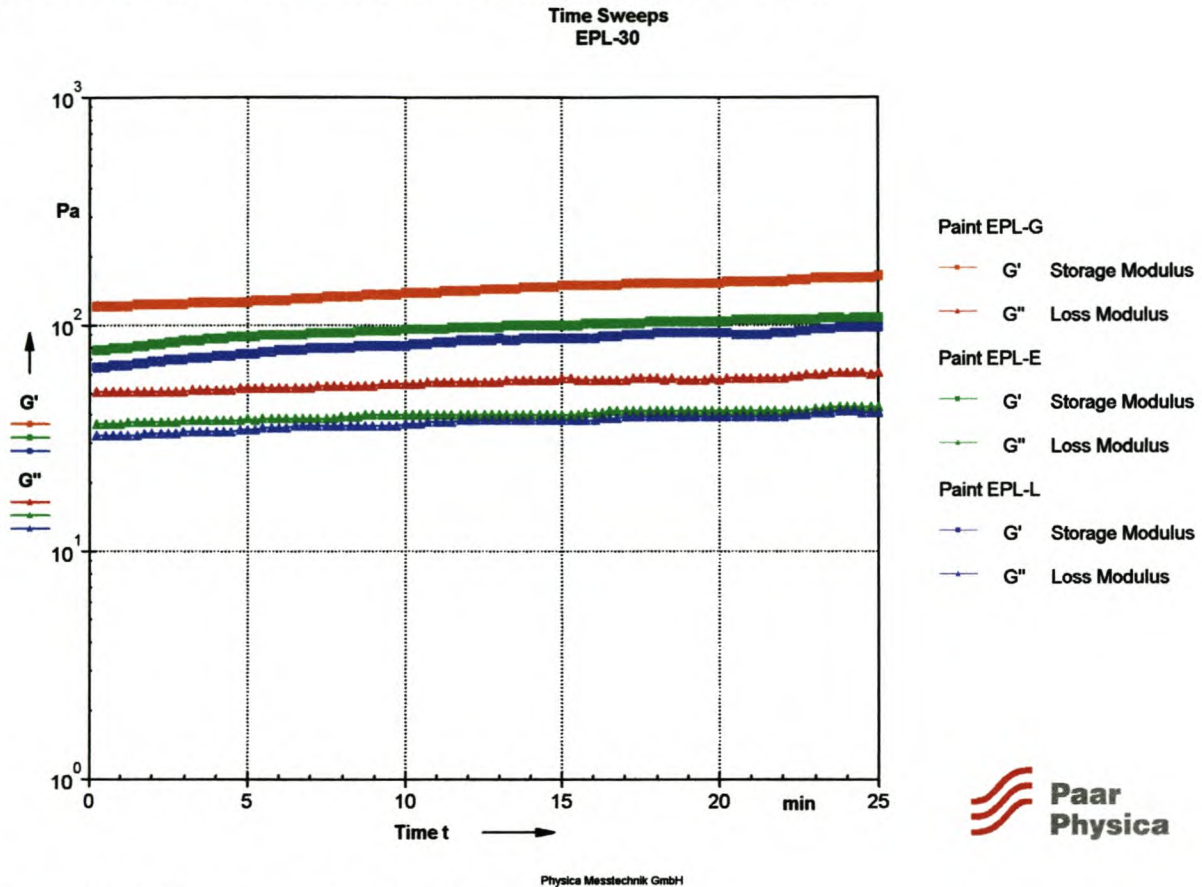


Figure 6-28: Time sweeps for EPL-30 paints

Figure 6-28 shows the following behaviour for the EPL-30 paints over a long duration of time:

- $G' > G''$ over the whole test range ($0 < t < 20$ min) for all three test samples, which indicates that the samples have a certain degree of structural strength and therefore the test indicates that the samples should be stable over a long period of time or during storage. All the samples therefore show good in-can stability and should not tend to sedimentate or undergo phase separation.
- The test indicates a slight degree of structural recovery (increase in G'). This recovery may be due to sample breakdown that occurred during handling of the sample. It is, however, important that the paints do not show structural breakdown (decreasing G' values) over a period of time to become unstable.

- Paint EPL-G has the highest degree of structural strength (according to G'), followed by paint EPL-E and paint EPL-L respectively. This same behaviour was also observed in the amplitude sweep.

6.4.5 Three-Interval-Thixotropy-Test (3-ITT)

The 3-ITT curves for the three paints are given in Figure 6-29 below.

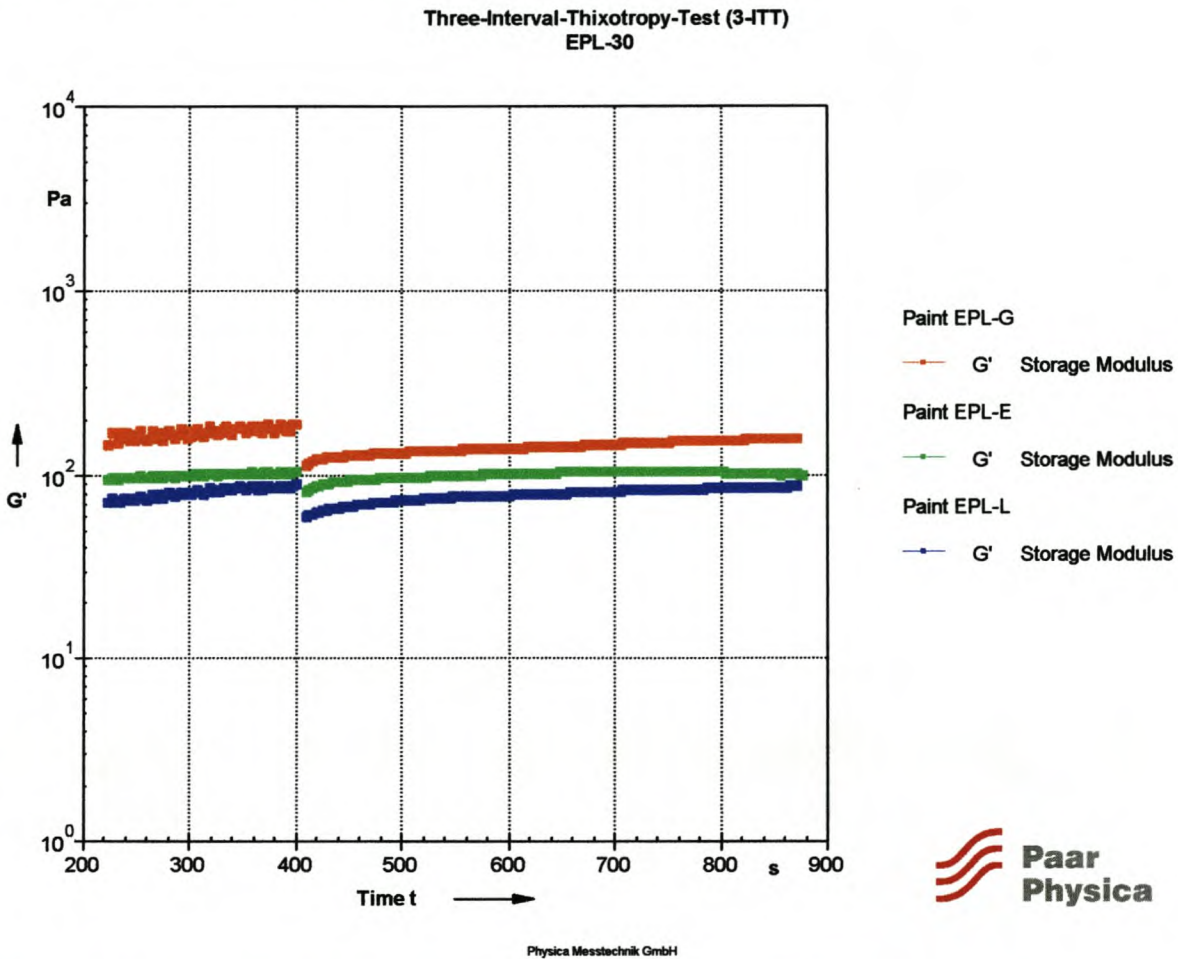


Figure 6-29: Three-interval-thixotropy-test curves for three EPL-30 paints.

Figure 6-29 gives the following information about the structural recovery after high shear:

- Although not illustrated in Figure 6-29, $G' > G''$ immediately after the shear load has been applied and therefore the structural recovery is examined only in terms of G' . The fact that $G' > G''$ directly after the high shear load indicates that all three paint samples do not flow directly after the application process and therefore should behave in the following way:

- will have poor levelling characteristics;
 - layer thickness will be thick;
 - will show good anti-sag behaviour.
- The following table gives the degree of structural recovery as a percentage of regeneration during the previously defined time period at a state of rest.

Table 6-21: Time for 75% structural recovery

Paint sample	Time for 75% structural recovery [s]
Paint EPL-G:	214
Paint EPL-E:	10
Paint EPL-L:	41

Therefore, it is clear that paint EPL-G have the longest structural recovery time and that there are big differences in the time to reach 75% structural recovery. The paints will therefore behave in very different ways during the structural recovery phase, resulting in very different final film properties. Paint EPL-G is likely to have a much thinner film thickness and is more likely to sag in comparison with the other two paints.

6.4.6 Conclusions

The following are the most important conclusions that can be drawn:

- The viscosity behaviour of a paint manufactured in two different batches differs by up to 62% in low-shear viscosity and up to 23% in high-shear viscosity and therefore differences exist in the flow and viscosity behaviour as a result of different manufacturing processes.
- Differences in the pseudoplasticity of the same type of paint exist as a result of their being manufactured at different factories.
- Differences in the structural strength (G') of all the paints exist, but this does not seem to have a drastic affect on the stability of the paints. Therefore all the paints are still stable at long time-scales and therefore show good in-can stability.

- According to the yield point values, the paints will show more or less the same sagging behaviour (which is not too much) and the same layer thickness of the final coating. However, large differences in terms of structural recovery after high shear exist. The paints will therefore behave in very different ways during the structural recovery phase, resulting in very different final film properties. It can be seen that the yield point alone is not sufficient in determining the behaviour after the paint has been applied to the surface of the wall.
- EPL-30 is more likely to spatter when it is manufactured in the Cape Town factory.

6.5 Conclusions

The following are the most important conclusions that can be drawn regarding paint rheology:

- The rheological data correlate well, although not always, with the end-use market the paints are designed for. This includes factors such as:
 - i. Quality;
 - ii. Consistency of structure at rest;
 - iii. Flow behaviour;
 - iv. Time-dependent behaviour directly after application.
- The rheological behaviour indicates that differences in the character of paints exist which are manufactured by two different companies. The paints, which are in the same class but from different companies, show diverse rheological behaviour.
- It is apparent from the rheology data why an inexpensive paint is incapable of fulfilling all the desired rheological requirements.
- Rheological inconsistency occurs as a result of the paint manufacturing process. That is, inconsistency occurs between different batches as well as between different manufacturing processes. Some of these inconsistencies may even lead to instability.

CHAPTER 7 Rheology Modifiers

7.1 Background

Latex paints rely on the use of rheology modifiers to a much greater extent than their solvent-based counterparts. A typical latex paint may contain up to four rheology modifiers depending on the end-use purpose. Often a combination of rheology modifiers is used to provide a good balance of container viscosity, application viscosity, anti-settling properties, spatter resistance, and flow and levelling behaviour [Ritchie, 1993]. The ideal situation for the paint formulator would be to adjust low, medium and high shear-rate viscosity independently, allowing optimisation of each property independently. In this chapter the rheological behaviour of four rheology modifiers and their contribution to the final performance properties of a latex paint are examined.

7.2 Chemistry of Rheology Modifiers

Rheology modifiers are water-soluble polymers which have been hydrophobically modified. They act by both thickening the water phase and by associating with other species present in the paint.

The following types of rheology modifiers were investigated:

- Acrysol ASE 60 ® - ASE chemistry
- Acrysol RM 8W ® - HEUR chemistry
- Acrysol RM 2020 ® - HEUR chemistry
- Acrysol RM 5 ® - HASE chemistry

ASE – *Alkali Swellable Emulsion*

HEUR – *Hydrophobically modified Ethylene Urethane oxide Rheology modifier*

HASE – *Hydrophobically modified Alkali Swellable Emulsion*

Rohm and Haas® supplied all of the rheology modifiers.

7.2.1 ASE Chemistry

These type of thickeners are made by polymerising an acid with a weakly hydrophobic monomer. These acid groups expand due to electrostatic repulsions upon addition of a base. This increases the effective volume fraction of the latex and thereby the viscosity of the aqueous medium.

Alkali swellable emulsions (ASE thickeners) are based on long chain acrylic polymers with carboxylate groups at intervals along the polymer backbone. In the emulsion state they are stabilised at a low pH (typically 3.0) and are low-viscosity, easily handled liquids. When neutralised to a pH above 7 with an amine, the polymer backbone unfolds as a result of carboxylate repulsion and thickening of the water phase occurs through molecular chain entanglement. Alkali swellable thickeners have the following disadvantages:

- More water sensitive;
- Fairly pseudoplastic;
- Poor resistance to roller spatter.

ASE thickeners are associative in behaviour and are usually very selective in application.

Acrysol ASE60 ®, an anionic thickener, is used as an example of an ASE rheology modifier.

7.2.2 HEUR Chemistry

The HEUR thickeners are built up from water-soluble poly-oxyethylene segments joined by urethane groups. The two ends of the molecule are very hydrophobic, while the centre is quite hydrophilic (see Figure 7-1). The hydrophobic groups associate with emulsion particles present through adsorption onto the particle surface. In addition, they aggregate together in the water phase in a similar way to that in which surfactants form micelles [Howard et al., 1992]. The multiple hydrophobic groups of the thickener molecules are thought to associate to form a network. This network formation results in a major increase in viscosity and also gives a uniform, stable dispersion of both pigment and emulsion particles. Variation of the end hydrophobic groups provides a very convenient and controllable way of manipulating the performance of HEUR thickeners. While there is evidence that the backbones of the HEUR rheology modifiers can also

associate with acid groups on the surface of the latex particles, most research indicates that hydrophobic association is the principal mechanism by which these rheology modifiers interact with latex particles [Howard et al., 1992].

The hydrophobic association and adsorption mechanism by which these rheology modifiers function is non-specific – the hydrophobes adsorb to any type of dispersed particle as long as it is relatively hydrophobic. They are driven by the tendency of the hydrophobic groups in the rheology modifiers to get out of the aqueous phase and seek hydrophobic environments.

The degree to which the hydrophobes associate with the polymer depends on a number of factors and this makes the performance of the associative thickener very specific with regard to the details of the formulation in which it is used. That is, one thickener will produce different results in different formulations, depending on the type and concentration of the dispersed particles, surfactants and cosolvents used in the formulation. In addition, the choice of latex can have a major effect on the interactions with the associative thickener. A schematic structure of a HEUR thickener is given in Figure 7-1.

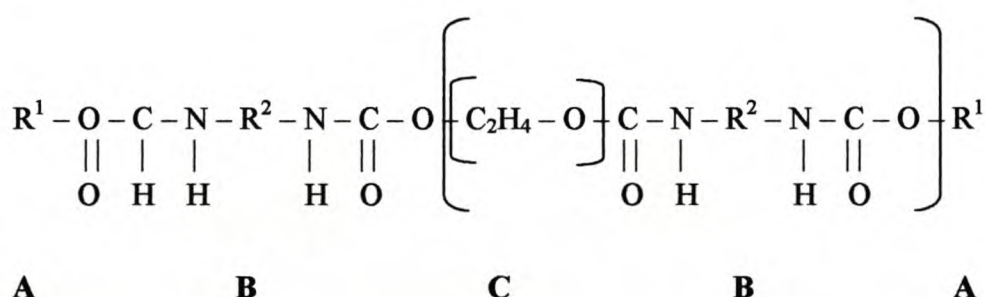


Figure 7-1: Chemical structure of typical HEUR thickener [Tafigel, 2001]

With the type and function of the molecule parts A, B, C as follows:

A: Hydrophobic end groups – hydrophobe-hydrophobe interactions between these groups and adsorption onto non-polar molecule surfaces (emulsion pigments) result in formation of a three-dimensional network;

B: Urethane groups – Links in the thickener between molecule parts A and C. Can also form hydrogen bonds;

C: Polymer backbone – Provides water compatibility of the thickener and formation of hydrogen bonds.

The combination of hydrophilic and hydrophobic groups gives the polymer surfactant properties.

7.2.3 HASE Chemistry

HASE rheology modifiers are anionic and thicken at a pH of above 7 through repulsion of carboxylate anions along the polymer backbone. In addition, the hydrophobes interact with the emulsion particles forming a network which tends to prevent flocculation. The HASE rheology modifiers employ a hydrophobic monomer enabling them to adsorb onto latex particles and also retain a carboxylate functionality. As a result, the rheology modifiers can adsorb onto the inorganic pigments and extenders in the same way as the dispersants.

Addition of surfactants does not result in low-shear viscosity reduction as for HEUR thickeners. This is because the water phase thickening tends to dominate over the association mechanism. In some cases addition of surfactant can result in low-shear viscosity increase caused by desorption of the hydrophobes and removal of the network structure, resulting in the onset of flocculation.

Acrysol RM 5, a low associative HASE thickener, cannot be used in masonry paints with low-quality binders. Under these conditions early water sensitivity can be a problem and the HEUR types would be a better choice. In addition HASE thickeners have a greater tendency than HEUR thickeners to adsorb onto pigment surfaces through attraction of the carboxylate groups. Therefore it is essential when formulating with HASE types to ensure that an adequate level of pigment dispersant is present to minimise this effect and ensure good viscosity stability on the paint storage [Prideaux, 1993].

7.3 Formulating with Rheology Modifiers

The physical properties of the latex paint are given in Table 7-1.

Table 7-1: Chemical composition of latex paint

Material Name	Chemical Composition	Particle Size [nm]	Percentage [%]
Vesiculated Beads:	Polystyrene/Styrene	5 000	83.24
AE748:	All-acrylic	89	14.48
Ucar ITB:	Ester/Alcohol	-	1.19
Ammonia:	NH ₃	-	1.09

The latex paint used in this case contains vesiculated beads which already contain PVOH (1.39%) and HEC (0.26%) as thickeners. These thickeners affect the whole viscosity shear-rate curve as illustrated in Chapter 4, while rheology modifiers change only part of the curve or alter its shape. Thickeners derived from cellulosics have an inflexible polymer backbone, which causes them to occupy a large volume in the water phase and therefore act by thickening the water.

In addition, the AE-748 emulsion, a pure acrylic, has an average particle size of 85 nm and is therefore highly associative. The HEC has a strong tendency to flocculate the polymer by filling all the volume in the water phase with their bulky molecules and forcing the emulsion particles together. HEC thickeners show special utility in acrylic latex formulations such as the AE-748, which is useful in coatings. This process is known as volume exclusion flocculation and limits gloss development in paint. It can therefore be seen that formulating flexibility is restricted with this type of thickener and therefore other types of rheological modifiers are investigated. ASE and HASE type rheology modifiers require pH adjustments. Figure 7-2 illustrates the relationship between pH and the stability of the paint for rheology modifiers that are pH sensitive, measured in terms of viscosity.

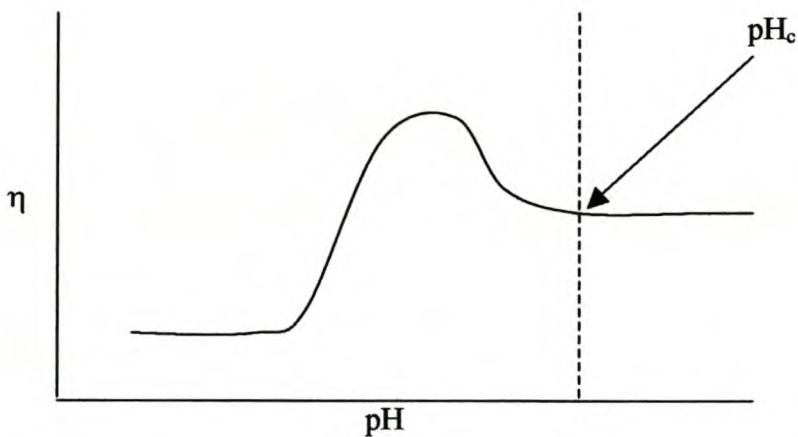


Figure 7-2: Effect of pH on viscosity for rheology modifiers that are pH sensitive

The paint behaves stably above a specific pH, pH_c . Above pH_c the paint is in an equilibrated state and small changes in pH will not result in any change in the stability, measured in terms of the viscosity. Therefore pH adjustments need to be performed first to determine the pH at which each rheology modifier performs stably.

Rohm and Haas® does not provide typical levels of rheology modifier to be used.

7.3.1 Formulating with Alkali Swellable Emulsions (ASE)

Selection of the grade and type of ASE thickener is important because of the associative nature of the additives. There are currently over 100 ASE thickeners to choose from. Acrysol ASE60 was chosen as an ASE thickener to be investigated in the paint formulation relying on a paint chemist's previous experience. All ASE thickeners have one thing in common – they all require pH adjustment. Generally the optimum pH range for ASE thickeners is between 8.0 and 10.0, but the effect on the viscosity for an individual ASE thickener needs to be investigated before it can be incorporated into the paint formulation. Figures 7-3 to 7-5 illustrate the effect of pH on the viscosity development of different levels of Acrysol ASE60.

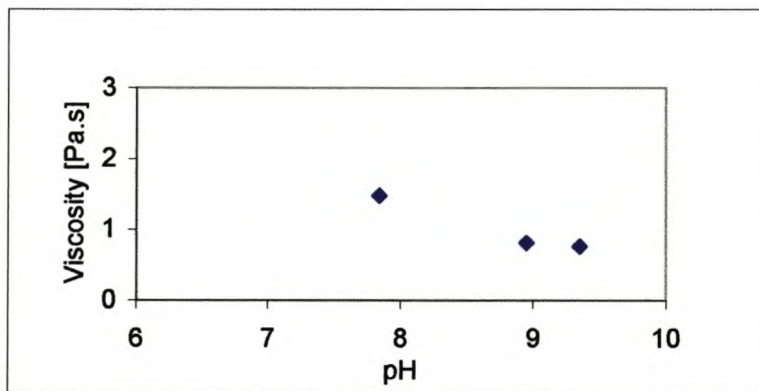


Figure 7-3: Effect of pH on viscosity¹ (0.54% Acrysol ASE 60)

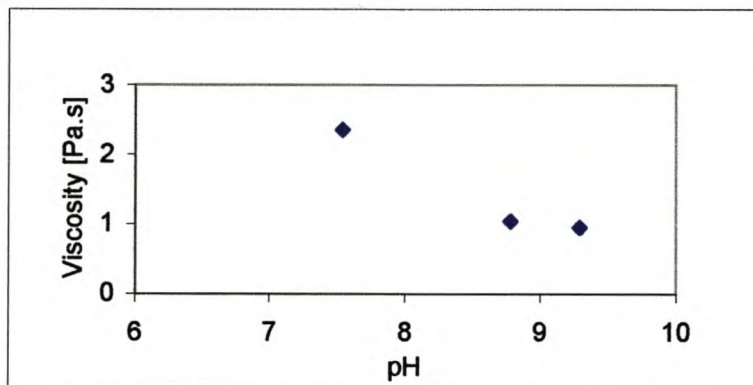


Figure 7-4: Effect of pH on viscosity² (0.89% Acrysol ASE 60)

¹ Steady-state viscosity measured at $\dot{\gamma} = 100 \text{ s}^{-1}$

² Steady-state viscosity measured at $\dot{\gamma} = 100 \text{ s}^{-1}$

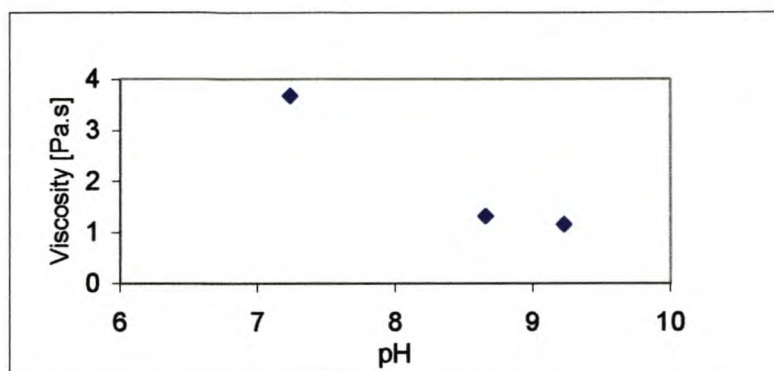


Figure 7-5: Effect of pH on viscosity³ (1.24% Acrysol ASE 60)

The viscosity points in Figures 7-3 to 7-5 for the different amounts of Acrysol ASE60 tend to have the same shape as that of Figure 7-2 and therefore indicate that equilibrium in the paint is reached at a pH of ± 9 . The samples are therefore formulated to have pH values above 9 so that stability of the paint is ensured.

7.3.2 Formulating with HEUR Rheology Modifiers

Due to the highly associative nature of HEUR rheology modifiers, adjustment of the level and type of latex polymer, varying particle size, surfactant, film forming aids, etc. is often required. These adjustments were not made in this specific paint formulation.

The sensitivities mentioned earlier in section 7.2.2 (HEUR Chemistry) result in a specific thickener producing different results in different formulations, depending on the type and concentration of the dispersed particles, surfactants and cosolvents used in the formulation. It may therefore be necessary to do some fine-tuning of the rheology in the final paint formulations based on a particular combination of latex grade and HEUR thickener [Howard, 1992].

Acrysol RM2020 is a relatively new rheology modifier and recent process improvements have made this type of thickener more suitable for general use in latex paints in combination with a more strongly associating type such as Acrysol RM8W.

³ Steady-state viscosity measured at $\dot{\gamma} = 100 \text{ s}^{-1}$

7.3.3 Formulating with HASE Rheology Modifiers

HASE rheology modifiers have lower manufacturing costs compared to HEUR rheology modifiers, but their high acid content can affect water-sensitive films. These combined properties have directed the use of such rheology modifiers to low-cost formulations such as PE-free paints. The HASE rheology modifiers were added to the paint formulation and then the pH adjustment followed. This approach, with the other variables held constant, highlights the influence of the rheology modifier on the rheology profile.

The rheology modifier Acrysol RM5 also requires pH adjustment and it was found that the paint formulations with Acrysol RM5 are stable at pH levels above 9 (same type of behaviour as in Figure 7-3 to 7-5).

7.3.4 The Compatibility Between Dispersants and Associative Thickeners (HASE and HEUR)

These rheology modifiers interact with a variety of other paint components in the same way as surfactants do. Not only do associative thickeners and surfactants behave in similar ways, but they also interact with the same ingredients. Both types function by adsorption onto particles in the paint formulation and under certain circumstances the associative thickener and the surfactant can interfere with each other's performance, with the possibility of adverse effects on paint properties. Too much surfactant in a formulation can result in the displacement of the associative thickener from the surfaces of the latex particles to the continuous phase. As a result the thickener associations are inhibited when this phenomenon occurs and behave more like HEC thickeners. Dispersant-thickener interactions may cause frequent instability in latex paints. When the thickener is displaced from the latex into the aqueous phase of the paint, it can thicken only through volume restriction flocculation, the mechanism employed by HEC. Paints thickened in this manner are shear thinning and prone to flocculation. As a result, they exhibit poor flow and levelling. Both HASE and HEUR are subject to displacement by surfactants, but the problem is far more severe with HASE products because they adsorb much less strongly. When used in relatively high levels they can tend to promote thickener desorption. PVOH is non-ionic and does not react significantly with HEUR thickeners [Kraus, 2001].

7.4 Discussion of Results

7.4.1 Acrysol ASE60

Rohm and Haas® states that Acrysol ASE60 has the following rheological characteristics [Rohm & Haas, 1996]:

- Outstanding in-can stability;
- Good application properties;
- Good paint stability and consistency.

The effect of Acrysol ASE60 on the PE-free paint formulation will be investigated keeping these characteristics in mind.

7.4.1.1 Viscosity Curves

The viscosity curves are given in Figure 7-6 below.

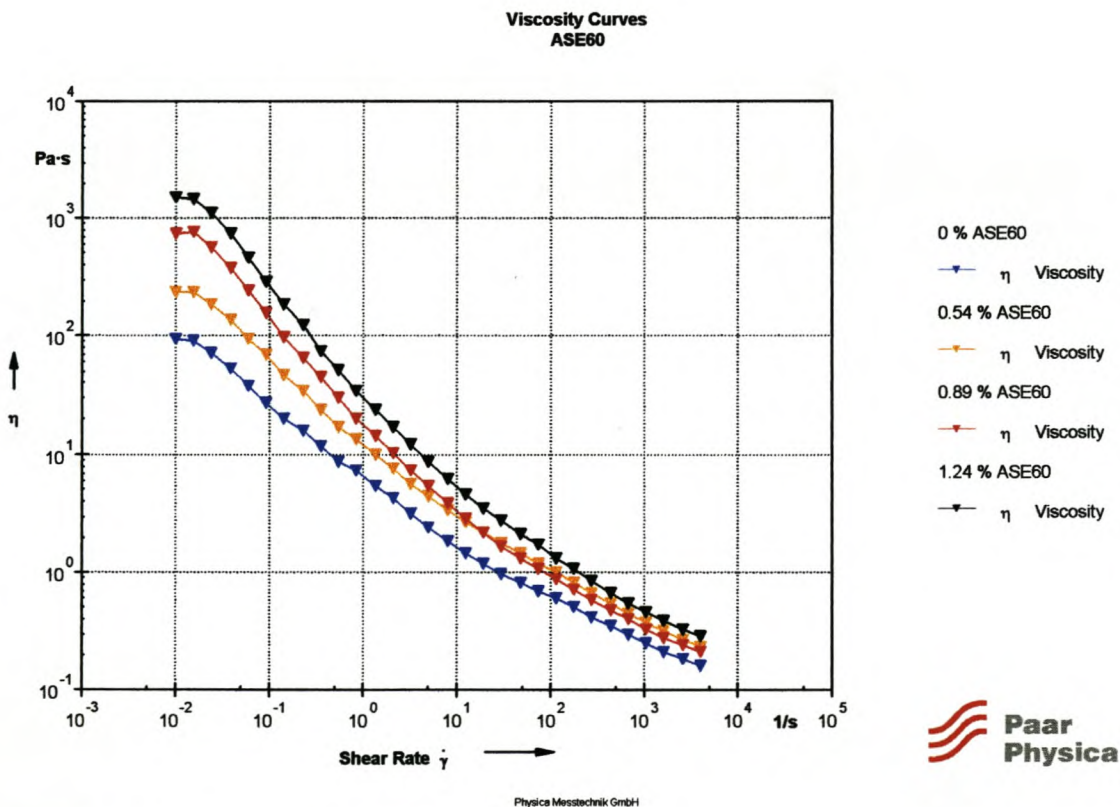


Figure 7-6: Viscosity curves with Acrysol ASE60

Acrysol ASE 60 has the following effect on the flow behaviour of the PE-free paint:

- The increase in low-shear viscosity can clearly be seen in the viscosity curves and will therefore result in an increase in the in-can stability of the paint. The primary use of Acrysol ASE60 is to increase the low-shear viscosity.
- Figure 7-6 also reveals that the viscosity in the high shear-rate range increases only slightly by the addition of Acrysol ASE60 and therefore still results in relatively good application behaviour, although impaired a little by the higher viscosity values.

7.4.1.2 Amplitude Sweeps

The amplitude sweeps are given in Figure 7-7 below.

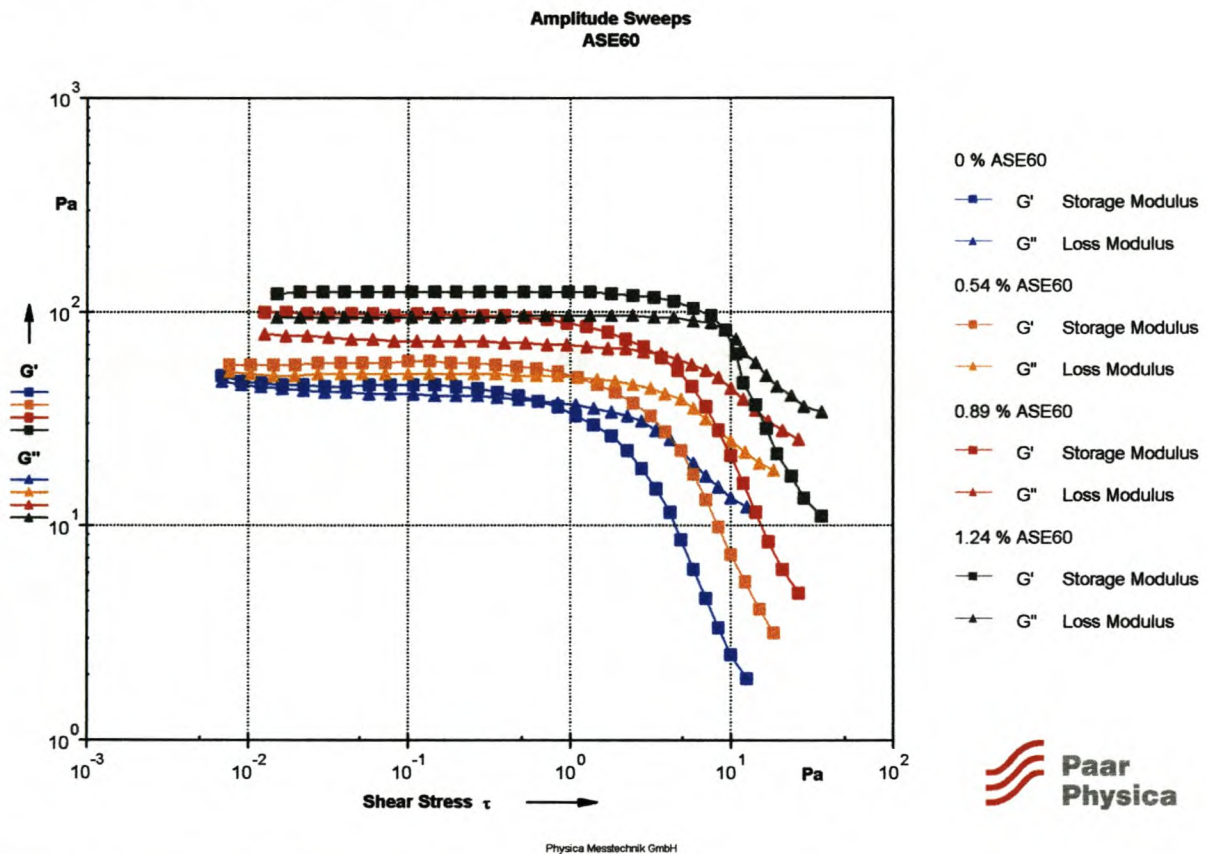


Figure 7-7: Amplitude sweeps for Acrysol ASE60

Figure 7-7 gives the following information about the character of the paints:

- $G' > G''$ in the LVER for all the samples and therefore the solid-like behaviour predominates over the liquid-like behaviour and all the samples show some degree of rigidity.
- An increase in the storage modulus (G') in the LVER with an increase in Acrysol ASE60 is observed. In other words, the structural strength increases and therefore assists with dispersion stability, resulting in favourable in-can stability.
- The yield point increases with an increase in Acrysol ASE60, also assisting in good in-can stability.
- The loss factor ($\tan \delta = G''/G'$) decreases with increase in Acrysol ASE60, indicating that the storage modulus (G') increases more than the loss modulus (G'') with each increase in Acrysol ASE60. This also indicates the increase in structural strength, resulting in good in-can stability.

7.4.1.3 Frequency Sweeps

The frequency sweeps are given in Figure 7-8 below.

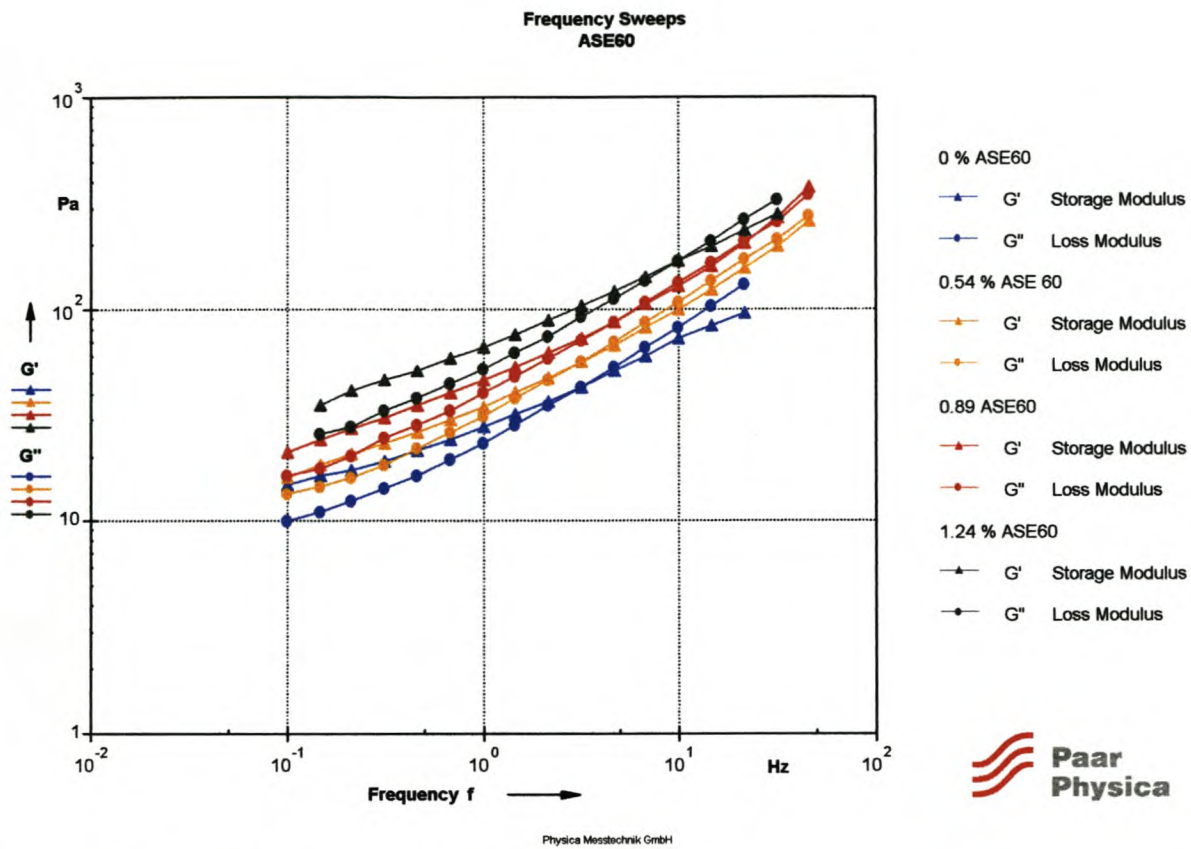


Figure 7-8: Frequency sweeps for Acrysol ASE60

The frequency sweeps gives the following information about the paints in the LVER:

- $G'' > G'$ in the high-frequency range and therefore the liquid-like behaviour predominates over the solid-like behaviour and all the paint samples are likely to spatter a lot during roller application. Prideaux [1993] also observed this type of behaviour with these types of rheology modifiers.
- $G' > G''$ in the low-frequency range and therefore the solid-like behaviour predominates over the liquid-like behaviour, resulting in good in-can stability because a structural network exists. This type of behaviour may, however, result in poor levelling properties as indicated by Whitton et al. [2001]. These properties often negate the advantages such as the excellent in-can stability.
- The curves of G' and G'' for all the levels of Acrysol ASE60 run almost parallel with little slope, therefore indicating stability of the paint.

- An increase in the G' values is observed, thereby indicating an increase in the structural strength.
- Figure 7-9 illustrates the structure of the sample at rest.



Figure 7-9: Storage stability of paint with Acrysol ASE60 (4 weeks)

Figure 7-9 illustrates the excellent in-can stability of the paint with Acrysol ASE60 added as rheology modifier (right). No phase separation or sedimentation occurs.

7.4.1.4 Three-Interval-Thixotropy-Test (3-ITT)

The structural recovery curves are given in Figure 7-10 below.

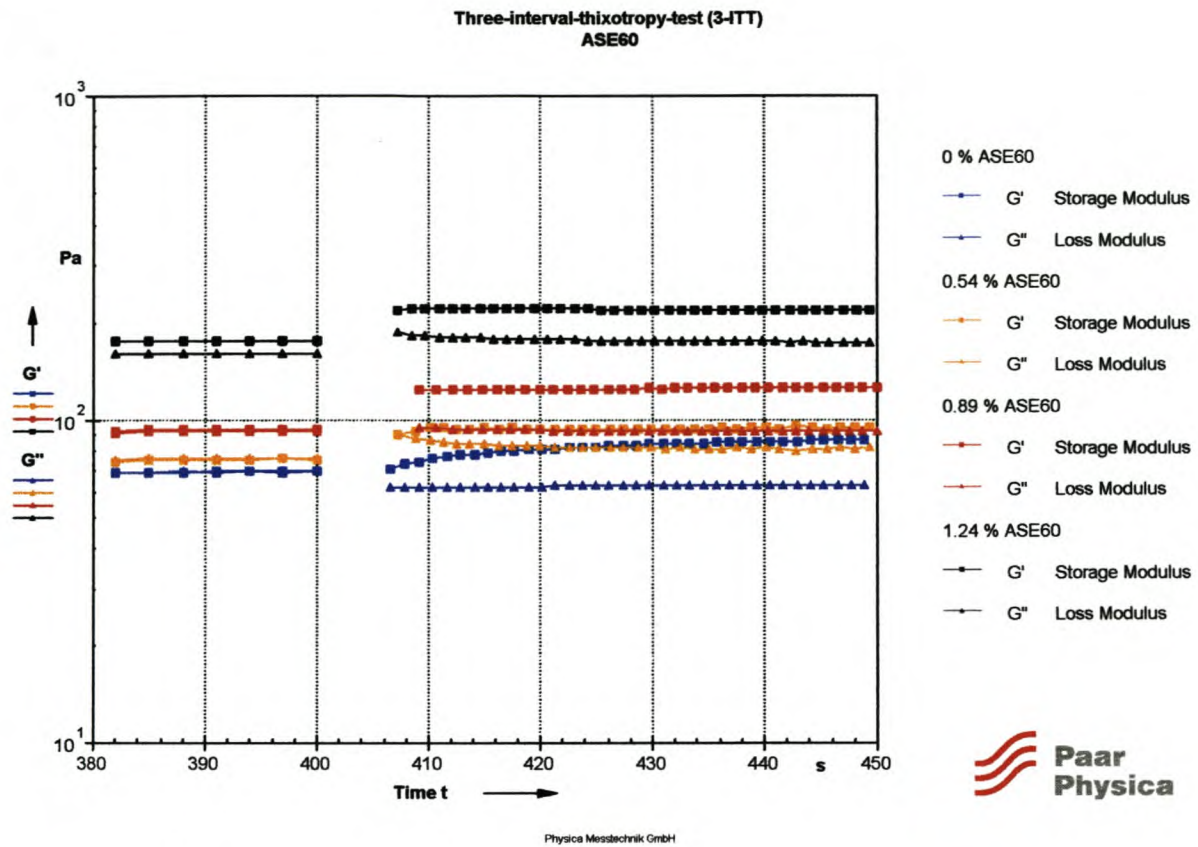


Figure 7-10: Structural recovery with Acrysol ASE60

Figure 7-10 shows the following behaviour of the paints after high shear:

- $G' > G''$ directly after the high-shear load for all the samples. Therefore the solid-like behaviour predominates over the liquid-like behaviour. This will result in relatively poor levelling behaviour, because the paint cannot flow directly after application.
- All the structures recover to G' values higher than originally in the rest phase. An increase in Acrysol ASE60 seems to result in an increase in the G' value in the recovery phase. This results in the paint having greater structural strength after application.
- The G' curve for the paint without any Acrysol ASE60 (0% ASE60) seems to recover over a period of time. In contrast, the samples with Acrysol ASE60 recover immediately to the constant plateau values of G' . In other words, the final structural strength of the samples with Acrysol ASE60 is reached immediately after application, while the sample without Acrysol ASE60 still indicates an increase in the structural strength. The immediate recovery

of the samples with the Acrysol ASE60 results in poor film properties because the solid particles in the paint film cannot orientate themselves into the most stable position.

7.4.1.5 Conclusions

The following conclusions can be drawn:

- The viscosity curves indicate that Acrysol ASE60 has an increasing effect on the in-can stability of the paint due to the higher low-shear viscosities. They also indicate that Acrysol ASE60 still allows for relative good application properties (although impaired a little) with relatively low increases in the high-shear viscosity with increases in the level of Acrysol ASE60.
- The amplitude sweeps also indicate the increase in structural strength (higher G' values and yield points, lower $\tan \delta$ values) with increasing amounts of Acrysol ASE60 and therefore resulting in better in-can stability.
- The frequency sweeps indicate that addition of Acrysol ASE60 does not result in lower spatter behaviour during roller application. They do, however, indicate that the stability of the paint increases by adding Acrysol ASE60 to the formulation, resulting in good in-can stability.
- Addition of Acrysol ASE60 to the formulation seems to impair the flow and levelling behaviour.

7.4.2 Acrysol RM8W and Acrysol RM2020 (HEUR Chemistry)

Acrysol RM8W and Acrysol RM2020 are used in a 1:1 ratio in the paint.

Rohm and Haas® states that the combined Acrysol RM2020/RM8 mixture has the following rheological characteristics [Rohm & Haas, 1996]:

- Excellent film build;
- Excellent flow and levelling;

- Excellent spatter resistance.

7.4.2.1 Viscosity Curves

Acrysol RM2020 is a relatively new rheology modifier that is designed to provide high shear-rate viscosities similar to that of traditional HEUR rheology modifiers, but the hydrophobic modification was adjusted to give much lower association, thereby reducing the low-shear viscosity to provide more near-Newtonian rheology. The effect of Acrysol RM2020/RM8W on the viscosity curves can be seen in Figure 7-11.

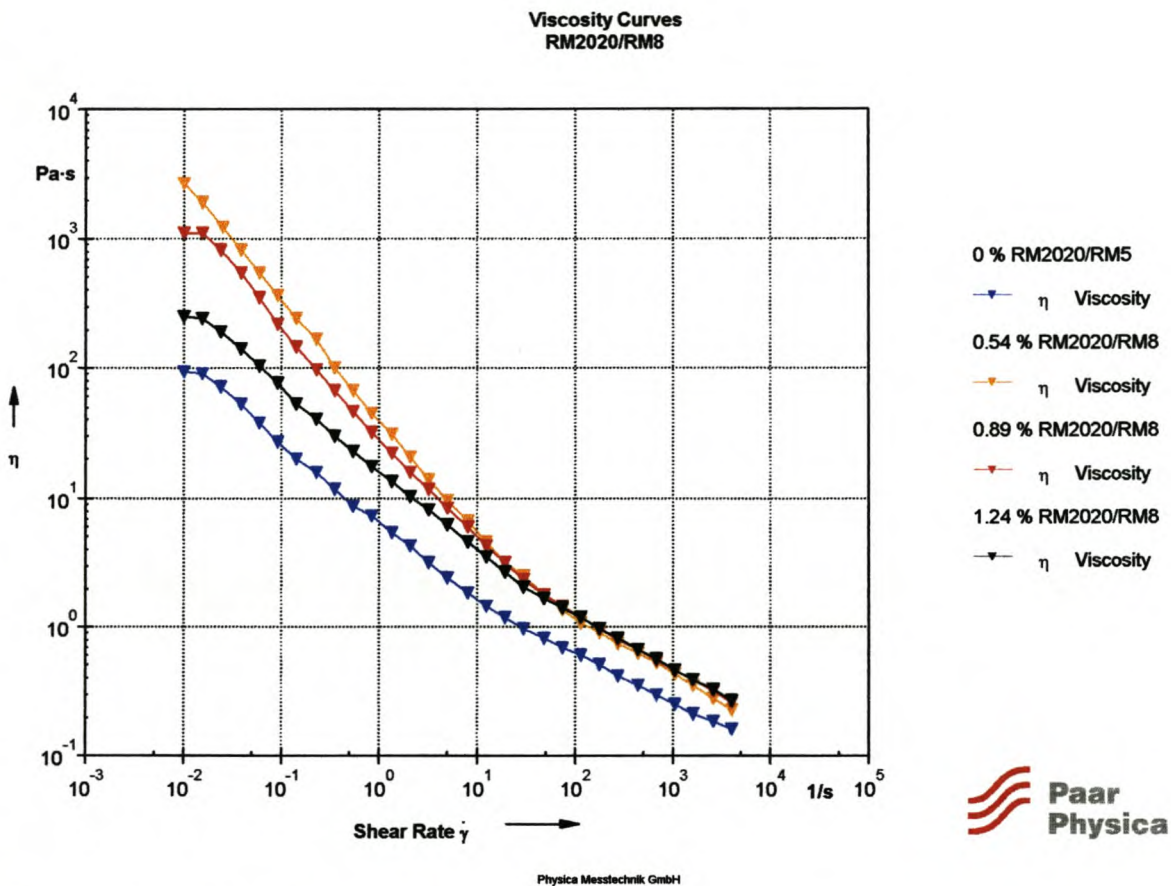


Figure 7-11: Effect of RM2020/RM8W on viscosity curves

The viscosity curves in Figure 7-11 give the following information about the flow behaviour of the paints:

- The viscosity curves reveal an overall increase in the viscosity with addition of Acrysol RM2020/RM8W.

- At shear rates higher than 50 s^{-1} , little difference is observed in the viscosity behaviour between the three samples with different amounts of Acrysol RM2020/RM8W. Knoef et al. [1992] states that the urethane groups may also form hydrogen bonds with chemical substances such as PVOH, which is adsorbed onto the polymer surface. These interactions will be fairly resistant to high shear forces, resulting in a more stable viscosity. Howard et al. [1992] has also observed very similar viscosity behaviour at high shear rates for a combination of two HEUR thickeners in a 50/50 ratio.
- At shear rates smaller than 50 s^{-1} large differences occur in the viscosity behaviour at different levels of Acrysol RM2020/RM8W. The viscosity seems to decrease with increasing amounts of the rheology modifier. The reason for this behaviour is mentioned in the first paragraph of this section – the hydrophobic groups of Acrysol RM2020 are adjusted to give much lower association, thereby reducing the low-shear viscosity to provide more nearly Newtonian rheology. Therefore the addition of a certain amount of Acrysol RM2020/RM8W will initially increase the low shear-rate viscosities resulting in better in-can stability, but further addition of Acrysol RM2020/RM8W will result in a decrease in the in-can stability of the sample. The lower viscosity with an increase in Acrysol RM2020/RM8W will result in better flow and levelling properties, as the manufacturer remarks.
- Attempts to understand the effect of shear on the viscosity-building mechanism on a more fundamental level so far have been inconclusive. Howard et al. [1992] states that the relationship between thickener association and the shear-dependent viscosity appears clear on an empirical basis, but attempts to understand the mechanism on a more fundamental level have been inconclusive.

Prideaux [1993] tries to explain the associative mechanism fundamentally by assuming that the thickening is dependent on the concentration of the hydrophobe micelles in the water phase (i.e. the concentration of rheology modifier present) and not on association with other particles.

7.4.2.2 Amplitude Sweeps

The amplitude sweeps are given in Figure 7-12 below.

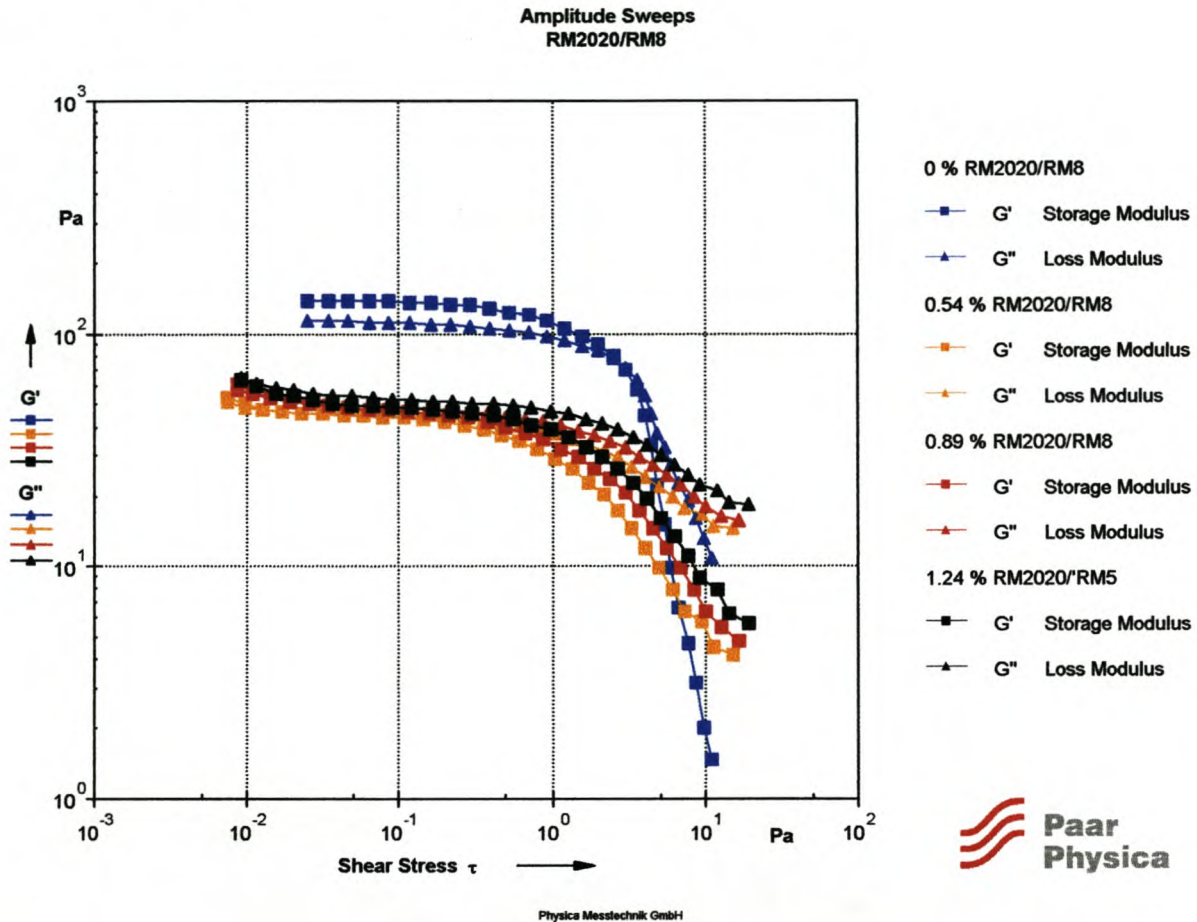


Figure 7-12: Effect of Acrysol RM2020/RM5 on the amplitude sweeps.

The following information about the character of the paint is obtained from Figure 7-12:

- The increase in liquid-like behaviour with the addition of Acrysol RM2020/RM8W can clearly be seen. The G' and G'' values for the samples with the Acrysol RM2020/RM8W are almost the same, in contrast to the sample without the Acrysol RM2020/RM8W, for which $G' > G''$. An increase in the amount of Acrysol RM2020/RM8W therefore results in an increase in the liquid-like character of the sample, which is an indication of possible instability that can result in phase separation or sedimentation.

- There is a decrease in the G' and G'' values with the Acrysol RM2020/RM8W added.
- The yield point also seems to decrease when Acrysol RM2020/RM8W is added.
- Therefore, addition of Acrysol RM2020/RM8W seems to have a degrading effect on the structural strength. This may lead to poorer in-can stability, although time-dependent tests are required to determine the long time-scale behaviour of the paints with Acrysol RM2020/RM8W as rheology modifier.

7.4.2.3 Frequency Sweeps

The frequency sweeps are given in Figure 7-13 below:

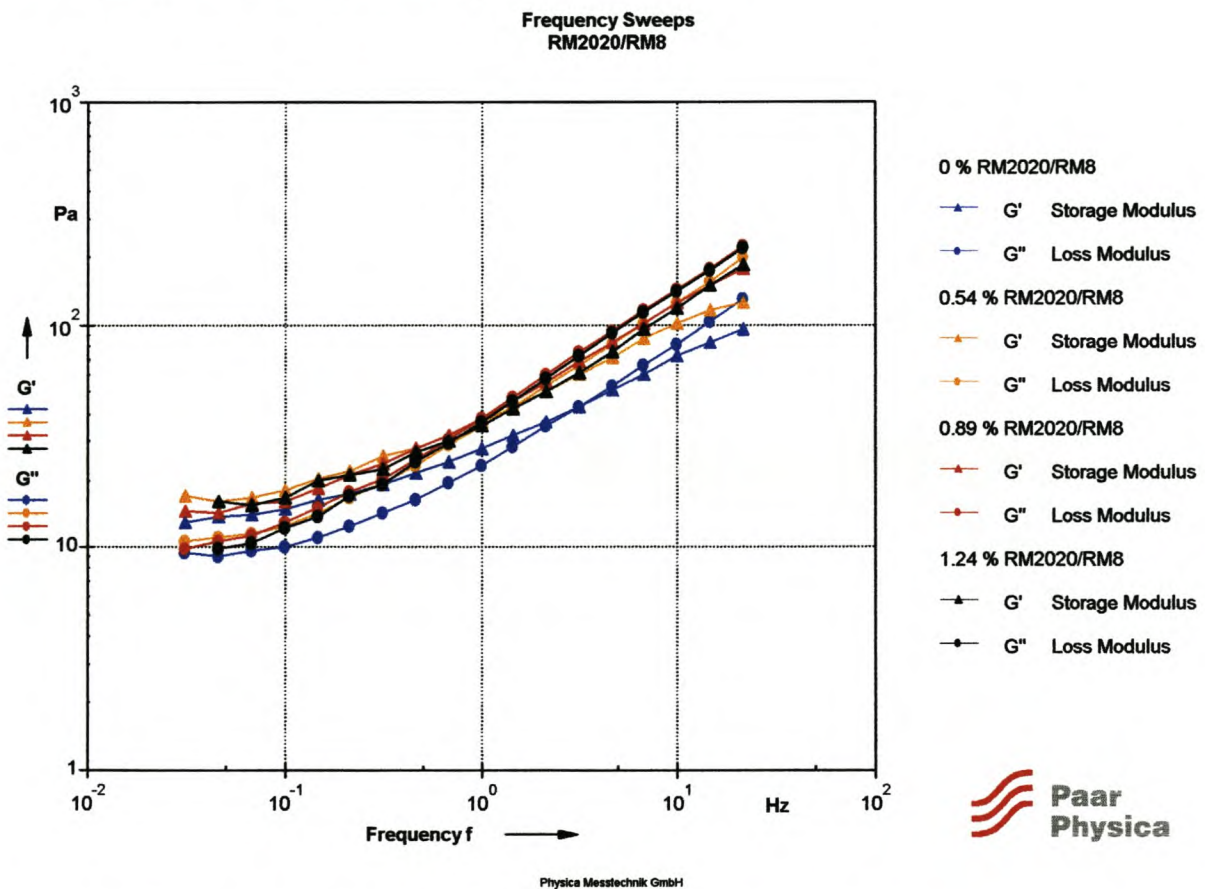


Figure 7-13: Effect of Acrysol RM2020/RM8W on the frequency sweeps

The following insights are obtained from Figure7-13:

- $G'' > G'$ in the high frequency range for the samples with added Acrysol RM2020/RM8W as well as the sample without Acrysol RM2020/RM8W and therefore the liquid-like behaviour predominates over the solid-like behaviour and the paint is more likely to spatter during roller application. The manufacturer states that this type of rheology modifier will give excellent anti-spatter behaviour, but it is clear that in this system it does not help to prevent spatter behaviour.
- In general, the paints with added Acrysol RM2020/RM8W behave in the same manner as the paint without the Acrysol RM2020/RM8W. The only difference is an increase in the gradients of the G' and G'' curve which indicates a decrease in the structural stability.
- The paint without the Acrysol RM2020/RM8W is stable in the low-frequency range (long time-scale behaviour). The paint samples with Acrysol RM2020/RM8W are also stable in the long-time scale behaviour and therefore stable in terms of phase separation behaviour.
- Figure 7-14 illustrates the structure of the sample at rest (in-can conditions).



Figure 7-14: Storage stability of paint with Acrysol RM2020/RM8W (4 weeks)

Figure 7-14 illustrates the good in-can stability of the paint with Acrysol RM2020/RM8W added as rheology modifier (right). No phase separation or sedimentation occurs. However, it appears as if a film has developed. Rohm and Haas® states that Acrysol RM2020/RM8W

allows for excellent film build after application, but in this specific paint it appears to be excessive and also affects the paint during storage.

7.4.2.4 Three-Interval-Thixotropy-Tests (3-ITT)

The structural recovery is given in Figure 7-15 below.

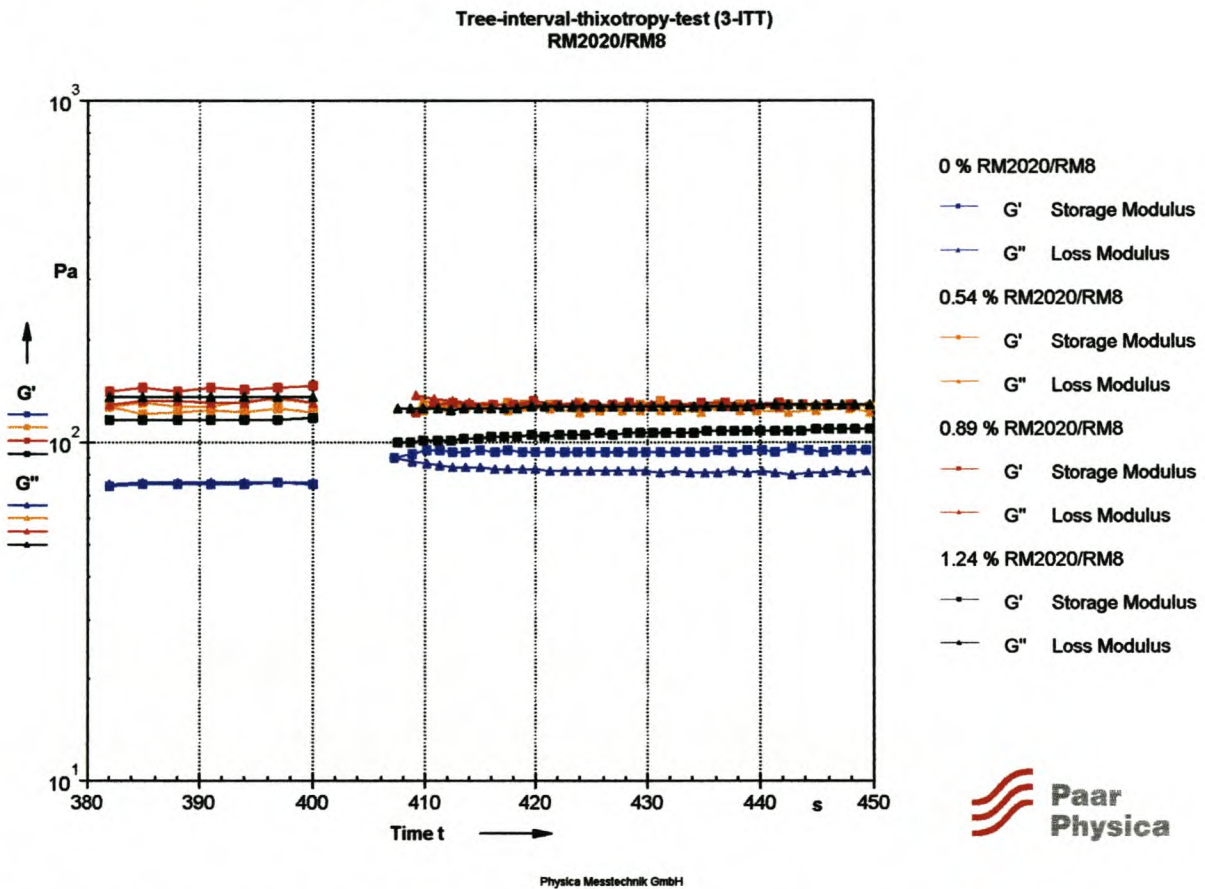


Figure 7-15: Effect of Acrysol RM2020/RM8W on the structural recovery

Figure 7-15 gives the following information about the structural recovery of the paints after high shear:

- $G' > G''$ directly after the shear load for the paint without Acrysol RM2020/RM8W (blue) and therefore the solid-like behaviour predominates over the liquid-like behaviour. The structure recovers immediately and does not allow for levelling, resulting in possible brush marks in the final coating and poor flow and levelling behaviour.

- The addition of 1.24% Acrysol RM2020/RM8W results in $G'' > G'$ and therefore the liquid-like behaviour predominates over the solid-like behaviour (black), resulting in good flow and levelling behaviour, as stated by the manufacturer of these rheology modifiers.
- The increase in the liquid-like behaviour directly after application might, however, result in sagging behaviour.

7.4.2.5 Conclusions

The following conclusions can be drawn:

- Addition of Acrysol RM2020/RM8W seems to increase the viscosity over the whole shear-rate range. However, the high-shear viscosity seems to be unaffected by different amounts of Acrysol RM2020/RM8W, while the low-shear viscosity is affected in a significant way. The relatively low viscosities in the high shear-rate-range will result in easy application behaviour. The lower viscosity in the low shear-rate range will result in better flow and levelling behaviour.
- The addition of Acrysol RM2020/RM8W leads to more liquid-like character and a lower yield point of the sample. This has an effect on the storage stability of the sample. A thin layer of low-viscosity liquid is found on the paint after 4 weeks. This thin layer is most probably the cause of the film that occurs after 4 weeks. The slight decrease in the stability of the paint is also observed in the frequency sweep (steeper G' and G'' curves) as well as in the 3-ITT after a high-shear load ($G'' > G'$).
- The addition of Acrysol RM2020/RM8W does not improve the spatter behaviour as the manufacturer claims.
- Addition of Acrysol RM2020/RM8W results in good flow and levelling properties, but may also result in sagging behaviour.

7.4.3 Acrysol RM5

Rohm and Haas® states that Acrysol RM5 has the following rheological characteristics [Rohm & Haas®, 1996]:

- Good high-shear viscosity;
- Excellent spatter resistance;
- Superior film build;
- Excellent flow and levelling.

7.4.3.1 Viscosity Curves

The viscosity curves are given in Figure 7-16 below.

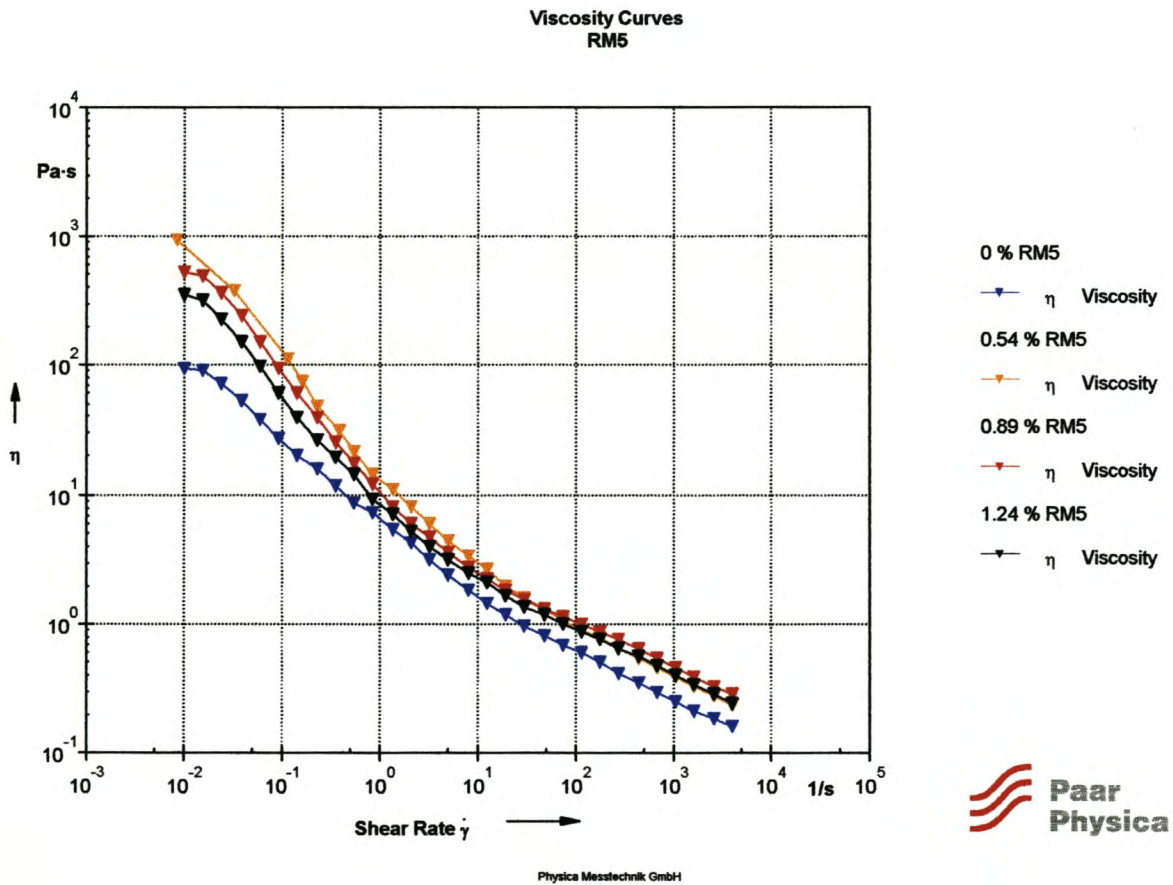


Figure 7-16: Effect of Acrysol RM5 on viscosity curves

Figure 7-16 shows the following flow behaviour:

- The viscosity curves reveal an overall increase in the viscosity with addition of Acrysol RM5.
- At high shear rates the viscosity behaviour seems to be unaffected by the level of Acrysol RM5 and therefore good application behaviour is retained, with an increase in the amount of rheology modifier.
- At lower shear rates the viscosity seems to decrease with increasing amounts of the rheology modifier. In other words, an increase in the amount of Acrysol RM5 results in a lower viscous, more Newtonian behaviour that will result in better flow and levelling behaviour, but at the same time the paint is more likely to sag. The lower viscosity behaviour may result in a decrease in the in-can stability of the sample.

7.4.3.2 Amplitude Sweeps

The amplitude sweeps are given in Figure 7-17 below.

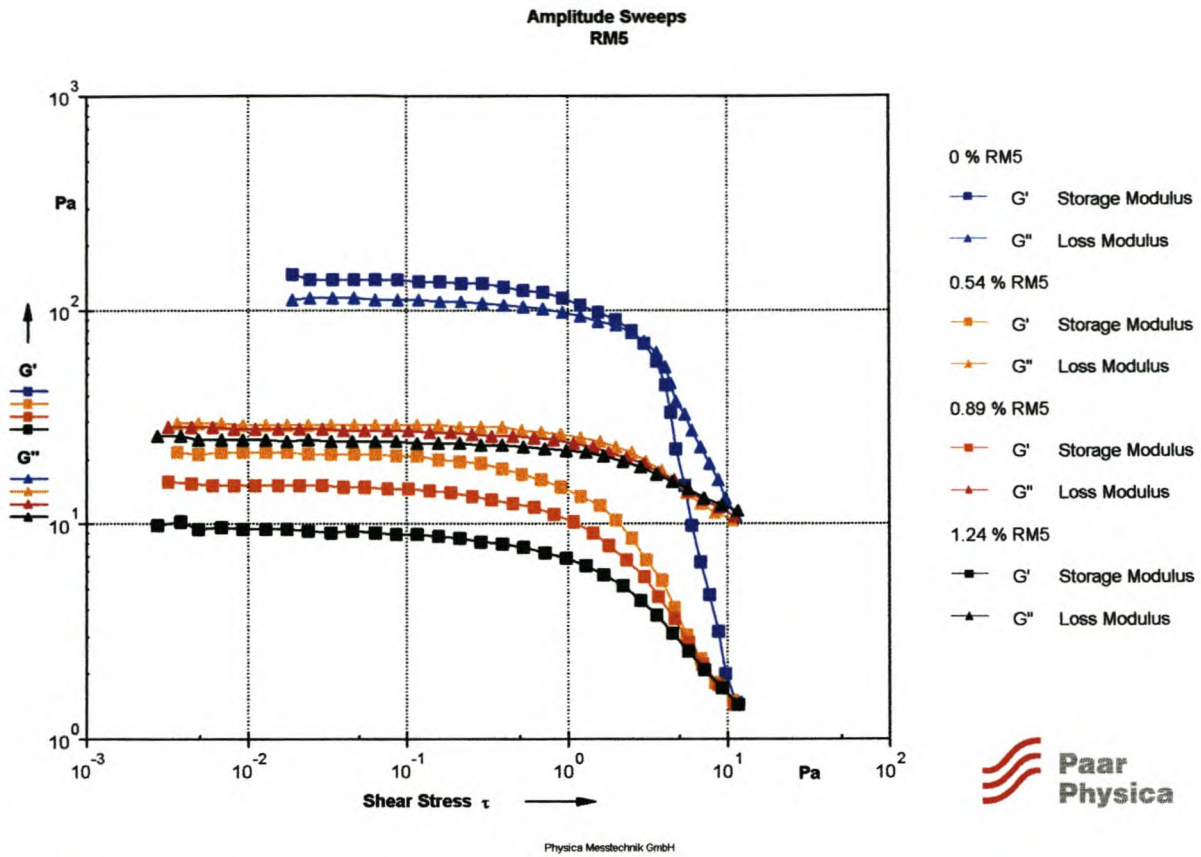


Figure 7-17: Effect of Acrysol RM5 on amplitude sweeps

Figure 7-17 reveals the following information about the character of the paints:

- $G'' > G'$ in the LVER for the samples with Acrysol RM5, while $G' > G''$ for the sample without the Acrysol RM5 and therefore the liquid-like character predominates over the solid-like character for the samples with the Acrysol RM5. This indicates possible instability during storage.
- Addition of Acrysol RM5 results in a decrease in the yield point (according to G').
- Addition of Acrysol RM5 causes a decrease in the structural strength (G') of the samples.

The three points mentioned above all indicate a decrease in the structural strength of the sample with addition of Acrysol RM5 and the paint is therefore very likely to show poor in-can stability due to the sharp decrease in the structural strength.

7.4.3.3 Frequency Sweeps

The frequency sweeps are given in Figure 7-18 below.

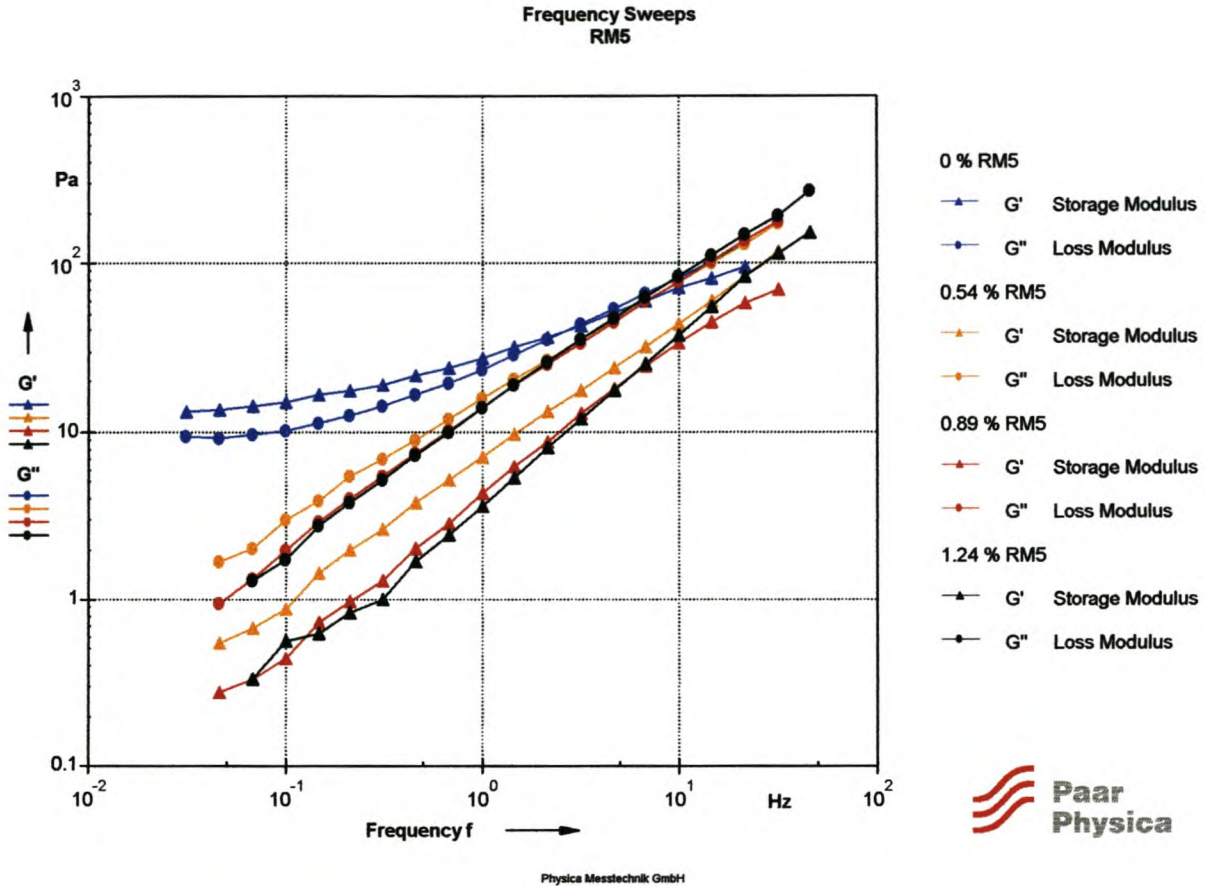


Figure 7-18: Effect of Acrysol RM5 on the frequency sweeps

The following information about the behaviour of the paints in the LVER is obtained from Figure 7-18:

- $G'' > G'$ over the whole frequency range for the samples with the Acrysol RM5 and therefore the liquid-like behaviour predominates over the solid-like behaviour, while $G' > G''$ for the sample without the Acrysol RM5. The G' and G'' curves also have very steep gradients. Therefore addition of Acrysol RM5 seems to decrease the structural stability of the paint drastically.
- $G'' > G'$ in the low-frequency range (long time-scale behaviour) and is therefore very likely to show sedimentation and phase separation behaviour.

- The liquid-like character predominates over the solid-like character over the whole frequency range, which makes the use of this type of rheology modifier inadequate.
- The structure of the sample at rest is given in Figure 7-19 below.

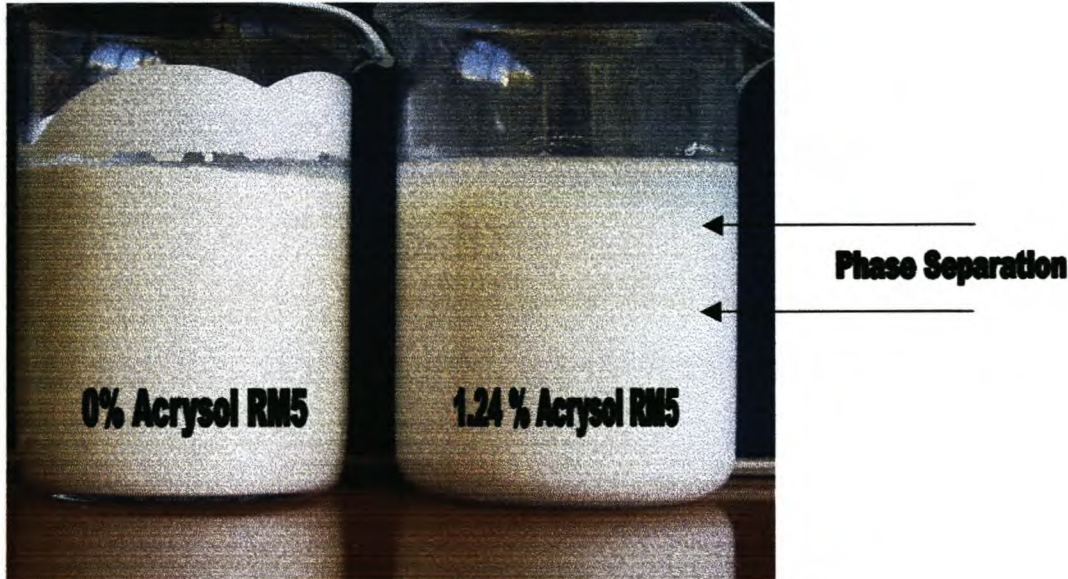


Figure 7-19: Storage stability of paint with Acrysol RM5 (4 weeks)

Figure 7-19 illustrates the instability caused by the addition of Acrysol RM5 (right). Phase separation occurs as indicated by the arrows.

Prideaux [1993] gives an explanation for this behaviour. Acrysol RM5, a low-associative HASE thickener, cannot be used in masonry paints with low-quality binders. Under these conditions early water sensitivity can be a problem. In addition HASE thickeners have a great tendency to adsorb onto pigment surfaces through attraction of the carboxylate groups. Therefore it is essential when formulating with HASE types to ensure that an adequate level of pigment dispersant is present to minimise this effect and ensure good viscosity stability on the paint storage.

7.4.3.4 Three-Interval-Thixotropy-Test (3-ITT)

The structural recovery after high shear is given in figure 7-20 below.

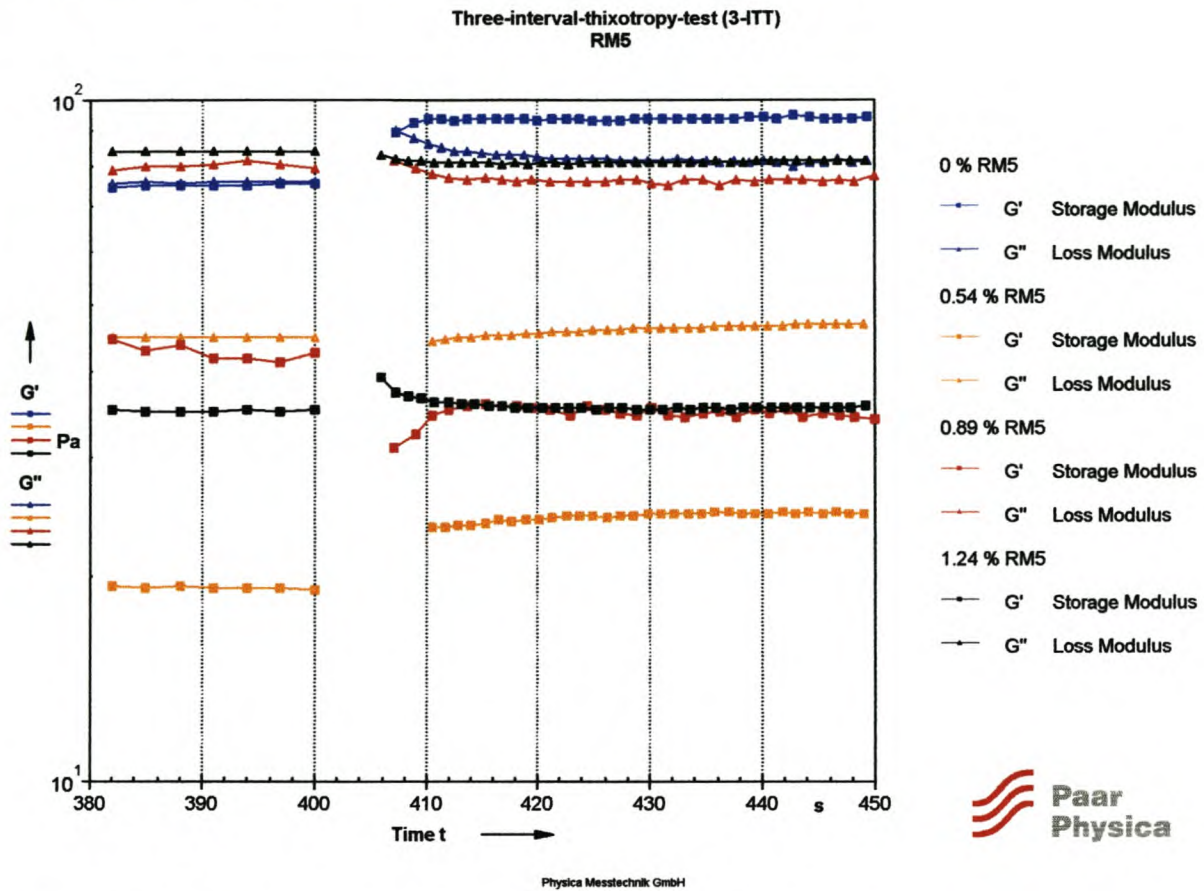


Figure 7-20: Effect of Acrysol RM5 on the structural recovery.

Figure 7-20 gives the following information about the structural recovery of the paints after high shear:

- $G'' > G'$ directly after the high-shear load for the samples with the Acrysol RM5 and therefore the liquid-like behaviour predominates over the solid-like behaviour and the paint is allowed to flow and results in good levelling behaviour showing few brush marks.
- Sagging is likely to occur due to the liquid-like character of the sample after high shear that predominates for too long.
- The elastic part (G') of the paint with 0.89% Acrysol RM5 as the rheology modifier is broken down quite significantly after the high-shear load. It then gradually reaches a plateau value, but does not recover to its original value.

7.4.3.5 Conclusions

The following conclusions can be drawn:

- Good high-shear viscosities are retained with the addition of Acrysol RM5, which makes application easy.
- The lower low-shear viscosity with addition of Acrysol RM5 will result in good flow and levelling behaviour, but the more Newtonian behaviour indicates that the paint with Acrysol RM5 is also likely to sag.
- Addition of Acrysol RM5 causes the dispersion to become unstable, resulting in phase separation and poor in-can stability.
- The liquid-like character after high shear ensures good levelling, but indicates possible sagging behaviour.

7.5 Conclusions

The following are the most important conclusions that can be drawn:

- PE-free paint is stable at pH levels of ± 9 for each of the rheology modifiers used.
- Table 7-2 summarises the effect of the various rheology modifiers on the PE-free paint:

Table 7-2: Effect of rheology modifiers on PE-free paint

Property	Acrysol ASE60	Acrysol RM2020/RM8W	Acrysol RM5
1. In-can stability:	Improve	Impair	Impair ⁴
2. Application behaviour:	Impair	Unaffected	Unaffected
3. Flow and levelling:	Impair	Improve	Improve
4. Spatter:	Unaffected	Unaffected	Impair
5. Sag:	Improve	Impair	Impair

It can be seen from Table 7-2 that there does not exist a single rheology modifier that results in ideal behaviour of the paint. Ideal properties of this paint are, however, not expected because of its lower quality.

1. In-can stability: Addition of the appropriate rheology modifier can result in an increase in the in-can stability of the paint. One of these rheology modifiers is Acrysol ASE60. However, addition of certain rheology modifiers such as Acrysol RM2020/RM8W results in a small decrease in the structural strength that leads to small degrees of phase separation, while addition of Acrysol RM5 leads to total instability with severe phase separation behaviour.
2. Application behaviour: Addition of a rheology modifier can impair the application behaviour by increasing the high-shear viscosity, such as Acrysol ASE60. Increasing the amount of Acrysol ASE60 steadily increases the high-shear viscosity, making application more difficult. Addition of Acrysol RM2020/RM8W and Acrysol RM5 initially also increase the high-shear viscosity, but further increases in the levels of these rheology modifiers do not have an effect on the high-shear viscosity.

⁴ Total instability with phase separation making paint useless.

3. Flow and levelling: Addition of the wrong rheology modifier can lead to poor flow and levelling behaviour due to a too rapid structural recovery, e.g. Acrysol ASE60, while other rheology modifiers such as Acrysol RM2020/RM8W and Acrysol RM5 result in good flow and levelling behaviour.
 4. The rheology modifiers do not always perform as the manufacturer claims they do. For example, the combination of Acrysol RM2020 and Acrysol RM8W does not result in better spatter behaviour in the PE-free paint. Neither of the other rheology modifiers seems to improve the spatter behaviour of the PE-free paint.
 5. Sag: Sag is a result of an increase in the liquid-like character of the sample after application. Therefore ideal sag and levelling behaviour seem to conflict with each other and an optimum has to be reached.
- The end-use of the paint determines the type of rheology modifier that will fit ideally to the PE-free paint. However, using Acrysol RM5 is ruled out due to total instability of the paint at rest. In most of the cases it can be seen that there is a trade-off between the high and low-shear rate properties – ideal in-can stability leads to impairment of application behaviour and vice versa. The remaining two rheology modifiers examined, Acrysol ASE60 and Acrysol RM2020/RM8W, offer good long time-scale and short time-scale behaviour respectively. Therefore, as stated in the Rohm and Haas® data sheets, addition of Acrysol ASE60 results in excellent in-can stability and addition of the combination of Acrysol RM2020/RM8W results in excellent flow and levelling behaviour.
 - HASE rheology modifiers have some of the lowest production costs, but their high acid content affects the water sensitivity of the PE-free paint and leads to instability. HEUR thickeners offer the best balance of application rheology and dry film performance and are generally considered to be the premium products among associative thickeners, but are more expensive than ASE thickeners.

CHAPTER 8 Modelling

8.1 Approximation Functions for Flow and Viscosity Curves of Paint

When comparison of data is required, e.g. for quality control, it is not useful to compare many measuring point values of one test with those of another. Mathematical model functions for curve approximation are therefore used to describe the complete flow or viscosity curve using a small number of curve parameters. This simplifies the comparison of measuring curves, as there are only a few model parameters left for comparison.

There are a number of existing models, but not every model function can be used for every kind of flow behaviour. If the correlation ratio¹ indicates insufficient agreement between the test data and the model function, it is best to try another model function. It is also important to keep in mind that model-specific coefficients and exponents are both purely mathematical variables and do not directly represent rheological parameters.

Since there are a number of models, the type of flow behaviour of paints is examined first to determine which model to adopt.

The specific aims of this study were to:

- Determine whether it is possible to model paints which show different types of flow and viscosity behaviour, with existing flow/viscosity models;
- Obtain a model that successfully describes the flow and viscosity behaviour of the standard vesiculated beads dispersion;
- Model certain rheological behaviour of a specific paint by using the simple linear regression model.

¹ The correlation ratio is calculated from data on a lin-log scale.

8.1.1 Possible Flow Behaviour of Paints

Figure 8-1 illustrates three different flow behaviours of paint which:

- Is shear-thinning in behaviour;
- Is Newtonian in behaviour in the low shear-rate range (without yield point);
- Is shear thinning with a definite yield point.

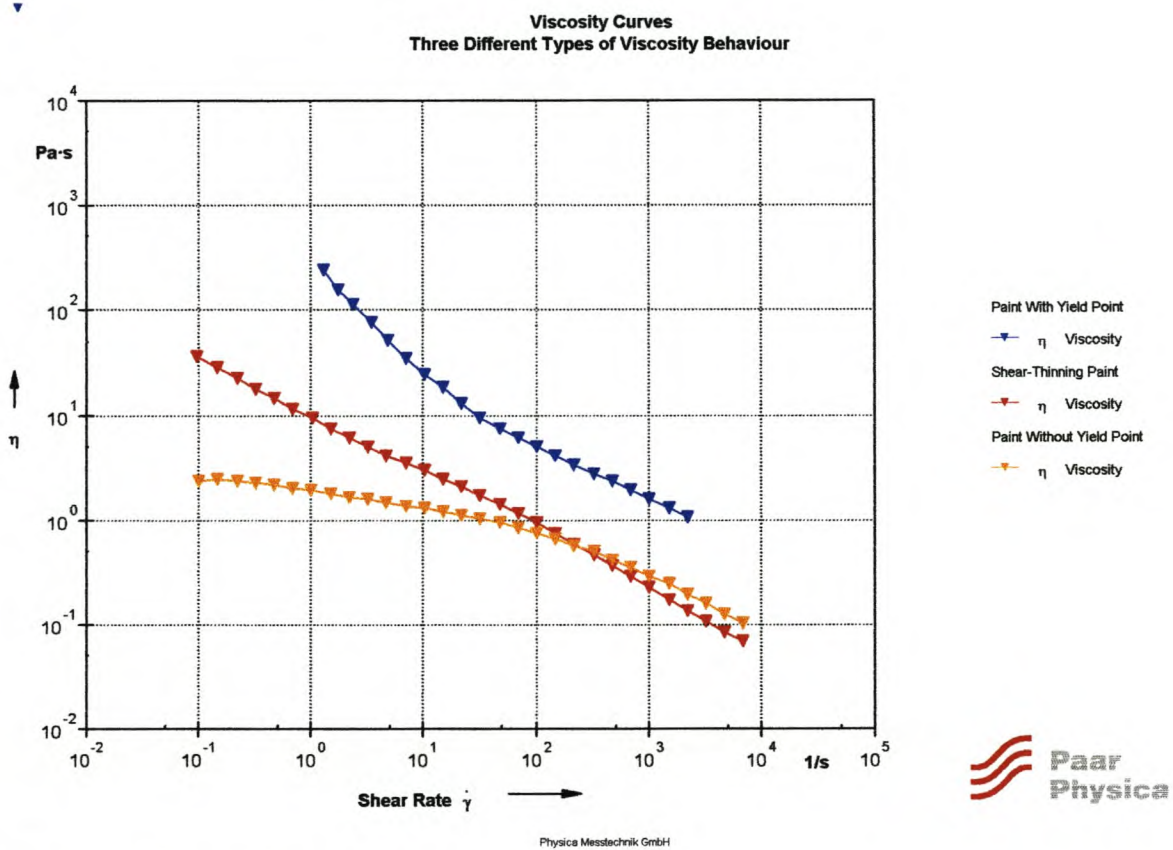


Figure 8-1: Different types of flow behaviour for paints

It is clear from Figure 8-1 that there are different types of flow behaviour for paints and therefore not every model function can be used for every kind of flow behaviour. The three paints in Figure 8-1 are used in the rest of the chapter when there are references to ‘paint with a yield point’, ‘paint that is shear-thinning’ and ‘paint without a yield point’.

8.1.2 Model Functions for Flow Behaviour for Paint with a Yield Point²

The Bingham, Casson and Herschel-Bulkley models are known to fit well to fluids with yield points.

8.1.2.1 The Bingham Model

The Bingham model is given by the following function:

$$\tau = \tau_B + \eta_B \dot{\gamma} \quad (8-1)$$

This is a flow curve model function ($\tau = f(\dot{\gamma})$) according to E.C. Bingham with the “Bingham yield point”, τ_B .

η_B is not the viscosity value – it is only a calculated coefficient used for the curve approximation and is referred to as the “Bingham flow coefficient”.

The model-fit to the flow and viscosity curves is given in Figure 8-2 below³.

² The figures discussed in section 8.1.2 refer to the flow behaviour of a paint with a yield point as illustrated in Figure 8-1. Therefore, when the legend of each figure states ‘with yield point’, this refers to the flow behaviour of the paint in Figure 8-1 with a yield point.

³ The term ‘Auto-regression’ in the legend of Figure 8-2 refers to the fitting of the specific model under investigation to the flow ($\tau = f(\dot{\gamma})$) and viscosity ($\eta = f(\dot{\gamma})$) curves of the paint ‘with a yield point’. The same applies for the rest of the chapter.

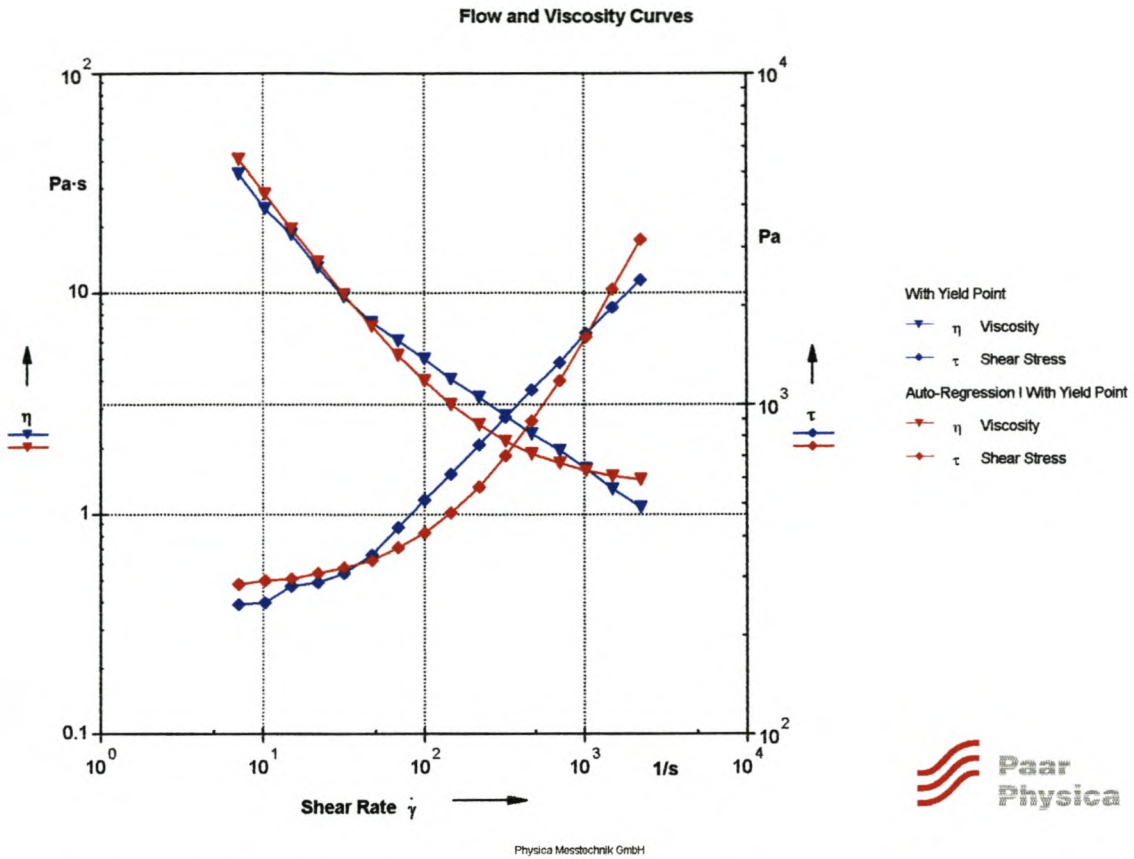


Figure 8-2: Bingham model fit for paint with a yield point

The model parameters for the Bingham model (eq. 8-1) fitted to the paint ‘with yield point’ are as follows:

- τ_B = 277 Pa (Bingham yield stress)
- η_B = 1.29 Pa.s (Infinite-shear viscosity, η_∞)
- correlation ratio = 0.971

The Bingham model was often used because the analysis is very easy (using the “Bingham straight line method”). However, the “Bingham yield point” describes the transition from the state of rest to flow relatively inaccurately and therefore this model should only be used for very simple quality control.

8.1.2.2 The Casson Model

The Casson model is given by the following function:

$$\tau^p = \tau_c + (\eta_c \dot{\gamma})^p \tag{8-2}$$

This is a flow curve model ($\tau = f(\dot{\gamma})$) with the “Casson yield point”, τ_c and the “Casson viscosity”, η_c (for η_c the same applies as mentioned above for η_B).

The model fit to the flow and viscosity curves is given in Figure 8-3 below.

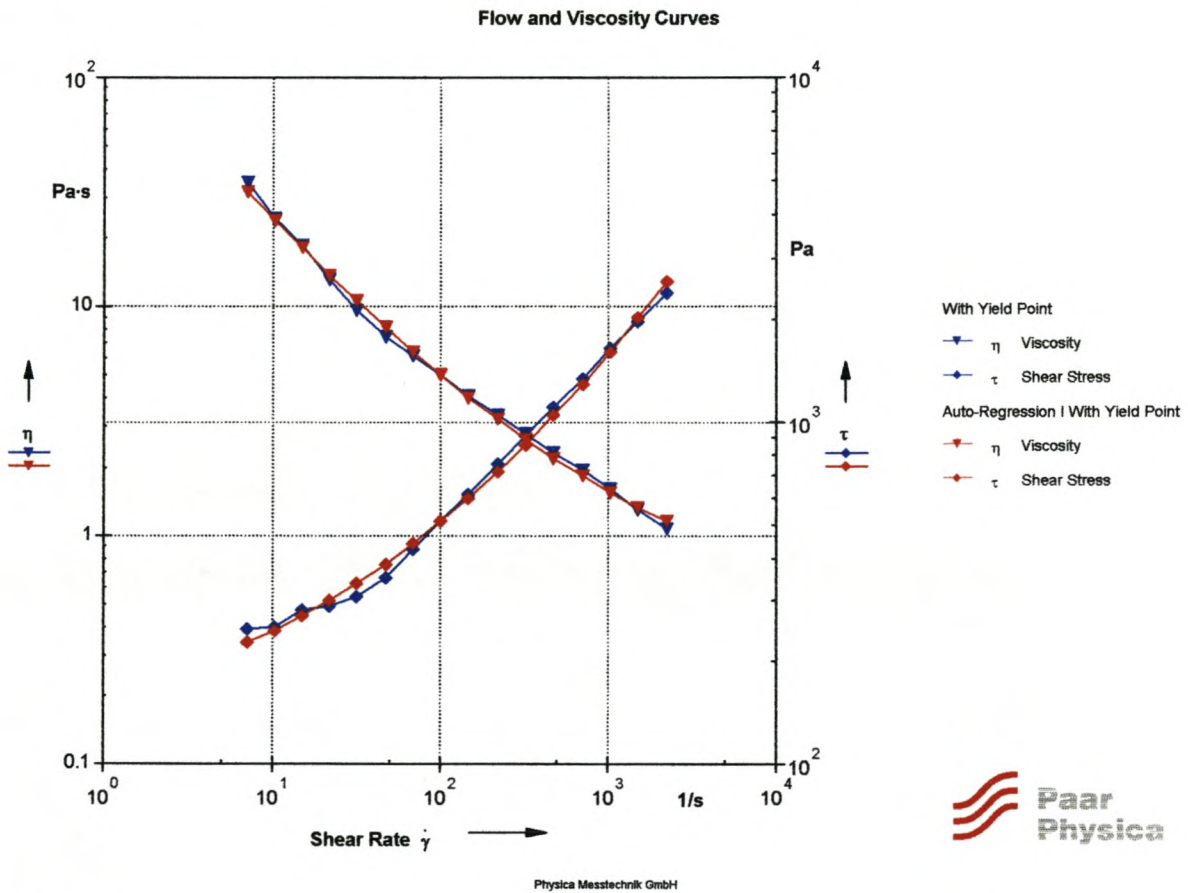


Figure 8-3: Casson model fit for paint with a yield point

The model parameters for the Casson model (eq. 8-2) fitted to the paint ‘with yield point’, are as follows:

τ_c	= 4 Pa (Casson yield stress)
η_c	= 0.67 Pa.s
p	=3.14 (p > 1 for shear-thinning)
correlation ratio	= 0.998
infinite shear viscosity	= 0.28 Pa.s

By comparison of the correlation ratio, it can be seen that the Casson model fits better (correlation ratio = 0.998) than the Bingham model (correlation ratio = 0.971)

8.1.2.3 The Herschel-Bulkley Model

The Herschel-Bulkley model is given by the following function:

$$\tau = \tau_{HB} + c\dot{\gamma}^p \quad (8-3)$$

This is a flow curve model ($\tau = f(\dot{\gamma})$) with the yield point according to “Herschel-Bulkley”, τ_{HB} . The flow coefficient, c, also called the “Herschel-Bulkley viscosity” and the exponent, p, also called the “Herschel-Bulkley index”.

The model fit to the flow and viscosity curves is given in Figure 8-4 below.

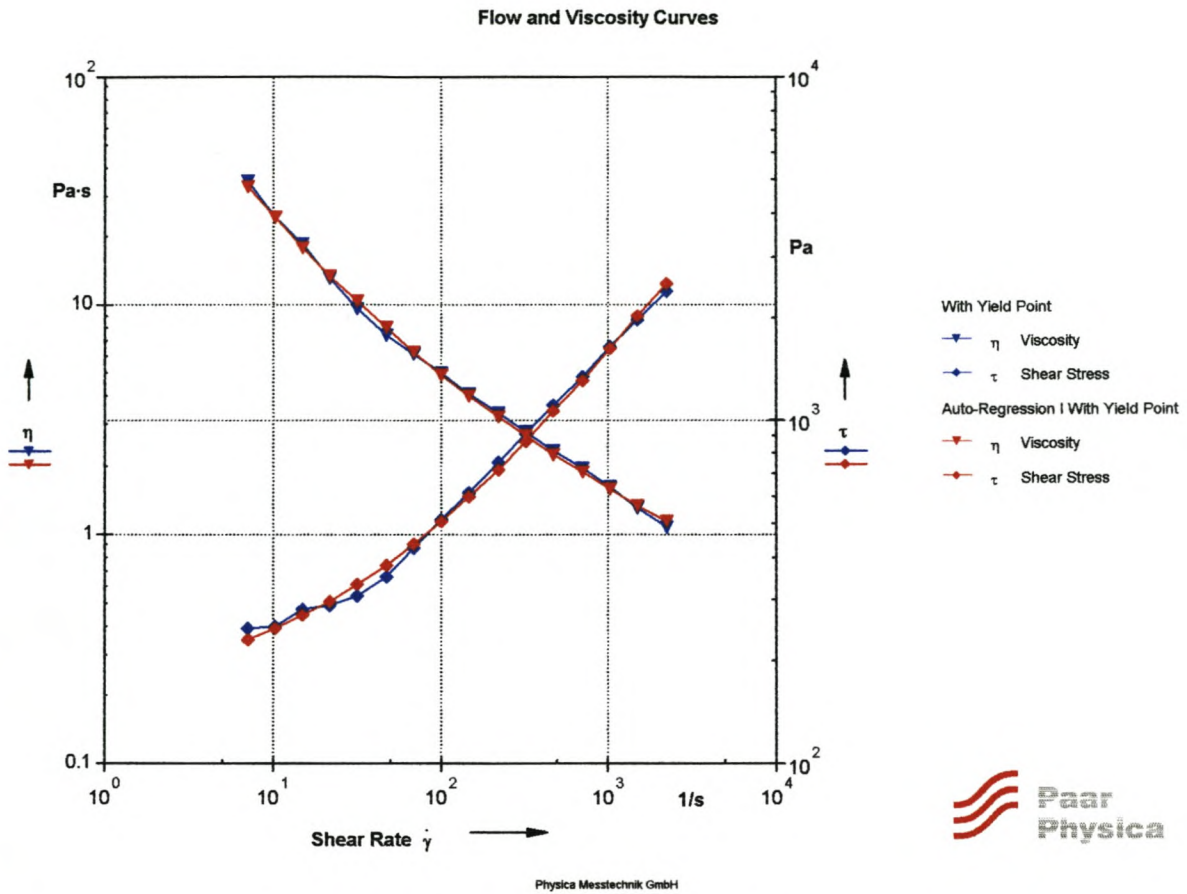


Figure 8-4: Herschel-Bulkley model-fit for paint with a yield point

The model parameters for the Herschel-Bulkley model (eq. 8-3) fitted to the paint ‘with yield point’ are as follows:

- τ_{HB} = 166 Pa (Herschel-Bulkley yield stress)
- c = 18.95 Pa.s
- p = 0.62 ($p < 1$ for shear-thinning)
- correlation ratio = 0.998

From the correlation ratios it can be seen that the Casson (correlation ratio = 0.998) and Herschel-Bulkley model (correlation ratio = 0.998) fit the curves equally well.

8.1.2.4 Yield Point Values Obtained from Models

The above-mentioned models predict the following yield points:

Table 8-1: Model predictions for yield points

Model	Yield Point [Pa]	Correlation Ratio [-]
Bingham:	277	0.971
Casson:	4	0.998
Herschel-Bulkley:	166	0.998

It is clear that the yield point obtained from the Bingham model is not that reliable due to the relatively low correlation ratio of 0.971 compared to the other values for the correlation ratios (both 0.998).

Both the Casson and Herschel-Bulkley give correlation ratios of 0.998, although the predicted yield points differ a lot. One would tend to say that the yield point is more likely to be closer to that of the Herschel-Bulkley yield point value (τ_{HB}) of 166 Pa because the Bingham yield point value (τ_B) is in the same order ($\tau_y > 100$ Pa). However, examination of the amplitude sweep for this paint shows the opposite – that the yield point is closer to that predicted by the Casson model. The amplitude sweep for this point is given below.

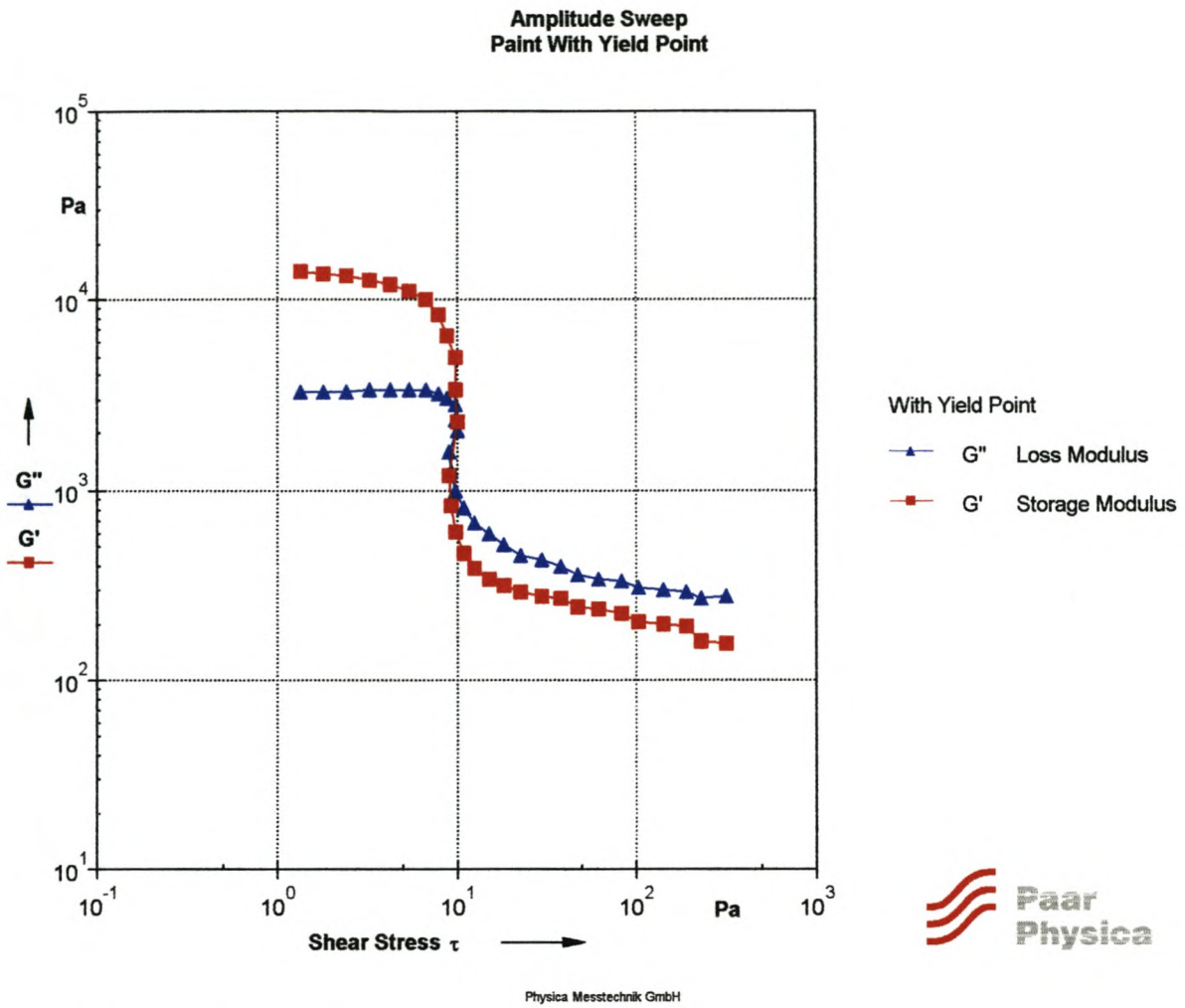


Figure 8-5: Amplitude sweep for paint with yield point

Figure 8-5 reveals that the yield point is definitely below 10 Pa. In fact, determining the yield point as 90% the value of the constant plateau value of G' results in a yield point of 3.25 Pa.

It can therefore be seen that, although the Herschel-Bulkley model has a correlation ratio which is the same as that of the Casson model, the Casson model gives a better representation of the yield point.

8.1.2.5 How to Choose a Model for Different Flow Behaviour of Paint

It is apparent that the models for paint can be divided into more or less three groups:

- Group I: Shear-thinning that is capable of giving an indication of the low-shear behaviour (yield point);
- Group II: Shear-thinning that is unable to give an indication of the low- and high-shear behaviour;
- Group III: More Newtonian-like behaviour (without yield point) in low-shear behaviour.

Table 8-2: Model groups for flow behaviour of paint

Model	Correlation ratio ⁴ [-]		
	Group I: with yield point	Group II: shear-thinning	Group III: without yield point
Ostwald/de Waal ⁵ : (average)	0.883 (0.883)	0.998 (0.998)	0.983 (0.983)
Bingham: Casson: Herschel-Bulkley: (average)	0.971 0.998 0.998 (0.989)	0.728 0.997 0.992 (0.905)	0.776 0.988 0.938 (0.901)
Cross: Philips-Deutsch ⁶ : (average)	0.897 0.962 (0.930)	0.996 0.799 (0.898)	0.998 - (0.998)

The highest average value for each group (I, II or III) indicates which models will be the most likely to fit the curves and therefore serves as a starting point for model fitting instead of fitting any random model to the flow behaviour.

⁴ The correlation ratio refers to the curves in Figure 8-1: with yield point, shear thinning, without yield point.

⁵ Mathematical expression for the Ostwald/de Waal model follows in section 8.1.3 (eq. 8-4)

⁶ Mathematical expressions for the Cross- and Phipips-Deutsch models follow in section 8.1.4 (eq. 8-5 and 8-6 respectively)

For example, if one wants to examine the shear-thinning behaviour as well as the low-shear behaviour (group I), then the best choice of models to start off with would be:

- Bingham
- Casson
- Herschel-Bulkley.

8.1.3 Model Functions for Flow Behaviour of Shear-Thinning Paints⁷

The power-law model is known to fit best to shear-thinning liquids. The power-law model in rheological terms are known as the Ostwald/de Waal model.

8.1.3.1 The Ostwald/deWaal Model

The Ostwald/de Waal model is given by the following function:

$$\tau = c\dot{\gamma}^p \quad (8-4)$$

This is a flow curve model ($\tau = f(\dot{\gamma})$) according to W. Ostwald and A. de Waal with the flow coefficient, c, and the exponent, p.

The model fit to the flow and viscosity curves is given in Figure 8-6 below.

⁷ The figures discussed in section 8.1.3 refer to the flow behaviour of a paint with shear-thinning behaviour as illustrated in Figure 8-1. Therefore, when the legend of each figure states '*shear-thinning*', it refers to the flow behaviour of the paint in Figure 8-1 with shear-thinning behaviour.

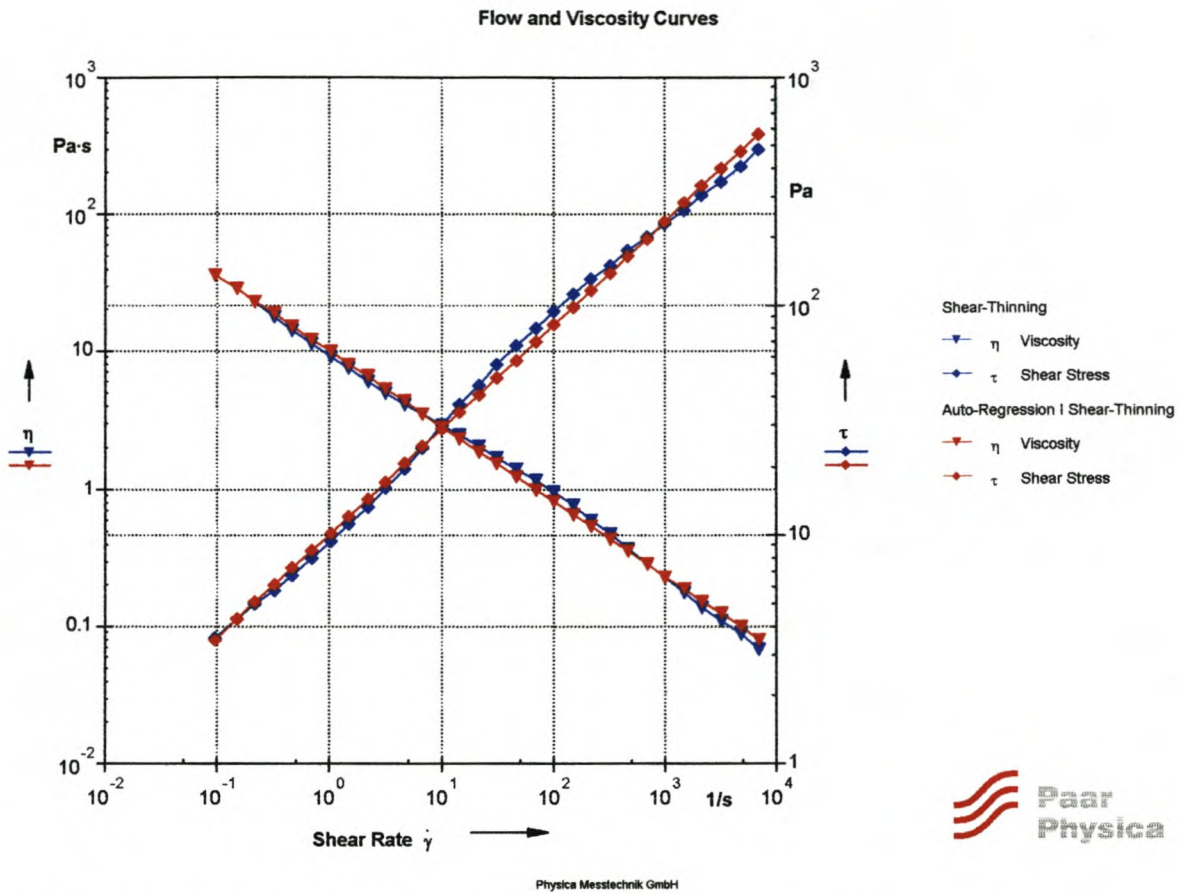


Figure 8-6: Ostwald/de Waal model fit for paint with shear-thinning behaviour

The model parameters for the Ostwald/de Waal model (eq. 8-4) fitted to the ‘shear thinning’ paint are as follows:

- c = 10.12 Pas.
- p = 0.45 (p < 1 for shear-thinning)
- correlation ratio = 0.998

The disadvantage of this model is that it cannot be fitted well to the curves at very low and very high shear rates and therefore can only give an indication of shear-thinning behaviour in the medium shear-rate range.

8.1.4 Model Functions for Flow Behaviour of Paints without Yield Point⁸

It is rather strange for a paint not to have a yield point and therefore these models are not ideal for substances such as paints. Nevertheless, as can be seen in Figure 8-1, there are paints that have Newtonian behaviour in the low shear-rate range and therefore indicate no, or a very low, yield point.

8.1.4.1 The Cross Model

The Cross model is given by the following function:

$$\eta = \frac{\eta_0 - \eta_\infty}{1 + c\dot{\gamma}^p} + \eta_\infty \quad (8-5)$$

This is a viscosity curve model ($\eta = f(\dot{\gamma})$) with the “Cross constant”, c , and the “Cross exponent”, p . Paints do not always demonstrate infinite-shear-viscosity, η_∞ .

The model fit to the flow and viscosity curves is given in Figure 8-7 below.

⁸ The figures discussed in section 8.1.4 refer to the flow behaviour of a paint without a yield point as illustrated in Figure 8-1. Therefore, when the legend of each figure states ‘*without yield point*’, it refers to the flow behaviour of the paint in Figure 8-1 without a yield point.

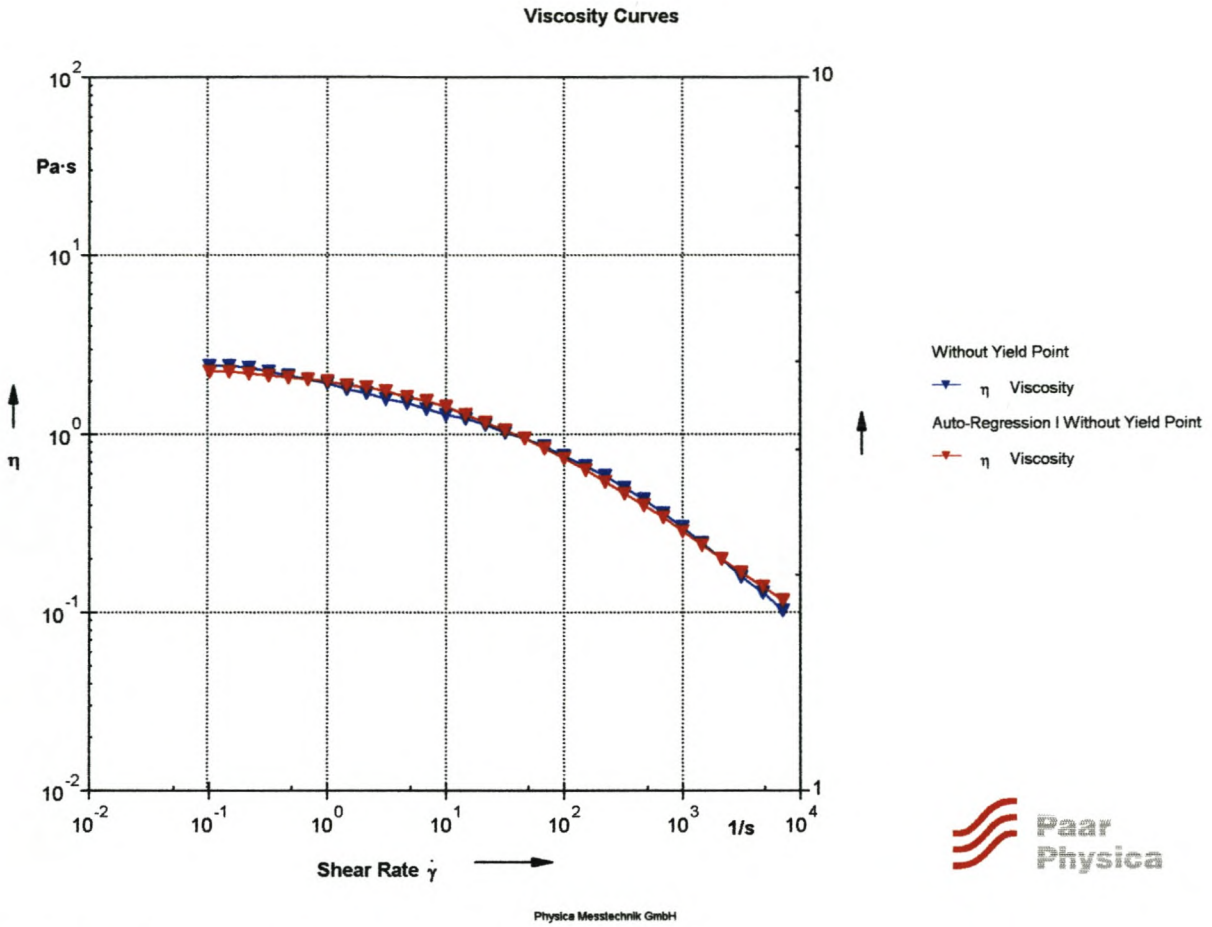


Figure 8-7: Cross model fit for paint without a yield point

The model parameters for the Cross model (eq. 8-5) fitted to the paint ‘without yield point’ are as follows:

$\eta_0 - \eta_\infty$	= 2.39 Pa
η_∞	= 1.21 E-05 Pa
c	= 0.22 s
p	= 0.51
correlation ratio	= 0.998

From the correlation ratio above it can be seen that the Cross model fits well to the paint without a yield point.

8.1.4.2 Philips-Deutsch

The Philips-Deutsch model is given by the following function:

$$\tau = c_1 \frac{(1 + c_2 \dot{\gamma}^2)}{(1 + c_3 \dot{\gamma}^2)} \dot{\gamma} \tag{8-6}$$

This is a flow curve model ($\tau = f(\dot{\gamma})$) with the viscosity factor, c_1 , the numerator coefficient, c_2 , and the denominator coefficient, c_3 .

The model fit to the flow and viscosity curves is given in Figure 8-8 below.

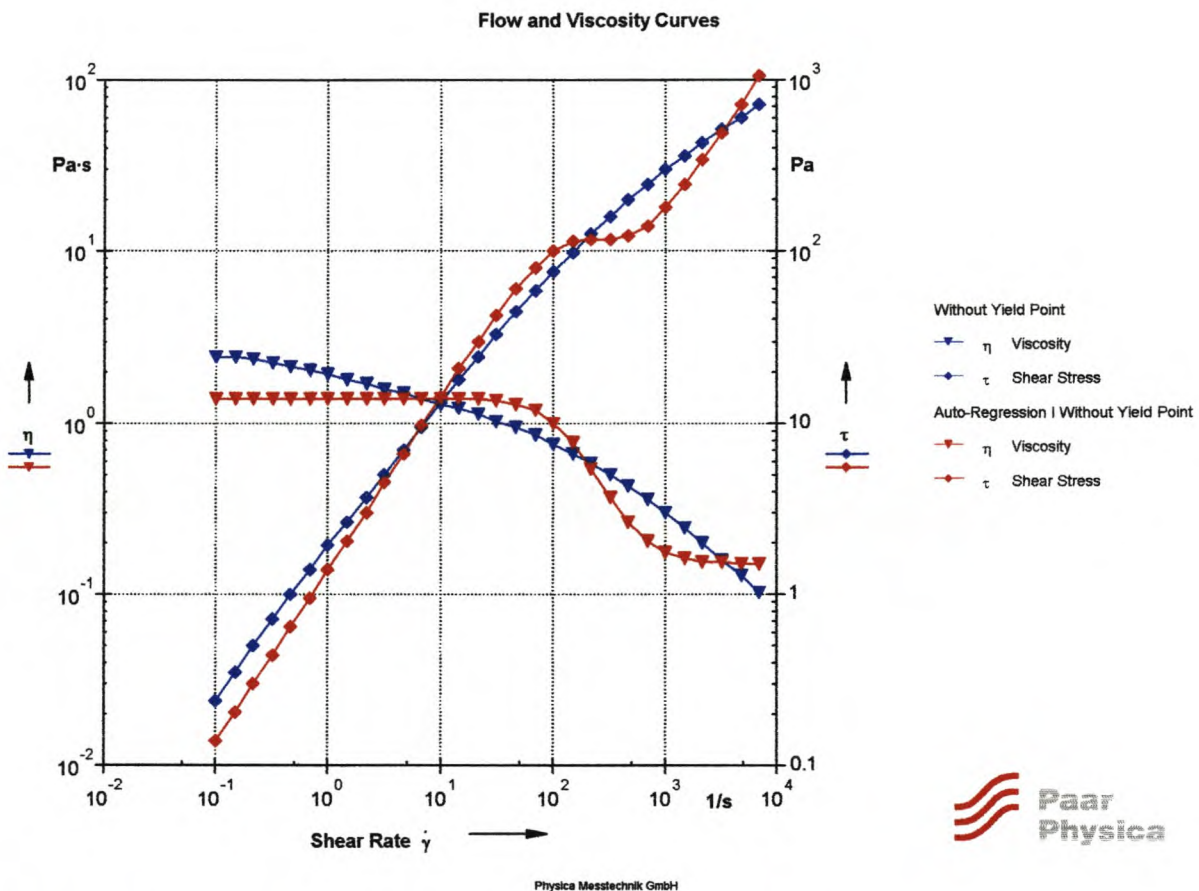


Figure 8-8: Philips-Deutsch model fit for paint without a yield point

It is clear from Figure 8-8 that this model does not fit well, especially in the high and low shear-rate range. This model is developed specifically for substances with zero and infinite shear viscosities. As was mentioned earlier, these types of models are not ideal for substances without infinite shear

viscosities such as paint. The model does not fit well and therefore the model parameters are not given.

8.2 Approximation Functions for Flow and Viscosity Curves of Dispersions

As observed from the previous model fittings, dispersions are unlikely to show zero-shear viscosities (η_0) or infinite shear viscosities (η_∞) but are more likely to show shear-thinning behaviour. Therefore, the model mentioned in section 8.3.1, the Ostwald/de Waal (power-law model), was fitted initially to a dispersion of vesiculated beads. A model for the standard vesiculated beads⁹ was determined so that the model can predict the flow properties.

8.2.1 The Ostwald/de Waal Model for Vesiculated Beads Dispersion

The model fit to the flow and viscosity curves is given in Figure 8-9 below.

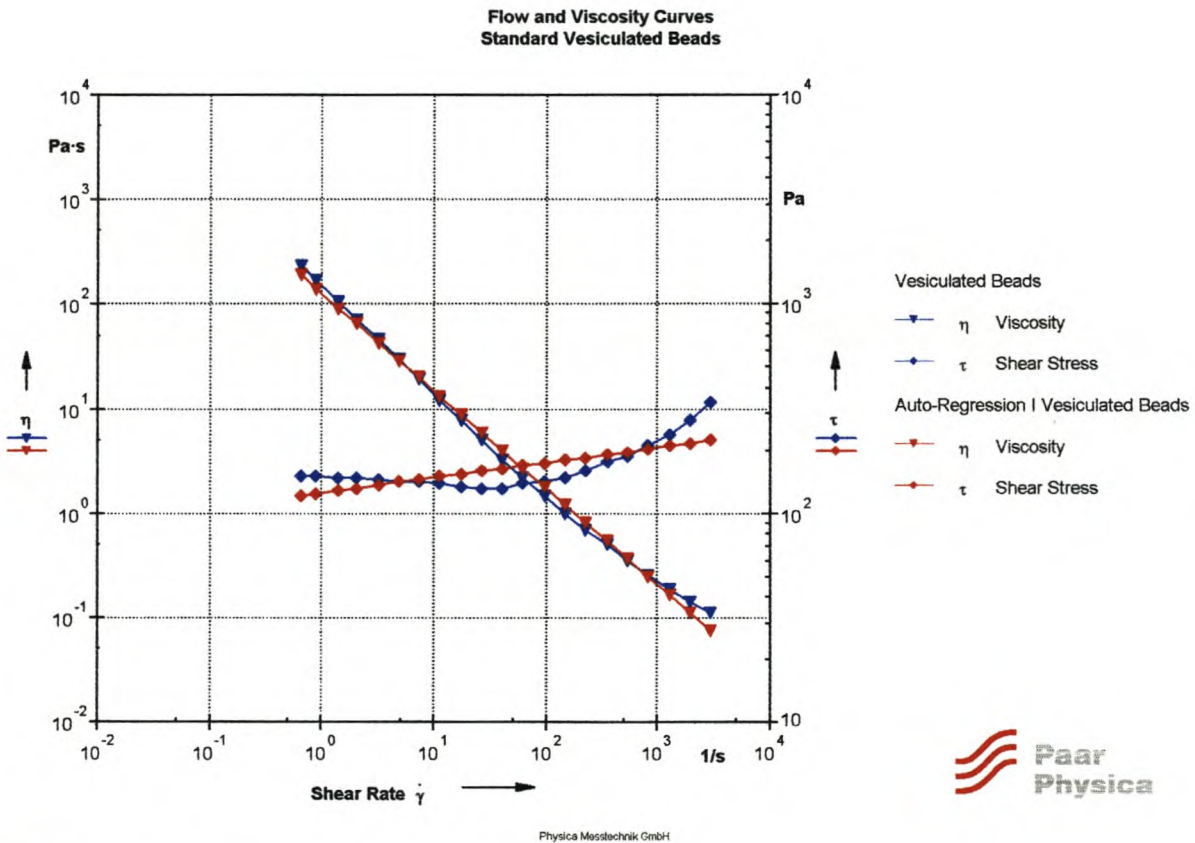


Figure 8-9: Ostwald / de Waal model-fit

⁹ Physical and chemical character of standard vesiculated beads are given in Appendix D.1 – Standard Vesiculated Beads

Figure 8-9 reveals that the Ostwald / de Waal model does not fit ideally for the flow and viscosity curves, with a correlation ratio of only 0.729. The flow curve illustrates that the behaviour is very much like that of a substance with a yield point (see section 8.1.2) and therefore a model that is known to fit flow curves that illustrates yield points, the Casson model, is also examined.

8.2.2 The Casson Model for Vesicated Beads Dispersion

The model fit to the flow and viscosity curves is given in Figure 8-10 below.

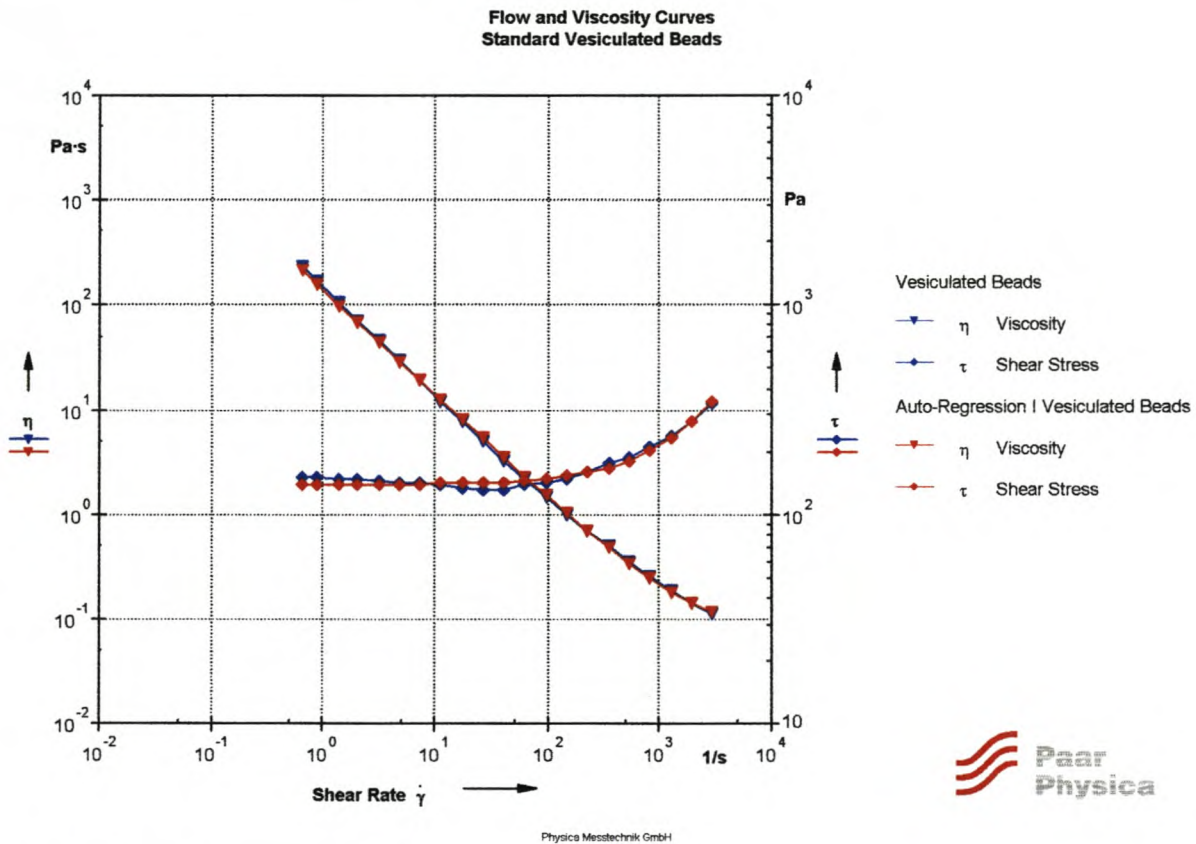


Figure 8-10: The Casson model fit

Figure 8-10 illustrates a very good fit and an improvement on the Ostwald/de Waal model. The Casson model (equation 8-2) and parameters fitted to the flow curve of the standard vesicated beads are as follows:

Casson model:
$$\tau^p = \tau_c + (\eta_c \dot{\gamma})^p$$

Parameters:

- τ_c = 90 Pa
- η_c = 0.07 Pa.s
- p = 1.09 (p > 1 for shear-thinning)
- correlation ratio = 0.982
- infinite-shear viscosity = 0.062 Pa.s

It can be seen that the Casson model fits well according to the correlation ratio of 0.982.

8.2.3 The Herschel-Bulkley Model for Vesiculated Beads Dispersion

The model fit to the flow and viscosity curves is given in Figure 8-11 below.

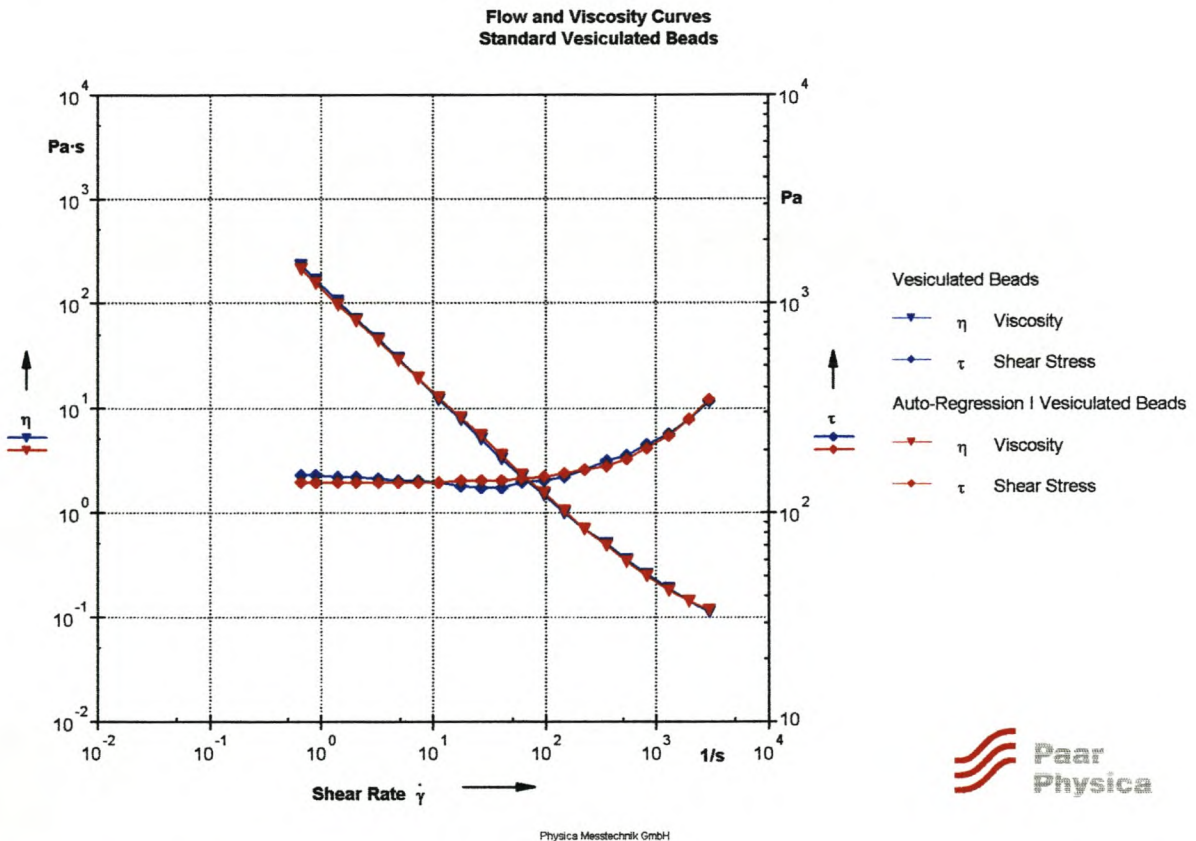


Figure 8-11: The Herschel-Bulkley model fit

Figure 8-11 also illustrates a very good fit and an improvement on the Ostwald/de Waal model for. The Herschel-Bulkley model (equation 8-3) and parameters fitted to the flow curve of the standard vesiculated beads are as follows:

Model:
$$\tau = \tau_{HB} + c\dot{\gamma}^p$$

Parameters:

- τ_{HB} = 139 Pa
- c = 0.13
- p = 0.91 (p < 1 for shear-thinning)
- correlation ratio = 0.982

Once again, the Herschel-Bulkley model fits equally well with a correlation ratio of 0.982.

The Bingham model is not tested due to its inaccuracy.

8.3 Paint Modelling - Simple Linear Regression

8.3.1 Background

A new way of making paint, Paint X, involving a so-called dispersion process, was studied in terms of certain paint properties by De Wet-Roos [2000]. The rheological behaviour of the paint were one of these properties, however; it must be stated that the rheological modelling did not form the central part of the modelling process. The high, intermediate and low levels of the factors were varied in the statistical design in order to identify the relative importance of the four variables used. These variables are given in Table 8-3.

Table 8-3: Factor levels for Paint X

Ingredient	Variable ID	High Value [g]	Intermediate [g]	Low Value [g]
Pigment	X ₁	219.01	182.56	146.05
Extender	X ₂	215.29	179.41	143.53
Emulsion	X ₃	395.08	329.23	263.38
Opacifier	X ₄	83.85	69.88	55.90

A three-level fractional design was used (see Appendix D.5 – Paint X formulation)

The objective of this study was to model the effect of variation of the ingredients mentioned in Table 8-3 on the following rheological characteristics:

- Yield point;
- Behaviour of Paint X in the LVER.

Previous modelling on Paint X has been done by De Wet-Roos [2000] and Van Wyk [2002]. This was, however, mostly done on physical properties of the paint such as gloss, chemical resistance, film thickness, scrub resistance, etc. Rheological modelling only included modelling of the viscosity. Modelling techniques investigated by De Wet-Roos [2000] are as follows:

- Fuzzy logic (FZ)
- Multiple linear regression (MLR)

Van Wyk [2002] investigated paint modelling with the following non-linear techniques:

- Genetic programming (GP)
- Neural network analysis (NN)

The accuracy of the modelling techniques used by De Wet-Roos and Van Wyk are compared in the following graph in terms of viscosity data.

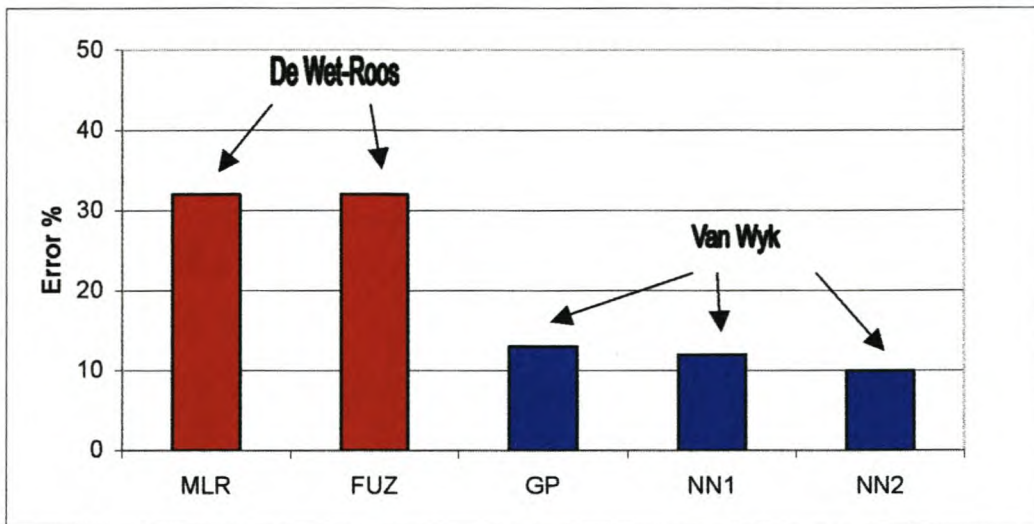


Figure 8-12: Error % for modelling of viscosity data by means of different modelling techniques (MLR – Multiple Linear Regression, FUZ – Fuzzy Logic, GP – Genetic Programming NN – Neural Network)

Very good regression results were obtained by Van Wyk [2002] with the genetic programming (GP) and neural network techniques (NN1 and NN2). The viscosity behaviour could be predicted with less than 20% average error and for some models even less than 10% average error, which is a large improvement on the fuzzy logic (FL) and multiple linear regression (MLR) techniques investigated by De Wet-Roos [2000], with average errors larger than 30%.

However, in this study, the simple linear regression technique will be used as a *first* approximation of the rheological data, although Van Wyk [2002] has indicated that genetic programming and neural network techniques seem to model the behaviour of Paint X more accurately.

8.3.2 Regression Model

The type of regression model used is the so-called *simple linear regression* model in which a constant and a slope are derived to fit a line of experimental data. The same principles operating for a simple linear regression model can be extended to larger models and non-linear models; however, this did not form part of this study. The basic equation used in the modelling approach is given by equation 8-7.

$$Y = a_0 + a_1X_1 + a_2X_2 + a_3X_3 + a_4X_4 + \varepsilon \tag{8-7}$$

In equation 8-7 a_0 is a constant and the variables in the equation (X_i) are scaled by means of regression coefficients ($a_i, i=1,2,3,4$) that represent the contribution of each variable to the output being modelled. The aim is to determine the regression coefficients, a_i , and to obtain the correlation coefficient¹⁰ (σ) by minimizing the error term, ε . This was carried out by the use of Matlab (see Appendix D – Matlab Program).

8.3.3 Modelling the Yield Point of Paint X

The following figure illustrates the correlation obtained between the actual and predicted yield points.

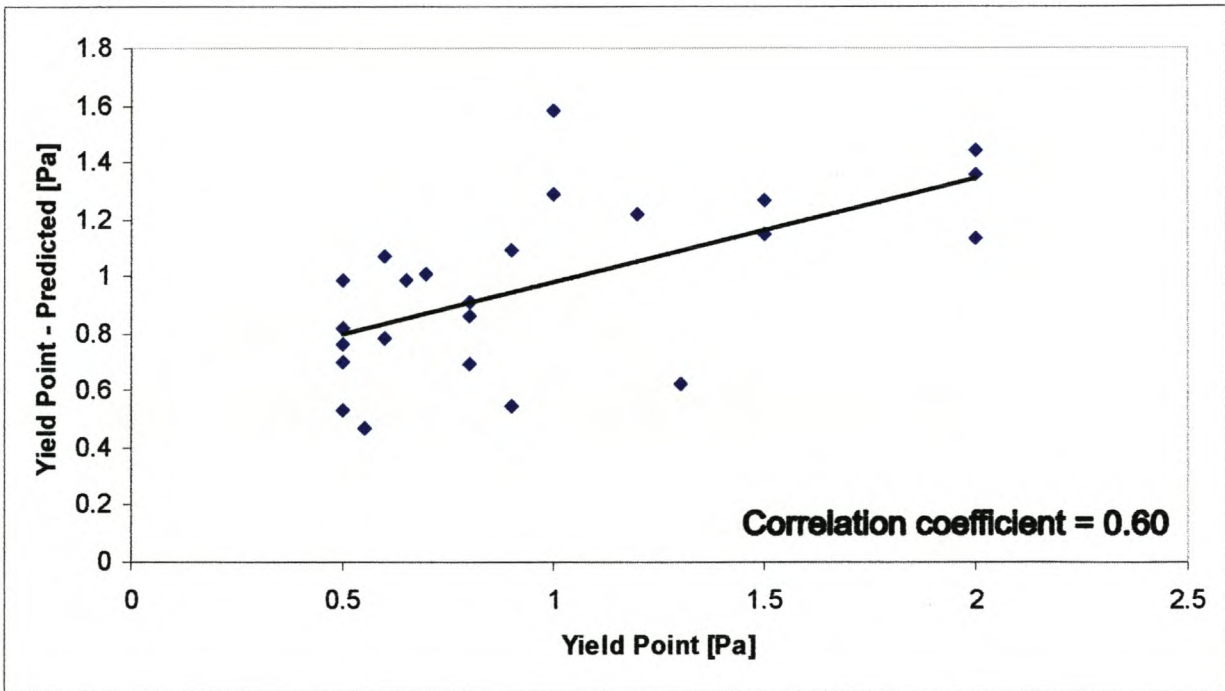


Figure 8-13: Modelled yield point data for paint X

$$^{10} \sigma = \frac{\sum(x_i - x_{mean})(y_i - y_{mean})}{\sqrt{\sum(x_i - x_{mean})^2} \cdot \sqrt{\sum(y_i - y_{mean})^2}}$$

It can be seen that a correlation coefficient of 0.60 is obtained between the predicted and actual yield points. Therefore, the simple linear regression model results in a relative low correlation between the predicted and actual yield points.

The following table illustrates the regression coefficients, a_i .

Table 8-4: Regression coefficients for simple linear regression model for predicting the yield points

Regression coefficients:	Value [-]	95% Confidence Level (Upper)	95% Confidence Level (Lower)
a_1 :	- 0.00602	0.00064	-0.01268
a_2 :	- 0.00840	-0.00190	-0.01490
a_3 :	0.00014	0.00353	-0.00326
a_4 :	0.01050	0.02748	-0.00657

It can be seen that the yield point is mainly affected by the variation in the level of the opacifier (variable X_4), while variation in the levels of the emulsion (variable X_3) barely affects the yield point behaviour.

8.3.4 Modelling the Behaviour of Paint X in the LVER

The cross-over point ($G' = G''$) in the LVER (see Appendix B – Typical rheological behaviour of coatings) for a paint is of great importance. It can either be examined in terms of the stress [Pa] or frequency [Hz] values.

The following figures illustrate the correlations obtained between the actual and predicted cross-over points, expressed in terms of stress (Figure 8-14) and frequency (Figure 8-15) values.

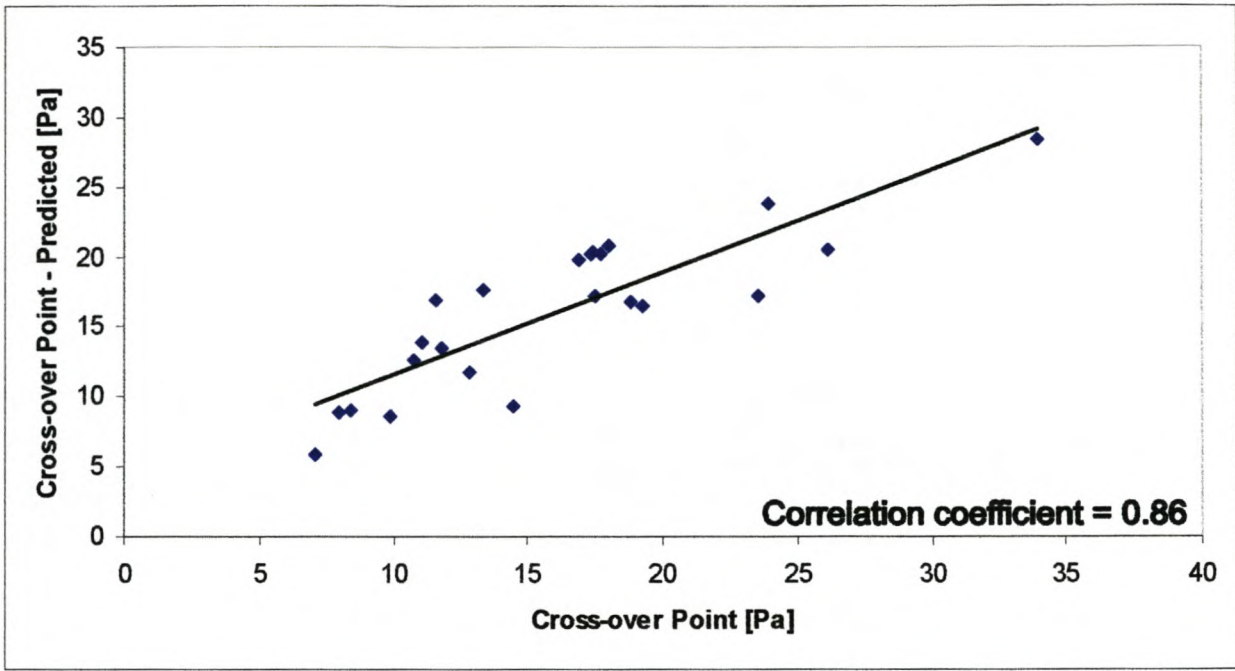


Figure 8-14: Modelled cross-over point (in terms of stress) for paint X

It can be seen that a correlation coefficient of 0.86 is obtained between the predicted and actual stress-related cross-over points. Therefore, the simple linear regression model models the data relatively accurately.

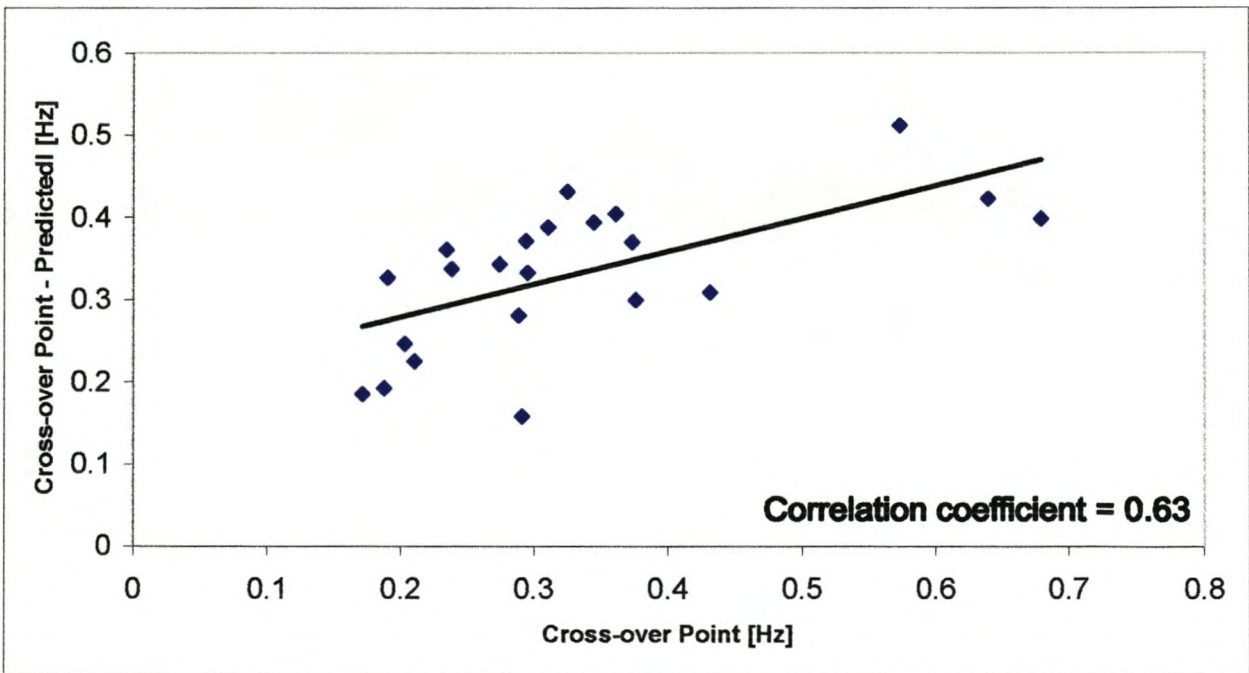


Figure 8-15: Modelled cross-over point (in terms of frequency) for paint X

It can be seen that a correlation coefficient of 0.63 is obtained between the predicted and actual frequency-related cross-over points. Therefore, the simple linear regression model results in a relative low correlation between the predicted and actual cross-over points.

The following table gives the regression coefficients for both the stress- and frequency-related cross-over points, as modelled by the simple linear regression model.

Table 8-5: Regression coefficients for simple linear regression model for predicting the cross-over point for paint X

Regression coefficients:	For stress-related cross-over points [-]	95% Confidence Level (Upper)	95% Confidence Level (Lower)	For frequency-related cross-over points [-]	95% Confidence Level (Upper)	95% Confidence Level (Lower)
a ₁ :	-0.0487	0.0069	-0.1043	-0.0014	0.0004	-0.0033
a ₂ :	-0.1306	-0.0735	-0.1876	-0.0005	0.0014	-0.0025
a ₃ :	-0.0733	-0.0461	-0.1084	-0.0012	-0.0002	-0.0022
a ₄ :	-0.1071	0.0371	-0.2513	-0.0033	0.0016	-0.0082

From Table 8-5 it can be seen that variations in the level of the extender (variable X₂) is modelled to affect the stress-related cross-over point the most of all the variables, followed by the variations in the level of opacifier (variable X₄). The frequency-related cross-over point is affected the most by variations in the level of the opacifier (variable X₄).

8.4 Conclusions

8.4.1 Modelling of Paints

- Paints show different types of flow behaviour that can be modelled as:
 - Shear thinning with a very definite yield point;
 - Shear-thinning;
 - Without a yield point.

- Paints that are shear-thinning *with a yield point* can be modelled with the following models:
 - Herschel-Bulkley with Herschel-Bulkley yield point, τ_{HB} ;
 - Bingham model with Bingham yield point, τ_B ;
 - Casson model with Casson yield point, τ_C .
- The Casson and Herschel-Bulkley models fit well to the paint ‘with a yield point’; however, the predicted yield points differ significantly. The amplitude sweep indicates that the Casson model predicts the yield point most accurately.
- Paints with shear-thinning behaviour can be accurately modelled (correlation ratio = 0.998) with the Ostwald / de Waal model (power-law model) to give an indication of the shear-thinning behaviour.
- Paints with no apparent yield point can be accurately modelled by the Cross model, while the Philips-Deutsch model seems to be inaccurate.
- Model-fitting can be made easier by first determining what type of flow behaviour exists.
- Paint can be modelled accurately by existing models.

8.4.2 Modelling of Vesicated Beads Dispersion

- The vesicated beads dispersion is modelled better as a fluid that is shear-thinning with a yield point (Casson and Herschel-Bulkley models) than as a fluid that is only shear-thinning (Ostwald / de Waal model).
- The Ostwald / de Waal model is derived to be able to predict shear-thinning behaviour but not low- or high-shear viscosity data and therefore cannot predict the yield point for the vesicated beads.
- The vesicated beads dispersion can be modelled accurately by existing models.

8.4.3 Simple Linear Regression Model for Modelling of Certain Rheological Behaviour of a Paint

- The following table illustrates the accuracy of the simple linear regression model for modelling of the behaviour of paint in the LVER.

Table 8-6: Correlation coefficients for simple linear regression modelling for behaviour of a paint in the LVER

Property:	Correlation coefficient [-]:
Yield Point:	0.60
Cross-over point (stress-related):	0.86
Cross-over point (frequency-related):	0.63

From Table 8-6 it can be seen that the simple linear regression technique results in correlation coefficients between 0.60 and 0.86, which are still not entirely acceptable. Therefore, the simple linear regression model only gives a rough idea of the actual data and one should consider other models such as the genetic programming and neural network models which have been proven by Van Wyk [2002] to be more accurate in predicting the paint properties.

- Variations in the level of opacifier (OP 96) affect the yield point behaviour of paint X the most.
- Variations in the level of extender pigment (Steabright) affect the cross-over point of paint X in the LVER the most, followed by variations in the level of opacifier (OP 96).

Chapter 9

Conclusions and Recommendations

9.1 Conclusions

The paint industry is highly dependent on the flow and deformation properties of the final coating. It has been observed throughout this study that rheology/rheometry can be used as a valuable tool to investigate the process of paint manufacturing as a whole. Rheological investigation included starting right at the beginning of the paint manufacturing process (raw materials) and ending in the prediction of paint properties (modelling). Rheological techniques were used successfully in the following areas of the paint manufacturing process:

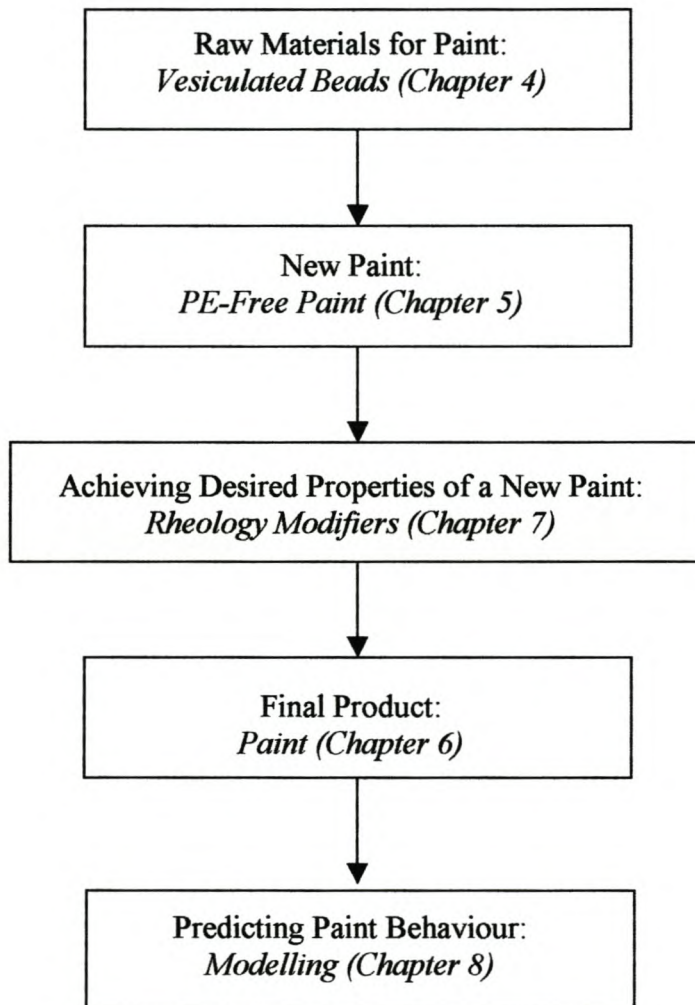


Figure 9-1: Rheology in the paint manufacturing process

The following can therefore be concluded from this study:

- Rheology can be used successfully to obtain the desired flow and deformation properties of the final coating by:
 - i. investigating the character of the paint;
 - ii. simulating actual processes in the coatings industry.

- Rheometry can be used in various aspects of the coating industry, ranging from process optimisation to quality control and was found to form an essential part of the coatings industry.

9.2 Recommendations

The following is the most important recommendation that can be made:

- Rheology in the coatings industry in South Africa seems to be less influential than some other aspects. Whether this is due to the lack of knowledge or expertise or due to resistance from paint manufacturers to 'trust' new measurement techniques is not entirely clear; however, it is evident from this study that valuable information *is* obtainable from rheological measurements.

It is therefore recommended for some sort of awareness campaign to be implemented, stressing the benefits of rheological measurements in the coating industry, starting off by making rheological measurements and interpretation of the data more user-friendly.

Chapter 10 Future Work

- This study has shown how rheology can be used as a valuable method for quality control for some of the most important physical processes which take place before, during and after the paint application process. However, rheology as quality control is a relatively new concept in the paint industry, with the development of new test methods being just as fast as the development of new technology in rheometry. Therefore it is not possible for every paint chemist to be a rheologist as well and, as a result, rheology is not yet used as a standard test method for quality control.

It should therefore be an aim to standardise rheological test methods for quality control with the outlined methods for interpretation of the rheological data to make rheology more accessible and user-friendly.

- It is apparent that there are an ever-increasing number of rheological parameters that can be used for rheological characterisation in the paint industry. The correlation between all these parameters and other existing parameters have not yet been fully developed. In other words, there seems to be a lack of a mathematical model that makes use of rheological/other parameters in the paint industry to model paint even more accurately.

Hence, it appears that there is room for further research in the field of rheological modelling of paint properties, which will aim to model rheological properties with modelling techniques such as neural networks, amongst others. This type of research seems fit for a PhD project.

References

- Barnes, H.A., *Measuring the viscosity of large particle (and flocculated) suspensions - a note on the necessary gap size of rotational viscometers*. Journal of non-Newtonian Fluid Mechanics, 2000. **94**(2): p. 213-217.
- Barnes, H.A., Hutton, J.F., Walters, K., *An introduction to rheology*. Rheology, Series 3. 1989: Elsevier: Ch. 1 - 7.
- Busato, F., *Coatings of the world*. 2001, Irfab Chemical Consultants: Brussels.
- Chander, S., *Challenges in characterisation of concentrated suspensions*. Colloids and surfaces, 1997. **133**: p. 143-150.
- Chiu, S., Pong, S., *Development of an on-line twin capillary rheometer*. Polymer degradation and stability, 1998. **64**.
- Coates, R.H., Gillan, J., *Process of preparing vesiculated polyester resin granules*, Patent Number: US4089819. 1978.
- Cohu, O., Magnin, A., *The levelling of thixotropic coatings*. Progress in Organic Coatings, 1994. **28**: p. 89-96.
- Eidam, D., *Using paints - Application and rheology*. Rheometer, 1997.
- Ferguson, J., Kemblowski, Z., *Applied fluid rheology*. 1991: Elsevier Science Publishers: p. 9 - 13.
- Ferry, J.D., *Viscoelastic properties of polymers*. 1980, New York: John Wiley and Sons: Ch. 4.
- Galvin, G.D., Hutton, J.F., Jones, B., *Development of a high-pressure, high-shear-rate capillary viscometer*. Journal of Non-Newtonian Fluid Mechanics, 1981. **8**: p. 11-28.
- Geoffrey, W., Hodge, J., *Bead polymerisation process*, Patent Number: US4363888. 1982: United states of America.
- Glass, J.E., *Adsorption of hydrophobically-modified, ethoxylated urethan thickeners on latex and titanium dioxide disperse phases*. Advances in colloid and interface science, 1999. **19**: p. 123-148.
- Gous, K., *Continuous processing of vesiculated beads*, MSc Ing Thesis, Department of Chemical Engineering. University of Stellenbosch, 2002.
- Gray, J.B., *Mixing theory and practice*, ed. V.W. Uhl. Vol. III. 1986. Ch. 7
- Gunning, R.H., *Process for making porous polyester granules*, Patent Number: US3923704. 1975.
- Gunning, R.H., Lubbock, F.J., *Process for making porous polyester granules*, Patent Number: US3891577. 1975.
- Gupta, R.K., *Polymer and composite rheology*. Second Edition ed. 2000. p. 225 - 262

- Howard, P.R., Leasure, E.D., Rosier, S.T., *Formulating with combinations of HEUR Associative Thickener*. Journal of Coatings Technology, 1992. **64**(804).
- Karickhoff, M., *Polymeric thickeners and coatings containing the same thickeners*, Patent Number: US4464524. 1984: United States of America.
- Kastner, U., *The impact of rheological modifiers on water-borne coatings*. Colloids and Surfaces, 2001. **183**: p. 805-821.
- Kestin, J., Sokolov, M., Wakeham, W., *Theory of capillary viscometers*. Applied Scientific Research, 1973. **27**: p. 241-264.
- Kiratzis, N., Faers, M., Luckham, P.F., *Depletion flocculation of particulate systems induced by HEC*. Colloids and Surfaces, 1998. **151**(3): p. 461-471.
- Kiratzis, N.E., Luckham, P.F., *The rheology of aqueous alumina suspensions in the presence of HEC*. Journal of the European Ceramic Society, 1999. **19**(15): p. 2605-2612.
- Knoef, A.J.M., Slingerland, H., *Urethane-based polymeric thickeners for aqueous coatings systems*. Water-borne Coatings, 1992. **9**.
- Kraus, S.S., Johnson, E.A., *The issue of compatibility between dispersants and associative thickeners*. Brush Strokes, 2001. **III**(I).
- Langenbacher, G., *Operating manual for US 200*. 2001: Stuttgart, Germany.
- Larson, R.G., *The structure and rheology of complex fluids*, ed. K.E. Gubbins. 2000, New York: Oxford University Press. p. 263 - 279.
- Lauger, J., Wollny, K., *New rheological test methods to simulate the processing of paper coatings*, *Physica*. 2001.
- Liang, W., Tadros, T.F., Luckham, P.F., *Investigations of depletion flocculation of concentrated sterically stabilised latex dispersions using viscous-elastic measurements and microscopy*. Journal of colloid and interface science, 1992. **158**: p. 152-158.
- Liang, W., Tadros, T.F., Luckham, P.F., *Rheological properties of concentrated sterically stabilised latex dispersions in the presence of HEC*. Journal of colloid and interface science, 1993. **160**.
- Liang, W., Tadros, T.H., Luckham, P.F., *Rheological studies on concentrated polystyrene latex sterically stabilised by poly(ethylene oxide) chains*. Journal of colloid and interface science, 1992. **153**(1).
- Liang, W., Tadros, T.H., Luckham, P.F., *Effect of volume fraction and particle size on depletion flocculation of sterically stabilised latex dispersion induced by addition of poly(ethylene oxide)*. Journal of colloid and interface science, 1992. **155**: p. 156-164.
- Macosko, C.W., *Rheology principles, measurements and applications*. 1993, New York: VCH Publishers, Inc. p. 425 - 470.

- Mewis, J., Vermant, J., *Rheology of sterically stabilised dispersions and latices*. Progress in organic coatings, 2000. **40**: p. 111-117.
- Mezger, T., *Quality Assurance - Rheological testing of the sagging behaviour of coatings*, *Physica Application Note - Rheology*. 1998.
- Mezger, T., *Rheological measurement for the simulation of process engineering techniques for paints*, *Physica Application Note - Rheology*. 1999.
- Mezger, T., *Thixotropic behaviour of paints and coatings*, *Physica application report*. 1999.
- Mezger, T., *The consistency of new and used offset ink*, *Physica Application Note - Rheology*. 2000.
- Mezger, T., *The rheology handbook*, ed. U. Zorll. 2002: Hannoprint. Ch. 1 - 11.
- Mezger, T., Lauger, J., *New rheological possibilities: Advantages for application technology*. Physica, 1998.
- Mezger, T., Lauger, J., *New techniques for paint and coating applications*, *Physica*. 1998.
- Mezger, T., Lauger, J., *Rheological characterisation of paper coatings*, *Physica Application Note - Rheology*. 1999.
- Murakami, T., Fernando, R.H., Glass, J.E., *The influence of hydrophobically modified, alkali-swellaable emulsions on the rheology of pigmented coatings*. Journal of oil and colour chemists' association, 1995.
- Nisogi, H., Bousfield, D.W., Le Poutre, P.F., *Influence of coating rheology on final coating properties*. Tappi Journal, 2000. **83**(2).
- Nommensen, P.A., Duits, M.H.G., Van den Ende, D., Mellema, J., *Probing the properties of grafted polymer layers on colloids by visco-elastic measurements*. 1999, Department of applied physics, University of Twente: Enschede.
- Nommensen, P.A., Duits, M.H.G., Van den Ende, H.T.M., Mellema, J., *Steady shear behaviour of polymerically stabilised suspensions: Experiments and lubrication based modeling*. 1999, University of Twente: Twente.
- Perez-Trejo, L., Perez-Gonzalez, J., De Vargas, L., *About the determination of steady state flow for polymer melts in capillary rheometers*. Polymer testing, 2001. **20**: p. 523-531.
- Perrins, N., Kelly, M.E., *Vesiculated Polymer Beads*, Patent Number: EP0622402. 1994.
- Prideaux, J., *Rheology modifiers and thickeners in aqueous paints*. Journal of the oil and colour chemists' association, 1993.
- Ritchie, P., *Spindrift pigmented vesiculated beads*, Surface coatings, raw materials and their usage. 1993, Chapman & Hall: London. p. 351-355.
- Rohm&Haas, *Additives for coatings*. 1996, Rohm and Haas Data Sheets.
- Schram, G., *A practical approach to rheology and rheometry*, HAAKE, 1994. p. 114 - 117.

- Sikorski, U.A., Lofstrom, J.R., Smith, P.M., Hesler, K.K., *Opacification of paint*, Patent Number: EP0113435. 1984: U.S.A.
- Tadros, T.F., *Control of the properties of suspension*. Journal of colloid surfaces, 1986. **18**.
- Tafigel, *Rheology Modifiers*. 2001, Munzing Chemie GmbH.
- Terblanche, J.C., *The development of vesiculated beads*, MSc Ing Thesis, Department of Chemical Engineering, University of Stellenbosch, South Africa. 2002: p. 71-77.
- Thorp, S., Von Doren, R.E., Whitton, A.J., *Rheological additives for latex paints*, in *Surface Coatings*. 1993, Chapman & Hall: London.
- Tioxide, *Bead polymerisation process*, Patent Number: EP0451940. 1981.
- Van Wyk, N.P., *Modelling of paint properties*, Final Report 478, Department of Chemical Engineering, University of Stellenbosch, South Africa. 2002: p. 1 - 23.
- Various, *Vesiculated particles, various aspects of manufacture*. 2001, Plascon Research Centre: Stellenbosch.
- Whitton, A.J., Van Doren, R.E., *Formulating with rheological additives for latex paints*. 2001.
- Wollny, K., *Spatte behaviour of coatings, Physica application report*, 2002.

APPENDIX A - Rheology

Rheology

The basic concepts of rheology are defined and discussed in this appendix. This chapter is largely an adaptation of the notes obtained from Thomas Mezger's *The Rheology Handbook*.

A.1. Rheology

Rheology is the science of flow and deformation of matter. The term "rheology" originates from the Greek: "rheos" meaning "the river". Thus, rheology is literally "flow science". However, rheological experiments do not merely reveal information about the flow behaviour of liquids, but also the deformation behaviour of solids.

All forms of shear behaviour can be viewed as lying between two extremes: the flow of ideal viscous liquids on the one hand and the deformation of ideal elastic solids on the other.

Rheometry is the measuring technology used to determine rheological data and includes the measuring systems, instruments and test and analysis methods.

A.2. Flow Behaviour

The Two-Plate-Model (figure A1) is used to define some of the fundamental rheological parameters.

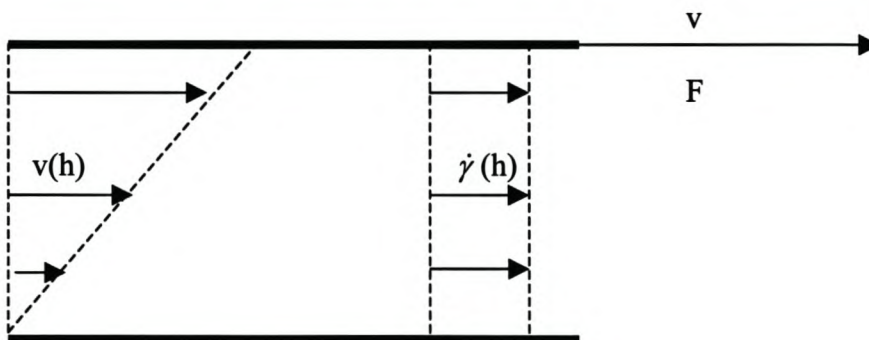


Figure A-1: Two-Plate-Model

The upper plate with the shear area (A) is moved by the shear force (F) and the resulting velocity (v) is measured. The distance (h) is the distance between the plates. The sample is sheared in this gap.

- Shear stress:

$$\tau = \frac{F}{A} \quad (\text{A-1})$$

- Shear rate:

$$\dot{\gamma} = \frac{v}{h} \quad (\text{A-2})$$

- Viscosity:

$$\eta = \frac{\tau}{\dot{\gamma}} \quad (\text{A-3})$$

A.2.1 Ideal Viscous Flow Behaviour

- Ideal liquid:

'A material that will continuously change its shape (will flow) when subjected to a given stress, irrespectively of how small that stress may be' [Barnes et al., 1989].

- Ideal viscous (Newtonian) flow behaviour is formally described by Newton's law:

$$\tau = \frac{\eta}{\dot{\gamma}} \quad (\text{A-4})$$

- The dashpot model:

The dashpot model (figure A-2) is used to illustrate the behaviour of ideal viscous liquids.

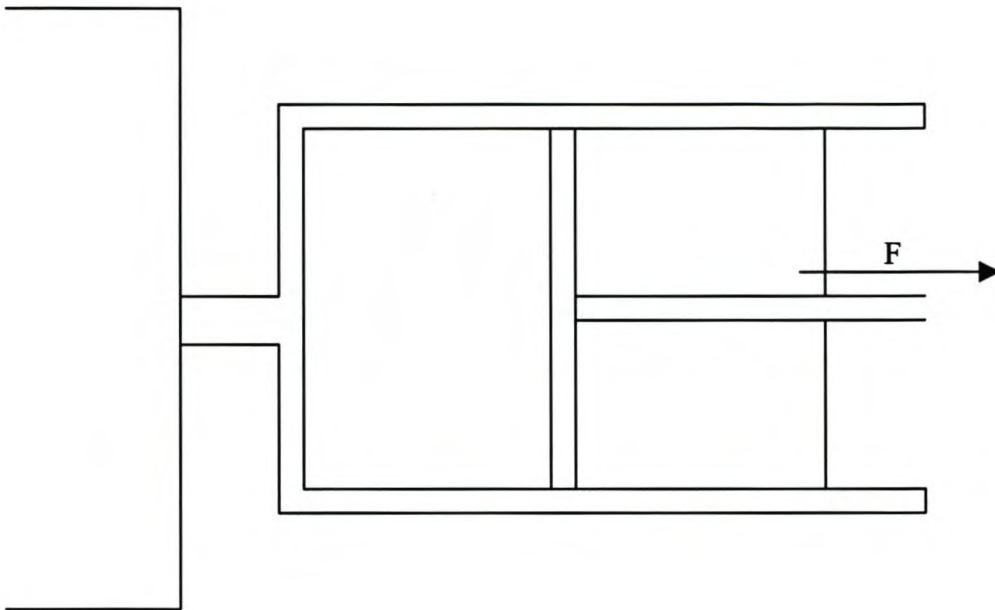


Figure A-2: The dashpot model for ideal viscous liquids

The piston moves continually under the constant shear force (F) as long as the force is supplied. As soon as the shear force is removed, the dashpot stops moving and remains in the position reached. In other words, after a load an ideal viscous fluid entirely remains in the deformed state.

A.2.2 Shear-Thinning/Pseudoplastic Flow Behaviour

For samples that display shear-thinning behaviour, the shear viscosity is dependent on the degree of shear load. The flow curve shows a decreasing curve slope with increasing shear. Shearing causes the particles to orientate themselves in the flow direction and in the direction of the shear gradient.

- Apparent shear viscosity:

If the ratio of shear stress to shear rate varies with the shear rate (non-Newtonian) then such ratios are referred to as apparent viscosity to make it clear that it is different from the constant viscosity of an ideal viscous fluid (Newtonian).

A.2.3 Shear-Thickening Flow Behaviour

The flow curve of a shear-thickening sample shows an increasing curve slope.

A.2.4 Yield Point

Samples with yield points only begin to flow when the external forces acting on the material are larger than the internal structural forces. Below the yield point the material show elastic behaviour.

- Apparent yield point:

Analysis methods for the yield point result in a value that is dependent on the measuring instrument. The value of the apparent yield point is dependent on the speed resolution of the rheometer and therefore apparent yield points are only used for simple quality control tests.

- True yield point:

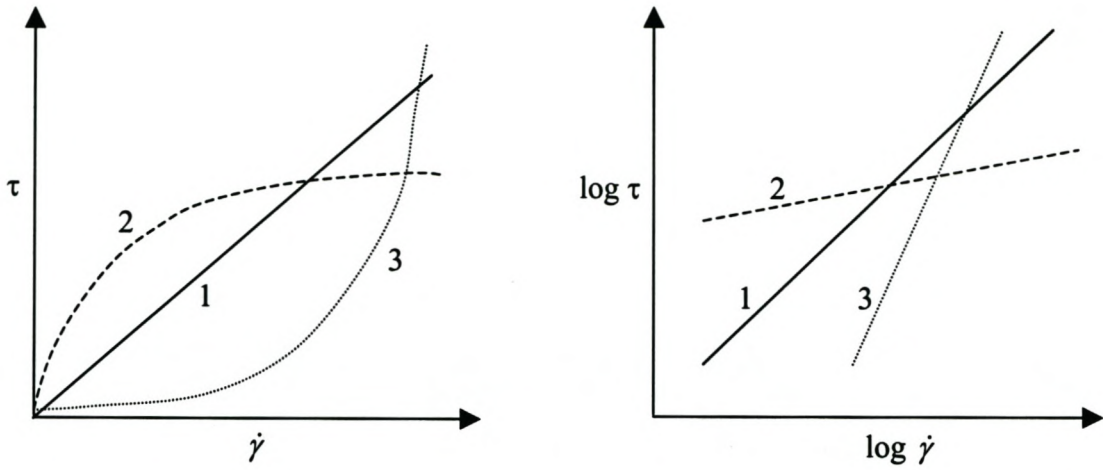
The true yield point is a material constant and is the *one* shear stress value at which point the range of the reversible elastic deformation ends and the range of irreversible viscous/viscoelastic flow begins.

A.2.5 Schematic Summary of Flow Behaviour

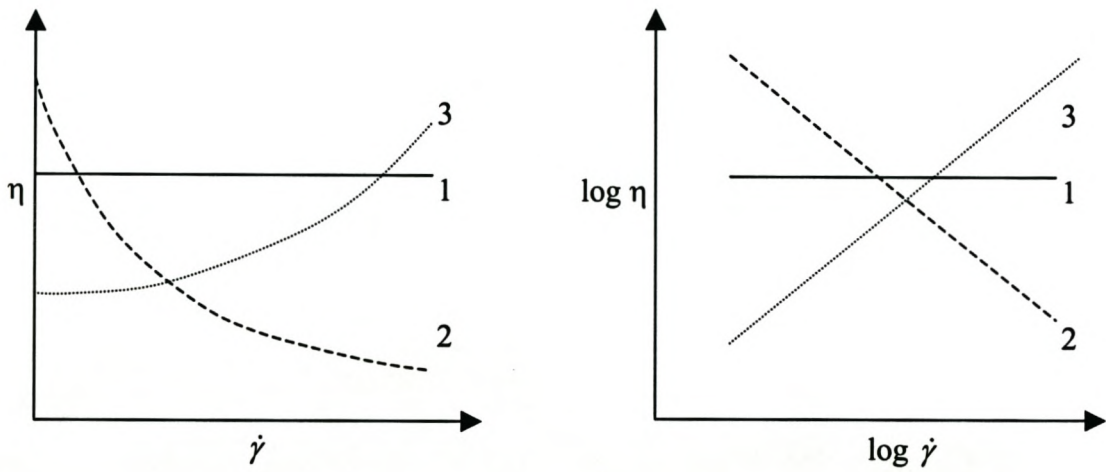
Figure A-3 illustrates the flow and viscosity curves for the behaviour discussed in the previous points.

- (1) Ideal viscous/Newtonian (slope = 1 for flow curve)
- (2) Shear-thinning (slope < 1 for flow curve)
- (3) Shear-thickening (slope > 1 for flow curve)
- (4) No yield point
- (5) With an apparent yield point

Comparison of flow curves:



Comparison of viscosity curves:



Comparison of flow and viscosity curves:

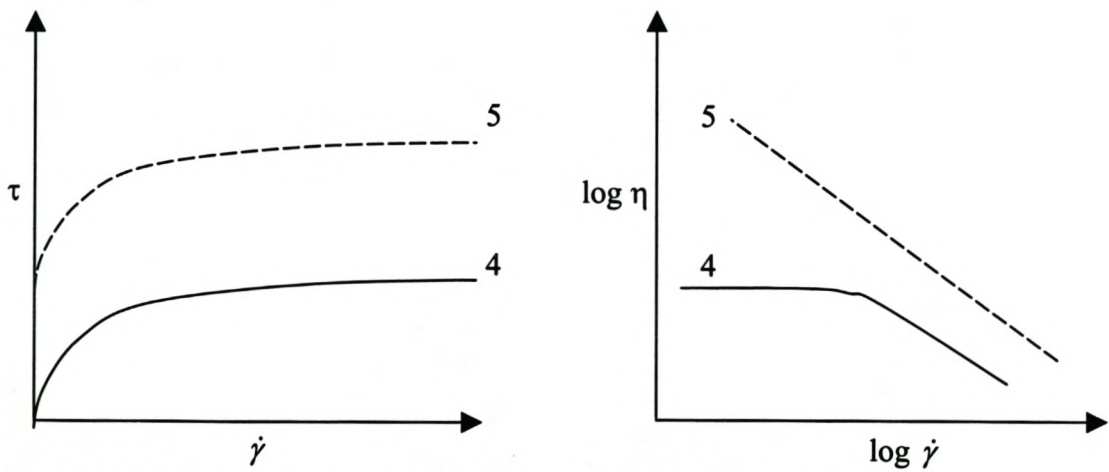


Figure A-3: Possible flow behaviour expressed by flow and viscosity curves

A.2.6 Time-Dependent Flow Behaviour

- Thixotropic behaviour:

Thixotropic behaviour means the reduction in structural strength during the shear load phase and the complete structural regeneration during the subsequent rest phase. Completely reversible structural change has taken place.

- Non-thixotropic behaviour:

A material is non-thixotropic if the initial structural strength does not completely return within an infinitely long period of rest time. Irreversible structural change has taken place.

- Rheopectic behaviour:

An increase in the structural strength during the load phase takes place with a complete decomposition of the increased structural strength during the subsequent period of rest.

A.3. Elastic Behaviour

The Two-Plate-Model (figure A-4) is used again to define some of the fundamental rheological parameters.

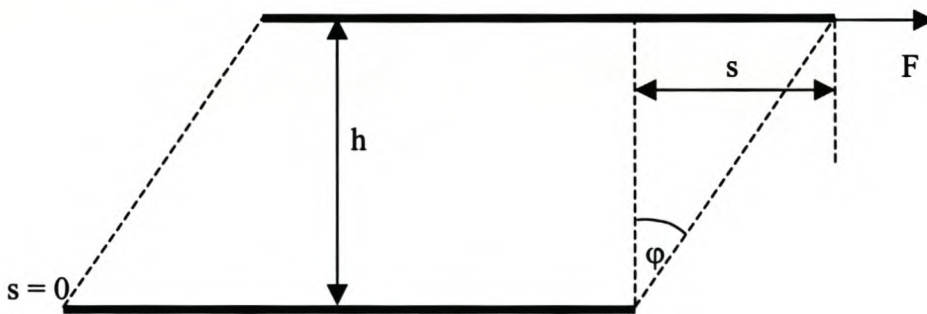


Figure A-4: Two-Plate-Model

The upper plate with the shear area (A) is deflected by the shear force (F) and the extent of the deflection (s) is measured. The distance (h) is the distance between the plates. The sample is sheared in this gap.

- Shear deformation (shear strain):

$$\gamma = \frac{s}{h} \quad (\text{A-5})$$

The shear rate ($\dot{\gamma}$) is the time-dependent rate of deformation.

- Shear modulus:

$$G = \frac{\tau}{\gamma} \quad (\text{A-6})$$

The shear modulus is a material constant and reveals information about the rigidity of the sample.

A.3.1 Ideal Elastic Deformation Behaviour

- Ideal solid:

'A material that will not continuously change its shape when subjected to a given stress'
[Barnes et al., 1989].

- Ideal elastic (Hookean) deformation behaviour is formally described by Hooke's law:

$$\tau = \frac{G}{\gamma} \quad (\text{A-7})$$

- The spring model:

The spring model (figure A-5) is used to illustrate the behaviour of ideal elastic solids.

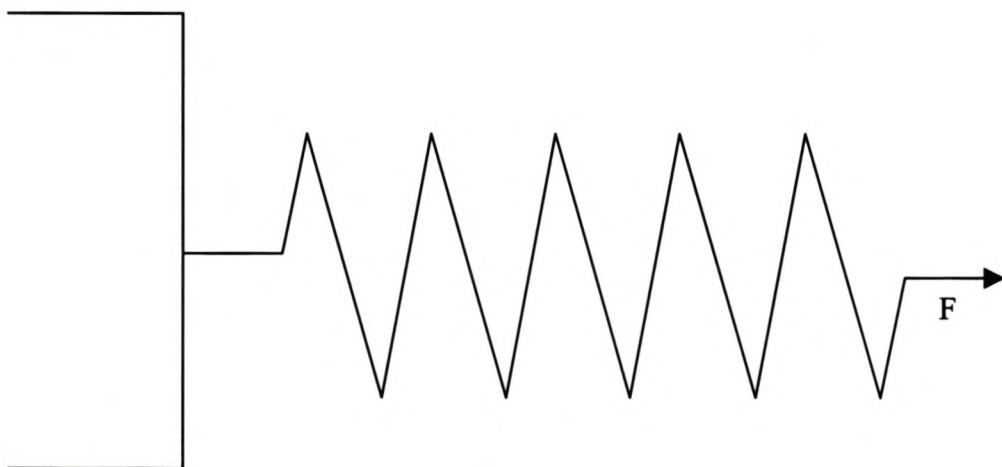


Figure A-5: The spring model for ideal elastic solids

The spring displays immediately the corresponding deformation which remains at a constant value as long as the force is applied. The force and the deflection are proportional and the proportionality factor corresponds to the rigidity of the spring. The spring returns immediately and completely to the initial state as soon as the force is removed. No permanent deformation remains, in contrast to the behaviour of Newtonian liquids (the dashpot model, see A.2.1). In other words, after a load an ideal elastic solid returns completely to its initial state.

A.4. Viscoelastic Behaviour

A viscoelastic material always shows viscous and elastic behaviour simultaneously. The viscous portion behaves according to Newton's law and the elastic portion behaves according to Hooke's law. Viscoelastic materials always display a delayed response when a load is applied and removed.

A.4.1 Viscoelastic Liquids According to Maxwell

- The Maxwell model:

The behaviour of a viscoelastic liquid can be illustrated using the combination of a spring and a dashpot in serial connection. Both components can be deflected independently of each other.

1) Before the load phase:

Both components are undeformed.

2) During the load phase:

- a) As soon as the load is applied, only the spring displays an immediate deformation until it reaches the state of constant deflection, where it remains. Therefore, immediately after the start of the load phase only the spring is deformed.
- b) The dashpot piston then moves continuously under the still acting constant force. After a certain period of time under load, both components show a

certain extent of deformation which corresponds to the degree of the force applied.

3) When the load is removed:

The spring moves back immediately and completely. The dashpot, however, remains deflected.

Therefore, after a load cycle, the sample remains partly deformed. The extent of reformation represents the elastic portion and the extent of permanently remaining deformation corresponds to the viscous portion.

A.4.2 Viscoelastic Behaviour

As mentioned earlier, a viscoelastic material behaves in a viscous and elastic manner simultaneously. The Two-Plate-Model is again used to define some of the fundamental rheological parameters. The upper plate oscillates in a sinusoidal manner. Figure A-6 and A-7 illustrates the response of an ideal liquid and ideal solid in the Two-Plate-Model respectively

i. Ideal viscous behaviour:

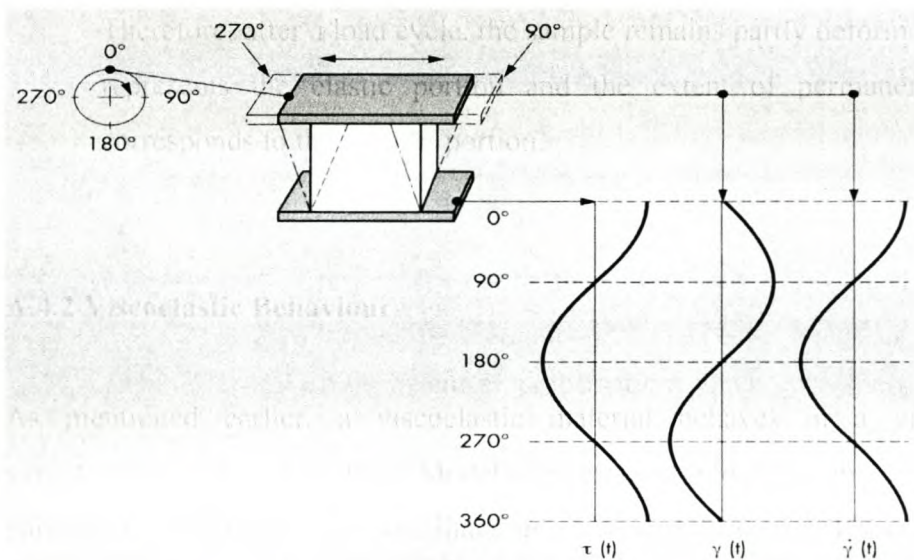


Figure A-6: Viscous behaviour of ideal liquid

For an ideal viscous fluid, Newton's law applies as follows:

$$\tau(t) = \eta^* \dot{\gamma}(t) \tag{A-8}$$

The (*) represents the property measured in the LVER as a result of harmonic-periodic changes. In the LVER the following applies:

$$\eta^* = \frac{\tau(t)}{\dot{\gamma}(t)} = \text{constant} \tag{A-9}$$

Therefore, the $\tau(t)$ curve is always in phase with the $\dot{\gamma}(t)$ curve, both running as cosine curves if the $\gamma(t)$ curve is represented as a sine curve.

For samples showing ideal viscous behaviour, a delay of the $\tau(t)$ curve in relation to the $\gamma(t)$ curve occurs with a phase shift of $\delta = 90^\circ$

ii. Ideal elastic behaviour:

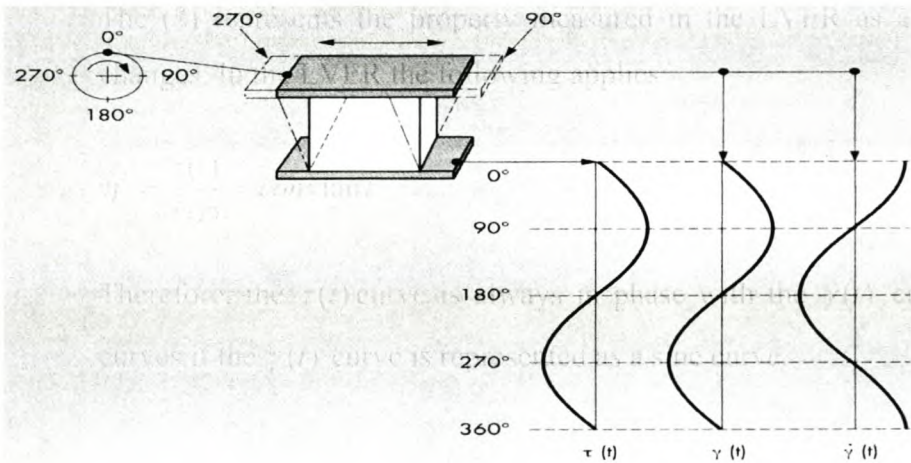


Figure A-7: Elastic behaviour of ideal solid

For an ideal elastic solid, Hooke's law applies as follows:

$$\tau(t) = G^* \gamma(t) \tag{A-10}$$

The (*) represents the rigidity measured in the LVER as a result of harmonic-periodic changes. In the LVER the following applies:

$$G^* = \frac{\tau(t)}{\gamma(t)} = \text{constant} \tag{A-11}$$

Therefore, the $\tau(t)$ curve is always in phase with the $\gamma(t)$ curve, both running as sine curves.

For samples showing ideal elastic behaviour, there is no phase shift between the $\gamma(t)$ and the $\tau(t)$ curves. A phase shift of $\delta = 0^\circ$

A viscoelastic material behaves in a combined manner of the ideal liquid (i) and ideal solid (ii). Therefore preset values of the controlled strain and stress functions will result in behaviour with a phase shift δ ($0^\circ \leq \delta \leq 90^\circ$), also referred to as the loss angle.

The following are terms used to describe viscoelastic behaviour:

- Complex shear modulus:

$$G^* = \frac{\tau(t)}{\gamma(t)} \quad (\text{A-12})$$

- Storage modulus:

$$G' = \frac{\tau(t)}{\gamma(t)} \cos \delta \quad (\text{A-13})$$

- Loss modulus:

$$G'' = \frac{\tau(t)}{\gamma(t)} \sin \delta \quad (\text{A-14})$$

- Loss factor:

$$\tan \delta = \frac{G''}{G'} \quad (\text{A-15})$$

- Complex viscosity:

$$\eta^* = \frac{\tau(t)}{\dot{\gamma}(t)} \quad (\text{A-16})$$

APPENDIX B Typical Rheological Behaviour of Coatings

Rheological Behaviour of Coatings

B.1 Viscosity Profile

Figure B-1 illustrates the typical viscosity profile of a coating.

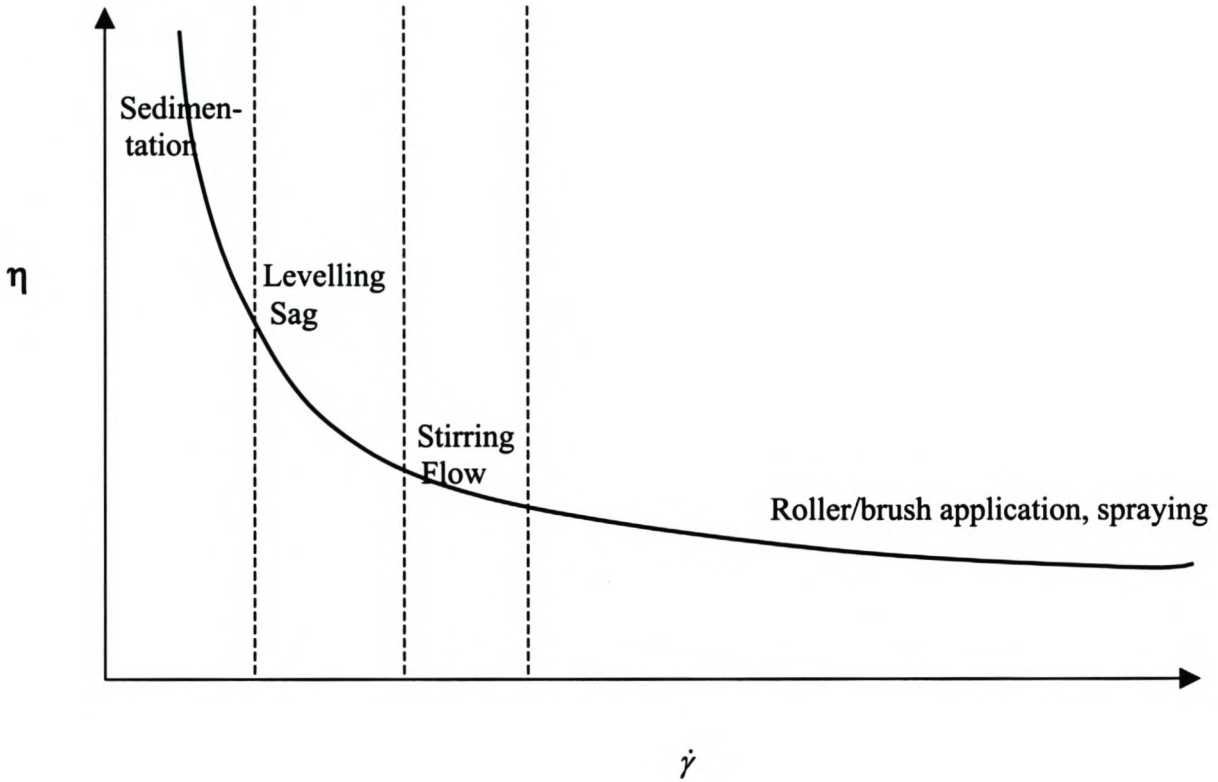


Figure B-1: Viscosity profile

Figure B-1 illustrates the ideal viscosity behaviour for a coating.

Typically, a coating must have a good balance of container viscosity, application viscosity, antissettling properties, spatter resistance and flow and levelling. In practical applications the following information is important concerning the rheological behaviour of a coating:

- Consistency of structure at rest
Practical use – Dispersion stability, long time storability
- Flow behaviour
Practical use – workability

- Time-dependent behaviour directly after sudden change in shear conditions
Practical use – Application behaviour (thixotropy), levelling, sagging, layer thickness, degassing

Typical values for the processes in figure B-1 is given in table B-1 below.

Table B-1: Shear-rate dependent processes

Process:	Shear rate, $\dot{\gamma}$ [s^{-1}]
Sedimentation of particles:	10^{-6} to 10^{-2}
Surface levelling:	10^{-2} to 10^{-1}
Sagging:	10^{-2} to 10^{-1}
Immersing:	10^0 to 10^2
Pipe flow, pumping:	10^0 to 10^3
Mixing, stirring:	10^1 to 10^3
Filling into containers:	10^2 to 10^4
Painting, brushing, spreading:	10^2 to 10^4
Rolling, printing:	10^2 to 10^6
Spraying:	10^3 to 10^6

B.2 Stability of a Coating

The sedimentation stability is a very significant aspect for the judgement of coatings.

B.2.1 Yield Point

The stronger a network of a substance is developed, the lower is the sedimentation tendency of particles. The stronger these solid particles are embedded into the super-structure, the higher the yield point and therefore the higher the stability. The yield point is that point in the G' curve of the amplitude sweep where it deviates from the constant plateau value for G' (see Figure B-2). This value is usually determined by reading off the value from the data tables at a 10% deviation from the G' plateau value.

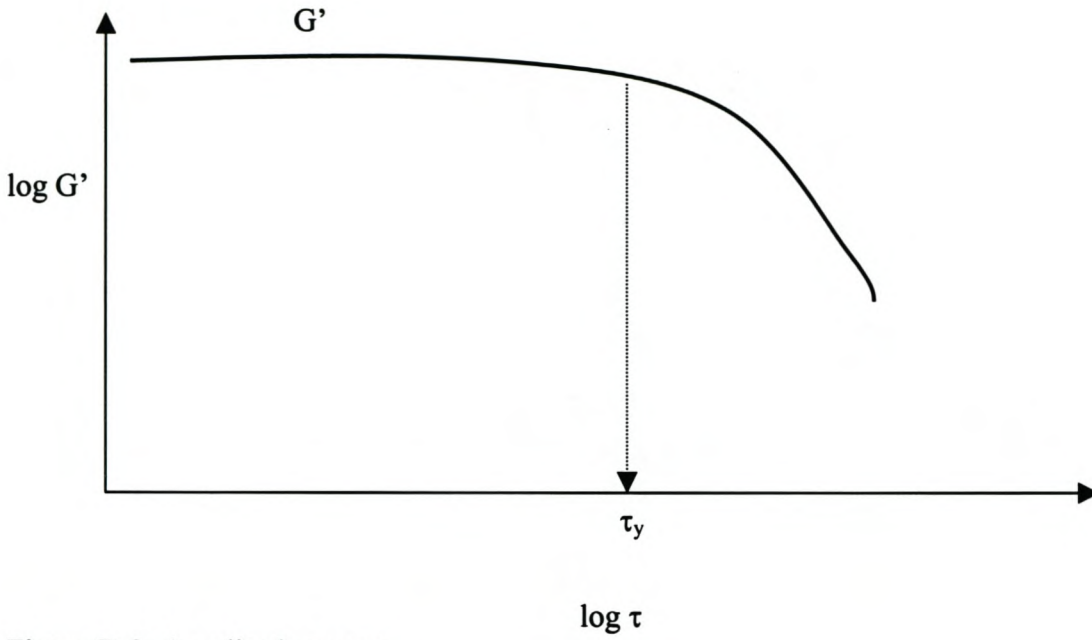


Figure B-2: Amplitude sweep

B.2.2 Storage Modulus G'

The storage modulus stands for the stability of the dispersion thus characterising the internal structure forces. A higher structural strength in rest measured in the LVER provides improved particle compound and counteracts phase separation. The increased stiffness of the superstructure avoids sedimentation processes and is indicated by higher G' values (see Figures B-3 and B-4).

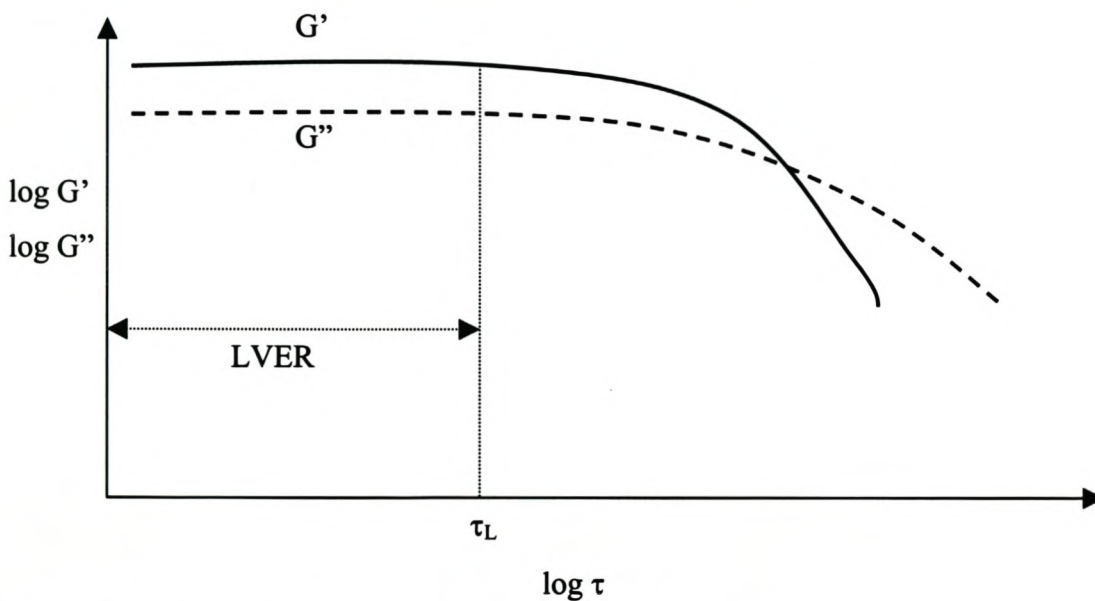


Figure B-3: Amplitude sweep of a stable coating ($G' > G''$)

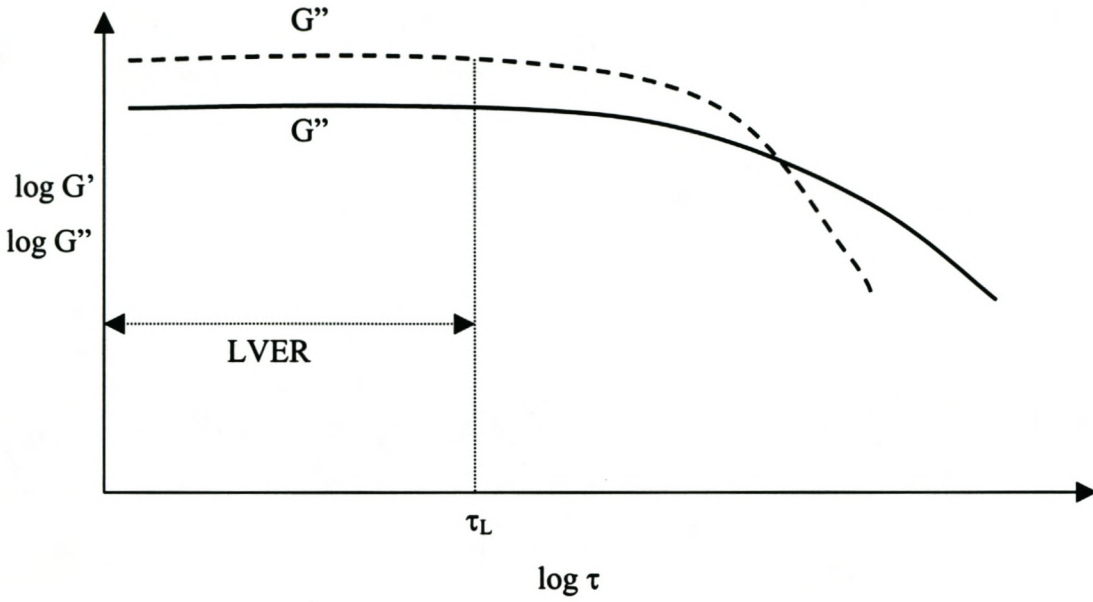


Figure B-4: Amplitude sweep of an unstable coating ($G'' > G'$)

B.2.3 Low-Shear Viscosity

The higher the low-shear viscosity, the higher is the resistance against sedimentation (see Figure B-5).

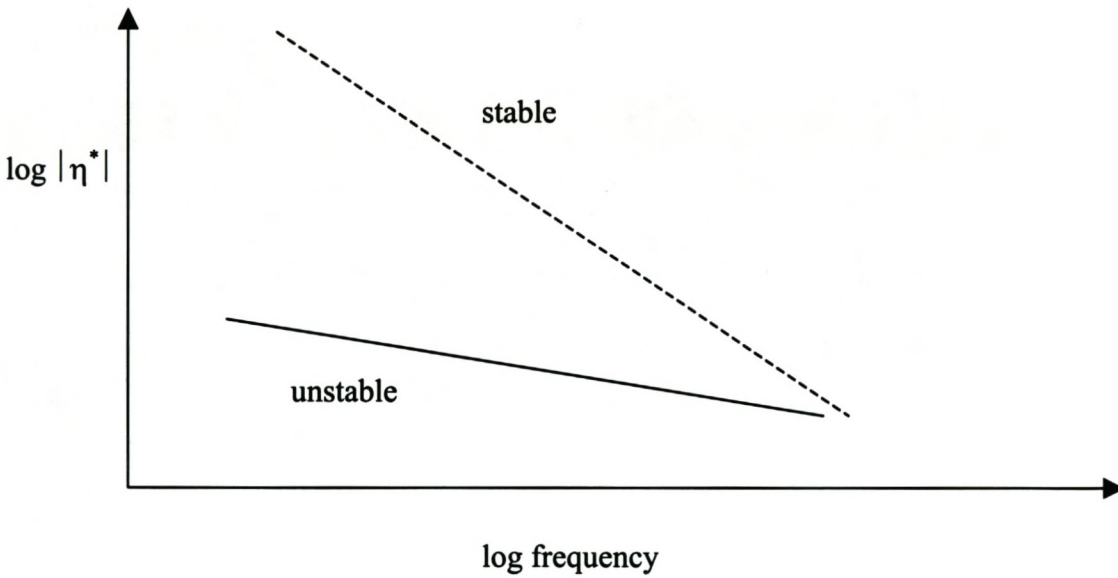


Figure B-5: Complex viscosity for a stable (-----) and unstable (——) dispersion

At low frequencies of the stable coating (- - - -), one can observe a continuous increase in the complex viscosity indicating the existence of a yield point. The unstable coating (—) shows a horizontal curve at low frequencies indicating very small or no yield points and therefore poor stability. It also tends to be more Newtonian in behaviour, indicating the liquid-like behaviour.

B.2.4 Long Time-Scale Behaviour

The long time-scale behaviour is represented by the low-frequency-range of the frequency sweep. Figure B-6 illustrates the differences between a stable and an unstable dispersion.

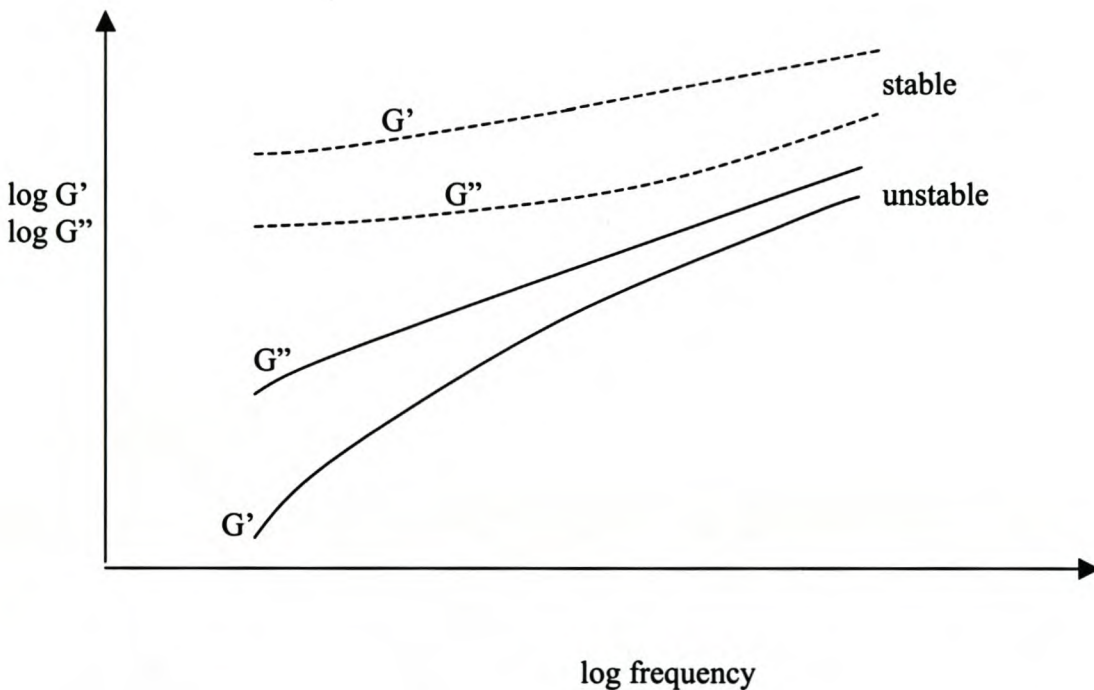


Figure B-6: Frequency sweep for a stable (-----) and unstable (——) dispersion

Instability of the dispersion is recognised in the following manner:

- $G'' > G'$ and therefore the liquid-like behaviour predominates over the solid-like behaviour
- The G' and G'' curves of the stable dispersion is almost parallel to each other showing little slope in the low-frequency range of the frequency sweep.
- In terms of the damping factor $\tan \delta$, because $\tan \delta = G''/G'$ and therefore if $\tan \delta > 1$, then $G'' > G'$ and the liquid like behaviour predominates over the solid-like behaviour.

B.3 Flow Behaviour

B.3.1 Shear-Thinning Behaviour

Most paints show pseudoplastic behaviour as in Figure B-1. In other words and decrease with the viscosity as the shear rate increases. Pseudoplastic behaviour is required to ensure high low-shear-rate viscosity and low high-shear-rate viscosity. Flow and viscosity curves are used to express the shear stress and viscosity curves respectively as a function of the shear rate. Pseudoplastic behaviour of a coating can be seen in Figure B-7.

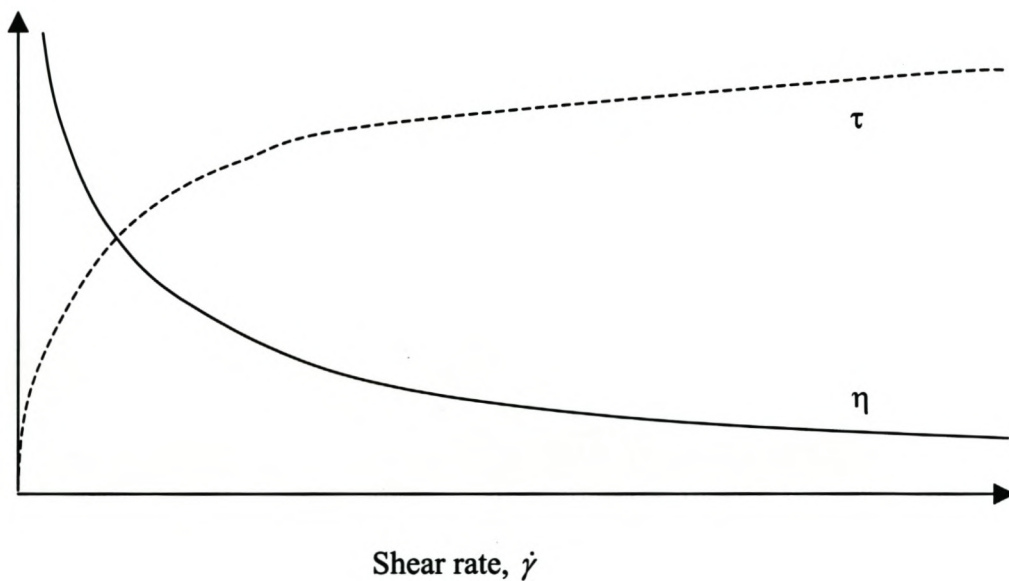


Figure B-7: Flow and viscosity curves of a pseudoplastic coating

B.3.2 Spatter

Spatter during roller application is most likely to occur when $G'' > G'$ in the high-frequency range of the frequency sweep, simulating rapid conditions.

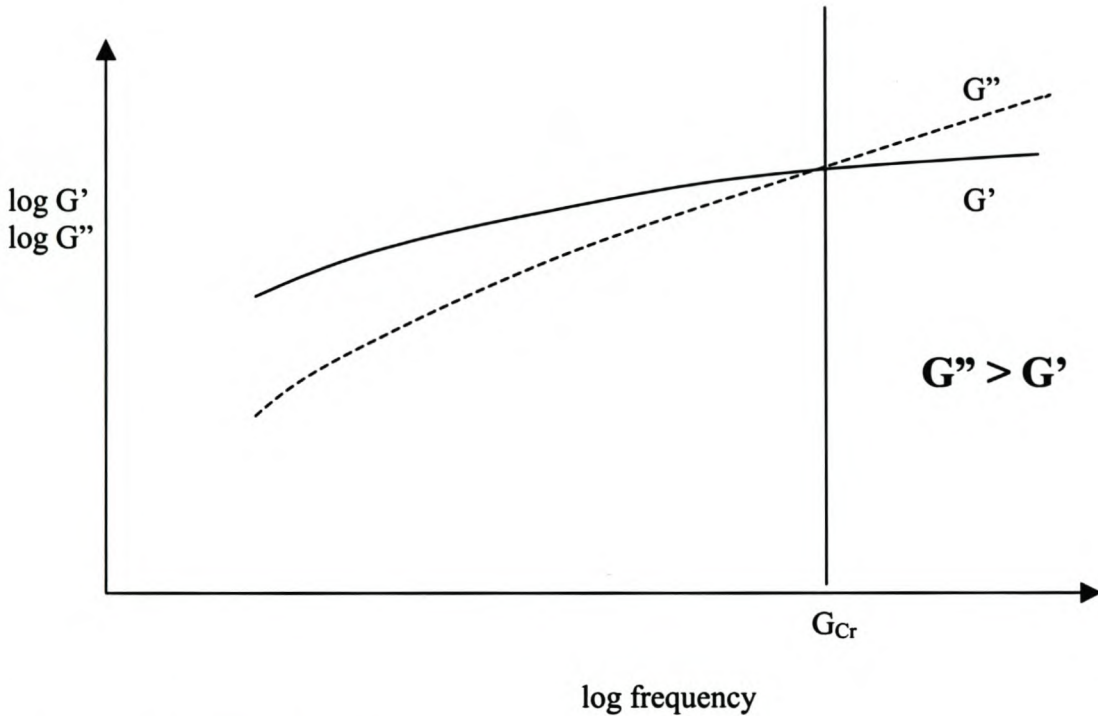


Figure B-8: Indication of spatter in frequency sweep

B.4 Behaviour After Application

Surface levelling and sagging behaviour significantly affects the quality of the coating. The internal superstructure must be built up within a certain period of time. During this period there should be enough time for gas bubbles to escape. Often, a smooth and glossy surface without any splashes or other inhomogeneities is required. When applying a coating on a vertical wall, sagging must be prevented.

All tests are based on the idea that a high shear load is followed by a period of minimum load. Different paints display different behaviour after application. Possible responses of paints in the recovery phase after a high shear load are as follows:

a) $G' > G''$ over whole recovery phase:

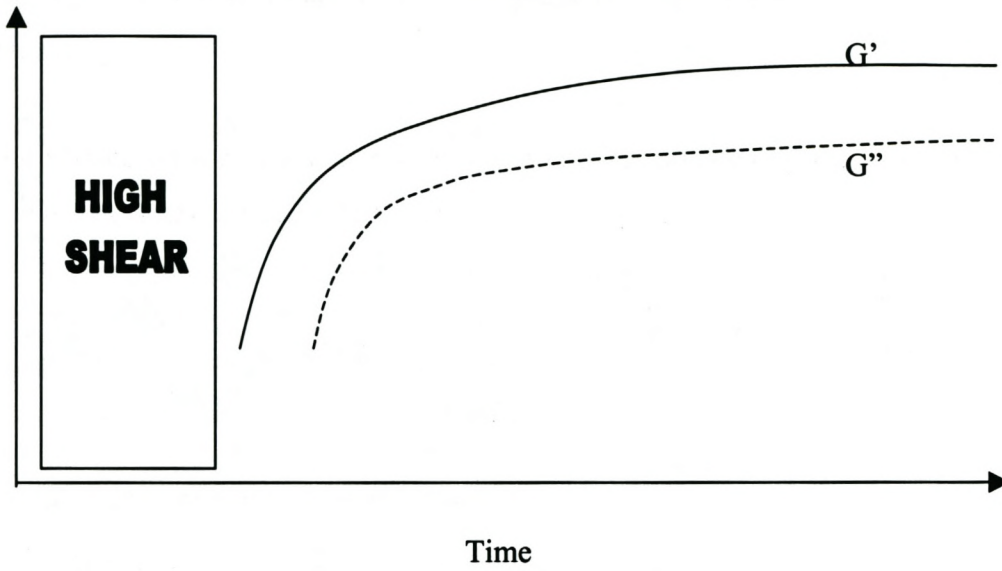


Figure B-9: Structure recovery after high shear load ($G' > G''$)

b) $G'' > G'$ over whole recovery phase:

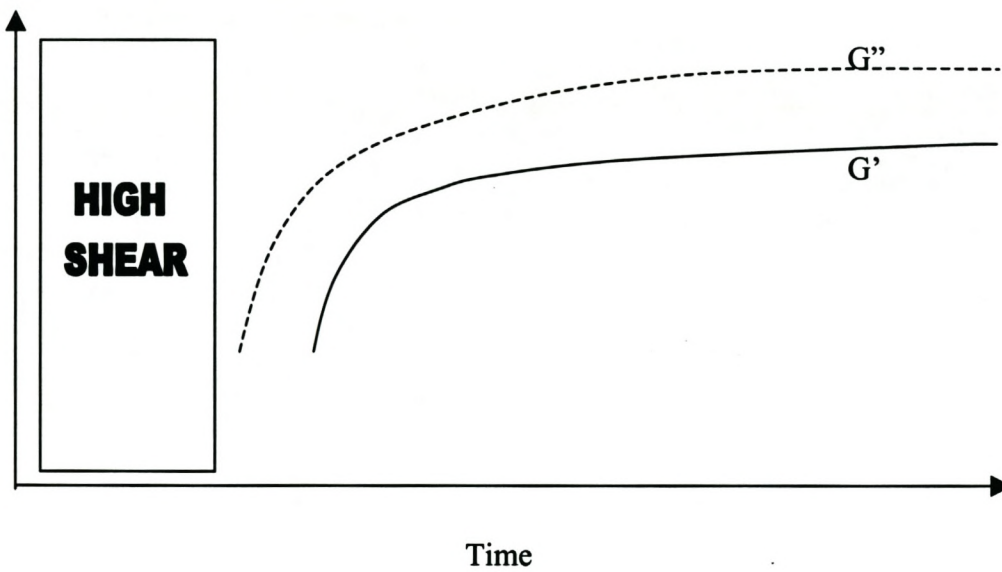


Figure B-10: Structure recovery after high shear load ($G'' > G'$)

c) $G'' > G'$ initially, but then cross-over ($G' = G''$) occurs so that $G' > G''$ in the end

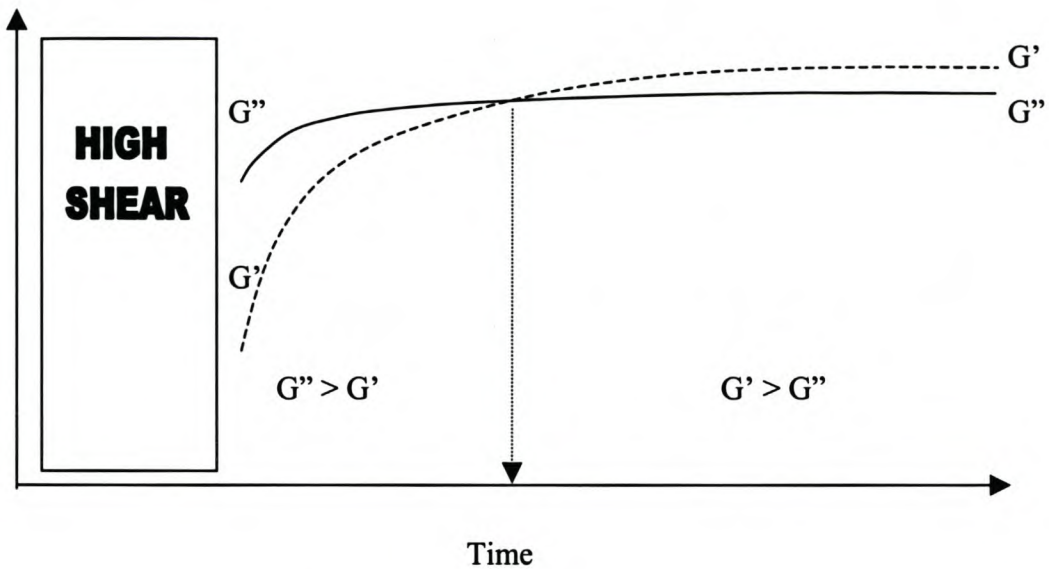


Figure B-11: Structure recovery with cross-over between G' and G''

The reverse behaviour of case (c) seldom happens.

B.4.1 Structure Recovery, Thixotropy

The internal structure reformation of a good paint is performed not too fast to allow appropriate levelling. If the internal structure reformation is performed too slowly, then too much paint will run down thus resulting in a too thin layer and sagging behaviour and the surface is covered inadequately. The structural recovery can be observed as the gradient of the G' -curves.

B.4.2 Surface Levelling and Sagging Behaviour

Sagging behaviour on a vertical wall takes place at very low shear rates (see Figure B-1). The surface levelling and sagging behaviour is dependent on the structure recovery as described in B.4.1.

- Too fast structure recovery can result in poor levelling with brush marks, while too long structure recovery can result in sagging behaviour.

- Sagging behaviour is also likely to occur when $G'' > G'$ directly after the high shear load without any cross-over point. See 'case b' above in Figure B-10.
- Poor levelling is also likely to occur when $G' > G''$ directly after the high shear load with G' indicating a fast rate of structure recovery. See 'case a' above in Figure B-9.
- Ideal levelling is most likely to occur when $G'' > G'$ directly after the high shear load, but not for too long so that a cross-over occurs between G' and G'' so that the structure strength recovers enough ($G' > G''$) to prevent further levelling and thereby resulting in a too thin layer and sagging behaviour. See 'case c' above in Figure B-11.

B.4.3 Layer Thickness

After applying the paint to a surface a definite layer thickness should remain. The yield point, the storage modulus and the low-shear-rate viscosity influences the layer thickness. The following rule is valid: the higher the yield point, the storage modulus and the low-shear viscosity, the thicker is the remaining layer on the surface.

However, the structure recovery after high shear gives one a clearer view on the layer thickness.

- Too fast structure recovery can result in too thick layer thickness, while too long structure recovery can result in too thin layer thickness.
- A too thin layer thickness is also likely to occur when $G'' > G'$ directly after the high shear load without any cross-over point. See 'case b' above in Figure B-10.
- A too thick layer thickness is also likely to occur when $G' > G''$ directly after the high shear load with G' indicating a fast rate of structure recovery. See 'case a' above in Figure B-9.
- Ideal layer thickness is most likely to occurs when $G'' > G'$ directly after the high shear load, but not for too long so that a cross-over occurs between G' and G'' so that the

structure strength recovers enough ($G' > G''$) to prevent further thinning of the layer and thereby resulting in a too thin layer. See 'case c' above in Figure B-11.

The term 'ideal' is used in a relative sense above. Ideal structure recovery is governed by the end-use the paint is designed for. For example, the ideal structure recovery of a paint that is designed to be highly durable will differ from the structure recovery behaviour from a paint that is designed to be a ceiling paint.

APPENDIX C Glossary of Rheological and Coating Terms

Glossary of Rheological and Coating Terms

The glossary is mainly an adaptation of rheological terms given by Barnes et al. [1989]

Apparent viscosity	The shear stress divided by the rate of shear when this quotient is dependent on the shear rate. Also called viscosity and shear viscosity.
Bingham model	A model with the behaviour of an elastic solid up to the yield stress. Above the yield stress, the shear rate is directly proportional to the shear stress minus the yield stress.
Complex fluid	A material that cannot be described purely by Newton or Hooke's laws for an ideal liquid and an ideal solid respectively.
Complex modulus	The mathematical representation of the shear modulus as the sum of a real and an imaginary part.
Complex viscosity	The mathematical representation of the viscosity as the sum of a real part and an imaginary part. The real part is usually called the dynamic viscosity and the imaginary part is related to the real part of the complex shear modulus.
Consistency	A general term for the property of a material by which it resists permanent change of shape.
Dashpot	A model for Newtonian viscous flow, typically represented by a piston moving in a cylinder of liquid.
Dead flat	Having no sheen or gloss.
Deformation	A change of shape and/or volume.
Dilatancy	The viscosity increase with increase in shear rate (shear thickening).

Durability	The degree to which a coating or sealant can withstand the destructive effects of the environment to which it is exposed. The term also refers to interior applications, including the ability to withstand scrubbing, abrasion, etc.
Ease of application	Characteristics of a paint or sealant that facilitate its application, e.g., spatter resistance, lapping properties, and open time.
Elastic liquid	A liquid showing elastic as well as viscous properties.
Elastic modulus	The stress divided by the corresponding elastic strain.
Elasticity	A reversible stress/strain behaviour.
Flocculation	Formation of clusters of particles separated by relatively weak mechanical forces or by change of physical forces at the interface between liquid and solid particles
Flow curve	A curve relating stress to shear rate.
Flow	A deformation, of which at least a part is non-recoverable
Hooke model	A model representing Hooke's law of elasticity.
Latex paint	Water-based paint made with a synthetic binder (latex), such as acrylic, vinyl acrylic, or styrene acrylic latex.
Levelling	The ability of a coating to form a smooth film without brush marks
Linear viscoelastic range (LVER)	The range where the G' and G'' values are independent of the strain.

Linear viscoelasticity	Viscoelasticity characterised by a linear relationship between stress and strain.
Liquid	A material that will continuously change its shape (will flow) when subjected to a given stress, irrespectively of how small that stress may be.
Loss angle	The phase difference between the stress and strain in an oscillatory deformation.
Loss modulus	The imaginary part of the complex modulus.
Maxwell model	A mechanical model consisting of a Hooke model and a Newtonian fluid model in series.
Model	An idealised relationship of rheological behaviour expressible in mathematical terms.
Modulus	In rheology, the ratio of the component of stress to the component of strain.
Navier-Stokes equations	The equations governing the motion of a Newtonian fluid.
Newtonian fluid model	A model characterised by a constant value for the quotient of the shear stress divided by the shear rate in a simple shear flow and with zero normal stress differences.
Non-Newtonian fluid	Any fluid whose behaviour is not characterised by the Navier-Stokes equations.
Opacity	The ability to keep light from passing through. A paint with a high opacity will hide the substrate well.

Power-law behaviour	Behaviour characterised by a linear relationship between the logarithm of the shear stress and the logarithm of the shear rate in simple shear flow.
Pseudoplasticity	Shear thinning.
Reynolds number	The product of a typical length and a typical fluid speed divided by the kinematic viscosity of the fluid.
Rheology	The study of the deformation and flow of matter.
Rheometer	An instrument for measuring rheological properties.
Sagging	Narrow downward movement of a paint or varnish film; may be caused by the application of too much coating, the collection of excess quantities of paint at irregularities in the surface (cracks, holes, etc.), or excessive material continuing to flow after the surrounding surface has set. Also referred to as runs or tears.
Semi-gloss	A paint with a gloss level between high gloss and eggshell/satin.
Settling	The sinking of pigments or other solid matter in a paint on standing in a container, with the subsequent accumulation on the bottom of the container.
Shear rate	The change of shear strain per unit time.
Shear stress	The component of stress parallel to the area considered.
Shear viscosity	Same as apparent viscosity.
Shear	The movement of a layer of material relative to parallel adjacent layers.

Shear-thickening	The increase of viscosity with increasing shear rate in a steady shear flow.
Shear-thinning	The reduction of viscosity with increasing shear rate in a steady shear flow.
Sheen	A moderately low degree of gloss; gloss with poor distinctness-of-image reflectance. Characteristic where a coating appears to be flat when viewed near to the perpendicular, but appears to be glossy when viewed from a low or grazing angle.
Solid	A material that will not continuously change its shape when subjected to a given stress.
Spatter	Droplets of paint that spin or mist off the roller as paint is being applied.
Strain energy	The energy stored in a material by the elastic strain.
Strain	The measurement of deformation relative to a reference configuration of length, area or volume.
Stress	A force per unit area.
Thixotropy	A decrease of the apparent viscosity under constant shear stress or shear rate, followed by a gradual recovery when the stress or shear rate is removed. The effect is time-dependent.
Viscoelastic liquid	A liquid with viscoelasticity.
Viscoelastic solid	A solid material with viscoelasticity.
Viscoelasticity	Having both viscous and elastic properties.

Viscometer	An instrument for measurement of viscosity.
Viscosity	The property of a material to resist deformation increasingly with increasing rate of deformation.
Water-based paint	Paint made with acrylic, vinyl or other latex resin types, and thinned with water. It dries more quickly than oil-based paint, has relatively low odour, some water vapour permeability, and cleans up easily. The liquid component is predominantly water.
Wet film thickness	Thickness of a liquid film immediately after application, before it begins to dry.
Yield stress	The stress corresponding to the transition from elastic to plastic deformation.
Zero-shear-viscosity	The constant viscosity value for the lower Newtonian region.

APPENDIX D Raw Data

Table D.1 - Properties of Standard Vesiculated Beads

Material name	Percentage [%]
Water:	74.54
Polyester:	14.67
Styrene:	6.39
Polyvinyl alcohol (PVOH):	1.39
Hydroxy ethyl cellulose (HEC):	0.26
Titanium dioxide (TiO ₂):	0.84
Cumene hydroperoxide (CHP):	0.12
Diethylene triamine (DETA):	0.27
Ferrous sulfate (FeSO ₄):	0.01
Acticide 14:	0.17
Disponil SUS 87:	0.85
Tween 80:	0.50
Physical/chemical character	
Solids [%]:	23.19
Average Particle size [μm]:	2.1
Particle Size Distribution [μm]	1.42
pH:	6.71

Table D.2 - Properties of Vesiculated Beads

Sample:	Solids [%]	Average Particle Size [μm]	Standard Deviation [μm]	Amount of Component [%]	pH	Stirrer Speed [rpm]
HEC1:	23.75	2.28	1.68	0.18	N/A	N/A
HEC2:	24.07	2.37	1.81	0.25	N/A	N/A
HEC3:	23.30	2.67	1.53	0.31	N/A	N/A
PH1:	23.65	2.40	1.83	1.00	N/A	N/A
PH2:	23.36	2.33	1.55	1.45	N/A	N/A
PH3:	23.47	2.13	1.44	1.69	N/A	N/A
DETA1:	23.42	2.11	1.46	0.27	6.71	N/A
DETA2:	23.19	2.10	1.42	0.34	7.26	N/A
Cowles1:	27.89	3.12	1.52	N/A	N/A	619
Cowles2:	27.69	4.82	2.40	N/A	N/A	498
Cowles3:	28.14	7.64	4.39	N/A	N/A	389

Table D.3 - Properties of PE-Free Paints

PE-free Paint	Vesiculated Beads [%]	Emulsion [%]	Coalescent type @ 1.1 % [-]	Pigment [%]	NH ₃ [%]	Rheology Modifier [%]
JE4/Ucar:	74.36	12.93	Ucar	9.70	0.97	0.97
JE4/Coasol:	74.36	12.93	Coasol	9.70	0.97	0.97
JE5/Ucar:	77.59	9.70	Ucar	9.70	0.97	0.97
JE5/Coasol:	77.59	9.70	Coasol	9.70	0.97	0.97
JE5.1/Ucar:	80.83	6.47	Ucar	9.70	0.97	0.97
JE5.1/Coasol:	80.83	6.47	Coasol	9.70	0.97	0.97
JE5.2/Ucar:	71.13	16.17	Ucar	9.70	0.97	0.97
JE5.2/Coasol:	71.13	16.17	Coasol	9.70	0.97	0.97

Table D.4 - Properties of PE-free Paints with Rheology Modifiers

Rheology Modifier:	Percentage Rheology Modifier [%]	pH
Acrysol ASE 60:	0.54	8.95
Acrysol ASE 60:	0.89	8.78
Acrysol ASE 60:	1.24	8.66
Acrysol RM2020/RM8W:	0.54	9.08
Acrysol RM2020/RM8W:	0.89	9.09
Acrysol RM2020/RM8W:	1.24	9.12
Acrysol RM5:	0.54	8.90
Acrysol RM5:	0.89	9.28
Acrysol RM5:	1.24	9.22

Table D.5 - Factor Levels in Paint X

Paint ID:	X1: pigment [g]	X2: extender [g]	X3: emulsion [g]	X4: opacifier [g]	Response Variables: Yield Point [Pa]		Response Variables: Cross-over [Pa]		Response Variables: Yield Point [Hz]	
					Actual:	Predicted:	Actual:	Predicted:	Actual:	Predicted:
1	146	143	263	56	1.0	1.29	33.93	28.42	0.57	0.61
2	146	143	329	83	1.0	1.58	17.45	20.43	0.27	0.34
3	146	143	395	69	2.0	1.44	18.80	16.83	0.43	0.30
4	146	179	263	83	1.5	1.27	18.00	20.83	0.36	0.40
5	146	179	329	69	2.0	1.13	17.49	17.23	0.37	0.37
6	146	179	395	56	0.7	1.01	11.79	13.52	0.29	0.33
7	146	215	263	69	0.5	0.82	13.35	17.63	0.32	0.43
8	146	215	329	56	0.8	0.69	11.07	13.92	0.34	0.39
9	146	215	395	83	0.7	0.99	7.10	5.93	0.21	0.22
10	182	143	263	83	2.0	1.36	23.91	23.78	0.29	0.37
11	182	143	329	69	1.2	1.22	17.68	20.18	0.24	0.33
12	182	143	395	56	0.9	10.9	19.27	16.47	0.37	0.29
13	182	179	263	69	0.8	0.91	26.15	20.58	0.68	0.39
14	182	179	329	56	0.6	0.78	11.59	16.87	0.23	0.36
15	182	179	395	83	0.6	1.07	8.00	8.88	0.18	0.19
16	182	215	263	56	0.6	0.47	23.54	17.27	0.63	0.42
17	182	215	329	83	0.5	0.76	14.49	9.27	0.19	0.32
18	182	215	395	69	1.3	0.62	16.91	19.76	0.29	0.15
19	219	143	263	69	0.5	0.98	12.87	11.77	0.31	0.38
20	219	143	329	56	0.8	0.86	17.36	20.19	0.17	0.18
21	219	143	395	83	1.5	1.15	9.90	8.57	0.28	0.28
22	219	179	263	56	0.9	0.55	10.77	12.58	0.20	0.24
23	219	179	329	83	0.5	0.70	4.42	8.97	0.65	0.38
24	219	179	395	69	0.5	0.53	7.65	9.82	0.48	0.42

Matlab Commands for Simple Linear Regression Model

1. Data are imported from EXCELL and get converted into ASCII code with the following command:

```
X=cell2num(exl_getmat)
```

2. The matrix used for calculations is defined by the following command:

```
y=X(:,1)  
x=X(:,2:end)
```

3. A column of ones is included in the matrix by the following command:

```
x=cat(2,ones(1,23)',x);
```

4. The matrix operation to obtain the array is given by the following command:

```
A=inv(X*X')*Y;
```

Test Procedure Followed on Rheometer

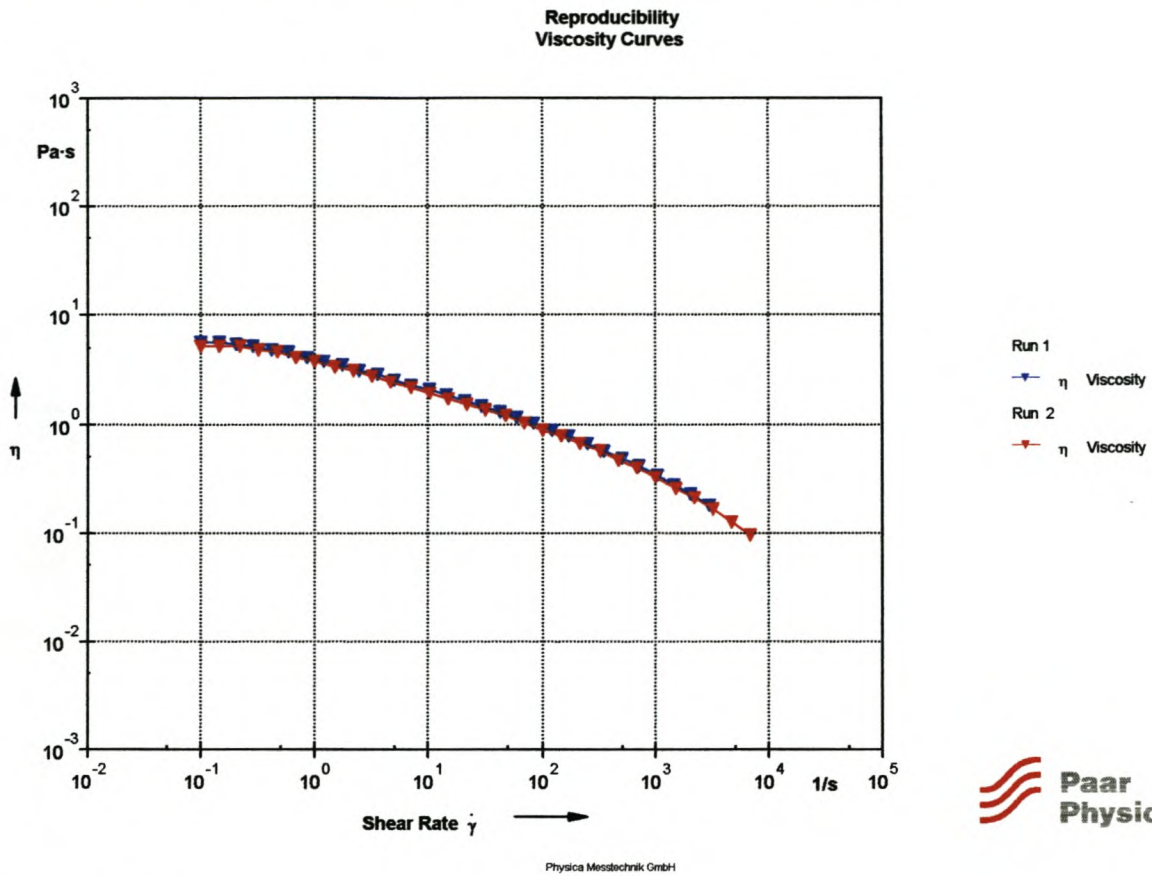
The following is a typical test procedure:

1. Start compressor so that there is pressure on the air bearing of the rheometer before it is switched on.
2. Switch on rheometer.
3. Open US 200 software program on computer.
4. Choose measuring device and connect it with rheometer coupling.
5. Set up test procedure.
6. 'Zero' the measuring device.
7. Place sample on lower plate.
8. Start test.
9. After the 'trim position' is reached, trim the excess sample and 'continue'.

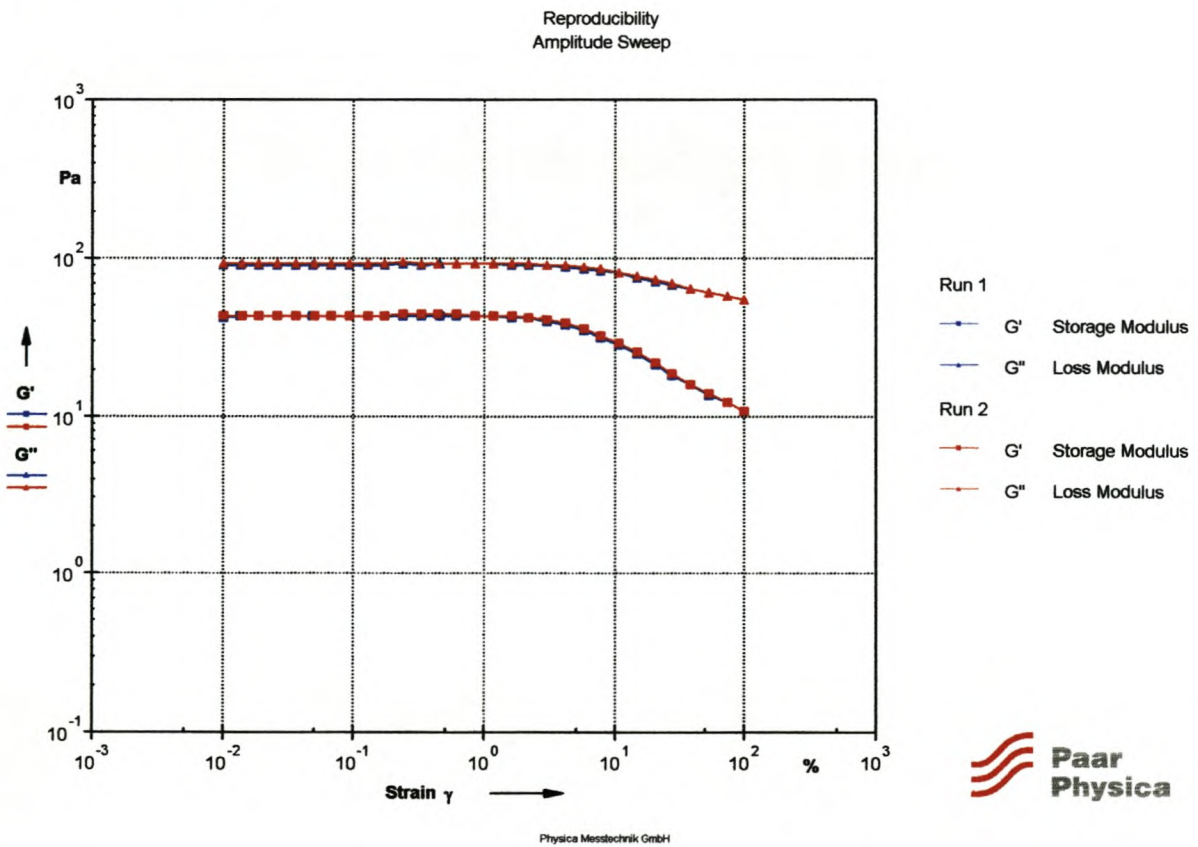
(The test is now being performed.)

10. Lift measuring device after test.
11. Clean measuring device and lower plate.
12. Save data.
13. Switch off rheometer before the compressor so that there is pressure on the air bearing the whole time.
14. Switch off compressor.

Reproducibility of Rheological Curves: 1. Viscosity Curves:



2. Amplitude Sweeps



3. Frequency Sweeps

Reproducibility
Frequency Sweeps

